Chemical Reactions Directed Peptide Self-Assembly

Ph.D. Thesis

by

Dnyaneshwar Baliram Rasale

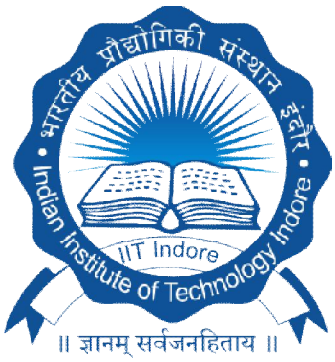

DISCIPLINE OF CHEMISTRY

INDIAN INSTITUTE OF TECHNOLOGY INDORE

APRIL 2014

Chemical Reactions Directed Peptide Self-Assembly

A THESIS

submitted in partial fulfillment of the requirements for the award of the degree of

DOCTOR OF PHILOSOPHY

by

Dnyaneshwar Baliram Rasale

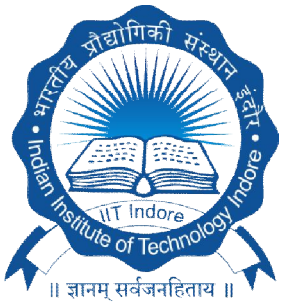

DISCIPLINE OF CHEMISTRY

INDIAN INSTITUTE OF TECHNOLOGY INDORE

APRIL 2014

INDIAN INSTITUTE OF TECHNOLOGY INDORE

CANDIDATE'S DECLARATION

I hereby certify that the work which is being presented in the thesis entitled **CHEMICAL REACTIONS DIRECTED PEPTIDE SELF-ASSEMBLY** in the partial fulfillment of the requirements for the award of the degree of **DOCTOR OF PHILOSOPHY** and submitted in the **DISCIPLINE OF CHEMISTRY, INDIAN INSTITUTE OF TECHNOLOGY INDORE**, is an authentic record of my own work carried out during the time period from March 2010 to April 2014 under the supervision of **Dr. APURBA K. DAS**, Assistant professor, Discipline of Chemistry.

The matter presented in this thesis has not been submitted by me for the award of any other degree of this or any other institute.

(DNYANESHWAR BALIRAM. RASALE)

This is to certify that the above statement made by the candidate is correct to the best of my knowledge.

(Dr. APURBA K. DAS)

DNYANESHWAR BALIRAM RASALE has successfully given his Ph.D. Oral Examination held on…….

Signature of Thesis Supervisor
Date:

Convener, DPGC
Date:

Signature of PSPC Member
Date:

Signature of PSPC Member
Date:

Signature of External Examiner
Date:

ACKNOWLEDGEMENTS

I would like to express my deep sense of gratitude and thanks to my supervisor Dr. Apurba Kumar Das for giving me the opportunity to work on such an exciting research area. His excellent supervision, advice and guidance from the very early stage made the completion of this study possible. I am indebted to him for his support, motivation and better understanding.

I would also like to extend my gratitude to Dr. Tushar Kanti Mukherjee and Dr. Shaibal Mukherjee for their valuable suggestions and guidance.

With great pleasure, I express my respect to Prof. Pradeep Mathur (Director, Indian Institute of Technology Indore) for his unending encouragement and providing all the facilities at Indian Institute of Technology Indore.

I am grateful to Dr. Chelvam Venkatesh (Head, Discipline of Chemistry, Indian Institute of Technology Indore) for his suggestions and guidance in various aspects. I am also grateful to Dr. Anjan Chakraborty, Dr. Tridib K. Sarma, Dr. Rajneesh Misra, Dr. Sampak Samanta, Dr. Suman Mukhopadhyay, Dr. Biswarup Pathak, Dr. Sanjay Singh, Dr. Shaikh M. Mobin and Dr. Satya S. Bulusu for their guidance and help during various activities.

I extend my profound thanks to my group members, Mr. Indrajit Maity, Mr. Maruthi Konda, Mr. Manoj K. Manna, Mr. Sagar Biswas, Mr. Soumitra Bhowmik, Mr. Sahidul Mondal and Mr. Ankan Biswas for their generous co-operation and help to make my work successful.

It has been wonderful to work with many friends together during my Ph.D., I would like to record my thanks to Mr. Prabhat Gautam,

Mr. Rajendar Nasani, Mr. Bhausaheb Dhokale, Mr. Bhagwati Sharma, Mrs. Raina Thakur, Ms. Tamalika Bhattacharya, Mr. Shivendra Singh, Ms. Anvita Srivastava, Mrs. Veenu Mishra, Ms. Manideepa Saha, Ms. Sonam Mandani, Mr. Debashis Majee, Mr. Anupam Das, Mr. Thaksen Jadhav, Mr. Biju Majumdar, Mr. Surajit Chattarjee, Dr. Pradeep K. Jaiswal, Dr. Deepa Dey and all friends for their generous co-operation and help.

I am also thankful to all my friends who helped me directly-indirectly during my Ph. D.

I am thankful to Ms. Sarita Batra, Mr. Kinney Pandey, Mr. Ghanshyam Bhavsar and Mr. Manish Kushwaha for their technical help and support.

I need to express my deepest love and gratitude to my lovable father Mr. Baliram Rasale and to my lovable mother Mrs. Shakuntala Rasale for their unconditional love with full support, unending encouragement and patience during this tenure.

Finally, I would like to take this opportunity to express my heartful regards to my lovable sisters Mrs. Shilesha, Mrs. Seema and Mrs. Jyoti for their care and affection.

Dnyaneshwar Baliram Rasale

Dedicated to My Beloved

Parents

ABSTRACT

In recent years, significant efforts have been made to develop functional materials in the field of nanoscience and biomedicine. Self-assembly is a prevalent process in nature and has exhibited great advantages in the development of functional architectures. Low molecular weight organic compounds are routinely being used in the construction of self-assembled nanostructures. Self-assembly of small peptides have attracted considerable attention due to their potential applications in tissue engineering, cell culture, drug delivery and biosensing. Peptide self-assembly is driven by various non-covalent interactions including hydrogen bonding, π-π stacking and hydrophobic interactions. To date, a number of stimuli have been used in the development of peptide self-assembly. Still, there is wide interest to develop novel biocompatible approaches for the fabrication of self-assembled soft materials and their further applications in biomedicine.

The main objectives of present study are:

- To synthesise small Nmoc-protected (Nmoc = Naphthalene-2-methoxycarbonyl) peptides and to study their self-assembly processes by novel approaches.
- Native chemical ligation is the most widely used method in protein synthesis. To achieve simple and efficient method for peptide self-assembly, our intention was to exploit oxo-ester mediated native chemical ligation in peptide coupling and subsequent formation of self-assembled peptide nanostructures.
- To develop a simple and easy orthogonal approach for peptide coupling and self-assembly process. We opted to synthesise Nmoc-protected-selenoesters which can readily undergo NCL reactions with N-terminal cysteine and cysteine based peptides.

- To exploit enzymatic peptide hydrolysis reaction in order to achieve a single predominating product from the dynamic peptide libraries via self-assembly.
- To study lipase catalyzed esterification reaction of Nmoc-protected peptides with gastrodigenin *p*-hydroxybenzyl alcohol in aqueous medium at physiological pH for the development of blue light emitting biomaterials.

1. Peptide self-assembly driven by oxo-ester mediated native chemical ligation

In this work, we have synthesized a series of Nmoc-protected dipeptides and Nmoc-amino acids which are finally coupled with *p*-nitrophenol to prepare active esters. All the active esters were subjected to native chemical ligation (NCL) reactions with cysteine in methanol-phosphate buffer medium at pH 7-8. The corresponding samples were analyzed with HPLC and ESI-MS. HPLC and ESI-MS results confirmed the formation of ligated products. Self-assembly was observed for compound **1** and **5** upon leaving undisturbed in atmospheric air. To further confirm the mechanism of self-assembly, reactions were carried out in inert atmosphere and kept undisturbed for long time. Self-assembly was not observed by any other ligated products. Thus, formation of disulfide bond after NCL reactions between two ligated products was responsible for the formation of self-assembled materials. This was further confirmed by treating the ligated products with reducing agent *tris*(2-carboxyethyl)phosphine (TCEP) that resulted in the dis-assembly of peptide gels. Self-assembly and dis-assembly were characterized by various techniques such as HPLC, rheology, circular dichroism, FTIR and electron microscopes.

2. In situ generation of redox active peptides driven by selenoester mediated native chemical ligation

To study the selenoester mediated native chemical ligation reactions, compounds **1-8** were synthesized. The Nmoc-protected amino acids were modified at C-terminal with phenyl selenoesters as well as thioesters. In this work, our objective was to make more facile and easy approach for peptide synthesis and self-assembly process. The synthesized compound **1** was dissolved in 10% ethanol in phosphate buffer followed by addition of Cys-Gly solution resulting in the formation of self-supporting gel within 1h. The self-assembled product was characterized by HPLC and ESI-MS which confirmed the formation of desired peptide. Similarly, compounds **2-4** were ligated with Cys-Gly and cysteine. The compound **2** was able to form self-assembled materials with different ligated products Cys-Gly and cysteine. Both ligated products of **2** were observed in oxidized form while ligated product of **1** was remained in reduced form. Cys-Gly is an active metabolite in biology whose higher concentration is related to increased risk in breast cancer. Such orthogonal reactions can be useful assays in clinical research. These redox active materials were characterized by using various techniques including HPLC, rheology, circular dichroism, FTIR, and electron microscopes.

3. Emerging π-stacked dynamic nanostructured library

Self-assembly is governed by various non-covalent interactions such as hydrogen bonding, π-π stacking and hydrophobic interactions. In this work, we reported the generation of dynamic library of small peptides with N-terminal aromatic protecting group i.e. naphthalene-2-methoxycarbonyl (Nmoc) that self-assembled to form self-supporting hydrogels and ultimately lead to a nanostructured predominating product via hydrogen bonding and π-stacking interactions. Nmoc-VVV **1** and Nmoc-FFF **2** were synthesized by conventional solution phase methodology. Nmoc-tripeptide **1** was dissolved in 2 mL of water and 1 mg of enzyme thermolysin was added to the solution of **1**. The self-supporting

hydrogel was formed after 24 h. The resulting hydrogel was analyzed by HPLC and ESI-MS which confirmed the formation of Nmoc-amino acid as a predominating product while Nmoc-tripeptide **2** gave uneven distribution of library components upon treatment with enzyme thermolysin and remained in solution form. Thus, self-assembly aids to drive the preferred product formation in dynamic combinatorial library (DCL) pool. Nmoc-amino acid gel was analyzed by fluorescence spectroscopy which confirms the formation of efficient π–π stacking interactions in the gel phase medium. Self-assembled hydrogel was further analyzed by rheology and TCSPC.

4. Lipase catalysed inclusion of gastrodigenin for the evolution of blue light emitting peptide nanofibers

Supramolecular ordered chromophoric π-conjugated aromatic systems serve as active materials in photoelectronic devices. Organic molecules with high fluorescence efficiency possess potential applications in organic light emitting diodes (OLEDs) and photonic devices. In this work, we reported lipase catalyzed incorporation of gastrodigenin *p*-hydroxybenzyl alcohol (HBA) in Nmoc-protected peptides followed by evolution of blue light emitting hydrogel. In this study, we have synthesized **1-3** Nmoc-protected dipeptides in which peptide **1** significantly undergoes 92% esterification reaction with *p*-HBA upon addition of *candida rugosa* lipase at physiological pH 7.4. The peptides **2** and **3** gave moderate 10% and 24% yields with HBA respectively. In case of peptide **1**, self-assembly drives esterification reaction at higher yield. The self-assembled fluorescence hydrogel was characterized by UV-vis and fluorescence spectroscopy. The emission peak appeared at 455-470 nm corresponding to blue light in the visible region of electromagnetic spectrum. The fluorescence microscopic study exhibits individual fluorescencent nanofibers in hydrogel state. Further, hydrogel was characterized with HPLC, rheology, CD, TCSPC and electron microscopy.

LIST OF PUBLICATIONS

1. Rasale D. B., Maity I., Das A. K. (2012), Emerging π-stacked dynamic nanostructured library, *RSC Adv.*, 2, 9791-9794 (DOI: 10.1039/C2RA21334F).
2. Rasale D. B., Maity I., Konda M., Das A. K. (2013), Peptide self-assembly driven by oxo-ester mediated native chemical ligation, *Chem. Commun.*, 49, 4815-4817 (DOI: 10.1039/C3CC41475B).
3. Rasale D. B., Maity I., Das A. K. (2014), Lipase catalyzed inclusion of gastrodigenin for the evolution of blue light emitting peptide nanofibers, *Chem. Commun.*, 50, 8685-8688 (DOI: 10.1039/C4CC02484B).
4. Rasale D. B., Maity I., Das A. K. (2014), In situ generation of redox active peptides driven by selenoester mediated native chemical ligation, *Chem. Commun.*, (DOI: 10.1039/ C4C C0 383 5E)
5. Rasale D. B., Maity I., Das A. K. (2013), Colorimetric enzyme sensing assays via *in situ* synthesis of gold nanoparticles, *J. Clus. Sci.*, 24, 1163-1170 (DOI 10.1007/s10876-013-0606-z).
6. Rasale D. B., Biswas S., Maity I., Das A. K., Biocatalytic evolution of nanostructured Nmoc (naphthalene-2-methoxycarbonyl) capped dynamic peptide libraries in hydrogel state, (*manuscript submitted 2014*).
7. Maity I., Rasale D. B., Das A. K. (2012), Sonication induced peptide-appended bolaamphiphile hydrogels for in situ generation and catalytic activity of Pt nanoparticles, *Soft Matter*, 8, 5301-5308 (DOI: 10.1039/C2SM25126D).
8. Maity I., Rasale D. B., Das A. K. (2013), Exploiting a self-assembly driven dynamic nanostructured library, *RSC Adv.*, 3, 6395-6400 (DOI: 10.1039/C3RA22401E).

9. Maity I., Rasale D. B., Das A. K. (2014), Peptide nanofibers decorated with Pd nanoparticles to enhance the catalytic activity for C-C coupling reactions in aerobic conditions, *RSC Adv.*, 4, 2984-2988 (DOI: 10.1039/C3RA44787A).
10. Maity I., Manna M. K., Rasale D. B., Das A. K. (2014), Peptide-nanofiber-supported palladium nanoparticles as an efficient catalyst for the removal of N-terminus protecting groups, *ChemPlusChem*, 79, 413-420 (DOI: 10.1002/ cplu. 201300348).
11. Maity I., Parmar H. B., Rasale D. B., Das A. K. (2014), Self-programmed nanovesicle to nanofiber transformation of a dipeptide appended bolaamphiphile and tts dose dependent cytotoxic behavior, *J. Mater. Chem. B*, 2, 5272-5279 (DOI: 10.1039/C4TB00365A).
12. Konda M., Maity I., Rasale D. B., Das A. K. (2014), A new class of phase selective synthetic β-amino acid based peptide gelator: from mechanistic aspects to oil spill recovery", *ChemPlusChem*, (DOI: 10.1002/cplu.201402120).

CONFERENCE PRESENTATION

1. Rasale D. B., Maity I., Das A. K., Peptide self-assembly via native chemical ligation, Fontier Lecture Series in Chemistry, Indian Institute of Technology Indore (30^{th}-31^{st} January 2014) Poster Presentation……..
2. Rasale D. B., Maity I., Das A. K., Dynamic peptide self-assembly", National Organic Symposium Trust, 9^{th} J-NOST Conference for Research Scholars, IISER Bhopal (04^{th}-06^{th} December 2013) Poster Presentation……..
3. Rasale D. B., Maity I., Das A. K., Enzyme Sensing and Enzyme-driven Dynamic Peptide Nanostructures", National Conference on Challenges and Prospective in Engineering,

Management and Pharmacy, B. M. College Indore (27^{th}-28^{th} April 2012) Oral Presentation……

TABLE OF CONTENTS

LIST OF FIGURES

Chapter 4. In Situ Generation of Redox Active Peptides Driven By Selenoester Mediated Native Chemical Ligation

Chapter 5. Emerging π-Stacked Dynamic Nanostructured Peptide Library

Chapter 6. Lipase Catalyzed Inclusion of Gastrodigenin for the Evolution of Blue Light Emitting Peptide Nanofibers

LIST OF TABLES

ACRONYMS

Abbreviations used for amino acids, peptides, derivatives, substituents, reagents, etc. are largely in acoordance with the recommendations of the IUPAC-IUB commission on Biochemical Nomenclature, 1974, Pure and Applied Chemistry, 40, 315-331. All amino acids are L-configuration. Standard three letter coding is used for all amino acids. Additional abbreviations used in this thesis are listed below.

Ala	Alanine
AFM	Atomic Force Microscopy
Boc	*tert*-butyloxycarbonyl
CD	Circular Dichroism
Cys-Gly	Cysteine-Glycine
C/Cys	Cysteine
CRL	Candida Rugosa Lipase
$CDCl_3$	Chloroform-d
DCL	Dynamic Combinatorial Library
DCM	Dichloromethane
DCC	Dicyclohexylcarbodiimide
DIP	Diisopropylcarbodiimde
DMSO	Dimethyl Sulfoxide
DMF	Dimethyl Formamide
EtOH	Ethanol
Et	Ethyl
EtOAc	Ethyl Acetate
EPL	Expressed Protein Ligation
ESI-MS	Electrospray Ionization Mass Spectrometry
FTIR	Fourier Transform Infrared Spectroscopy
F/ Phe	Phenylalanine
Fmoc	Fluorenylmethyloxycarbonyl
G/Gly	Glycine

HOBt	1-Hydroxybenzotriazole
HPLC	High Performance Liquid Chromatograpy
HCl	Hydrochloric Acid
HBA	4-Hydroxybenzyl Alcohol
L/Leu	Leucine
MeOH	Methanol
Me	Methyl
M	Molar
Nmoc	Naphthalene-2-methoxycarbonyl
Nmoc-VVV	Nmoc-Val-Val-Val-OH
Nmoc-FFF	Nmoc-Phe-Phe-Phe-OH
Nmoc-V	Nmoc-Val
Nmoc-F	Nmoc-Phe
Nmoc-L	Nmoc-Leu
Nmoc-A	Nmoc-Ala
Nmoc-Y	Nmoc-Tyr
Nmoc-Y-W	Nmoc-Tyr-Trp-OH
Nmoc-L-W	Nmoc-Trp-Tyr-OH
NCL	Native Chemical Ligation
NaCl	Sodium Chloride
NaOH	Sodium Hydroxide
$NaHCO_3$	Sodium Hydrogen Carbonate
NMR	Nuclear Magnetic Resonance
Nph	Naphthyl
OBz	Benzyl ester
OCH_3	Methyl ester
Ph	Phenyl
PB	Phosphate Buffer
pH	The negative logarithm hydrogen-ion activity $(-\log_{10} [H_3O^+])$
p-NP	*p*-Nitrophenol

s	Singlet
SEM	Scanning Electron Microscope
THF	Tetrahydrofuran
TCEP	Tris-(2-carboxylethyl)phosphine)
TEM	Transmission Electron Microscope
TFA	Trifluoroacetic Acid
TLC	Thin Layer Chromatograpy
TCSPC	Time Correlated Single Photon Counting
Tyr	Tyrosine
UV-Vis	UV-Visible Spectroscopy
V/Val	Valine
W/Trp	Tryptophan

NOMENCLATURE

θ	Angle
λ	Wavelength
α	Alfa
β	Beta
Å	Angstrom
nm	Nanometer
ω	Angular frequency
τ	Life time
δ	delta
µm	Micrometer
π	Pi
φ	Phi
ψ	Psi
σ	Sigma
γ	Gamma
G’	Storage modulus
G’’	Loss Modulu

Chapter 1

General Introduction

The spontaneous formation of ordered structures at nanoscale is usually referred as self-assembly.[1] When the constitutive components are molecules, the process is generally termed as molecular self-assembly. The molecular self-assembly is again divided into intramolecular and intermolecular self-assembly. The term molecular self-assembly refers to intermolecular self-assembly and the intramolecular analog is more commonly called folding. Scenarios guide research on origin of life stated that there must have been process by which prebiotic organic compounds were sufficiently concentrated[2,3] to undergo physical and chemical interactions. The physical properties of certain kind of molecules lead to formation of complex structures with emergent properties. Such emergent phenomena are referred to as self-assembly processes or self-organization. Cellular life began when self-assembled membrane-bound polymers had ability to not only polymerize, but also replicate their linear sequence of monomers.[4] Thus, self-assembly is a basic process by which contemporary cellular life produces membranes, duplex DNA and folding proteins. It has been demonstrated that the first cell must have been formed by the same intermolecular interactions and self-assembled structures. The self-assembly is a prevalent process in nature which plays important role in maintaining integrity of cell[5,6] to perform various functions of cell.[7] The cellular components such as actin filaments, microtubules, DNA, vesicles and micelles are the classic representation of molecular self-assembly in biological pools.[9]

Microtubules are long hollow cylinders made up of α and β tubulin dimmers (Figure 1.1). These dimers polymerize end to end in proto filaments which are being considered as building block of the microtubule

structures. They are highly dynamic and involved in many important cellular processes.[10] Their rapid assembly and dis-assembly play important role in the anaphase of mitosis. They are also involved in maintaining the structures of the cell along with microfilament and intermediate filament to form the cytoplasm.

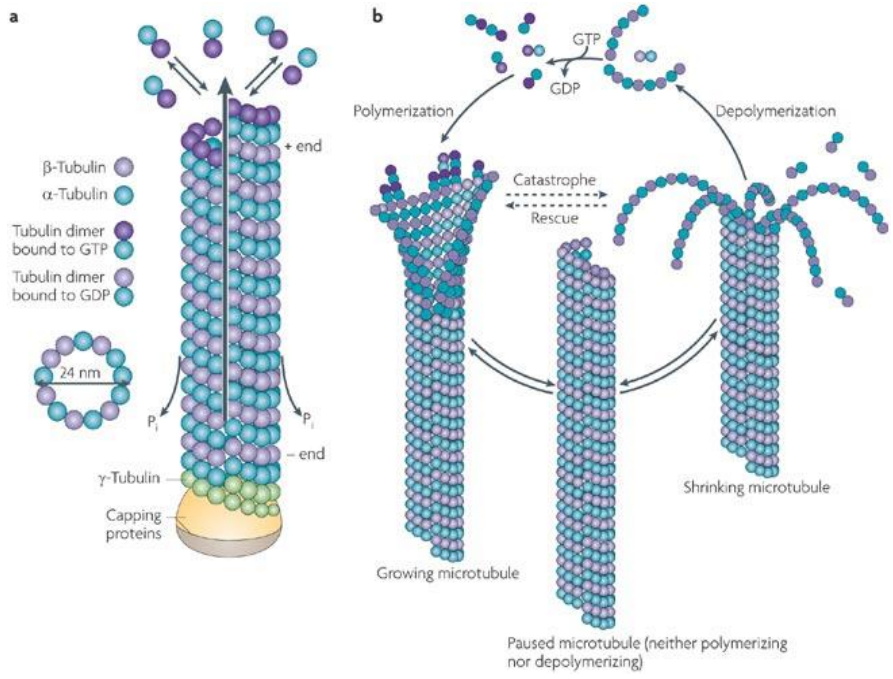

Figure 1.1*. Basics of microtubules.*

DNA is a basic example of molecular self-assembly in all living things. The transformation of genetic information occurs during the cell division and chromosomes are duplicated providing each cell its own complete set of chromosomes. All these important roles are performed by DNA in its self-assembled form. The dynamic and self-replicating abilities of DNA to transfer its genetic information has inspired scientist to mimic the nanostructures in the development of biotechnology. The unique material properties of DNA have made it an attractive molecule for material scientists and engineers interested in micro- and nano-fabrication.[11,12,13,14,15] The self-assembled nanostructures have a great impact on nanotechnology and biomedicine.[16 17,18,19,20] Natural preference

for bio precursors in constructing nanostructures comes from the biological world. The production of amino acids and their condensation to polypeptides to complex biopolymers under plausible prebiotic conditions has been known as the origin of life.[21,22,23] Amino acids have been considered as a building block of life.[24] The simple functionality and easy condensation to polypeptide made it an attractive molecule in the development of self-assembled nanostructures.[25,26,27,28] One of the naturally occurring examples of self-assembled peptide is Insulin which regulates the carbohydrate and fat metabolism in the body. The stability of insulin is maintained by formation of hexameric self-assembly.[29,30,31,32] The self-assembly of a single or more linear polymer of polypeptide chains leads to formation of complex structures. These complexities of structures are commonly known as proteins.[33,34] Proteins are essential part of organisms and participate in virtually every process within cells. The formation of the essential haemoglobin is a classic example of molecular self-assembly in biology in which four globular proteins assemble to form the haemoglobin structure.[35] Collagen is the main structural protein of the various connective tissues in which polypeptide chains are associated to form triple helix which further self-assembled to form collagen.[36,37,38] *Protein* is generally used to refer to the complete biological molecule in a stable conformation, whereas *peptide* is generally reserved for short amino acid oligomers often lacking a stable three-dimensional structure yet some short peptides acquire secondary structure in its self-assembled form.[39,40,41]

1.1 Peptide Conformation

1.1.1 Primary Structure of Peptide

There are 20 different natural L-amino acids used by cells for protein construction. Amino acids, as their name indicates, contain both a basic amino group and an acidic carboxyl group. This difunctionality allows the

individual amino acids to join together in long chains by forming peptide bonds (Figure 1.2).

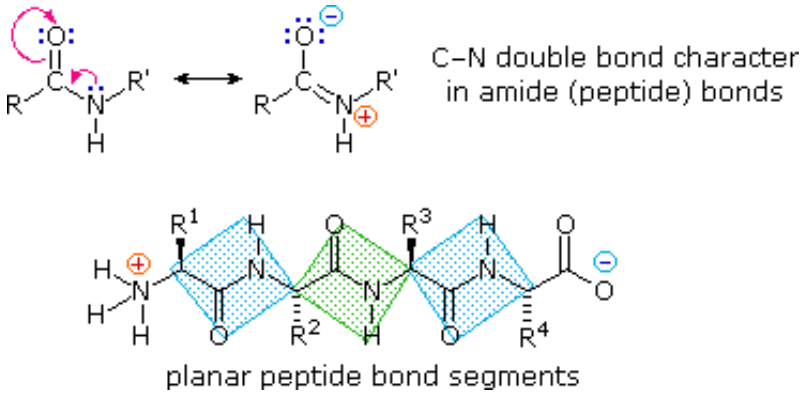

Figure 1. 2. *Primary planar peptide bond.*

1.1.2 Secondary Structures

In 1951, Linus Pauling and coworkers described that there are two main types of secondary structure, the α helix and β sheets.[42] These secondary structures are defined by patterns of hydrogen bonds between the main-chain peptide groups.[43] They have a regular geometry, being constrained to specific values of the dihedral angles ψ and φ on the Ramachandran plot (Figure 1.3). Both the α helix and β sheets represent a way of saturating all the hydrogen bond donors and acceptors in the peptide backbone. The backbone conformation of a polypeptide chain is defined by its main chain torsion angles. The torsion angle describes the rotations of the polypeptide backbone around the bonds between N-C^{α} (Phi, φ) and C^{α}-C (Psi, ψ). The Ramachandran plot provides an easy way to view the distribution of torsion angles of a protein structure.[44] It also provides an overview of allowed and disallowed regions of torsion angle values.[45] The third possible torsion angle within the proteins or peptides backbone (omega, ω) is essentially flat and fixed to 180^{o}. Usually the *trans* conformation (ω = 180^{o}) of peptide bond is preferred over the *cis* conformation (ω= 0^{o}) to avoid steric crowding of bulky side chains present at C^{α} carbon atoms of

amino acid residues. There are only three small sterically allowed regions in the Ramachandran plot that are physically accessible to a polypeptide chain and within this region the φ-ψ values produces the right-handed α-helix, the parallel and anti parallel β-pleated sheets and the collagen triple helix.[46,47,48]

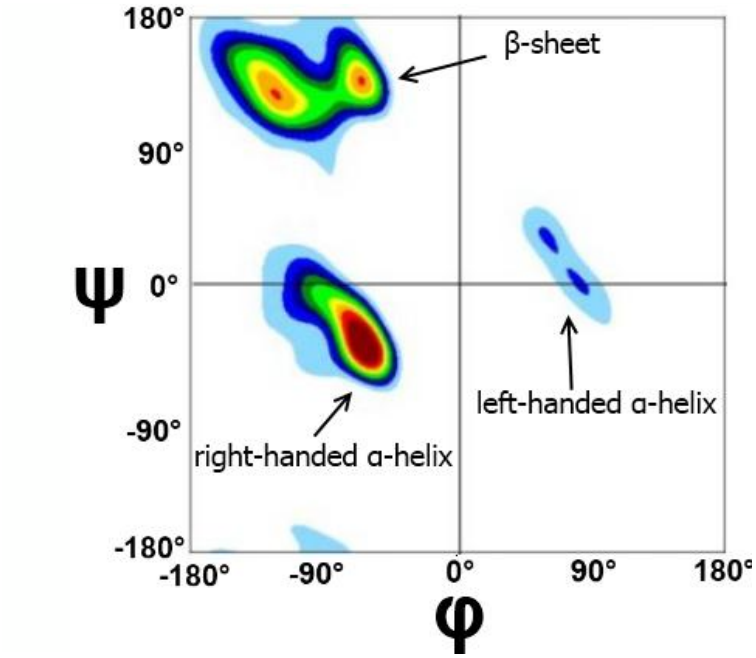

Figure 1.3. *The positions of commonly found regular conformations of the proteins on a Ramachandran plot.*

1.1.3 α- Helix

α-helices are formed by hydrogen bonding in amino acids via their carbonyl oxygen and amide protons. In a helix, every backbone NH group donates hydrogen bond to the backbone C=O group of the amino acid four residue earlier (Figure 1.4). Such an association of amino acids gives rise to a structure that resembles a cork screw. Each turn of the helix is made up of 3.6 amino acids (residues). Each turn of the helix propagates 5.4 Å along the helical axis. This distance is also known as the pitch of the helix. On average the φ angle in an alpha helix is -60° while the ψ angles can be in the range of -45 to -50 degrees. The α-helix can exist as either right handed helical structure or left handed helix. However, the left handed

helix is not favored by natural L-amino acids. Typically α- helices adopt backbone (φ, ψ) dihedral angles around (-60°, -45°), as shown in the image at right. In more general terms, they adopt dihedral angles such that the ψ dihedral angle of one residue and the φ dihedral angle of the next residue sum to roughly -105°. As a consequence, α-helical dihedral angles fall on a diagonal stripe on the Ramachandran plot ranging from (-90°, -15°) to (-35°, -70°). Similar structures include the 3_{10} helix ($i + 3 \rightarrow i$) and the π-helix ($i + 4 \rightarrow i$) also exit in polypeptide backbone.

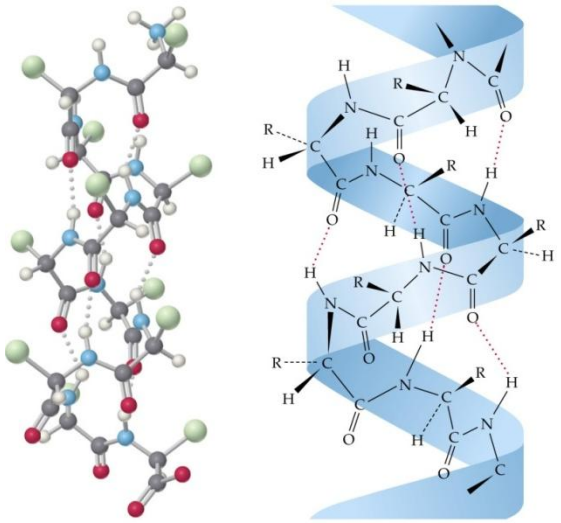

Figure 1.4. *Diagram shows the α-helix is held together by hydrogen bonds between N-H and C=O groups in each turn.*

1.1.4 β-Sheet

The β-sheet or β-pleated sheet is the second form of regular secondary structure in proteins. β-sheet is long chain of polypeptide typically 3 to 10 amino acids with backbone in fully extended conformation. The majority of β-strands are arranged adjacent to other strands and form an extensive hydrogen bond network with their neighboring N-H groups in the backbone of one strand and the C=O groups in the backbone of the other adjacent strands. The sideways distance between adjacent C^{α} atoms in hydrogen-bonded β-strands is roughly 5 Å. The energetically preferred dihedral angles near (φ, ψ) = (–135°, 135°) broadly, the upper

left region of the Ramachandran plot. The parallel β-sheet and antiparallel β-sheet are the major class of β-sheet structures.[49]

The parallel β-sheet is characterized by two peptide strands running in the same direction held together by hydrogen bonds between the strands. (figure 1.5). The antiparallel β-sheet is characterized by two peptide strands running in opposite directions held together by hydrogen bonds between the strands.

The anti-parallel β-sheet strand is known to be more stable than the parallel β-sheet arrangement because hydrogen bonds between carbonyls and amines are planar which gives preferred orientation. The peptide backbone dihedral angles (φ, ψ) are about (-140°, 135°) in antiparallel sheets. The parallel β-sheet strand introduces non planarity in the inter-strand hydrogen bonding pattern. The dihedral angles (φ, ψ) are about (-120°, 115°) in parallel sheets. However, β-sheet arrangement is more prominent in many self-assembling peptides and proteins. The higher-level association of β sheets has been implicated in the formation of protein aggregates and fibrils observed in many human diseases such as Alzheimer's disease.[50,51]

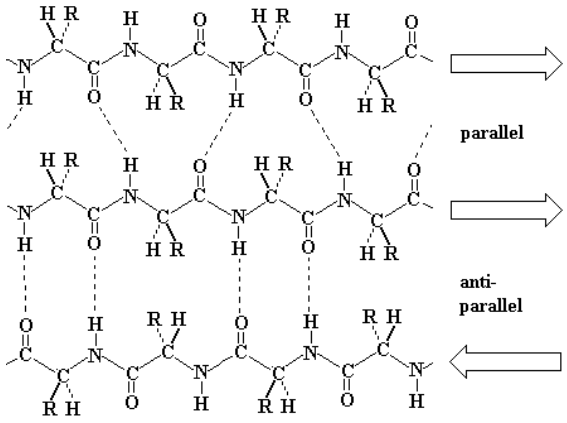

Figure 1.5. *Diagram shows hydrogen bonding pattern in parallel and anti-parallel β-pleated sheet structures. The dotted lines indicates the hydrogen bonding between N-H and C=O groups.*

1.2 Development of Molecular Self-assembly

Molecular self-assembly[52] is the spontaneous association of molecules under equilibrium conditions into stable, structurally well-defined aggregates joined by non-colavlent bonds. Molecular self-assembly is prevalent process in biological systems and underlies the formation of a wide variety of complex biological structures.[53,54] The understanding of self-assembly process and associated non-covalent interactions[55,56] that connect the complementary interacting molecular backbones in biological aggregates is a central concern in chemical biology. Besides the biomacromolecular nanostructures, certain small organic molecules are capable to self-assemble in a particular solvent, resulting in self-supporting gel.[57,58,59,61,62,63] If the self-assembly occurs in an aqueous medium, the resulting gel is referred to a supramolecular hydrogel.[64,65] The design of biomolecules that can self-assemble into higher order structure, has received increasing attention over the past few years, because of their applications in supramolecular electronics,[66] drug delivery,[67,68,69] wound healing, biosensing[70,71] and tissue engineering.[72,73,74] There are many weak interactions such as hydrogen bonding, hydrophobic interactions and π-π interactions that govern the assembly of everything from DNA in its double helix to the bonding of H_2O molecule in liquid water. Self-assembly is also the only practical approach for building a wide variety of nanostructures. [75,76]

The development of nanoscale structures and devices can be accomplished through "bottom-up approach" or "top-down" methods. In the bottom-up approach, small building blocks assemble into larger structures[77,78] (Figure 1.6). Examples of this approach include chemical synthesis,[79] molecular self assembly,[80] and colloidal aggregation.[81,82,83] The most of the self-assemblies are directed by small molecular weight organic molecules and bioactive molecules. With the increasing applications of supramoluclar hydrogels in the biomedicine, there is wide interest in the

development of supramolecular soft materials.[84] Several, physical stimuli such as pH, temperature, light, enzymes, and sonication are used to control peptide self-assembly.

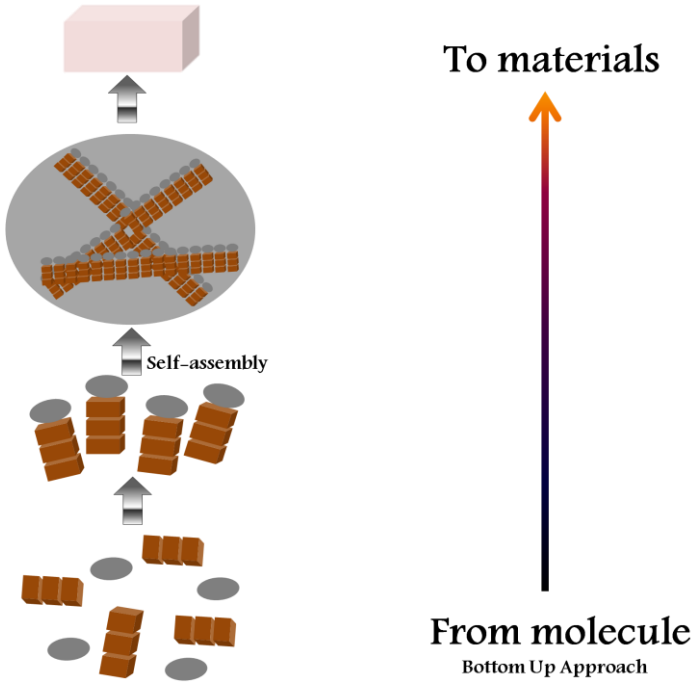

Figure 1.6. *The ''bottom-up'' approach is based on the interaction of simple monomers to form building blocks. The building blocks assemble to form well-ordered self-assembly by means of molecular interactions. This well order assembly leads to generation of a functional material.*

1.2.1 pH Modulated Molecular Self-assembly

Self-assembly is a powerful strategy for the preparation of ordered and dynamic supramolecular nanomaterials. Peptide based building blocks are prominent supramolecular synthons to produce hierarchical functional materials in water.[85,86,87] Self-assembled smart hydrogels are increasingly important class of materials for biomedicine,[88,89] pharmaceutics, coatings and cosmetics.[90,91] Three dimensional networks formed by supramolecular hydrogels are result of covalent or non-covalent

interactions. Within the range of several external stimuli, pH-responsive self-assembly is of particular interest for biomedical applications, since different intra- and extracellular compartments maintain varying levels of acidity or alkalinity. A highly relevant example is variation in pH between the healthy tissue and tumor tissue.[92,93,94] There are several reports on pH triggered self-assembly for many applications. Hawker *et al. (2013)* reported pH triggered self-assembly of biocompatible histamine-functionalized triblock copolymers which shows abrupt and reversible hydrogelation above pH 7.0 due to hydrophilic/hydrophobic transition of the histamine units to form a network of hydrophobic domains bridged by hydrophilic PEO matrix.[95] Zang and coworker described 1D self-assembly of water soluble perylene diimide molecule by pH triggered hydrogelation with electronic and optical properties for self-assembled nanofibers.[96]

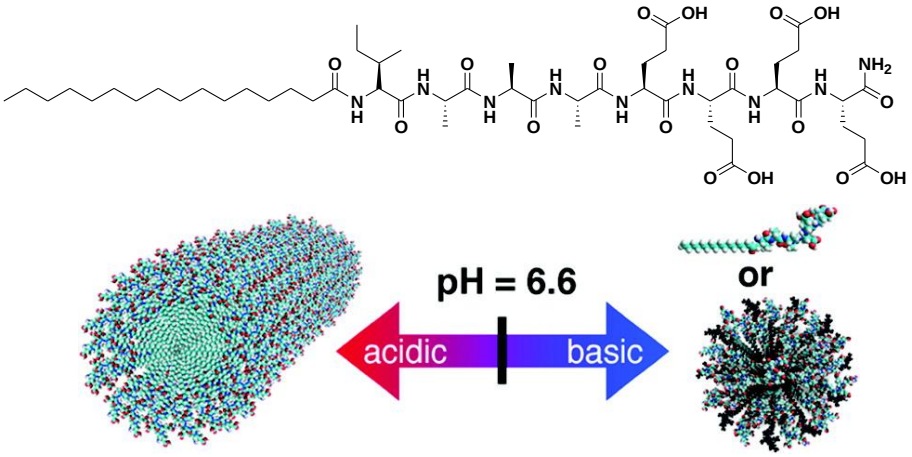

Figure 1.7. *pH-triggered morphological transition of self-assembling peptide amphiphiles.*

Goldberger and coworkers *(2012)* developed a series of self-assembling peptide amphiphile molecules that transforms either isolated molecules (Figure 1.7) or spherical micelles into nanofibers when the pH is slightly reduced from 7.4 to 6.6.[97] Escuder group described a new family of isomeric tetrapeptides containing aromatic and polar amino acids residues

that are able to form molecular hydrogels following a smooth change in pH.[98,99]

1.2.2 Sonication Induced Molecular Self-assembly

Generally, sonication is used to solubilise and disperse compounds through disruption of weak non-covalent interactions between molecules. Sometimes it can help the small organic molecules to self-assemble into supramolecular structure and tune the gelation properties.[100] Ultrasound breaks the non-covalent weak interactions and provides sufficient energy to achieve self-assembly through reorientation of the assembly process, such as intramolecular hydrogen bonding to intermolecular hydrogen bonding, extension of π-π stacking interactions and elongating the fiber to form network structures. Wang group reported sonication-induced self-assembly of flexible tris(ureidobenzyl)amine from its dimeric aggregates to supramolecular gel[101] (Figure 1.8).

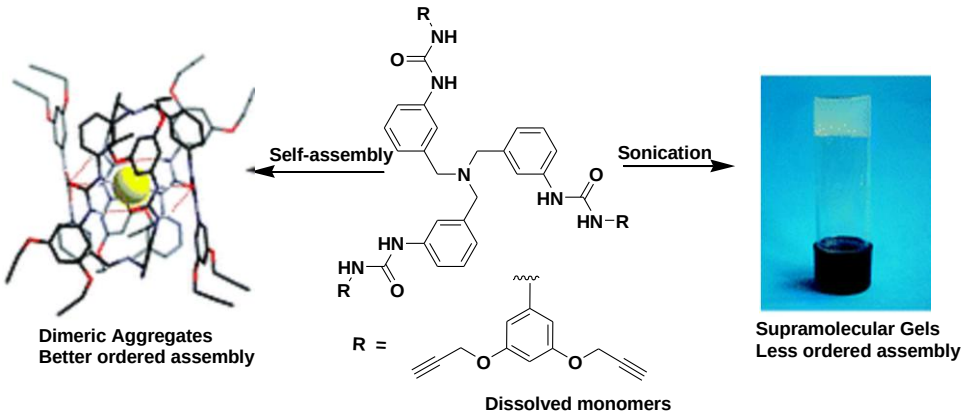

Figure 1.8. *Possibility of the tris(ureidobenzyl) amine to the transformation between dimeric capsules and supramolecular gels by sonication.*

Das and coworkers *(2012)* described sonication induced peptide-appended bolaamphiphile hydrogels which can act as a nanoreactor for *in situ* synthesis and stabilization of platinum (Pt) nanoparticles within the gel-phase network. In situ synthesized Pt nanoparticles, with a diameter of 1-3

nm, can reduce *p*-nitroaniline to *p*-phenylenediamine.[102] Zhang and coworker designed and synthesized a series of monocholesterol substituted quinacridone derivatives which can gelate a wide range of organic solvents upon ultrasound irradiation and afford intriguing well-defined nanostructures composed of three-dimensional sponge-like superstructures or fibrous networks.[103]

1.2.3 Chemical Reactions Mediated Self-assembly

A chemical reaction is a process that leads to the transformation of one set of chemical substances to another, which are usually characterized by chemical changes. Chemical reactions are used for the synthesis of new compounds from natural raw materials such as petroleum and mineral ores. It has a crucial role not only in everyday life but also in biology where it is referred as metabolism. In the living organisms, the biochemical reactions are mainly controlled by enzymes. One of the most important biochemical reaction is anabolism, in which different DNA and enzyme-controlled processes result in the production of large molecules such as proteins and carbohydrates from smaller units.[104] There has been wide interest to achieve such processes in the laboratory to develop some complex architecture exhibiting structural complexity ranging from nano- to mesoscale which is of fundamental importance for various proteins-related diseases but also hold great promise for various nano- and biotechnological applications.[105] Several physical perturbations are known to develop such complex self-assembled architectures. However, chemical reactions find wide scope in the development of self-assembled biomaterials due to its one pot propensity.[106] Generally, the efforts are made to develop orthogonal chemical reactions to further explore in the biomedical applications.[107,108] The self-assembly is mainly governed by non-covalent interactions which maintain the delicate balance between intermolecular interactions among the self-assembling molecules which could be achieved by adding or removing constrain moiety from the

molecules and subsequently leads to self-assembly.[109] Escuder and coworkers *(2013)*, demonstrated the use of chemical stimuli in control molecular gelation.[110]

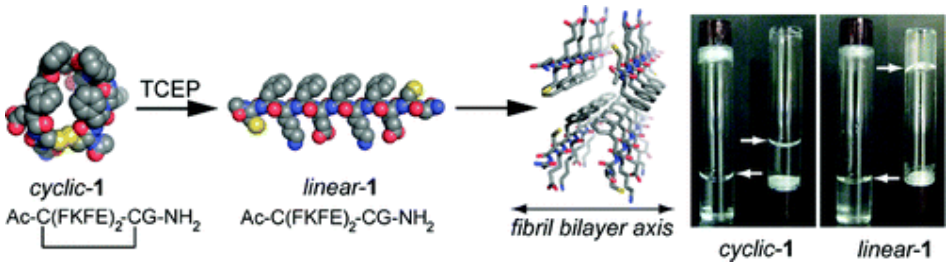

Figure 1.9. *Cyclic to linear peptide conformational switch using a chemical reductive trigger.*

Nilsson *et al. (2010)* described that imposing a conformational constraint that prevents adoption of the β-sheet secondary structure required for the self-assembly of short peptides is a possible strategy for controlling peptide self-assembly[111] (Figure 1.9). They flanked a short self-assembling peptide sequence with cysteine (Cys) residues which enabled the macrocyclization of these peptides, preventing β-sheet formation and self-assembly in the cyclic form. Thus, using TCEP, constraint was removed by simple reduction of the disulfide bond which resulted in relaxation to the stable β-strand and subsequently formation of self-assembly.

Van Esch and coworkers *(2010)* reported dissipative self-assembly system in which a synthetic DSA fibrous network uses chemical fuel as an energy source[112] (Figure 1.10). A gelator precursor dibenzoyl-(L)-cystine (DBC) is converted into self-supporting gel by reaction with a chemical fuel methyl iodide at pH=7 leading to formation of diester. Hydrolysis of the gelator, which is labile under ambient conditions, leads to energy dissipation and dis-assembly of the formed structures. Yang *et al. (2013)*

reported redox controllable self-assembly properties of selenium containing peptides.

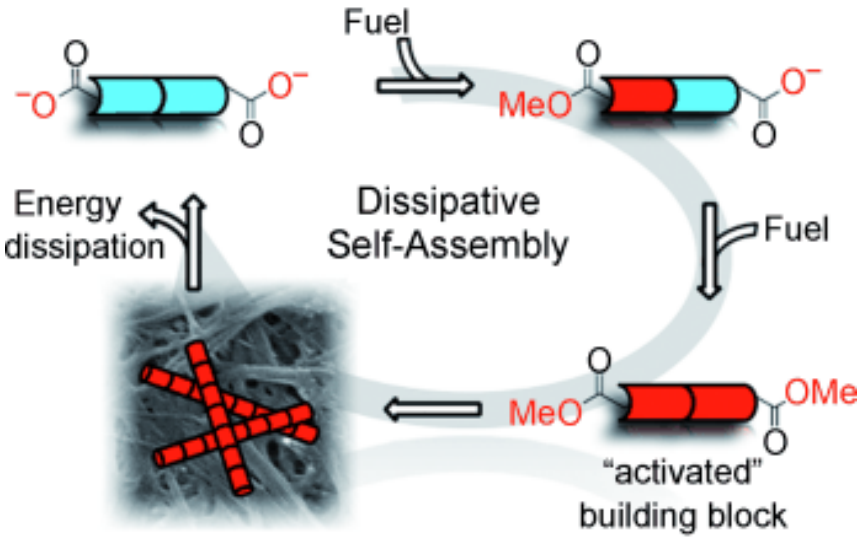

Figure 1.10. *A monomeric building block (blue) is activated by fuel consumption and is able to assemble (forming red fibers). In the assembled state, it can dissipate its energy and revert to its monomeric state (blue).*

An N-capped 4-phenyl-selenyl butanoic acid peptide was converted to selenoxide upon oxidation with H_2O_2 which is easily soluble in phosphate buffer saline.[113] However, chemical treatment with vitamin C converts selenoxide into less soluble selenide in aqueous medium leading to the formation of self-assembling nanostructures. Lehn and coworkers *(2005)* described that guanosine hydrazide yields a stable supramolecular hydrogel based on the formation of a guanine quartet (G-quartet) in the presence of metal cations. Guanosine hydrazide and its assemblies can be reversibly decorated by acylhydrazone formation upon reaction with various aldehydes, resulting in the formation of highly viscous dynamic hydrogels.[114] The dynamic system selects an aldehyde from the mixture of aldehydes, which leads to the formation of the most stable gel. Rao *et al. (2010)* demonstrated a biocompatible condensation reaction for controlled assembly of nanostructures in living cells using 1, 2 aminothiol and 2-cyanobenzothiazole.[114] Ajayan reported *(2011)* uniform and

crystalline nanofibers of perylene-3,4,9,10-tetracarboxylic dianhydride (PTCDA), an insoluble organic semiconducting molecule which have been achieved by self-assembling molecules using chemical reaction mediated conversion of an appropriately designed soluble precursor perylene tetracarboxylic acid (PTCA) using carbodiimide chemistry.[115] Das group *(2013)* exploited reversible acid catalyzed esterification reaction and alkylation reactions that lead to the formation of a single predominant product among the library members using dimethyl sulfate (DMS) as chemical fuel.[116] The library members formed a self-supporting hydrogel and showed the formation of a single predominant product. Otto and coworkers *(2010)* developed two self-replicating peptide-derived macrocycles that emerge from a small dynamic combinatorial library through oxidative disulfide formation from their pendant thiol groups in presence of oxygen and compete for a common feedstock. Replication is driven by nanostructure formation resulting from self-assembly of peptide.[117]

1.2.4 Photo-Switched Molecular Self-assembly

The self-assembly of bio-organic molecules into nanostructures is an attractive route to fabricate functional materials. For example, diphenylalanine (Phe-Phe, FF), an aromatic dipeptide consisting of two covalently linked phenylalanine units, can form various nanostructures such as nanotubes,[118,119] nanowires and nanosphere[120] under different processing conditions.[121] FF-based nanostructures can readily self-assemble in a simple way and possess the functional flexibility and molecular recognition capability suitable for a wide range of applications, such as biosensors,[122] imaging, guest encapsulation and nanofabrication.[123,124,125] Zhang *et al. (2013)* reported an azobenzene-linked symmetrical gemini α-helical peptide which reversibly transforms

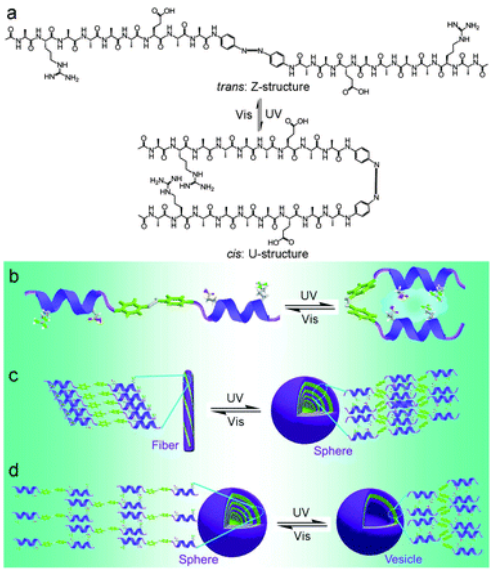

Figure 1.11. *Schematic illustration of the light-switched self-assembly of the gemini α-helical peptide. (a) Molecular structure of the gemini α-helical peptide and light-triggered reversible change between Z- and U-structures. (b) Model of light-triggered reversible structural change in the gemini α-helical peptide. (c) Light-switched self-assembly behaviors of the gemini α-helical peptide in acidic (pH 3.0), and (d) in basic (8.0) medium.*

between the *trans*- (Z-) and *cis*-structure (U-structure) under UV (λ=365 nm) and subsequently visible light irradiation[126] (Figure 1.11). This also affects self-assembly behavior of the gemini α-helical peptide. Park developed a light-harvesting peptide nanotubes that integrate photosynthetic units for mimicking natural photosynthesis.[127] Zinic *et al. (2002)* demonstrated that a bis(phenylalanine) maleic acid shows irreversible photoinduced gelation in water that works on photochemical isomerization of nongelling maleic acid amide to gelling fumaric acid amide.[128]

1.3 Enzyme Catalyzed Peptide Self-assembly

Enzymes are a class of highly efficient and specific catalysts in nature. Enzyme-regulated molecular self-assembly plays a critical role in many cell processes.[129] The formation of microtubules, which governs mitosis,

is one example.[130] The polymerization of actins which governs the focal adhesion of cells, is essentially a self-assembly process of seemingly miraculous sophistication that is regulated by enzymes. These natural self-assemblies inspire the development of enzymatic hydrogelation of small molecules. Compared with physical or conventional chemical perturbations, enzymatic regulation promises a unique opportunity to integrate molecular self-assembly in water with natural biological processes. Moreover, as a new method to make biomaterials, the enzyme-catalyzed formation of hydrogels of small molecules has already shown promise in biomedical applications.[131,132, 133] Xu and coworkers *(2012)* reported a method to image enzyme-triggered self-assembly of small molecules inside live cells[134] (Figure 1.12). George *et al. (2006)* have focused on the enzyme catalysis self-assembly strategy to develop molecularly defined and functional materials.[135] Ulijn groups exploited several enzymes including phosphatases, esterases and proteases, to trigger the self-assembly of aromatic peptide amphiphiles by converting non-assembling precursors into self-assembling components. [136 ,137 ,138, 139,140] Saiani and coworkers reported the effect of enzyme concentration of the morphology and properties of enzymatically triggered peptide hydrogels.[141]

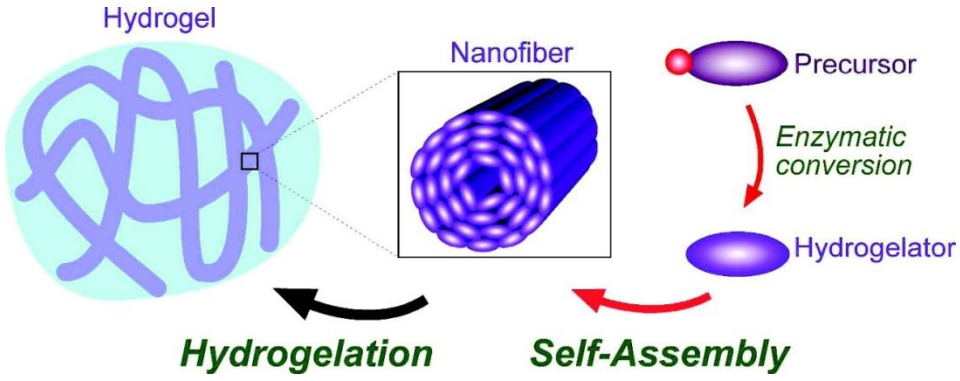

Figure 1.12. *The essential steps in the enzymatic hydrogelation of small molecules.*

1.3.1 Self-assembly Driven by Peptide Hydrolysis

Generally, hydrolysis is a chemical process in which a molecule of water is added to a substance and this addition causes both substance and water molecule to split into two parts. Acid-base-catalysed hydrolyses are very common. One of such example is the hydrolysis of amides or esters.[142] The amide bond in peptide is more rigid due to significant delocalisation of the lone pair of electrons on the nitrogen atom giving the bond a partial double bond character. Therefore, the hydrolysis reactions are very slow in water. Usually in the laboratory hydrolysis of proteins or peptides is being carried out by using 6N HCl at 110 °C.[143] However, use of this method leads to partial destruction of many amino acids including serine, threonine and cysteine. Tryptophan is totally destroyed by this procedure. In living system, most biochemical reactions including ATP hydrolysis take place by the catalysis of enzymes. The catalytic action of enzymes allows the hydrolysis of proteins, fats, oils, and carbohydrates. Protease enzyme aids digestion by causing hydrolysis of peptide bond in proteins.[144] In recent years, there is growing interest in the development of peptide nanostructure using biocatalytic method via peptide bond hydrolysis. Researchers are interested to exploit enzyme for development of peptide self-assembly for further biomedical applications without destruction of any amino acids. Shao *et al*. *(2011)* reported self-assembly of a peptide amphiphile based on hydrolysed Bombyx mori silk fibroin usin α-chymotrypsin.[145]

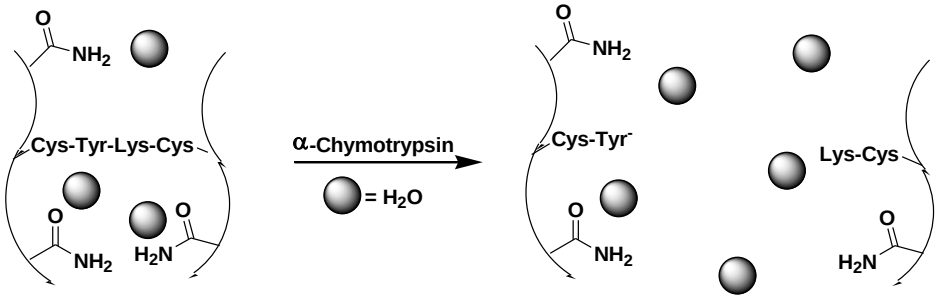

Figure 1.13. *A CYKC-cross-linked hydrogel degraded with α-chymotrypsin.*

Moore and coworkers *(2005)* described the chymotrypsin responsive hydrogel in which tetrapeptide CYKC was used as a cross-linker to create poly(acrylamide) hydrogel[146] (Figure 1.13). In the sequence of CYKC hydrolysis of tyrosine-lysine bond by chymotrypsin leads degradation of hydrogel. Gazit *et al*. showed emzymatic degradation of self-assembled peptide nanotubes, resulted in the production of discrete nanowires with a long persistence length.[247]

1.3.2 Peptide Self-assembly Driven by Reverse-Hydrolysis

Reverse hydrolysis of peptide is exactly opposite to the hydrolysis of amide bonds in peptides. Usually some protease show ability to reversibly synthesis the amide bond as well as hydrolyze the amide bond in dilute aqueous conditions. It is reported that self-assembly drives the reverse hydrolysis of peptides and prefers the most stable product formation in gel phase medium.[113] Thus, an enzyme thermolysin is preferably used to exploit in peptide self-assembly. Self-assembly of macroscopic materials from small molecular building blocks provides a route to design molecular biomaterials. The control development of biomaterials is on high demand in the context of biomedical applications. The stimuli that trigger self-assembly include various physical chemical perturbations. The enzyme triggered self-assembly is particularly interesting due to mild and physiological reaction conditions. Enzymatic hydrogelation of peptides causes to have desirable response in a biological environment.[147] Herein, some of the examples demonstrate the hydrogelation of peptides via reverse hydrolysis of amide bonds in peptides.

Uljin and coworkers *(2006)* have used a protease enzyme that normally hydrolyzes peptide bonds in aqueous medium.

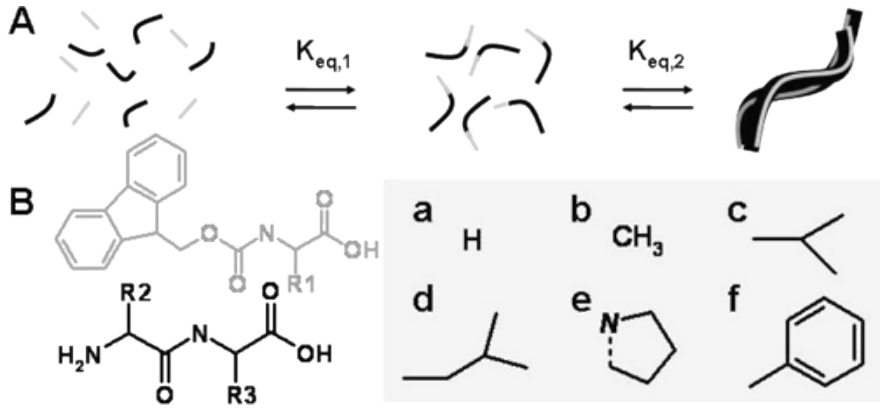

Figure 1.14. *(A) Proposed mechanism: Fmoc amino acids (gray) are enzymatically coupled to dipeptides (black) by a protease to form Fmoc-tripeptides that self-assemble to higher-order aggregates driven by π-π interactions between fluorenyl groups.* $K_{eq,1}$ *represents the equilibrium constant for peptide synthesis/hydrolysis,* $K_{eq,2}$ *for self-assembly. (B) Chemical structures of Fmoc-amino acids, dipeptide precursors and amino acid side chains:* ***a*** *Gly,* ***b*** *Ala,* ***c*** *Val,* ***d*** *Leu,* ***e*** *Pro,* ***f*** *Phe.*

They described a conceptually novel approach by using thermolysin to perform the reverse reaction (*i.e.* peptide synthesis or amide formation) which can produce amphiphilic peptide hydrogelators and self-assembles to form nanofibrous structures[148] (Figure 1.14). Uljin group *(2009)* also reported the use of reversible enzyme-catalysed reactions to drive self-assembly. They demonstrated that this system combines three features such as (i) self-correction-fully reversible self-assembly under thermodynamic control; (ii) component-selection-the ability to amplify the most stable molecular self-assembly structures in dynamic combinatorial libraries and (iii) spatiotemporal confinement of nucleation and structure growth.[149] Enzyme-assisted self-assembly therefore provides control in bottom-up fabrication of nanomaterials that could ultimately lead to functional nanostructures with enhanced complexities and fewer defects.

1.3.3 Lipase Catalyzed Peptide Self-assembly

Lipase is an important class of enzyme that catalyzes the hydrolysis of fats (lipid). Lipases are among the most broadly deployed biocatalysts because

of their ability to produce chiral products[150] with high enantiomeric purity. Lipases are used as catalyst for hydrolysis, alcoholysis, esterification[151] and transestrification of carboxylic acids or esters reactions.[152,153,154] They also work in organic as well as in aqueous medium which makes it a versatile candidate in the broad research area. One of the important aspects in chemical synthesis of drugs is to retain a single enantiomer, which is often a difficult task. Thus, one of the commercially attractive and environmentally compatible ways of making enantiomerically pure drug is biotransformation. In addition, peptides acylated with fatty acids become capable of being anchored to liposomes, translocating across lipid membranes, penetrating intact cells, and penetrating through the blood-brain barrier. However, selective acylation is a formidable task to a chemist due to the presence of numerous reactive groups in peptides. Klibanov *et al. (1991)* reported a lipase catalyze selective acylation of a dipeptide L-Phe-α-L-Lys-O^{t}Bu.[155] It has two primary amino groups. The α-NH_2 group of Phe and the ω-NH_2 group of Lys offer a challenge for selective acylation. Thus, lipase selectively acylate ω-NH_2 group of Lys in dipeptide in presence of excess trifluoroethyl acetate. Besides its useful applications in the organic synthesis, lipases are being used in the development of molecular self-assembly. Recently, the use of enzymes for the fabrication of biomaterials, starting from small molecular building blocks, to promote the synthesis of self-assembling materials has become an emerging area of research activity. Additionally, the structure of these (bio) materials can be easily controlled and tuned by using biological catalysts taking advantage of chemo-, regio- and enantioselective synthesis and of mild reaction conditions. In general, there are two routes to drive enzymatic molecular self-assembly through either breaking or making of covalent bonds. Interestingly, both the routes lead to self-assemble by maintaining the hydrophobic and hydrophilic balance between the self-assembling molecules. Important efforts have been made to get more insight into the

molecular self-assembly. These studies have proved that non-covalent interactions such as π-π stacking, hydrogen bonding and hydrophobic interactions play a key role in the development of such systems. Recently, thermolysin is used to generat dynamic combinatorial libraries for the discovery of stable self-assembling nanostructures. Although lipases are primarily used in esterification and transesterification of carboxylic acids, there are few examples where the lipases have been used to develop peptide self-assembly through amide bond synthesis. Palocci and coworkers *(2010)* reported peptide self-assembly via coupling of Fmoc-phenylalanine and diphenylalanine using lipase as catalyst at physiological conditions[156] (Figure 1.15). This is an excellent example of synthesis of peptide bond instead of using expensive protease. Lipase is known as an industrial biocatalyst and can be exploited to study such self-assembling systems. In his another work, Palocci described the self-assembly of homochiral and heterochiral lipase catalyzed Fmoc-based peptides with control drug release from hydrogel metrix.[157]

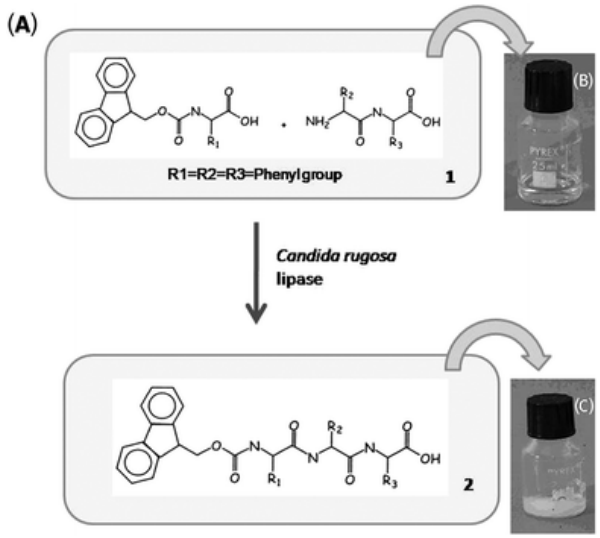

Figure 1.15. *(A) Chemical structures of the precursor (**1**) and its corresponding hydrogelator (**2**) and the schematic gelation process, (B) optical images of a solution of **1** in phosphate buffer (pH 7.4) and (C) the hydrogel of **2** formed by adding lipase to a solution of **1**.*

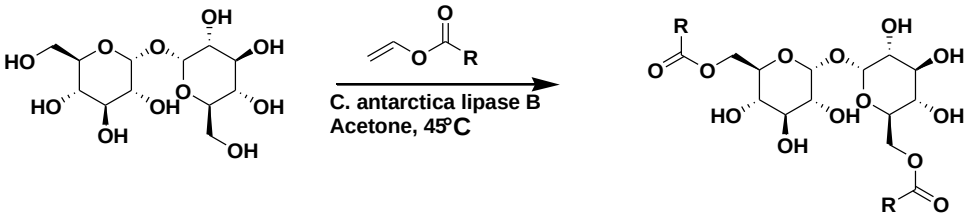

Compounds 1, 2, 3, 4, 5, 6,

R= $-CH_3$, $-(CH_2)_2CH$, $-(CH_2)_8CH_3$, $-(CH_2)_{12}CH_3$, $-(CH_2)_{16}CH_3$, -CH=CH

Figure 1.16. *Lipase catalyzed acylation of the disaccharide trehalose generated a family of low-molecular-weight gelators via transesterification.*

Dordick et al. *(2006)* demonstrated lipase catalyzed sugar-containing self-assembled organogels with nanostructured morphologies[158] (Figure 1.16). The lipase activity and thermostability can be increased upon immobilization with many supports. The self-assembled peptide architectures have also been used for the better activity of lipase. Matsui and coworkers (*2005*) reported lipase incorporated peptide nanotubes.[159] However, there are some nonspecific proteases which have been used for ester hydrolysis followed by self-assembly. Although, lipases are widely used in ester hydrolysis and transesterification, it is less explored in molecular self-assembly.

1.4 Dynamic Library Influenced by Self-assembly

Dynamic combinatorial chemistry (DCC) is promising tool to create and study the complexity of chemical reaction. DCC is often correlated with evolution of life. Thus, chemists are taking inspiration from nature to create dynamic molecular libraries and study the synthetic route for the evolution of unexpected molecules. The dynamic library is based on the reversible exchange of building blocks through chemical bonds. The distribution of library components are typically governed by thermodynamics and may alters upon changing the reaction condition. Initially, dynamic libraries have been generated by adding external

template which is inert to reversible chemistry of building blocks. The molecular recognization between template and library member alter the distribution of library members. The binding library member to template often leads to amplification of library member in the dynamic system. This effect may be utilized for the discovery of synthetic receptors and ligands for biomacromolecules, in many cases leading to unexpected supramolecular structures.

Lehn and Sreenivasachary described the reversible acyl hydrazone formation of guanosine hydrazide upon mixing with a mixture of aldehydes. This system leads to formation of dynamic libraries of hydrazone components. The amplified single component among the library member leads to stable gel formation.[128] The formation of preferential component works under the pressure of gelation because of the collective interactions in the assemblies of G-quartets. Otto *et al.* reported two self-replicating peptide-derived macrocycles that emerge from a small dynamic combinatorial library and compete for a common feedstock. Replication is driven by nanostructure formation, resulting from the assembly of the peptides into fibers held together by β- sheets[132] (Figure 1.17).

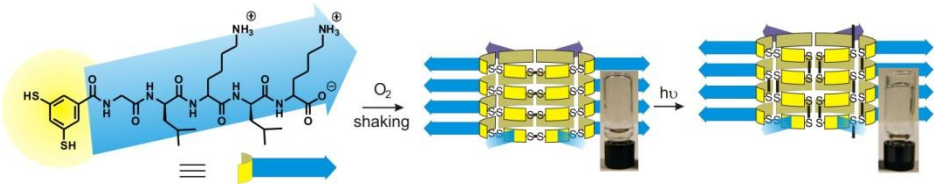

Figure 1.17. *Schematic illustration of a small dynamic combinatorial library made from dithiol building blocks.*

1.5 Bioorthogonal Chemical Reactions

Innovations in chemical ligation reactions have been essential for major breakthroughs in biology and medicine. At the heart of bioorthogonal

chemical reactions is the development of uniquely reactive functional groups that allow specific covalent ligation of molecules in biological systems. Despite the challenges of performing specific chemical reactions in biological settings, a variety of bioorthogonal ligation methods such as native chemical ligation, Staudinger ligation and many cycloaddition reactions have been developed. The native chemical ligation is the most revolutionary method for total or semi-synthesis of proteins discovered by Kent and co-worker in 1994.[160] In general, NCL involves reaction between an unprotected peptide with a C-terminal thioester and another unprotected peptide carrying an N-terminal cysteine. The sulfhydryl group of N-terminal peptide undergoes transthioesterification with C-terminal thioester. The resulting thioester-linked intermediate spontaneously and rapidly rearranges through an intramolecular S→N acyl shift to yield a native peptide bond (Figure 1.18). The term bioorthogonal chemistry was coined by Carolyn R. Bertozzi in 2003[161] and refers to any chemical reaction that can occur inside of living systems without interferring with native biochemical processes.[162,163,164] The concept of the bioorthogonal reaction has enabled the study of biomolecules such as glycans, proteins, and lipids in real time in living systems without cellular toxicity.

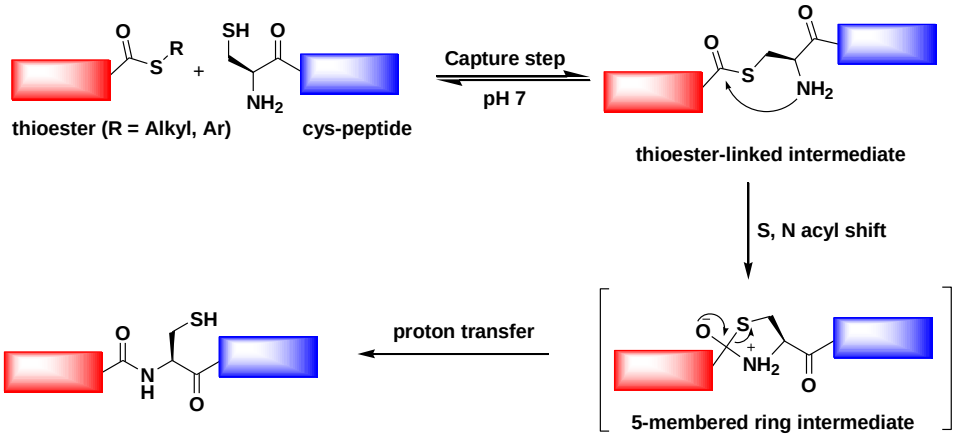

Figure 1.18. *Native chemical ligation (NCL) mechanism.*

A number of chemical ligation strategies have been developed that fulfill the requirements of bioorthogonality, including 1,3-dipolar cycloaddition between azide and cyclooctynes (copper free-click chemistry),[165] nitrones and cyclooctynes,[166] oximes/hydrazone formation from aldehydes and ketones (tetrazine ligation),[167] the isonitrile-based click reaction[168] and most recently, the quadricyclane ligation. Bertozzi group has developed the Staudinger ligation based on Staudinger reactions of azides with triarylphosphines[169] (Figure 1.19). The Staudinger ligation has been used in both live cells and live mice. Another interesting reaction was developed by Bertozzi group which is copper-free click reaction based on the work by Sharpless *et al*.[170] Unlike CuAAC, Cu-free click chemistry has been modified to bioorthogonal reactions by eliminating cytotoxic copper catalyst (Figure 1.20), allowing reactions to proceed quickly and without live cell toxicity. Instead of Cu in CuAAC, the reaction is a strain-promoted alkyne-azide cycloaddition reactions (**SPAAC**).

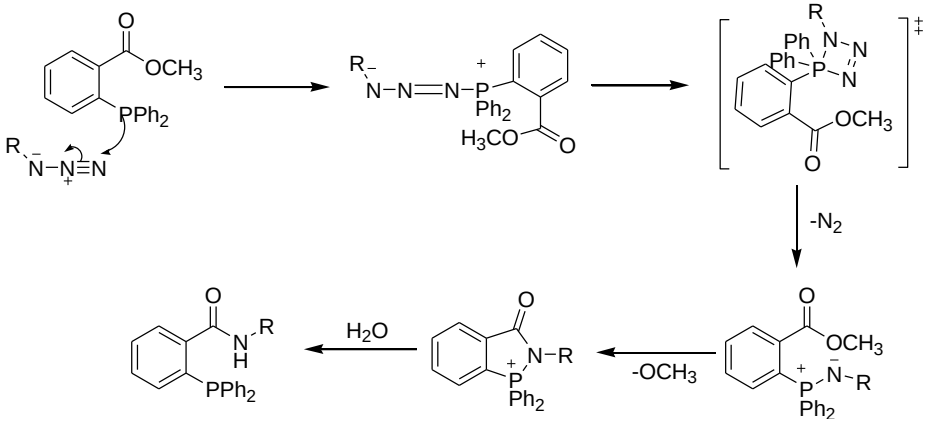

Figure 1.19. *Staudinger ligation mechanism.*

It was developed as a faster alternative to the Staudinger ligation. The incredible bioorthogonality of the reaction has allowed the Cu-free click reaction to be applied within cultured cells, live zebrafish and mice. The classic copper-catalyzed azide-alkyne cycloaddition has been an extremely

fast and effective click reaction for bioconjugation, but it is not suitable for use in live cells due to the toxicity of Cu(I) ions.

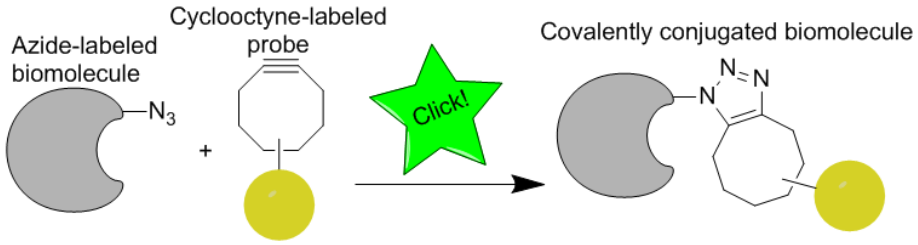

Figure 1.20. *Strain-promoted alkyne-azide cycloaddition (Copper free click reaction).*

The azide group is particularly bioorthogonal because it is extremely small (favorable for cell permeability and avoids perturbations), metabolically stable and does not naturally exist in cells and thus has no competing biological side reactions. Although azides are not the most reactive 1,3-dipolar compounds available for reaction, they are preferred for their relative lack of side reactions and stability in typical synthetic conditions.[171] The alkyne is not small, but it still has the stability and orthogonality necessary for *in vivo* labeling. Cyclooctynes were selected as the smallest stable alkyne ring which increases reactivity through ring strain which is calculated to be 19.9 kcal/mol.[172] The reaction proceeds as a standard 1,3-dipolar cycloaddition, a type of asynchronous concerted pericyclic shift. Thus, the application of this bioorthogonal chemistry in biology through functionalized chemical reporters has enabled the imaging and large-scale analysis of nucleic acids, proteins, glycans, lipids and other metabolites in vitro as well as in vivo in all kingdoms of life including bacteria, plants and mammals. In addition, to monitor biomolecules, bioorthogonal chemistry has allowed the functionalization of molecules for target identification of drugs and semi-synthesis of biomolecules for basic science as well as diagnostic and therapeutic agents. Considering the biological relevance of these bioorthogonal reactions, these methods open wide scope in various fields of Chemistry. Native chemical ligation is widely used method for coupling

of peptide fragments in protein synthesis. Considering its utility and feasibility, we were inspired to use native chemical ligation reactions in the development of dynamic peptide self-assembly.

1.5.1 Native Chemical Ligation

Native chemical ligation or NCL is an important extension of the chemical ligation discovered by Kent and co-workers in 1994. It is widely used method for the synthesis of total or semi-synthesis proteins. Native chemical ligation involves the chemoselective reaction of two unprotected peptides in aqueous solution to give a single covalently linked ligation product (Figure 1.21). In fact, in 1953, Wieland and co-workers discovered the chemical foundation of this reaction.[173] The reaction of valine-thioester and cysteine amino acid in aqueous buffer was shown to yield the dipeptide valine-cysteine. The reaction proceeded through the intermediacy of a thioester containing the sulfur of the cysteine residue. However, Wieland's work led to the 'active ester' method for making protected peptide segments in conventional solution synthesis in organic solvents.

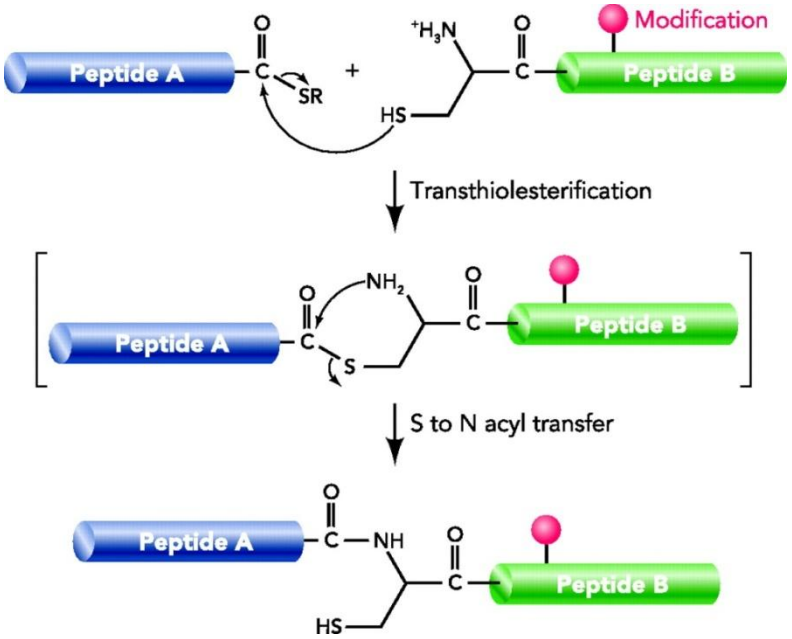

Figure 1.21. *Native chemical ligation mechanism.*

The native chemical ligation is the first practical method to ligate large unprotected peptide fragments was invented by Kent group. Native Chemical Ligation has become an extremely powerful method for the routine synthesis of small to moderate-sized proteins (approximately 150 amino acids), and it involves a chemoselective reaction between an unprotected peptide-α-carboxy thioester (-αCOSR) and an unprotected peptide with an N-terminal cysteine residue in solution. The mechanistic aspects describe that NCL proceeds through transthioesterification of C-terminal thioester of peptide with sulfhydryl group of N-terminal cysteine residue, which further spontaneously and rapidly undergoes S→N acyl transfer to give amide bond. The key features of this NCL reaction are that it occurs in aqueous buffer at physiological pH~7 and room temperature. The rate of ligation is dependent on the identity of the C-terminal amino acid in the peptide-thioester.[174] The ligation at sterically less hindered amino acid such as Gly- or Ala-RCOSR (R is an alkyl group) proceeds more quickly than ligation at sterically hindered *β*-branched C-terminal residues such as Ile- or Val-RCOSR. The ligation rate also affects on the nature of leaving group. Ligation with a highly activated 5-thio-2-nitrobenzoic acid thioester proceeds to completion within 10 min at pH 7.0, whereas ligation with an alkyl thioester is very slow and can take days to reach completion. The rate-limiting step in native chemical ligation is the transthioesterification with the thiol moiety of the side chain of the N-terminal cysteine. In general, the alkyl thioester are unreactive at normal NCL reaction conditions. Thus, exogenous thiol catalysts are required to be added to native chemical ligation reactions to promote the *in situ* formation of more active thioesters and thus increase the kinetics of ligation. The most common thiol catalysts to date have been used are either a mixture of thiophenyl, 4-mercaptophenylacetic acid (MPAA), or 2-mercaptoethanesulfonate (MESNa) in the NCL reactions.[175] The NCL reaction is highly chemoselective as no side-products are formed from reaction with the other functional groups present in either peptide segment

such as acids or basic amino groups and phenolic hydroxyls. Peptide and protein thioesters are extremely useful in chemistry and chemical biology and are essential for the synthesis of site-specifically modified peptides and proteins by NCL. The traditional method to synthesis peptide-thioesters is based on the activation of carboxylic acid of amino acids. Thioester can also be prepared by Boc chemistry using solid phase peptide synthesis.

1.5.2 Intein

In 1990, similar S→N acyl shift analogy of natural protein intein was observed to generate medium-sized proteins via native chemical ligation.[176,177] Intein mediated self-catalyzed protein splicing begins with the intramolecular rearrangement of N-terminal cysteine residue resulting into the formation of thioester intermediate (Figure 1.22). A transesterification occurs when the side chain of the first residue of the C-extein attacks the newly formed thioester inetrmediate to free the N-terminal end of the intein. The branched intermediate forms which undergoes excision by cyaclization of asparagine at the C-terminus of the intein splice junction. Finally, the free amino group of the C-extein attacks on thioester and undergoes NCL like S→N acyl shift to form a peptide bond of fuctional protein.[178,179] A protein semisynthesis method that involves a chemoselective reaction between an intein-generated protein thioester with a synthetic cysteinyl peptide to provide access to larger proteins (greater than about 150 amino acids) is termed Expressed Protein Ligation (EPL) (or semisynthesis), and was introduced by Muir Laboratory.[180]

EPL can be used for various applications[181,182,183] including introduction of fluorescent probe into proteins, to regulate post-translational modification, isotopic labeling and in protein engineering.

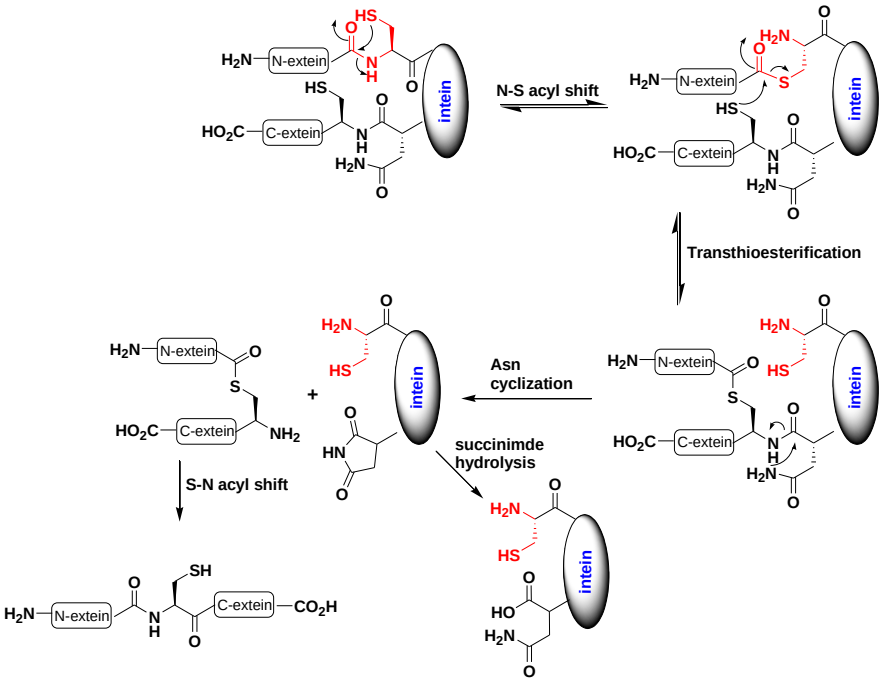

Figure 1.22. *The mechanism of protein splicing involves in inteins.*

Kent group *(2006)* reported a "kinetically control ligation" method during the convergent synthesis of proteins.[184] The method is based on the relative rate of ligation in thioester and N-terminal cysteine peptides. Typically, NCL reaction of alkyl thiolester was carried out with addition of thiol catalyst. However, Kent and co-workers modified the C-terminal with new 4-mercaptophenyl acetic acid (MPAA)-based linker which enables much fast ligation of cys-peptide than the alkylthiolester. In the competitive experiment in the absence of thiophenol, this large rate difference makes peptide-alkylthioester effectively unreactive. These chemoselective ligation reactions are being exploited by various research groups to synthesis long peptides, proteins as well as post-translational modification of proteins.

1.6 Applications of Native Chemical Ligation

1.6.1 Total Synthesis of HIV-1 Protease

The HIV-1 protease (HIV-1 PR) is a virally encoded 21.4 kDa aspartyl protease made up of two identical 99-residue polypeptide chains that together form an enzyme molecule with a single active site. Kent and co-workers *(2007)* successfully synthesized the mature 99-residue polypeptide by native chemical ligation by overcoming the frustrating solubility problems by adding 10 residues from the reverse transcriptase (RT) protein adjacent to the HIV-1 PR sequence in the Gag- Pol polyprotein to the C-terminus of the 95-99 peptide, followed by 10 arginine residues to act as a solubilizing "tag" to keep the polypeptide intermediates in solution[185] (Figure 1.23). Finally the conversion of cysteine to alanine was done by Raney nickel desulfurization.

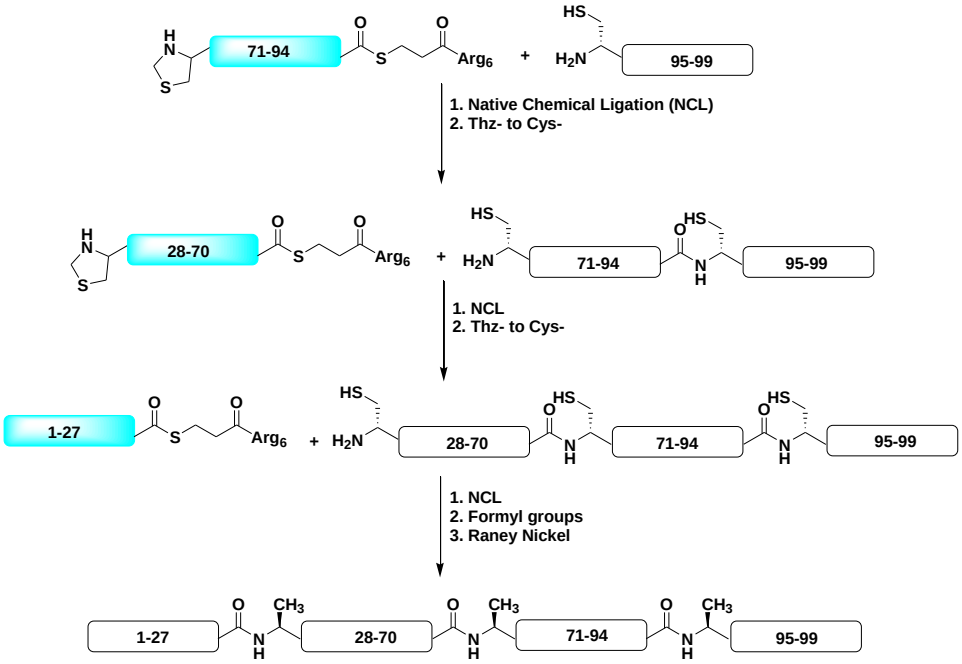

Figure 1.23. *Total synthesis of HIV-1 protease via native chemical ligation and conversion of cysteines into alanines by Raney nickel desulfurization. (Numbers indicate amino acid residues).*

1.6.2 Post-Translational Modifications of Histones

The N-terminal tail of histone H3 protrudes from the globular nucleosome core and can undergo several different types of post-translational modification that influence cellular processes. Peterson *et al. (2003)* described a native chemical ligation strategy that permits the reconstitution of nucleosomal arrays that harbor a wide range of individual or combinations of histone modifications, including serine phosphorylation, lysine acetylation, and lysine methylation. The solid phase peptide synthesis was used to generate a histone N-terminal tail domain that contains modified amino acids at any desired location. Native chemical ligation strategy was used to assemble full-length recombinant histone, which is reconstituted into histones octamer and subsequently assembled into nucleosomal arrays. The nucleosomal array was modified by phosphorylating serine at position 10 of each histone H3 proteins.[186]

1.6.3 Semisynthesis of Glycoprotein CAM-1

Glycosylation is a vital protein modification for the normal growth and development of organisms. Macmillan and Bertozzi *(2004)* prepared multi-glycosylated protein CAM-1 using semisynthesis[187] (Figure 1.24). A mucin-like glycoprotein functions as a ligand for the leukocyte adhesion molecule L-selectin. Two distinct motifs of this protein are separated by mucin domain which undergoes N-acetyl galactosamine (GalNAc) α-O-glycosylation on the hydroxyl groups of Ser/Thr residues. Three glycosylated forms of CAM-1 were prepared by using chemoselctive ligation having glycosylated residues at the N-terminal, C-terminal and simultaneously N- and C-termini regions. Despite efficiency and application of NCL reactions, various groups are looking to extend the scope of NCL reactions.

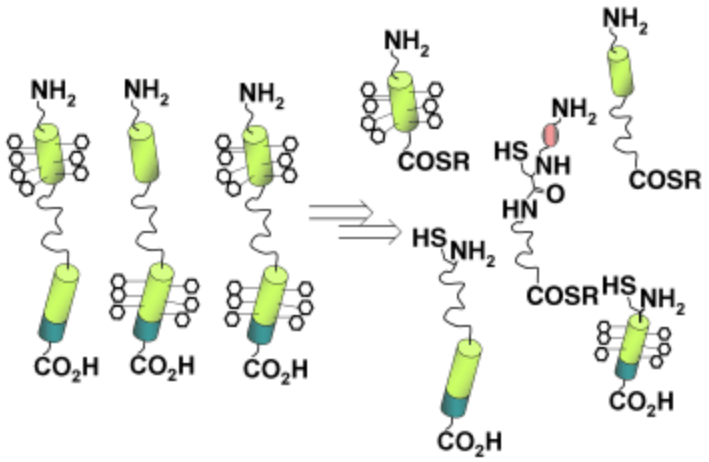

Figure 1.24. *Retrosynthetic rout to semisynthesis of glycoprotein CAM-1 via native chemical ligation.*

1.7 Extended Native Chemical Ligation

A limitation of native chemical ligation reaction is the requirement of N-terminal cysteine residue in the ligated peptide. However, most of the naturally occurring peptides and proteins are lacking the abundance of cysteine residue that promoted the development of post-ligation desulfurization chemistry. The Cys residue is used to facilitate the ligation which can be desulfurized to provide an alanine (Ala) residue either through hydrogenation or via a radical mediated approach, for example, through the use of the popular water-soluble radical initiator 2,2′-azobis[2-(2-imidazolin-2-yl)propane] dihydrochloride (VA-044).[188,189,190] Therefore, to extend the scope of native chemical ligation, extensive research efforts have recently focused on the synthesis of β-, γ-, and δ-thiol-derived amino acids as well as thiol-derived aromatic amino acids, which can be implemented in ligation-desulfurization chemistry through a similar mechanism to native chemical ligation (Figure 1.25). Seitz *et al. (2008)* extended the ligation reaction at valine site followed by desulfurization of penicillyl residues using reported method (VA-044, TCEP, EtSH, and tBuSH). Furthermore, they modified the reaction conditions for better yield.[191]

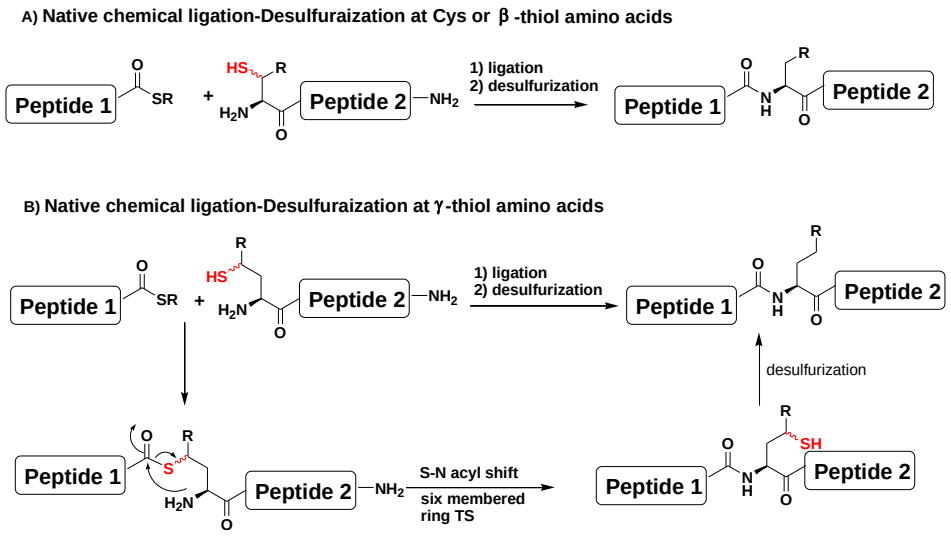

Figure 1.25. *A) Native chemical ligation-desulfurization at Cys or β-thiol amino acids. B) γ-thiol-mediated ligation desulfurization.*

Crich and Banerjee *(2007)* carried out native chemical ligation at *β*-phenylalanine. They anticipated that facile reductive cleavage of the benzylic C-S bond would ensure compatibility with other sulfur containing AAs.[192] The desulfurization was done with nickel boride which was obtained in situ by sodium borohydride reduction of nickel chloride. Danishefsky and co-workers (*2011*) demonstrated an advance in proline ligation. Ligation at C-terminal proline site is not readily accomplished due to poor reactivity of proline thioesters.[193] Here, they showed that ligation at N-terminal proline is feasible. An efficient methodology for ligation at glutamate (Glu) was described by Payne group. They first synthesized a suitably protected γ-thiol-Glu building block through a short and scalable route and further extended its utility in peptide ligation-desulfurization chemistry.[194] Payne and co-workers *(2011)* also successfully carried out ligation at β-aspartate as well as at β-tryptophan followed by desulfurization of sulfhydryl group.[195,196] Similarly, the expansion of native chemical ligation at side chain bearing thiol group facilitates ligation reaction in similar way to cysteine. The concept has also been applied for expansion of ligation reaction at C-

terminal thioester peptides. Despite the advances and utility of thioester mediated native chemical ligation, several groups expanded ligation reactions beyond C-terminal peptide thioester (Figure 1.26). There has been continuous advancement in native chemical ligation reaction by modifying various functionalities at C-terminal of peptides. Danishefsky *et al.* (*2008*) first reported oxo-ester mediated native chemical ligation using active *p*-nitrophenol ester at C-terminal of peptides.[197] Liu *et al.* (*2012*) described the ligation of peptide hydrazides that is complementary to native chemical ligation which proceeds through a chemoselective reaction between a C-terminal peptide hydrazide and a Cys-peptide to yield a native peptide bond.[198] White and Offer (*2012*) reported a simplified procedure for the chemical ligation of peptides by using the N-methylsulfonamide linker.[199]

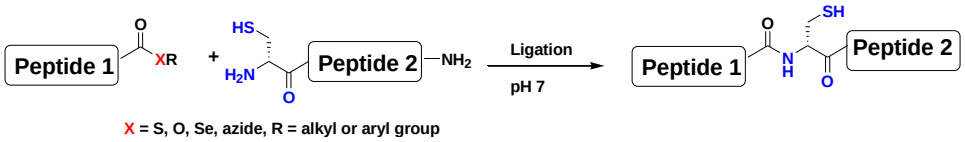

Figure 1.26. *Native chemical ligation at C-terminal of thioester, oxo-ester, selenoesters and azide.*

Durek *et al. (2011)* enabled the native chemical ligation reaction at selenoester by first converting thiolester to selenoacid followed by alkylation with 2-iodoacetamide at pH 4.[200] Considering the versatility of native chemical ligation reaction, there is growing interest to exploit NCL reactions in various fields of science and nanosciences. NCL reactions are successfully used for coupling of peptide and glycoconjugates bearing N-terminal cysteine based peptide to activated surfaces.

1.8 Peptide Self-assembly Driven by Native Chemical Ligation

1.8.1 Thioester Mediated Native Chemical Ligation

As posited in a "Thioester World," thioesters are possible precursors to life.[201] It is revealed that thioesters are obligatory intermediates in several key processes in which ATP is either used or regenerated. Thioesters are involved in the synthesis of all esters, including those found in complex lipids. The biosynthesis of lignin, which comprises a large fraction of biomass, proceeds via thioester derivative of caffeic acid.[202] Acetyl CoA is an important molecule in metabolism. The chemical structure of Acetyl CoA includes a thioester between coenzyme A (a thiol) and acetic acid which is produced during the second step of aerobic cellular respiration in Krebs cycle. The C-terminal peptides or protein thioesters are essential in NCL. The synthetic thioester preparation is generally carried out via conventional carboxyl activation chemistry rather than the N→S route so elegantly directed by intein. Thioesters can also be prepared via ter-butyloxycarbonyl (Boc)-based solid-phase peptide synthesis (SPPS) on a thioester resin or 9-fluorenylmethoxycarbonyl (Fmoc)-based SPPS which involves mild bases during synthesis.[203] Melnyk and co-workers *(2011)* reported a solid-phase *N→S* acyl transfer for thioester synthesis after peptide chain assembly using Fmoc/*t*-Bu chemistry in combination with the sulfonamide safety-catch linker.[204] Once, thioester is synthesized that can easily be subjected to NCL reaction at physiological conditions. Since the beginning of thioester mediated NCL reaction, it is being exploited for total synthesis of proteins or peptides and dendrimers[205] and is combined with peptide self-assembly. Recently, NCL reaction has attracted wide research group for the development of functional biomaterials.

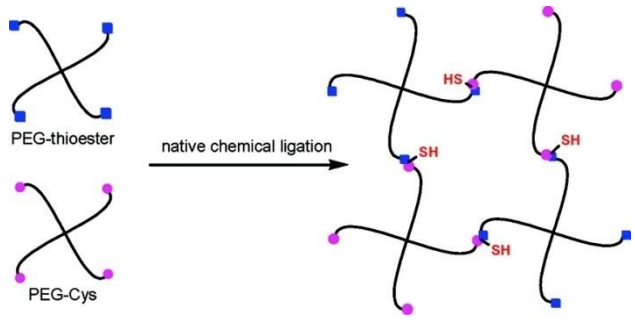

Figure 1.27. *Native chemical ligation is used in cross-linking of hydrogel.*

Woolfson *et al. (2007)* described the combination of chemical ligation with peptide self-assembly to deliver extremely long polypeptide chains with stipulated, repeated sequences. The self-assembling fibers were used to align peptide from their N to C-terminals which facilitate the liagtion reaction without usual requirement of N-terminal catalytic cysteine residue.[206] Collier and co-workers *(2008)* investigated a novel method for rapidly increasing the stiffness of self-assembled β-sheet fibrillar peptide hydrogels using native chemical ligation (NCL)[207] (Figure 1.27). Messersmith *et al.* (2009) illustrated the use of NCL as a strategy to form covalently cross-linked polymer hydrogels under mild conditions and in the absence of catalysts.[208] The thioester based polymer and N-terminal cysteine polymer bioconjugate were synthesized to bring up hydrolgelation by native chemical ligation reaction and viscoelastic nature of hydrogel was studied by oscillatory rheology.

1.8.2 Oxo-ester Mediated Native Chemical Ligation

Amino acid and peptide oxo-esters have played an important role in peptide chemistry for many years. Various amino acid esters are commonly used as protecting groups for peptide synthesis in conventional solution phase methodology. Moreover, activated phenyl ester derivatives have been used for chemical ligation of peptides. Several modifications of thioester mediated NCL reaction have been made in an effort to expand

the utility of the method. Danishefsky and co-workers *(2004)* first reported the use of oxo-ester in NCL reactions through indirect approach involving *o*-thiophenolic ester[209] which was followed later by a direct approach utilizing *p*-nitrophenyl (*p*NP) activated C-terminal ester (Figure 1.28). The oxo-ester mediated native chemical ligation reactions were successfully carried out with sterically hindered C-terminal amino acids which is rather problematic with thioester mediated NCL. Hackeng et al. *(1999)* observed that *β*-branched amino acids such as Thr, Val and Ile in this position react extremely slow under standard NCL reaction conditions (>48 h).[210] Long NCL reaction times are generally discouraged, due to potential side-reactions (thioester hydrolysis, desulfurization of cysteine and methionine oxidation)[211] under the NCL conditions employed. Moreover, proline in this position was found to react even more sluggishly with, at best, conversions of around 20% after 48 h.[212,213] However, the *p*-nitrophenol oxo-esters are more labile acyl donor than thioester in NCL reactions.

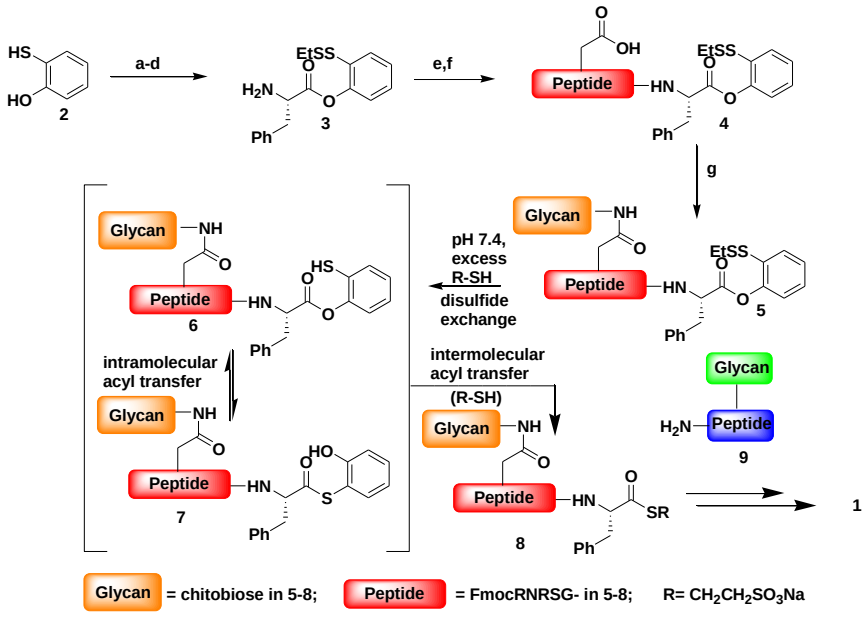

Figure 1.28. *Oxo-ester mediated native chemical ligation, reagents and conditions: (a) I_2, MeOH, H_2O; (b) BF_3-OEt_2, EtSSEt,CH_2Cl_2, 99%, 2 steps; (c) Boc-Phe-OH, EDCI, DMAP, CH_2Cl_2/THF, 93%; (d) 4 N HCl/dioxane, 94%; (e) Fmoc-Arg(Pbf)-Asp(tBu)-Arg(Pbf)-Ser(tBu)-Gly-OH, HATU, DIEA, DMF, 61%; (f) TFA/phenol/Et_3SiH/H_2O, 35:2:1:1, 60%; (g) GlcNAcβ1→4GlcNAcβ1-NH_2, HATU, DIEA, DMSO, 52%.*

Synthesis of *p*-nitrophenol ester is easy and less problematic. Weissenborn *et al. (2012)* described oxo-ester mediated NCL on oxo-ester activated surfaces and found that 2,3,4,5,6-pentafluorophenyl (PFP) is more efficient acyl donor than than *p*-nitrophenol and N-hydroxysuccinimide (NHS) activating agents.[214] Liu and co-workers *(2010)* reported a simple and less activated phenyl oxo-ester of peptide for chemoselective NCL reactions.[215] Borner *et al. (2006)* investigated peptide guided assembly of PEO-peptide conjugate via intramolecular O→N acyl transfer to restore native amide bond.[216] Messersmith *et al. (2013)* described polymer hydrogel formation *via* oxo-ester mediated NCL between branched polymer precursors containing NHS activated ester and N-terminal cysteine group and showed cytocompatibility and *in vivo* acute inflammatory response[217](figure 1.29).

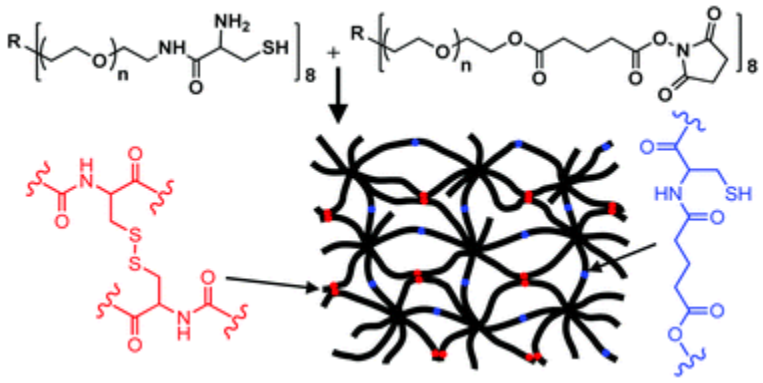

Figure 1.29. *Peptide self-assembly via oxo-ester mediated native chemical ligation*

1.8.3 Selenoester Mediated Native Chemical Ligation

Over the past decades, selenium and organoselenium compounds are gaining increasing attention due to their properties as antioxidant and antitumor agents, as apoptosis inducers, and in the effective chemoprevention of cancer in a variety of organs.[218,219,220,221,222] Selenoesters are important intermediates in several organic

transformations. The compounds in this class have been used as precursors of acyl radicals[223,224,225] and anions[226] and have attracted attention for the synthesis of new molecular materials, especially superconducting materials, liquid crystals and self-assembled biomaterials. The hydrolysis of selenoesters subsequently generates ionic species of selenium (such as selenols) which can readily participate in redox processes. These charged seleno compounds may possess inherent biological activity, and it would be beneficial if they could enhance the cytotoxic impact on cancer cells. In case of aryl selenoester, the magnitude of selenoesters hydrolysis as well as its expected biological activity can be tuned by the placement of different substituent on the aryl ring. The synthesis of selenoesters can be achieved by solution phase methodology as well as Boc solid phase peptide synthesis in peptide chemistry. Durek et al. *(2011)* reported solution phase method for selenoester synthesis, in which unprotected peptide thioesters were converted to selenoacids by treatment with NaHSe at pH 7 followed by alkylation with alkyl halides at pH 4 to yield the corresponding selenoesters.[190] However, in solid phase peptide synthesis, the starting pre-loaded Ile-OCH_2-PAM-resin, 3-bromo- or 3-iodopropionic acid was coupled by using symmetric anhydride conditions and dicyclohexylcarbodiimide (DCC). The mixture of (Li_2Se_2) was used to selenate the halogenated resin under inert conditions. Diselenides were reduced with 1,4-dithiothreitol (DTT) in DMF and the selenol acylated with the first Boc-protected amino acid building block using standard SPPS protocols with an extended coupling time (1 h).[227] The completed peptide selenoester was cleaved from the resin with concomitant side chain deprotection using HF/*p*-cresol (9:1 (v/v)) at - 5 ^{o}C. The reactivity of selenoesters was found higher than the comparable thioesters towards thiol nucleophiles in the first transesterification step of NCL. Therefore, selenoesters have been expanded to the synthesis of proteins by chemical ligation of chalcogenol esters,[228,229] to the synthesis of substrates which

undergo facile and efficient radical decarbonylation, as well as to the synthesis of the natural alkaloid (+)-geissoschizine.[230]

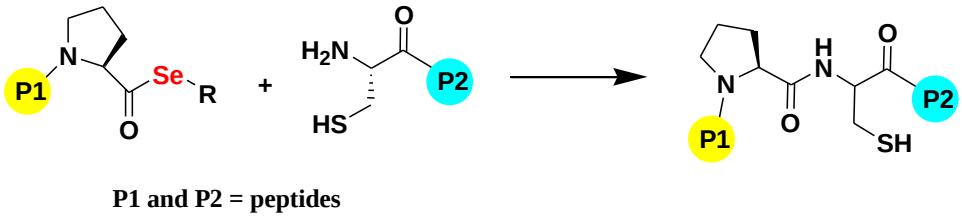

P1 and P2 = peptides

Figure 1.30. *Seleno-ester mediated native chemical ligation.*

Durek and coworkers first reported the utility of selenoester in NCL reactions (Figure 1.30). However, their utility and potential in the peptide self-assembly via selenoester mediated native chemical ligation reaction has not been investigated.

1.9 Applications of Peptide Self-assembly

There are many applications in the biomedical field where self-assembled peptide nanostructures could play an important role as part of biosensing platforms, as efficient drug-delivery systems, cell cultures or as a hydrogels for tissue reparation. This section presents the advantages of such biomaterials.

1.9.1 Antimicrobial Activities

There is increasing demand to develop new antimicrobial agents due to the increasing resistance of microbes against conventional antibiotics. Like some of the traditional antibiotics, the short cationic antimicrobial peptides kill the microbes by interacting and disrupting bacterial cell membranes. Effectiveness of antimicrobial activity depends on the cationic charges and the hydrophobicity of peptides.[231] These varying extent of antimicrobial activities are supported by evident permeation and disruption to the

bacterial membranes.[232] Shai and coworkers investigated the influence of PAs (palmitoyl) containing cationic K-based di- and tri-peptides on antimicrobial and antifungal activity using a range of Gram-negative and Gram-positive bacteria, and two fungal strains[233] (Figure 1.31). The amphiphilic peptides self-assemble into micelles and were shown to be effective against S. aureus infection in mice and rabbits. In the latter case, transport across the blood-brain barrier and reduction of bacterial growth in infected brains were demonstrated.[234] Mitra *et al*. studied lipopeptide-based molecules with proline (P), phenylalanine (F) or tryptophan (W) as part of the head groups and C_{14} as tails. These lipopeptides showed remarkable growth inhibition activity on both Gram-positive and Gram-negative bacteria and fungus. In addition, they have good biocompatibility to different mammalian cell lines like HepG2, HeLa and SiHa.[235]

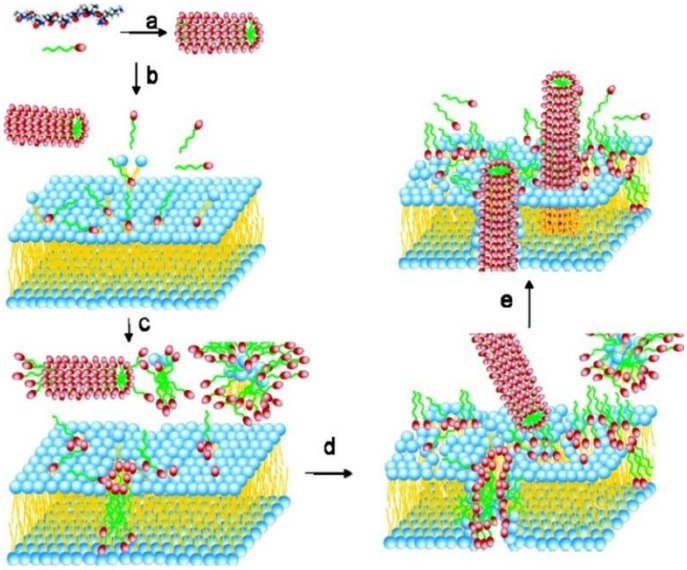

Figure 1.31. *Schematic illustration of mechanisms of action adopted by A9K for the bacterial membrane permeation and disruption. The red rods represent A9K nanorods. The A9K molecules assemble into nanorods with the positive charges outside (step a). The monomers may also flap on and become inserted into the outer membrane surface (step b). They can then flip and become inserted into the inner leaf of the membrane, forming a ''through barrel'' or micelle to cause leakage or lysis (step c). Nanorods formed may also attack cell membrane through electrostatic attraction or local hydrophobic affinity, lifting some lipids out of the membrane and making the membrane unstable, causing the nanorods to flop into the membrane bilayer (step d and e).*

1.9.2 Cell Culture

The self-assembled architectures in associated gel networks and antimicrobial activities of peptide amphiphiles make them potential candidates as cell culture matrices or scaffolds in tissue engineering and regenerative medicine. Extensive study of these self-assembled biomaterials has already proved their biocompatibility.[236] Self-assembly of amphiphilic peptides bearing N-terminal hydrophobic aromatic moiety has been used in cell cultures by several groups. The Fmoc-based dipeptide, tripepeptide are regularly used by several groups as scaffold in cell cultures.

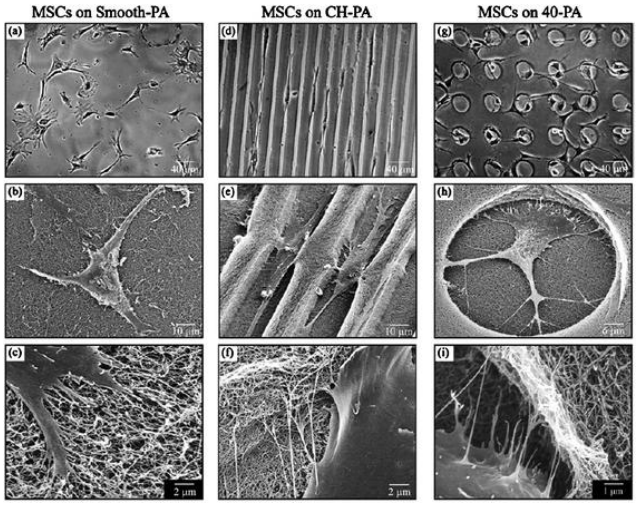

Figure 1.32. *Morphological characteristics of cells on various peptide amphiphile (PA) substrates. (a-c) Cells on smooth peptide amphiphile exhibited broad flattened shape with randomly oriented processes. (d-f) In contrast, hMSCs on CH-PA (10 mm wide channels separated by 20 mm distances) exhibited narrower cell bodies that aligned along the microchannel axis while (g-i) those growing on 40-PA (surfaces with 8 mm deep holes that were 40 mm in diameter, and 8 mm high) tended to migrate and spread inside the 40 mm diameter holes. On all substrates, hMSCs interacted with the PA nanofiber bundles (c, f, i), which were especially evident along the vertical geometries of the channels (f) and holes (i).*

A simple peptide Fmoc-RGD mimicking the extracellular matrix (ECM) has recently been reported, where Fmoc as a hydrophobic moiety was linked to the tri-peptide sequence RGD forming an elegant peptide

amphiphile. These molecules self-assembled into nanofibers and bioactive hydrogels through π-π stacking of the Fmoc groups, leaving the RGD groups outside the nanofiber surfaces. The self-assembled hydrogels displayed excellent performance in 3D cell culture using human adult dermal fibroblast cells.[237] Peptide amphiphiles have shown potential application to create 3D microscale topographical patterns to study the behaviour of human mesenchymal stem cells (hMSCs)[238] (Figure 1.32). In vivo delivery of luciferase-expressing cells using the binary lipopeptide nanofiber system into the mouse model revealed the enhanced viability and proliferation of associated bone marrow derived stem and progenitor cells. Lipopeptides with branched head groups containing Arg-Gly-Asp-Ser (RGDS) also showed excellent performance as scaffolds for the growth of human bladder smooth muscle cells.[239] Nguyen *et al. (2013)* reported a peptide hydrogel that shows superior physiological properties as an in vitro matrix for 3D cell culture. Human epithelial cancer cells, MCF-7, are encapsulated homogeneously in the hydrogel matrix during hydrogelation. Compared with two-dimensional (2D) monolayer culture, cells residing in the hydrogel matrix grow as tumor-like clusters in 3D formation. Relevant parameters related to cell morphology, survival, proliferation, and apoptosis were analyzed using MCF-7 cells in 3D hydrogels.[240] Inetersetingly, upon treatment with cisplatin, an anti-cancer drug, can cause a significant decrease of cell viability of MCF-7 clusters in hydrogels. These results provided evidence that this peptide hydrogel is a promising 3D cell culture material for drug testing.

1.9.3 Drug Delivery System

Supramolecular self-assembly of rationally designed peptidic sequences is emerging as a promising route to novel biofunctional materials. The biocompatibility and immunogenicity of these self-assembled nanostructures will bring important information that will define the possibility to use this biomaterial in applications such as drug-delivery

systems or tissue reparation in humans. Several groups have reported that molecular hydrogels have been widely used as carriers for the delivery of therapeutic agents.[241,242,243,244] There are two ways for delivery of therapeutic agent. One can either physically entraps the drug in the matrix of self-assembled hydrogel or covalently links to hydrogelators via hydrolysable bonds.[245,246,247] These encapsulated therapeutic agent can be released from the matrix of hydrogel by hydrolysis of this hydrolysable bond or enzymatic degradation of the gel.[248] Besides the self-assembled hydrogels as carriers in drug delivery system, focus has been given to the development of molecular hydrogel of therapeutic agent as 'self-delivery'.[249] Yang and coworkers developed molecular hydrogel of a hydrophobic therapeutic agent such as taxol. The original drug molecules can be released upon ester bond hydrolysis.

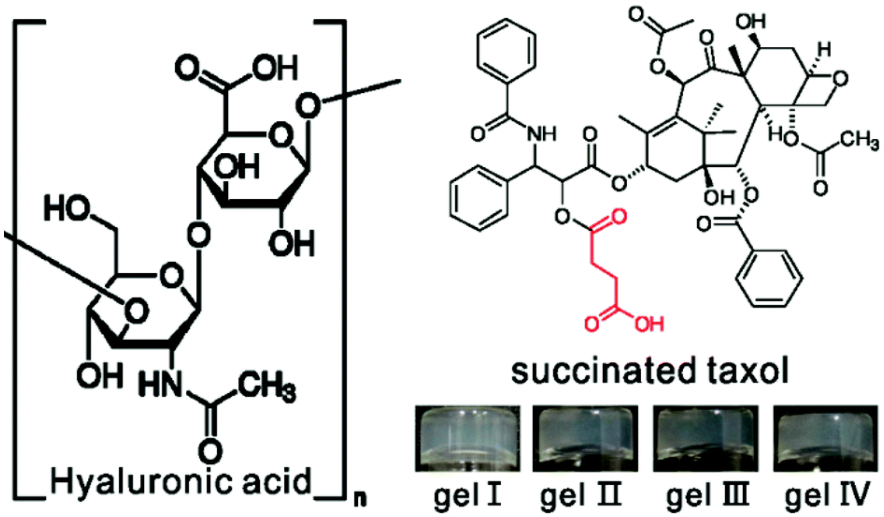

Figure 1.33. *Chemical structures of succinated taxol and hyaluronic acid and optical images of the hydrogels in PBS solution (pH = 7.4) containing 1 wt% of the succinated taxol (gel I: without HA, gel II–IV: with 0.1, 0.3, 0.6 wt% of HA, respectively).*

Yang group *(2013)* covalently coupled the taxol molecule to succinic acid which formed self-supporting hydrogel upon sonication[250] (figure 1.33). The release profile of anti-cancer drug from gel was monitored at 37 °C. All hydrogels released succinated taxol during the 24 h experimental time. Both gel I and gel II exhibited similar release behaviors and there were

about 1.48 and 1.58% of succinated taxol being released from gel I and gel II over 24 hours, respectively. Gel III and gel IV with more than 3 mg mL^{-1} of HA possessed slightly slower release profiles, and there were about 1.27 and 1.15% of succinated taxol being released from gel III and gel IV over 24 hours, respectively. There were no burst releases for four gels, suggesting its good potential for long term release of anti-cancer drugs for cancer therapy.

1.9.4 Wound Healing, Skin Care and Cosmetics

Short peptide amphiphiles are able to self-assemble into complex fibrous structures in water. These architectures can retain more than 99.9% of water and possess sufficiently strong mechanical strengths for the use as biological scaffolds. Self-assembling peptide (SAP) nanofiber scaffold combined with epidermal growth factors (EGFs) could serve as a bioactive wound dressing. These scaffolds closely mimic the structure and porosity of extracellular matrices in that growth factors and nutrients freely diffuse in and out of the scaffold at very slow rates. Egles *et al*. (2008) used wounded HSEs to study the capacity of SAP scaffolds that are combined with EGF, to modulate the wound healing rate in tissues that closely mimic the human wound response in vivo.[251] Peptide amphiphiles can not only act as surfactants, but they also have inherent biological functions such as anti-wrinkle, antimicrobial activities, and can be directly used as nutrients. They have great potential for cosmetic applications.[252] Palmitoyl pentapeptide-3 or 4 (Matrixyl) is a typical lipopeptide with a C_{16} acyl chain as tail and a peptide sequence KTTKS as head. The short peptide is a structural mimic of part of the sequence of collagen type I. The attachment of the fatty acid tail clearly enhances its oil solubility and improves skin penetration. The peptide sequence, when used in the culture of fibroblast cells, stimulates the synthesis of the key constituents of the skin matrix such as collagen, elastin and glucosaminoglycans. Although the exact mechanism is not well understood, the lipopeptide has been used

in a variety of anti-aging products and has exhibited effectiveness against wrinkles with no skin irritation. C_{16}-GHK is another important component of matrixyl^{TM} 3000 which can presumably stimulate skin matrix replenishment and reduce wrinkles.[253]

1.9.5 Templates for Nanofabrication

Molecular self-assembly offers new routes for the fabrication of nanomaterials. However, self-assembling peptide amphiphiles have sought great potential as templates for nanofabrication such as biomineralization, nucleation, nanowires, nanocircuits.[254] The self-assembled nanofibers have also been used as templates for the nucleation and growth of CdS nanocrystals.[255] Cui and Liu, *(2013)* reported a new approach that combines electron-induced molecular self-assembly with simultaneous nanoparticle formation by room temperature electron reduction to develop peptide thin films with highly dispersed noble metal nanoparticles.[256] Gazit *et al*. *(2003)* reported self-assembly of very short peptide, Alzheimer's β-amyloid diphenylalanine structural motif, into descrete and stiff nanotubes. Nanotublar structures formed by self-assembling peptide were further exploited in the fabrication of silver nanowires (Figure 1.34).

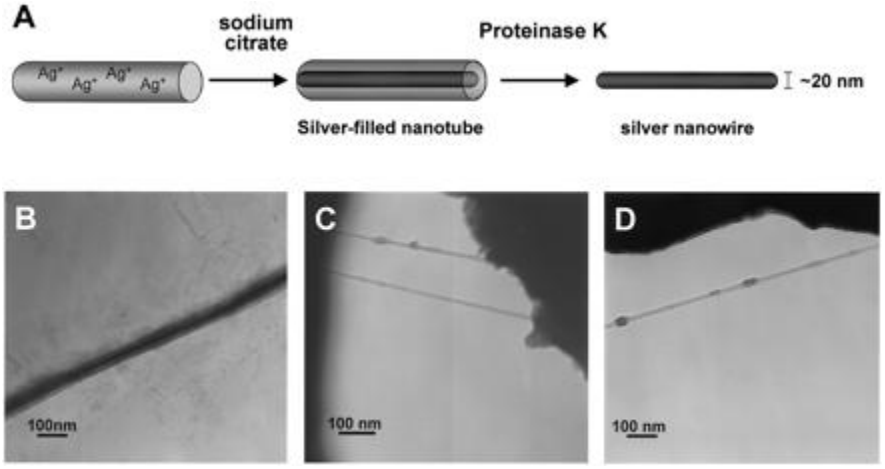

Figure 1.34. *Casting of silver nanowiers with the peptide nanotubes. A) The nanowires were formed by reduction of silver ions within the tubes, followed by enzymatic degradation of the peptde mold. B) TEM analysis nanotubes filled with silver nanowires. (C and D) nanowires upon enzymatic degradation of the peptide mold.*

The reduction of ionic silver within the nanotubes, followed by enzymatic degradation of peptide backbone leads to formation of long persistent nanowires.[257] Therefore, such fabrication may have applications in supramolecular electronics. Peptide bolaamphiphiles self-assembly have been used for the synthesis and stabilization of palladium nanoparticle under physiological conditions. The catalytic activity of these peptide-nanofiber-supported Pd nanoparticles have used for the removal of N-terminus protecting groups of amino acids and peptides.[258]

1.10 Organization of the Thesis

The initial aim of this project was to explore different chemical strategies to drive the peptide self-assembly for further applications in nanosciences and biomedicine. This was to be achieved by synthesizing various Nmoc-protected peptides and Nmoc-protected active esters. The peptide self-assembly of Nmoc-protected peptides was to be achieved by enzyme catalyzed chemical reactions while self-assembly of Nmoc-protected ester was to be carried out by chemoselective native chemical ligation reactions.

Chapter 2: This chapter includes materials and experimental techniques which weres used in this thesis.

Chapter 3: Native chemical ligation is the most widely used method in protein synthesis. In this chapter, we have exploited simple and efficient method for peptide self-assembly. Our intention was to exploit oxo-ester mediated native chemical ligation in peptide coupling and subsequent formation of self-assembled peptide nanostructures.

Chapter 4: In this chapter, Nmoc-protected-selenoesters were synthesized to *in situ* generation of redox active peptides via native chemical ligation.

Chapter 5: In this chapter, we have exploited enzymatic peptide hydrolysis reaction in order to achieve a single predominating product from the dynamic peptide libraries via self-assembly.

Chapter 6: Lipase catalyzed chemical reaction was used to include gastrodigenin for the evolution of blue light emitting peptide nanofibers.

1.11 References

1. Whitesides G. M., Mathias J. P., Seto C. T. (1991), Molecular self-assembly and nanochemistry: a chemical strategy for the synthesis of nanostructures, *Science*, 254, 1312-1319 (DOI: 10.1126/science.1962191)
2. Yanagawa H., Kojima K., Ito M., Handa N. (1990), Synthesis of polypeptides by microwave heating I. Formation of polypeptides during repeated hydration-dehydration cycles and their characterization, *J. Mol. Evol*., 31, 180-186.
3. Ito M., Handa N., Yanagawa H. (1990), Synthesis of polypeptides by microwave heating II. Function of polypeptides synthesized during repeated hydration-dehydration cycles, *J. Mol. Evol*. 31, 187-194.
4. Lee D. H., Granja J. R., Martinez J. A., Severin K., Ghadiri M. R. (1996), A self-replicating peptide, *Nature*, 382, 525-528 (DOI:10.1038/382525a0).
5. Timpl R., Brown J. C. (1996), Supramolecular assembly of basement membranes, *Bioessays*, 18, 123-132 (DOI: 10.1002/bies.950180208).
6. Schnur J. M. (1993), Lipid tubules: A paradigm for molecularly engineered structures, *Science*, 262, 1669-1676 (DOI: 10.1126/science.262.5140.1669).

7. Qi S. Y., Groves J. T., Chakraborty A. K., (2001), Synaptic pattern formation during cellular recognition, *Proc. Natl. Acad. Sci. U.S.A.* 98, 6548-6553 (DOI: 10.1073/pnas.111536798).
8. Lodish H., Berk A., Matsudaira P., Kaiser C. A., Krieger M., Scott M. P., Zipursky S. L., Darnell J. (2003), *Molecular Cell Biology*, Fifth ed. Freeman, New York.
9. Conde C., Caceres A. (2009), Microtubule assembly, organization and dynamics in axons and dendrites, *Nat. Rev. Neur.*, 10, 319-332 (DOI:10.1038/nrn2631).
10. Li H., Carter J. D., LaBean T. H., (2009), Nanofabrication by DNA self-assembly, *Materials Today*, 12, 24-32.
11. Seeman N. C. (2003), Double helix, *Nature*, 421 (6921), 427 (DOI:10.1038/nature01406).
12. Seeman N. C. (2007), An overview of structural DNA nanotechnology, *Mol. Biotechnol*., 37, 246-257 (DOI:10.1007/s12033-007-0059-4).
13. Aldaye F. A., Palmer A. L., Sleiman H. F. (2008), Assembling materials with DNA as the guide, *Science*, 321, 1795-1799 (DOI: 10.1126/science.1154533).
14. Gothelf K. V., LaBean, T. H. (2005), DNA-programmed assembly of nanostructures, *Org. Biomol. Chem.*, 3, 4023-4037 (DOI: 10.1039/B510551J).
15. LaBean T. H., Li H. (2007), Constructing novel materials with DNA, *Nano Today*, 2, 26-35.
16. Seeman N. C. (2010), Nanomaterials based on DNA, *Annu. Rev. Biochem.*, 79, 65-87 (DOI: 10.1146/annurev-biochem-060308-102244).
17. Bath J., Turberfield, A. J. (2007), DNA nanomachines *Nat. Nanotechnol.*, 2, 275-284 (DOI:10.1038/nnano.2007.104).

18. Drmanac R., Sparks A. B. (2010), Human genome sequencing using unchained base reads on self-assembling DNA nanoarrays, *Science,* 327, 78-81 (DOI: 10.1126/science.1181498).
19. Genereux J. C., Barton J. K. (2009), Mechanisms for DNA charge transport, *Chem. Rev*., 110, 1642-1662 (DOI: 10.1021/cr900228f).
20. McManus S. A., Li Y. (2013), Turning a kinase deoxyribozyme into a sensor, *J. Am. Chem. Soc.,* 135, 7181-7186 (DOI: 10.1021/ja311850u).
21. Miller S. L., (1953), A production of amino acids under possible primitive earth conditions, *Science,* 117, 528-529 (DOI: 10.1126/science.117.3046.528).
22. Brack A. (2007), From interstellar amino acids to prebiotic catalytic peptides, *A Review, Chemistry & Biodiversity,* 4, 665-679 (DOI: 10.1002/cbdv.200790057).
23. Bar-Nun A., Bar-Nun N., Bauer S. H., Sagan C. (1970), Shock synthesis of amino acids in simulated primitive environments, *Science,* 168, 470-473.
24. Goldman N., Reed E. J., Fried L. E., Kuo I.-F. W., Maiti, A. (2010), Synthesis of glycine-containing complexes in impacts of comets on early Earth, *Nat. Chem.*, 2, 949-954 (DOI:10.1038/nchem.827).
25. Webber M. J., Newcomb C. J., Bitton R., Stupp S. I. (2011), Switching of self-assembly in a peptide nanostructure with a specific enzyme, *Soft Matter*, 7, 9665-9672 (DOI:10.1039/c1sm05610g).
26. Wang J.-X., Lei Q., Luo G.-F., Cai T.-T., Li J. L., Cheng S. X., Zhuo R. X., Zhang X.-Z. (2013), Controlled arrays of self-assembled peptide nanostructures in solution and at interface, *Langmuir*, 29, 6996-7004 (DOI: 10.1021/la4010714.).
27. Adler-Abramovich L., Aronov D., Gazit E., Rosenman G. (2009), Patterned arrays of ordered peptide nanostructures, *J. Nanosci. Nanotechnol.,* 9, 1701-1708 (DOI: 10.1166/jnn.2009.SI02).

28. Azuri I., Adler-Abramovich L., Gazit E., Hod O., Kronik L., (2014), Why are diphenylalanine-based peptide nanostructures so rigid? Insights from first principles calculations, *J. Am. Chem. Soc.*, 136, 963-969 (DOI: 10.1021/ja408713x.).

29. Nettleton E. J., Tito P., Sunde M., Bouchard M., Dobson C. M, Robinson C. V. (2000), Characterization of the oligomeric states of insulin in self-assembly and amyloid fibril formation by mass spectrometry, *Biophysical Journal*, 79, 1053-1065.

30. Dzwolak W., Anna Loksztejn L., Smirnovas V. (2006), New insights into the self-assembly of insulin amyloid fibrils: An H-D exchange FT-IR study, *Biochemistry*, 45, 8143-8151 (DOI: 10.1021/bi060341a).

31. Adams M. J., Bludell T. L., Dodson E. J., Dodson G. G., Vijayan M., Baker E. N., Harding M. M., Hodgkin D. C., Rimmer B., Sheat S. (1969), Structure of rhombohedral 2-zinc insulin crystals, *Nature*, 224, 491-495 (DOI: 10.1038/224491a0).

32. Munch H. K., Heide S. T., Christensen N. J., Hoeg-Jensen T., Thulstrup P. W., Jensen K. J., (2011), Controlled self-assembly of re-engineered insulin by Fe(II), *Chem. Eur. J.*, 17, 7198-7204 (DOI: 10.1002/chem.201100495).

33. Lynch M. (2005), Simple evolutionary pathways to complex proteins, *Protein Sci.*, 14, 2217-2225 (DOI:10.1110/ps.041171805).

34. Dobson M. J., Pearlman R. E., Karaiskakis A., Spyropoulos B., Moens P. B. (1994), Synaptonemal complex proteins: occurrence, epitope mapping and chromosome disjunction, *J Cell Sci.*, 10, 2749-2760.

35. Lehningr A. L. (1986), *Principles of Biochemistry*, First Ed. Chapter, 8, worth Publishers, Inc. USA.

36. Lodish H., Berk A., Zipursky S. L. *et al*. (2000), *Molecular Cell Biology*. Fourth Ed. W. H. Freeman, New York.

37. Chapman J. A., Tzaphlidou M., Meek K. M., Kadler K. E. (1990), The collagen fibril- a model system for studying the staining and fixation of a protein, *Electron Microsc. Rev*., 3,143-182.

38. Kadler K. E., Holmes D. F., Trotter J. A., Chapman J. A. (1996), Collagen fibril formation, *Biochem. J.*, 316, 1-11.

39. Forood B., Feliciano E. J., Nambiar K. P. (1993), Stabilization of α-helical structures in short peptides via end capping, *Proc. Natl. Acad. Sci. USA*, 90, 838-842 (DOI: 10.1073/pnas.90.3.838).

40. Seebach D., Ciceri P. E., Overhand M., Jaun B., Rigo D., Oberer L., Hommel U., Amstutz R., Widmer, H. (1996), Probing the helical secondary structure of short-chain β-peptides, *Helvetica Chimica Acta*, 79, 2043-2066 (DOI: 10.1002/hlca.19960790802).

41. Pannuzzo M., Raudino A., Milardi D., La Rosa C., Karttunen M. (2013), α-Helical structures drive early stages of self-assembly of amyloidogenic amyloid polypeptide aggregate formation in membranes, *Sci. Rep.*, 3, 2781-2791 (DOI: 10.1038/srep02781).

42. Pauling L., Corey R. B. (1951), Configurations of polypeptide chains with favoured orientations around single bonds: Two new pleated sheets, *Proc. Natl. Acad. Sci. U.S.A*, 37, 729-740 (PMCID: PMC1063460).

43. Salemme F. R., (1983), Structural properties of protein β-sheets, *Biophysics & Molecular Biology*, 42, 95-133 (DOI:10.1016/0079-6107(83)90005-6).

44. Ramachandran G. N., Ramakrishnan C., Sasisekharan V. (1963), Stereochemistry of polypeptide chain configurations, *J. Mol. Biol*., 7, 95-99 (DOI:10.1016/S0022-2836(63)80023-6).

45. Gunasekaran K., Ramakrishnan C., Balaram P. (1996), Disallowed ramachandran conformations of amino acid residues in protein

structures, *J. Mol. Biol.*, 264, 191-198 (DOI:10.1006/jmbi.1996.0633).

46. Hollingsworth S. A., Karplus P. A. (2010), A fresh look at the Ramachandran plot and the occurrence of standard structures in proteins, *Biomol. Concepts*, 1, 271-283 (DOI: 10.1515/bmc.2010.022).

47. Mandel N., Mandel G., Trus B. L., Rosenberg J., Carlson G., Dickerson R. E. (1977), Tuna cytochrome c at 2.0 Å resolution, *J. Biol. Chem.*, 252, 4619-4636.

48. Pal, D., Chakrabarti P. (2002), On residues in the disallowed region of the Ramachandran map, *Biopolymers*, 63, 195-206 (DOI: 10.1002/bip.10051).

49. Lifson S., Sander C. (1979), Antiparallel and parallel β-strands differ in amino acid residue preferences, *Nature*, 282, 109-111 (DOI:10.1038/282109a0).

50. Hardy J., Selkoe D. J. (2002), The amyloid hypothesis of alzheimer's disease: Progress and problems on the road to therapeutics, *Science*, 297, 353-356 (DOI: 10.1126/science.1072994).

51. Cerf E., Sarroukh R., Tamamizu-Kato S., Breydo L., Derclaye S., Dufrêne Y. F., Narayanaswami V., Goormaghtigh E., Ruysschaert J.-M., Raussens V. (2009), Antiparallel β-sheet: A signature structure of the oligomeric amyloid β-peptide, *Biochem. J.*, 421, 415-423 (DOI:10.1042/BJ20090379).

52. Jones M. R., Osberg K. D., Macfarlane R. J., Langille M. R., Mirkin C. A. (2011), Templated techniques for the synthesis and assembly of plasmonic nanostructures, *Chem. Rev.*, 111, 3736-3827 (DOI: 10.1021/cr1004452).

53. Nogales E., Wolf S., Downing K. H. (1998), Structure of the α, β tubulin dimer by electron crystallography, *Nature*, 391, 199-203 (DOI:10.1038/34465).

54. Desai A., Mitchison T. (1997), Microtubule polymerization dynamics, *Annu. Rev. Cell Dev. Biol*. 13, 83-117.

55. Uhlenheuer D. A., Petkau K., Brunsveld L. (2010), Combining supramolecular chemistry with biology, *Chem. Soc. Rev*., 39, 2817-2826 (DOI: 10.1039/B820283B).

56. Collier J. H. (2008), Modular self-assembling biomaterials for directing cellular responses, *Soft Matter*, 4, 2310-2315 (DOI: 10.1039/B805563G).

57. Xu H., Song J., Tian T., Feng R. (2012), Estimation of organogel formation and influence of solvent viscosity and molecular size on gel properties and aggregate structures, *Soft Matter*, 8, 3478-3486 (DOI: 10.1039/C2SM07387K).

58. Dunna B., Zink J. (1991), Optical properties of sol-gel glasses doped with organic molecules, *J. Mater. Chem*., 1, 903-913 (DOI: 10.1039/JM9910100903).

59. Chen Q., Lv Y., Zhang D., Zhang G., Liu C., Zhu D. (2010) Cysteine and pH-responsive hydrogel based on a saccharide derivative with an aldehyde group, *Langmuir*, 26, 3165-3168 (DOI: 10.1021/la903102z).

60. Ajayaghosh A., Praveen V. K., Vijayakumar C. (2008), Organogels as scaffolds for excitation energy transfer and light harvesting *Chem. Soc. Rev.*, 37, 109-122 (DOI: 10.1039/B704456A).

61. George M., Weiss R. G. (2006), Molecular organogels soft matter comprised of low-molecular-mass organic gelators and organic liquids, *Acc. Chem. Res.* 39, 489-497 (DOI: 10.1021/ar0500923).

62. Koley P., Pramanik A. (2012), Multilayer vesicles, tubes, various porous structures and organo gels through the solvent-assisted self-

assembly of two modified tripeptidesand their different applications, *Soft Matter***,** 8**,** 5364-5374 (DOI: 10.1039/C2SM25205H).

63. Adhikari B., Banerjee A. (2011), Short peptide based hydrogels: incorporation of graphene into the hydrogel, *Soft Matter*, 7, 9259–9266 (DOI: 10.1039/c1sm06330h).

64. Roy S., Banerjee A. (2011), Amino acid based smart hydrogel: formation, characterization and fluorescence properties of silver nanoclusters within the hydrogel matrix, *Soft Matter*, 7, 5300-5308 (DOI: 10.1039/c1sm05034f).

65. Xu H., Das A. K., Horie M., Shaik M. S., Smith A. M., Luo Y., Lu X., Collins R., Liem S. Y., Song A., Popelier P. L. A., Turner M. L., Xiao P., Kinloch I. A., Ulijn R. V. (2010), An investigation of the conductivity of peptide nanotube networks prepared by enzyme-triggered self-assembly, *Nanoscale*, 2, 960-966 (DOI: 10.1039/B9NR00233B).

66. Ma D., Tu K., Zhang L. M. (2010), Bioactive supramolecular hydrogel with controlled dual drug release characteristics, *Biomacromolecules*, 11, 2204-2212 (DOI: 10.1021/bm100676a).

67. Naskar J., Palui G., Banerjee A. (2009), Tetrapeptide-based hydrogels: For incapsulation and slow release of an anticancer drug at physiological pH, *J. Phys. Chem. B*, 113, 11787-11792 (DOI: 10.1021/jp904251j).

68. Koley P., Gayen A., Drew M. G. B., Mukhopadhyay C., Pramanik A. (2012), Design and self-assembly of a leucine-enkephalin analogue in different nanostructures: application of nanovesicles, *Small*, 8, 984-990 (DOI: 10.1002/smll.201101685).

69. Wada A., Tamaru S., Ikeda M., Hamachi I. (2009), MCM-Enzyme-Supramolecular Hydrogel Hybrid as a Fluorescence Sensing Material for Polyanions of Biological Significance, *J. Am. Chem. Soc.*, 131, 5321-5330 (DOI: 10.1021/ja900500j).

70. Yemini M., Reches M., Rishpon J., Gazit E. (2005), Novel electrochemical biosensing platform using self-assembled peptide nanotubes, *Nano Lett.,* 5, 183-186 **(**DOI: 10.1021/nl0484189).

71. Lee K. Y., Mooney D. J. (2001), Hydrogels for tissue engineering, *Chem. Rev.,* 101, 1869-1880 (DOI: 10.1021/cr000108x).

72. Tsitsilianis C. (2010), Responsive reversible hydrogels from associative "smart" macromolecules, *Soft Matter*, 6, 2372-2388 (DOI: 10.1039/B923947B).

73. Zhao X. B., Pan F., Xu H., Yaseen M., Shan H., Hauser C. A. E., Zhang S., Lu J. R. (2010), Molecular self-assembly and applications of designer peptide amphiphiles, *Chem. Soc. Rev*., 39, 3480-3498 (DOI: 10.1039/b915923c).

74. Li J., Fan C., Pei H., Shi J., Huang Q. (2013), Smart drug delivery nanocarriers with self-assembled DNA nanostructures, *Adv. Mater.*, 25, 4386-4396 (DOI: 10.1002/adma.201300875).

75. Rahmawan Y., Xu L., Yang S. (2013), Self assembly of nanostructures towards transparent, superhydrophobic surfaces, *J. Mater. Chem. A***,** 1, 2955-2969 (DOI: 10.1039/C2TA00288D).

76. Berl V., Huc I., Khoury R. G., Krische M. J., Lehn J. M. (2000), Interconversion of single and double helices formed from synthetic molecular strands, *Nature*, 407, 720-723 (doi:10.1038/35037545).

77. Ramstrom O., Bunyapaiboonsri T., Lohmann S., Lehn J. M. (2002), Chemical biology of dynamic combinatorial libraries, *Biochim. Biophys. Acta*, 1572, 178-186.

78. Mercuri F., Baldoniab M., Sgamellottia A. (2012), Towards nano-organic chemistry: perspectives for a bottom-up approach to the synthesis of low-dimensional carbon nanostructures, *Nanoscale,* 4, 369-379 (DOI: 10.1039/C1NR11112D).

79. Zhang S. (2003), Fabrication of novel biomaterials through molecular self-assembly, *Nat. Biotech.,* 21, 1171-1178 (PMID:14520402).

80. Wang Y., Xia Y. (2004), Bottom-up and top-down approaches to the synthesis of monodispersed spherical colloids of low melting-point metals, *Nano Lett.*, 4, 2047-2050 (DOI: 10.1021/nl048689j).

81. Velev O. D., Lenhoff A M. (2000), Colloidal crystals as templates for porous materials, *Curr. Opin. Colloid Interface Sci.* 5, 56-63 (DOI:10.1016/S1359-0294(00)00039-X).

82. Xia Y., Gates B., Yin Y., Lu Y. (2000), Monodispersed colloidal spheres: Old materials with new applications, *Adv. Mater.*, 12, 693-713(DOI: 10.1002/(SICI)1521-4095 (200005) 12:10<693:: AID-ADMA693>3.0.CO;2-J)

83. Sajisha V. S., Maitra U. (2013), Multi-component, self-assembled, functional soft materials, *Chemia*, 67, 44-50 (DOI: 10.2533/chimia.2013.44).

84. Ghadiri M. R., Granja J. R., Buehler L. K. (1994), Artificial transmembrane ion channels from self-assembling peptide nanotubes, *Nature*, 369, 301-304 (DOI:10.1038/369301a0).

85. Hamley I. W. (2007), Peptide fibrillization, Angew. *Chem. Int. Ed.*, 46, 8128-8147 (DOI: 10.1002/anie.200700861).

86. Ulijn R. V., Smith A. M. (2008), Designing peptide based nanomaterials, *Chem. Soc. Rev.*, 37, 664-675 (DOI: 10.1039/B609047H).

87. Li J. (2010), Self-assembled supramolecular hydrogels based on polymer-cyclodextrin inclusion complexes for drug delivery, *NPG Asia Materials*, 2, 112-118 (DOI:10.1038/asiamat.2010.84)

88. Chaterji S., Kwon K., Park K. (2007), Smart polymeric gels: redefining the limits of biomedical devices, *Prog. Polym. Sci.*, 32, 1083-1122.

89. Lee E., Kim B. (2011), Smart delivery system for cosmetic ingredients using pH-sensitive polymer hydrogel particles, Korean *J. Chem. Eng.* 28, 1347-1350.

90. Morales M. E., Gallardo V., Clarés B., García M. B., Ruiz M. A. (2009), Study and description of hydrogels and organogels as vehicles for cosmetic active ingredients, *J. Cosmet. Sci.*, 60, 627-636.

91. Roos A., Boron W. F. (1981), Intracellular pH, *Physiol. Rev*., 61, 296-434 (PMID:7012859).

92. Glynn S. A. Albanes D.(1994), Folate and cancer: a review of the literature, *Nutr. Cancer*, 22, 101-119 (PMID:14502840).

93. Tannock I. F., Rotin D. (1989), Acid pH in tumors and its potential for therapeutic exploitation, *Cancer Res.*, 49, 4373-4384 (PMID:2545340).

94. Lundberg P., Lynd N. A., Zhang Y., Zeng X., Krogstad D. V., Paffen T., Malkoch M., Nystromb A. M., Hawker C. J. (2013), pH-triggered self-assembly of biocompatible histamine-functionalized triblock copolymers, *Soft Matter*, 9, 82-89 (DOI: 10.1039/C2SM26996A).

95. Datar A., Balakrishnan K., Zang L. (2013), One-dimensional self-assembly of a water soluble perylene diimide molecule by pH triggered hydrogelation, *Chem. Commun.*, 49, 6894-6896 (DOI: 10.1039/C3CC43359E).

96. Ghosh A., Haverick M., Stump K., Yang X., Tweedle M. F., Goldberger J. E. (2012), Fine-tuning the pH trigger of self-assembly, *J. Am. Chem. Soc.*, 134, 3647-3650 (DOI: 10.1021/ja211113n).

97. Tena-Solsona M., Miravet J. F., Escuder B. (2014) Tetrapeptidic molecular hydrogels: Self-assembly and co-aggregation with amyloid fragment Ab1-40, *Chem. Eur. J.* 20, 1023-1031 (DOI: 10.1002/chem.201302651).

98. Castelletto V., Hamley I. W., Segarra-Maset M. D., Gumbau C. B., Miravet J. F., Escuder B., Seitsonen J., Ruokolainen J. (2014), Tuning chelation by the surfactant-like peptide A6H using predetermined pH values, *Biomacromolecules*, 15, 591-598 (DOI: 10.1021/bm401640j).

99. Salick D. A., Kretsinger J. K., Pochan D. J., Schneider J. P. (2007), Inherent antibacterial activity of a peptide-based β-hairpin hydrogel, *J. Am. Chem. Soc.*, 129, 14793-14799 (DOI:10.1021/ja076300z).

100. Deng C., Fang R., Guan Y., Jiang J., Lin C., Wang L. (2012), Sonication-induced self-assembly of flexible tris (ureidobenzyl) amine: from dimeric aggregates to supramolecular gels, *Chem. Commun.*, 48, 7973-7975 (DOI: 10.1039/C2CC33408A).

101. Maity I., Rasale D. B., Das A. K. (2012), Sonication induced peptide-appended bolaamphiphile hydrogels for *in situ* generation and catalytic activity of Pt nanoparticles, *Soft Matter*, 8, 5301-5308 (DOI: 10.1039/C2SM25126D).

102. Dou C., Li D., Gao H., Wang C., Zhang H., Wang Y. (2010), Sonication-induced molecular gels based on mono-cholesterol substituted quinacridone derivatives, *Langmuir*, 26, 2113-2118 (DOI: 10.1021/la902663z).

103. Dickinson J. M., Volpi E., Rasmussen B. B. (2013), Exercise and nutrition to target protein synthesis impairments in aging skeletal muscle aging and muscle protein anabolism, 41, 216- 223. 104) S. Zhang, *Nat. Biotech*., 12, 1171.

105. Ikeda M., Tanida T., Yoshii T., Hamachi I. (2011), Rational molecular design of stimulus-responsive supramolecular hydrogels based on dipeptides, *Adv. Mater.*, 23, 2819-2822 (DOI: 10.1002/adma.201004658).

106. Jewett J. C., Sletten E. M., Bertozzi C. R. (2010), Rapid Cu-free click chemistry with readily synthesized biarylazacyclooctynones, *J. Am. Chem. Soc.*, 132, 3688-3690 (DOI: 10.1021/ja100014q).

107. Changa P. V., Preschera J. A., Slettena E. M., Baskina J. M., Millera I. A., Agarda N. J., Loa A., Bertozzia C. R. (2010), Copper-free click chemistry in living animals, *Proc. Natl. Acad. Sci. U.S.A.*, 107**,** 1821-1826 (DOI: 10.1073/pnas.0911116107).

108. Yang Z., Xu B. (2004), A simple visual assay based on small molecule hydrogels for detectinginhibitors of enzymes, *Chem. Commun.*, 2424-2425 (DOI: 10.1039/B408897B).

109. Segarra-Maset M. D., Nebot V. J., Miravet J. F., and Escuder B. (2013), Control of molecular gelation by chemical stimuli, *Chem. Soc. Rev*, 42, 7086-7098 (DOI: 10.1039/c2cs35436e).

110. Bowerman C. J., Nilsson B. L. (2010), A reductive trigger for peptide self-assembly and hydrogelation, *J. Am. Chem. Soc*., 132, 9526-9527 (DOI: 10.1021/ja1025535).

111. Boekhoven J., Brizard A. M., Kowlgi K. N. K., Koper G. J. M., Eelkema R., van Esch J. H. (2010), Dissipative self-assembly of a molecular gelator by using a chemical fuel, *Angew. Chem. Int. Ed.*, 49, 4825-4828 (DOI: 10.1002/anie.201001511).

112. Miao X., Cao W., Zheng W., Wang J., Zhang X., Gao J., Yang C., Kong D., Xu H., Wang L., Yang Z. (2013), Switchable catalytic activity: selenium-containing peptides with redox-controllable self-assembly properties, *Angew. Chem. Int. Ed*., 52, 7781-7785 (DOI: 10.1002 / anie. 201303199).

113. Sreenivasachary N., Lehn J.-M. (2005), Gelation-driven component selection in the generation of constitutional dynamic hydrogels based on guanine-quartet formation, *Proc. Natl. Acad. Sci. U.S.A.*, 102, 5938-5943 (DOI: 10.1073/pnas.0501663102).

114. Liang G., Ren H., Rao J. (2010), A biocompatible condensation reaction for controlled assembly of nanostructures in living cells, *Nat. Chem.*, 2, 54-60 (DOI: 10.1038/nchem.480).

115. Sayyad A. S., Balakrishnan K., Ajayan P. M. (2011), Chemical reaction mediated self-assembly of PTCDA into nanofibers, *Nanoscale*, 3, 3605-3608 (DOI : 10. 1039/ C1NR 10579E).

116. Maity I., Rasale D. B., Das A. K. (2013), Exploiting a self-assembly driven dynamic nanostructured library, *RSC Adv.*, 3, 6395-6400 (DOI: 10.1039/c3ra22401e).

117. Carnall J. M. A., Waudby C. A., Belenguer A. M., Stuart M. C. A., Peyralans J. J. P., Otto S. (2010), Mechanosensitive self-replication driven by self-organization, *Science*, 327, 1502-1506 (DOI:10.1126/science.1182767).

118. Na N., Mu X., Liu Q., Wen J., Wang F., Ouyang J. (2013), Self-assembly of diphenylalanine peptides into microtubes with "turn on" fluorescence using an aggregation-induced emission molecule, *Chem. Commun.*, 49, 10076-10078 (DOI: 10.1039/c3cc45320k).

119. Kumaraswamy P., Lakshmanan R., Sethuraman S., Krishnan U. M. (2011), Self-assembly of peptides: influence of substrate, pH and medium on the formation of supramolecular assemblies, *Soft Matter*, 7, 2744-2745 (DOI: 10.1039/C0SM00897D).

120. Guo C., Luo Y., Zhou R. H., Wei G. H., (2012), Probing the self-assembly mechanism of diphenylalanine-based peptide nanovesicles and nanotubes, *ACS Nano*, 6, 3907-3918 (DOI: 10.1021/nn300015g).

121. Yan X., Su Y., Li J., Fruh J., Mçhwald H. (2011), Uniaxially oriented peptide crystals for active optical waveguiding, *Angew. Chem. Int. Ed.*, 50, 11186-11191 (DOI: 10.1002/anie.201103941).

122. Kim J. H., Lim S. Y., Nam D. H., Ryu J., Ku S. H., Park C. B. (2011), Self-assembled, photoluminescent peptide hydrogel as a versatile platform for enzyme-based optical biosensors,

Biosensors and Bioelectronics, 26, 1860-1865 (DOI:10.1016/j.bios.2010.01.026).

123. Zhu P., Yan X., Su Y., Yang Y., Li J. (2010), Solvent-induced structural transition of self-assembled dipeptide: From organogels to microcrystals, *Chem. Eur J.*, 16, 3176-3183 (DOI: 10.1002/ chem. 200902139).

124. Yan X. H., He Q., Wang K., Duan L., Cui y., Li J. B. (2007), Transition of cationic dipeptide nanotubes into vesicles and oligonucleotide delivery, *Angew. Chem., Int. Ed.,* 46, 2431-2434 (DOI: 10.1002/anie.200603387).

125. Mehler A., Reches M., Rechter M., Cohen S., Gazit E. (2006), Rigid self-assembled hydrogel composed of a modified aromatic dipeptide, *Adv. Mater.,* 18, 1365-1370 (DOI : 10. 1002/ adma. 200501765).

126. Chen C.-S., Xu X.-D., Li, R.-X., Zhuo S.-Y., Zhang X.-Z. (2013), Photo-switched self-assembly of a gemini α-helical peptide into supramolecular architectures, *Nanoscale*, 5, 6270-6274 (DOI: 10.1039/c3nr01967e).

127. Kim J. H., Lee M., Lee J. S, Park C. B. (2012), Self-assembled light-harvesting peptide nanotubes for mimicking natural photosynthesis, *Angew. Chem. Int. Ed.,* 51, 517-520 (DOI: 10.1002/anie.201103244).

128. Frkanec L., Jokic M., Makarevic J., Wolsperger K., Zinic M. (2002), Bis(PheOH) Maleic acid amide-fumaric acid amide photoizomerization induces microsphere-to-gel fiber morphological transition: The photoinduced gelation system, *J. Am. Chem. Soc*. 124, 9716-9717 (DOI: 10.1021/ja027189u).

129. Walsh C. (2001), Correction: Enabling the chemistry of life, *Nature*, 409, 226-231 (DOI:10.1038/35081124).

130. Purich D. L., Scaife R. M. (1988), Enzymatic modulation of cytoskeletal self-assembly: ADP ribosylation of microtubule protein components, *Enzyme Dynamics and Regulation*, 217-223.

131. Um S. H., Lee J. B., Park N., Kwon S. Y., Umbach C. C., Luo D. (2006), Enzyme-catalysed assembly of DNA hydrogel, *Nat. Mater*., 5, 797-801 (PMID: 16998469).

132. Yang Z., Xu B. (2006), Using enzymes to control molecular hydrogelatio *Adv. Mater.*, 18, 3043-3046 (DOI : 10. 1002 / adma. 200600400).

133. Peppas N. A., Sefton M. V. (2004), Molecular and cellular foundations of biomaterials, advances in chemical engineering, Elsevier, Amsterdam, The Netherlands 29.

134. Gao Y., Shi J., Yuan D., Xu B. (2012), Imaging enzyme-triggered self-assembly of small molecules inside live cells, *Nat. Commun.* 3, 1033 (DOI: 10.1038/ncomms 2040).

135. Praveen K. V. Jun L., George J. (2006), Enzyme catalysis: Tool to make and break amygdalin hydrogelators from renewable resources: A delivery model for hydrophobic drugs, *J. Am. Chem. Soc.*, 128, 8932-8938 (DOI: 10.1021/ja062650u).

136. Das A. K., Collins R., Ulijn R. V. (2008), Exploiting enzymatic (Reversed) hydrolysis in directed self-assembly of peptide nanostructures, *Small*, 4, 279-287 (DOI : 10. 1002 / smll. 200700889).

137. Das A. K., Hirstb A. R., Ulijn R. V. (2009), Evolving nanomaterials using enzyme-driven dynamic peptide libraries (eDPL), *Faraday Discuss.*, 143, 293-303 (DOI : 10. 1039/ B902065A).

138. Sadownik J. W., Ulijn R. V. (2010), Locking an oxidation-sensitive dynamic peptide system in the gel state, *Chem. Commun.*, 46, 3481-3483 (DOI: 10.1039/C001982H).

139. Hirst A. R., Roy S., Arora M., Das A. K., Hodson N., Murray P., Marshall S., Javid N., Sefcik J., Boekhoven J., van Esch J. H., Santabarbara S., Hunt N. T., Ulijn R. V. (2010), Biocatalytic induction of supramolecular order, *Nat. Chem.*, 2, 1089-1094 (DOI: 10.1038/NCHEM.861).

140. Roy S., Javid N., Sefcik J., Halling P. J., Ulijn R. V. (2012), Salt-induced control of supramolecular order in biocatalytic hydrogelation, *Langmuir*, 48, 16664-16670 (DOI: 10.1021/la303388s).

141. Guilbaud, J.-B., Rochas C., Miller A. F., Saiani A. (2013), effect of enzyme concentration of the morphology and properties of enzymatically triggered peptide hydrogel, *Biomacromolecules*, 14, 1403-1411 (DOI: 10.1021/bm4000663).

142. Robinson B. A., Tester J. W., (1990), Kinetics of alkaline hydrolysis of organic esters and amides in neutrally-buffered solution, Inter. *J. Chem. Kin.*, 22, 431-448 (DOI: 10.1002/kin.550220502).

143. Inglis A. S., Nicholls P. W., Roxburgh O. M. (1971), Hydrolysis of the peptide bond and amino acid modification with hydriodic acid, *Aust. J. Biol. Sci.*, 24, 1235-1240.

144. Rebecchi K. R., Go E. P., Xu L., Woodin C. L., Mure M., Desaire H. (2011), A general protease digestion procedure for optimal protein sequence coverage and post-translational modifications analysis of recombinant glycoproteins: application to the characterization of human lysyl oxidase-like 2 glycosylation, *Anal. Chem.*, 83, 8484-8491 (DOI: 10.1021/ac2017037).

145. Zhang J., Hao R., Huang L., Yao J., Chen X., Shao Z. (2011), Self-assembly of a peptide amphiphile based on hydrolysed Bombyx mori silk fibroin, *Chem. Commun*., 47, 10296-10298 (DOI: 10.1039/C1CC12633D).

146. Plunkett K. N., Berkowski K. L., Moore J. S. (2005), Chymotrypsin responsive hydrogel: Application of a disulfide exchange protocol for the preparation of methacrylamide containing peptides, *Biomacromolecules*, 6, 632-637 (DOI: 10.1021/bm049349v).

147. Li J. Y., Gao Y., Kuang Y., Shi J. F., Du X., Zhou J., Wang H. M., Yang Z., Xu B. (2013), Dephosphorylation of D-peptide derivatives to form biofunctional, supramolecular nanofibers/hydrogels and their potential applications for intracellular imaging and intratumoral chemotherapy, *J. Am. Chem. Soc.*, 135, 9907-9914 (DOI: 10.1021/ja404215g).

148. Toledano S., Williams R. J., Jayawarna V., Ulijn R. V. (2006), Enzyme-triggered self-assembly of peptide hydrogels via reversed hydrolysis, *J. Am. Chem. Soc.*, 128, 1070-1071 (DOI: 10.1021/ja056549l).

149. Williams R. J. Smith A. M., Collins R. Hodson N., Das A. K., Ulijn R. V. (2009), Enzyme-assisted self-assembly under thermodynamic control, *Nat. Nanotech.*, 4, 19-24 (DOI:10.1038/nnano.2008.378).

150. Wu Q., Soni P., Reetz M. T. (2013), Laboratory evolution of enantiocomplementary candida antarctica lipase B mutants with broad substrate scope, *J. Am. Chem. Soc.* 135, 1872-1881 (DOI: 10.1021/ja310455t).

151. Bezbradica D., Karalazi I., Ohnjanovi N., Anmijin D., Ilser-Marinkovi S., Knezevic Z. (2006), *J. Serb. Chem. Soc.* 71, 31.

152. Schmid R. D., Verger R. (1998), Lipases: Interfacial enzymes with attractive applications, *Angew. Chem., Int. Ed.* 37, 1608-1633 (DOI: 10.1002/(SICI)1521-3773(19980703)37:12<1608::AID-ANIE1608>3.0.CO;2-V).

153. Naik S., Basu A., Saikia R., Madan B., Paul P., Chaterjee R., Brask J., Svendsen A. (2010), Lipases for use in industrial biocatalysis: Specificity of selected structural groups of lipases, *J. Mol. Catal. B*: *Enzym.*, 65, 18-23.

154. Sharma D., Sharma B., Shukla A. K. (2011), Biotechnological approach for microbial lipase: A review (2011), *Biotechnology*, 10, 23-40 (DOI: 10.3923/biotech.2011.23.40).

155. Gardossi L., Bianchi D., Klibanov A. M. (1991), Selective acylation of peptides catalyzed by lipases in organic solvents, *J. Am. Chem. Soc.*, 113,6328-6329 (DOI: 10.1021/ja00016a091).

156. Chronopoulou L., Lorenzoni S., Masci G., Dentini M., Togna A. R., Togna G., Bordic F., Palocci C. (2010), Lipase-supported synthesis of peptidic hydrogels, *Soft Matter*, 6, 2525-2532 (DOI: 10.1039/C001658F).

157. Chronopoulou L., Sennato S., Bordi F., Giannella D., Nitto A. D., Barbetta A., Dentini M., Togna A. R., Togna G. I., Moschinic S., Palocci C. (2014), Designing unconventional Fmoc-peptide-based biomaterials: structure and related properties, *Soft Matter*, 10, 1944-1952 (DOI: 10.1039/c3sm52457d).

158. John G., Zhu G., Li J., Dordick J. S. (2006), Enzymatically derived sugar-containing self-Assembled organogels with nanostructured morphologies, *Angew. Chem. Int. Ed.* 45, 4772-4775 (DOI: 10.1002/anie.200600989).

159. Yu L., Banerjee I. A., Gao X., Matsui H. (2005), *Polymer Preprints* 46, 36.

160. Dawson P. E., Muir T. W., Clark-Lewis I., Kent S. B. H. (1994), Synthesis of proteins by native chemical ligation, *Science*, 266, 776-779 (DOI: 10.1126/science.7973629).

161. Sletten E. M., Bertozzi C. R. (2011), From mechanism to mouse: A tale of two bioorthogonal reactions, *Acc. Chem. Res*., 44, 666-676 (DOI: 10.1021/ar200148z).

162. Sletten E. M., Bertozzi C. R. (2009), Bioorthogonal chemistry: fishing for selectivity in a sea of functionality, *Angew. Chem. Int. Ed.*, 48, 6974-6998 (DOI: 10.1002/anie.200900942).

163. Prescher J. A., Dube D. H., Bertozzi C. R. (2004), Chemical remodelling of cell surfaces in living animals, *Nature*, 430, 873-877 (DOI:10.1038/nature02791).

164. Prescher J. A., Bertozzi C. R. (2005), Chemistry in living systems, *Nature Chemical Biology*, 1, 13-21 (DOI:10.1038/nchembio 0605-13).

165. Baskin J. M., Prescher J. A., Laughlin S. T., Agard N. J., Chang P. V., Miller I. A., Lo A., Codelli J. A., Bertozzi C. R. (2007), Copper-free click chemistry fordynamic *in vivo* imaging, *Proc. Natl. Acad. Sci. U.S.A*, 104, 16793-16797 (DOI: 10.1073/pnas.0707090104).

166. Ning X., Temming R. P., Dommerholt J., Guo J., Ania D. B., Debets M. F., Wolfert M. A., Boons G.-J., van Delft F. L. (2010), Protein modification by strain-promoted alkyne-nitrone cycloaddition, *Angew. Chem. Int. Ed.*, 49, 3065-3086 (DOI: 10.1002/anie.201000408).

167. Blackman M. L., Royzen M., Fox J. (2008), Tetrazine ligation: Fast bioconjugation based on inverse-electron-demand diels-alder reactivity, *J. Am. Chem. Soc.*, 130 13518-13519 (DOI: 10.1021/ ja8053805).

168. Stöckmann H., Neves A. A., Stairs S., Brindle K. M., Leeper F. J. (2011), Exploring isonitrile-based click chemistry for ligation with biomolecules, *Org. Biomol. Chem.*, 9, 7303-7305 (DOI: 10.1039/C1OB06424J).

169. Saxon E., Bertozz C. R. (2000), Cell surface engineering by a modified staudinger reaction, *Science*, 287, 5460 (DOI: 10.1126/science.287.5460.2007).

170. Rostovtsev V. V. , Green L. G., Fokin V. V., Sharpless K. B. (2002), A stepwise huisgen cycloaddition process: Copper(I)-catalyzed regioselective "ligation" of azides and terminal alkynes, *Angew. Chem. Int. Ed., 41*, 2596-2599 (DOI: 10.1002/1521-3773(20020715)41:14<2596::AID-ANIE2596>3.0.CO;2-4).

171. Huisgen R. (1976) 1,3-Dipolar cycloadditions concerted nature of 1,3-dipolar cycloadditions and the question of diradical intermediates, *J. Org. Chem.*, 1976, 41, 403-419 (DOI : 10. 1021/ jo00865a001).

172. Schoenebeck F., Ess D. H., Jones G. O., Houk K. N. (2009), Reactivity and regioselectivity in 1,3-Dipolar cycloadditions of azides to strained alkynes and alkenes: A computational study, *J. Am. Chem. Soc.,* 131, 8121-8133 (DOI: 10.1021/ja9003624).

173. Wieland T., Bokelmann E., Bauer L., Lang H. U., Lau H. (1953), Über peptidsynthesen. 8. mitteilung bildung von S-haltigen peptiden durch intramolekulare wanderung von aminoacylresten, *Justus Liebigs Ann. Chem*., 583, 129-149 (DOI: 10.1002/jlac.19535830110).

174. Kemp D. S., Galakatos N. G., Dranginis S., Asthon C., Fotouhi N., Curran T. P. (1986), Peptide synthesis by prior thiol capture. 4. Amide bond formation. The effect of a side-chain substituent on the rates of intramolecular O, N-acyl transfer, *J. Org. Chem.* 51, 3320-3324 (DOI: 10.1021/jo00367a013).

175. Johnson E. C. B., Kent S. B. H. (2006), Insights into the mechanism and catalysis of the native chemical ligation reaction, *J. Am. Chem. Soc.,* 128, 6640-6646 (DOI: 10.1021/ja058344i).

176. Hirata R., Ohsumi Y., Nakano A., Kawasaki H., Suzuki K., Anraku Y. (1990), Molecular structure of a gene, VMAI, encoding the catalytic subunit of H^+-translocating adenosine triphosphatase from vacuolar membranes of succharomyces cereuisiae, *J. Biol. Chem*., 265, 6726-6733.

177. Kane P. M., Yamashiro C. T., Wolczyk D. F., Neff N., Goebl M., Stevens T. H. (1990), Protein splicing converts the yeast TFP1 gene product to the 69-kD subunit of the vacuolar $H^{(+)}$-adenosine triphosphatase, *Science*, 250, 651-657 (PMID:2146742).

178. Anraku Y., Mizutani R., Satow Y. (2005), Protein splicing: its discovery and structural insight into novel chemical mechanisms, *IUBMB Life*, 57, 563-574 (PMID:16118114)

179. Xu M.-Q., Perler F. B. (1996), The mechanism of protein splicing and its modulation by mutation, *EMBO J.*, 15, 5146-5153.

180. Muir T. W., Sondhi D., Cole P. A. (1998), Expressed protein ligation: A general method for protein engineering, *Proc. Natl. Acad. Sci. U.S.A.*, 95, 6705-6710.

181. Lu W., Gong D., Bar-Sagi D., Cole P. A. (2001), Site-specific incorporation of a phosphotyrosine mimetic reveals a role for tyrosine phosphorylation of SHP-2 in cell signaling, *Mol. Cell*, 8, 759-769 (PMID:11684012).

182. Valiyaveetil F. I., Mekedat M., Muir T. W., MacKinnon R. (2004), Semisynthesis of a functional K+ channel, *Angew. Chem., Int. Ed. Engl*. 43, 2504-2507 (DOI: 10.1002/anie.200453849).

183. Singla N., Erdjument-Bromage H., Himanen J. P., Muir T. W., Nikolov D. B. (2011), A semisynthetic Eph receptor tyrosine kinase provides insight into ligand-induced kinase activation, *Chem. Biol.*, 18, 361-371 (DOI: 10.1016/ j.chembiol. 2011.01.011).

184. Bang D., Pentelute B. L., Kent S. B. H. (2006), Kinetically controlled ligation for the convergent chemical synthesis of proteins, *Angew. Chem. Int. Ed.*, 45, 3985-3988 (DOI: 10.1002/anie.200600702).

185. Johnson E. C. B., Malito E., Shen Y., Rich D., Tang W.-J., Kent S. B. H. (2007), Modular total chemical synthesis of a human

immunodeficiency virus type 1 protease, *J. Am. Chem. Soc.*, 129, 11481-11490 (DOI: 10.1021/ja072870n).

186. Shogren-Knaak M. A., Fry C. J., Peterson C. L., (2003), A native peptide ligation strategy for deciphering nucleosomal histone modifications, *J. Bio. chem.*, 278, 15744-15748 (DOI:10.1074/jbc.M3014 -45200).

187. Macmillan D. Bertozzi C. R. (2004), Modular assembly of glycoproteins: Towards the synthesis of glyCAM-1 by using expressed protein ligation, *Angew. Chem., Int. Ed.*, 116, 1379-1383 (DOI: 10.1002/ange.200352673).

188. Dawson P. E. (2011), Native chemical ligation combined with desulfurization and deselenization: A general strategy for chemical protein synthesis, *Isr. J. Chem.*, 51, 862-867 (DOI: 10.1002/ ijch.201100128).

189. Rohde H., Seitz O. (2010), Invited reviewligation-desulfurization: A powerful combination in the synthesis of peptides and glycopeptides, *Biopolymers*, 94, 551-559 (DOI: 10.1002/ bip.21442).

190. Wan Q., Danishefsky S. J. (2007), Free-radical-based, specific desulfurization of cysteine: a powerful advance in the synthesis of polypeptides and glycopolypeptides, Angew. *Chem., Int. Ed.*, 46, 9248-9252 (DOI: 10.1002/anie.200704195).

191. Haase C., Rohde H., Seitz O. (2008), Native chemical ligation at valine, *Angew. Chem. Int. Ed.*, 47, 6807-6810 (DOI: 10.1002/ anie.200801590).

192. Crich D., Banerjee A. (2007), Native chemical ligation at phenylalanine, *J. Am. Chem. Soc.*, 129, 10064-10065 (DOI: 10.1021/ja072804l).

193. Shang S., Tan Z., Dong S., Danishefsky S. J. (2011), An advance in proline ligation, *J. Am. Chem. Soc.* 133, 10784-10786 (DOI: 10.1021/ja204277b).

194. Cergol K. M., Thompson R. E., Malins L. R., Turner P., Payne R. J. (2014) One-pot peptide ligation-desulfurization at glutamate, *Org Lett.* 16, 290-293 (DOI: 10.1021/ol403288n).

195. Thomas G. L., Hsieh Y. S. Y., Chun C. K. Y., Cai Z.-L., Reimers J. R., Payne R. J. (2011), Peptide ligations accelerated by N-terminal aspartate and glutamate residues, *Org. Lett.*, 13, 4770-4773 (DOI: 10.1021/ol2017356).

196. Malins L. R., Cergola K. M., Payne R. J. (2014), Chemoselective sulfenylation and peptide ligation at tryptophan, *Chem. Sci.*, 5, 260-266 (DOI: 10.1039/c3sc51497h).

197. Wan Q. Chen J. Yuan Y., Danishefsky S. J. (2008) Oxo-ester mediated native chemical ligation: Concept and applications, *J. Am. Chem. Soc.*, 130, 15814-15816 (DOI: 10.1021/ja804993y).

198. Fang G.-M., Wang J.-X., Liu L. (2012), Convergent chemical synthesis of proteins by ligation of peptide hydrazides, *Angew. Chem. Int. Ed.*, 51, 10347-10350 (DOI: 10.1002/anie.201203843).

199. Burlina F., Morris C., Behrendt R., White P., Offer J. (2012), Simplifying native chemical ligation with an N-acylsulfonamide linker, *Chem. Commun.*, 48, 2579-2581 (DOI: 10.1039/ c2cc15911b).

200. Durek T., Alewood P. F. (2011), Preformed selenoesters enable Rapid native chemical ligation at intractable sites, *Angew. Chem. Int. Ed*., 50, 12042-12045 (DOI: 10.1002/anie.201105512).

201. de Duve C. (1995), The beginnings of life on earth, *American Scientist*, 83, 428-437.

202. Lehninger A. L., Nelson D. L., Cox M. M. (2000), *Principles of Biochemistry*, 3rd ed., Worth Publishing, New York.

203. Hojo H., Aimoto S. (1991), *Bull. Soc. Chem. Jpn.* 64, 111.

204. Dheur J., Ollivier N., Melnyk O. (2011), Synthesis of thiazolidine thioester peptides and acceleration of native chemical ligation, *Org. Lett.*, 13, 1560-1563 (DOI: 10.1021/ol2002804).

205. Dirksen A., Meijer E. W., Adriaens W., Hackeng T. M. (2006), Strategy for the synthesis of multivalent peptide-based nonsymmetric dendrimers by native chemical ligation, *Chem. Commun.* 1667-1669 (DOI: 10.1039/B600286B).

206. Ryadnov M. G., Woolfson D. N. (2007), Self-assembled templates for polypeptide synthesis, *J. Am. Chem. Soc.* 129, 14074-14081 (DOI: 10.1021/ja072960s).

207. Jung J. P., Jones J. L., Cronier S. A., Collier J. H. (2008), Modulating the mechanical properties of self-assembled peptide hydrogels via native chemical ligation, *Biomaterials*, 29, 2143-2151 (DOI:10.1016/j.biomaterials.2008.01.008).

208. Hu B.-H., Su J., Messersmith P. B. (2009), Hydrogels cross-linked by native chemical ligation, *Biomacromolecules,* 10, 2194-2000 (DOI: 10.1021/bm900366e).

209. Warren J. D., Miller J. S., Keding S. J., Danishefsky S.J. (2004), Toward fully synthetic glycoproteins by ultimately convergent routes: A solution to a long-standing problem, *J. Am. Chem. Soc.*, 126, 6576-6578 (DOI: 10.1021/ja0491836).

210. Hackeng T. M., Griffin J. H., Dawson P. E. (1999), Protein synthesis by native chemical ligation: Expanded scope by using straightforward methodology, *Proc. Natl. Acad. Sci. U.S.A.* 96, 10068-10073 (DOI: 10.1073/pnas.96.18.10068).

211. Metanis N., Keinan E., Dawson P. E. (2010), Traceless ligation of cysteine peptides using selective deselenization, *Angew. Chem., Int. Ed.*, 49, 7049-7053 (DOI: 10.1002/anie.201001900).

212. Pollock S. B., Kent S. B. (2011), An investigation into the origin of the dramatically reduced reactivity of peptide-prolyl-thioesters in native chemical ligation, Chem. *Commun.*, 2011, 2342-2344 (DOI: 10.1039/c0cc04120c).

213. Townsend S. D., Tan Z. P., Dong S. W., Shang S. Y., Brailsford, J. A., Danishefsky S. J. (2012), Advances in proline ligation, *J. Am. Chem. Soc.,* 134, 3912-3916 (**DOI:** 10.1021/ja212182q).

214. Weissenborn M. J., Castangia R., Wehner J. W., Sardzik R., Lindhorst T. K., Flitsch S. L. (2012) Oxo-ester mediated native chemical ligation on microarrays: An efficient and chemoselective coupling methodology *Chem. Commun.*, 48, 4444-4446 (DOI: 10.1039/c2cc30844d).

215. Fang G.-M., Cui H.-K., Zheng J.-S., Liu L. (2010), Chemoselective ligation of peptide phenyl esters with N-terminal cysteines *ChemBioChem,* 11, 1061-1065 (DOI: 10.1002/ cbic.201000165).

216. Hentschel J., Krause E., Borner H. G. (2006), Switch-peptides to trigger the peptide guided assembly of poly(ethylene oxide)-peptide conjugates into tape structures, *J. Am. Chem. Soc*., 128, 7722-7723 (DOI: 10.1021/ja060759w).

217. Strehin I., Gourevitch D., Zhang Y., Katzb E. H., Messersmith P. B. (2013), Hydrogels formed by oxo-ester mediated native chemical ligation, *Biomater. Sci.*, 1, 603-613 (DOI: 10.1039/ c3bm00201b).

218. Jacob C., Giles G. I., Giles N. M., Sies H. (2003), Sulfur and selenium: The role of oxidation state in protein structure and function, *Angew. Chem. Int. Ed.*, 42, 4742-4758 (DOI: 10.1002/ anie.200300573).

219. Mugesh G., Singh H. B. (2000), Synthetic organoselenium compounds as antioxidants: Glutathione peroxidase activity, *Chem. Soc. Rev*., 29, 347-357 (DOI: 10.1039/A908114C).

220. Mugesh G., du Mont W. W., Sies H. (2001), Chemistry of biologically important synthetic organoselenium compounds, *Chem. Rev*., 101, 2125-2179 (DOI: 10.1021/cr000426w).

221. Nogueira C. W., Zeni G., Rocha J. B. T. (2004), Organoselenium and organotellurium compounds: Toxicology and pharmacology, *Chem. Rev.*, 104, 6255-6268 (DOI: 10.1021/cr0406559).

222. Nishino T., Okada M., Kuroki T., Watanabe T., Nishiyama Y., Sonoda N. (2002), One-pot synthetic method of unsymmetrical diorganyl selenides: Reaction of diphenyl diselenide with alkyl halides in the presence of lanthanum metal, *J. Org. Chem.*, 2002, 67, 8696-8698 (DOI: 10.1021/jo026032h).

223. Keck G. E., Grier M. C. (1999), Generation and reactivity of oxazolidinone derived N-acyl radicals, *Synlett*, 1657-1659 (DOI: 10.1055/s-1999-2913).

224. Boger D. L., Mathvink R. J. (1992), Acyl radicals: intermolecular and intramolecular alkene addition reactions, *J. Org. Chem.*, 57, 1429-1443 (DOI: 10.1021/jo00031a021).

225. Chen C., Crich D., Papadatos A. (1992), The chemistry of acyl tellurides: generation and trapping of acyl radicals, including aryltellurium group transfer, *J. Am. Chem. Soc.*, 114, 8313-8314 (DOI: 10.1021/ja00047a066).

226. Hiiro T. Morita Y., Inoue T., Kambe N., Ogawa A., Ryu I., Sonoda N. (1990), A new access to acyl- and aroyllithiums via lithium-tellurium exchange, *J. Am. Chem. Soc.*, 112, 455-457 **(**DOI: 10.1021/ja00157a074).

227. Schnölzer M., Alewood P., Jones A., Alewood D., Kent S. B. (1992), In situ neutralization in Boc-chemistry solid phase peptide synthesis. Rapid, high yield assembly of difficult sequences, *Int. J. Pept. Protein Res.* 40, 180-193 (PMID:1478777).

228. Baca M., Muir T., Schonolzer M., Kent S. B. H. (1995), Chemical ligation of cysteine-containing peptides: Synthesis of a 22 kDa tethered dimer of HIV-1 protease, *J. Am. Chem. Soc.*, 117, 1881-1887 (DOI: 10.1021/ja00112a003).

229. Inoue M., Yamahita S., Ishihara Y., Hirama M. (2006), Two convergent routes to the left-wing fragment of ciguatoxin CTX3C using *O*, *S*-acetals as key intermediates, *Org. Lett.*, 8, 5805-5808 **(**DOI: 10.1021/ol062350h).

230. Martin S. F., Chen K. X., Eary C. T. (1999), An enantioselective total synthesis of (+)-geissoschizine, *Org. Lett.*, 1, 79-82 (DOI: 10.1021/ol990554a).

231. Chu-Kung A. F., Bozzelli K. N., Lockwood N. A., Haseman J. R., Mayo K. H., Tirrell M. V. (2004), Promotion of peptide antimicrobial activity by fatty acid conjugation, *Bioconjugate Chemistry*, 15, 530-535 (DOI: 10.1021/bc0341573).

232. Chen C. X., Pan F., Zhang S. Z., Hu J., Cao M. W., Wang J., Xu H., Zhao X. B., Lu J. R. (2010), Antibacterial activities of short designer peptides: a link between propensity for nanostructuring and capacity for membrane destabilization, *Biomacromolecules*, 11, 402-411 (DOI: 10.1021/bm901130u).

233. Makovitzki A., Baram J., Shai Y. (2008), Antimicrobial lipopolypeptides composed of palmitoyl di- and tricationic peptides: *In vitro* and *in vivo* activities, self-assembly to nanostructures, and a plausible mode of action, *Biochemistry*, 47, 10630-10636 (DOI: 10.1021/bi8011675).

234. Liu L. H., Xu K. J., Wang H. Y., Tan P. K. J., Fan W. M., Venkatraman S. S., Li L. J., Yang Y. Y. (2009), Self-assembled cationic peptide nanoparticles as an efficient antimicrobial agent, *Nature Nanotech.*, 4, 457-463 (DOI:10.1038/nnano.2009.153).

235. Mitra R. N., Shome A., Paul P., Das P. K. (2009), Antimicrobial activity, biocompatibility and hydrogelation ability of dipeptide-based amphiphiles, *Org. Biomol. Chem.*, 7, 94-102 (DOI: 10.1039/b815368j).

236. Ghanaati S., Webber M. J., Unger R. E., Orth C., Hulvat J. F., Kiehna S. E., Barbeck M., Rasic A., Stupp S. I., Kirkpatrick C. J.

(2009), Dynamic in vivo biocompatibility of angiogenic peptide amphiphile nanofibers, *Biomaterials*, 30, 6202-6212 (DOI: 10.1016/j.biomaterials.2009.07.063).

237. Zhou M., Smith A. M., Das A. K., Hodson N. W., Collins R. F., Ulijn R. V., Gough J. E. (2009), Self-assembled peptide-based hydrogels as scaffolds for anchorage-dependent cells, *Biomaterials*, 30, 2523-2530 (DOI: 10.1016/ j.biomaterials. 2009.01.010).

238. Mata A., Hsu L., Capito R., Aparicio C., Henriksonc K., Stupp S. I. (2009), Micropatterning of bioactive self-assembling gels, *Soft Matter*, 5, 1228-1236 (DOI: 10.1039/B819002J).

239. Harrington D. A., Cheng E. Y., Guler M. O., Lee L. K., Donovan J. L., Claussen R. C., Stupp S. I. (2006), Branched peptide-amphiphiles as self-assembling coatings for tissue engineering scaffolds, *J. Biomed. Mater. Res., Part A*, 78, 157-167 (DOI: 10.1002/jbm.a.30718).

240. Huang H., Ding Y., Sun X. S., Nguyen T. A. (2013), Peptide hydrogelation and cell encapsulation for 3D culture of MCF-7 breast cancer cells, *PLoS One.* (DOI: 10.1371/ journal. pone.0059482).

241. Gao Y., Kuang Y., Guo Z. -F., Guo Z., Krauss I. J., Xu B. (2009), Enzyme-instructed molecular self-assembly confers nanofibers and a supramolecular hydrogel of taxol derivative, *J. Am. Chem. Soc*., 131, 13576-13577 (DOI: 10.1021/ja904411z).

242. Altunbas A., Lee S. J., Rajasekaran S. A., Schneider J. P., Pochan D. J. (2011), Encapsulation of curcumin in self-assembling peptide hydrogels as injectable drug delivery vehicles, *Biomaterials*, 32, 5906-5914 (DOI: 10.1016/j.biomaterials.2011.04.069).

243. Vemula P. K., Li J., John G. (2006), Enzyme catalysis: Tool to make and break amygdalin hydrogelators from renewable

resources: A delivery model for hydrophobic drugs, *J. Am. Chem. Soc*., 128, 8932-8938 (DOI**:** 10.1021/ja062650u).

244. Vemula P. K., Cruikshank G. A., Karp J. M., John G. (2009), Self-assembled prodrugs: an enzymatically triggered drug-delivery platform, *Biomaterials*, 30, 383-393 (DOI: 10.1016/j. biomaterials. 2008.09.045).

245. Sutton S., Campbell N. L., Cooper A. I., Kirkland M., Frith W. J., Adams D. J. (2009), Controlled release from modified amino acid hydrogels governed by molecular size or network dynamics, *Langmuir*, 25, 10285-10291 (DOI: 10.1021/la9011058).

246. Nagai Y., Unsworth L. D., Koutsopoulos S., Zhang S. (2006), Slow release of molecules in self-assembling peptide nanofiber scaffold, *J. Controlled Release*, 115, 18-25 (DOI:10.1016/ j.jconrel.2006.06.031).

247. Zhao Y., Tanaka M., Kinoshita T., Higuchi M., Tan T. (2010), Self-assembling peptide nanofiber scaffolds for controlled release governed by gelator design and guest size, *J. Controlled Release*, 147, 392-399 (DOI: 10.1016/j.jconrel.2010.08.002).

248. Matson J. B., Newcomb C. J., Bitton R., Stupp S. I. (2012), Nanostructure-templated control of drug release from peptide amphiphile nanofiber gels, *Soft Matter*, 8, 3586-3595 (DOI: 10.1039/C2SM07420F).

249. Zhao F., Ma M. L., Xu B. (2009), Molecular hydrogels of therapeutic agents, *Chem. Soc. Rev.*, 38, 883-891 **(**DOI**:** 10.1039/B806410P**).**

250. Yang C., Bian M., Yang Z. (2013), A polymer additive boosts the anti-cancer efficacy of supramolecular nanofibers of taxol, *Biomater. Sci.* 2**,** 651-654 (DOI: 10.1039/c3bm60252d).

251. Schneider A., Garlick J. A., Egles C. (2008), Self-assembling Peptide nanofiber scaffolds accelerate wound healing, *PLoS ONE*, 1, 1410 (DOI: 10.1371/journal.pone.0001410).

252. Kanlayavattanakul M., Lourith N. (2010), Lipopeptides in cosmetics, *Int. J. Cosmet. Sci.*, 32, 1-8 (DOI: 10.1111/j.1468-2494.2009.00543.x).

253. Chirita R.-I., Chaimbault P., Archambault J. -C., Robert I., Elfakir C. (2009), Development of a LC-MS/MS method to monitor palmitoyl peptides content in anti-wrinkle cosmetics, *Anal. Chim. Acta*, 641, 95-100 (DOI: 10.1016/j.aca.2009.03.015).

254. Dickerson M. B., Sandhage K. H., Naik R. R. (2008), Protein- and peptide-directed syntheses of inorganic materials, *Chem. Rev.*, 108, 4935-4978 (DOI: 10.1021/cr8002328).

255. Sone E. D., Stupp S. I. (2004), Semiconductor-encapsulated peptide-amphiphile nanofibers, *J. Am. Chem. Soc.*, 126, 12756-12757 (DOI: 10.1021/ja0499344).

256. Yan J., Pan Y., Cheetham A. G., Lin Y. A., Wang W., Cui H., Liu C. -J. (2013), One-step fabrication of self-assembled peptide thin films with highly dispersed noble metal nanoparticles, *Langmuir*, 29, 16051-16057 (DOI: 10.1021/la4036908).

257. Reches M., Gazit E. (2003), Casting metal nanowires within discrete self-assembled peptide nanotubes, *Science*, 300, 625-627 (DOI: 10.1126/science.1082387).

258. Maity I., Manna M. K., Rasale D. B., Das A. K. (2014), Peptide-nanofiber-supported palladium nanoparticles as an efficient catalyst for the removal of N-terminus protecting groups, *ChemPlusChem*, 79, 413-420 (DOI: 10.1002/cplu.201300348).

Chapter 2

Materials and Experimental Techniques

2.1 Introduction

This chapter presents the materials used and general synthetic procedures employed in this thesis for solution phase peptide synthesis. This chapter covers the range of characterization techniques used in this work. The respective chapter described the specific synthetic procedures pertaining to sequences studies in this thesis.

2.2 Experimental Procedures

2.2.1 Source of Chemicals

All the amino acids, *tert*-butylpyrocarbonate, dicyclohexylcarbodiimide (DCC), 1-hydroxybenzotriazole (HOBt), *p*-nitrophenol, 4-dimethylamino pyridine (DMAP), selenophenol, 2-naphthalenemethanol, phosgene, ethylchloroformate, triethylamine, *p*-hydroxybenzyl alcohol and benzyl alcohol were obtained from Sigma Chemical Company, St. Louis Missouri, U. S. A.; Aldrich, U. S. A.; E- Merck, Germany, Lancaster, England, and SRL, India. Deuterated solvents for NMR studies, $CDCl_3$, and $(CD_3)_2SO$ were purchased form Sigma Chemical Company, St. Louis Missouri, U. S. A. Silica gel (100-200 mesh) for column chromatography was purchased from SRL and TLC pre-coated silica gel plates (Kieselgel 60F254, Merck) were obtained from Merck, India. All other local chemicals were obtained from local manufactures like SD Fine Chemicals Pvt. Ltd., SRL India, and E-Merck India *etc*. Enzyme themolysin from *Bacillus thermoproteolyticus rokko* and Lipase from *candida rugosa* were obtained from Sigma Chemical Company, St. Louis Missouri U. S. A.

2.2.2 Purification of Solvents and Reagents

In order to obtained satisfactory results in many synthesis involving air moisture sensitive reactions, it is necessary to remove oxygen or impurities from the solvents. The solvents used during the course of synthesis were purified by a commonly employed still method. Ethyl acetate, chloroform and hexane were distilled prior to use. Dichloromethane and dioxane were passed through basic alumina before use. Methanol was purified by drying over an effective drying agent calcium oxide and fractionally distilled before further use.[1] Thionyl chloride was simply distilled and used. Dimethylformamide (DMF) was fractionally distilled using condenser packed with fenske helices under reduced pressure over calcium hydride (3 g L^{-1}).

2.2.3 Amino Acid Derivatives

All the required amino acid methyl ester hydrochlorides were prepared in good to excellent yields by the room temperature reaction of amino acids with methanol in the presence of thionylchloride.[2] The amino acid benzyl ester was prepared using a normal method of preparation for benzyl ester involves heating of amino acid with benzyl alcohol in presence of *p*-toluene sulphonic aicd. The Boc-amino acids used in this work were prepared by Schnabel's method.[3]

2.2.4 Solution Phase Peptide Synthesis

Solution-phase peptide synthesis[4] is a classical approach to peptide synthesis. It has been replaced in most of the lab by solid-phase peptide synthesis for long peptides. All the peptides used in this works were synthesized by solution-phase peptide synthesis using conventional coupling agent dicyclohexylcarbodiimide/1-hydroxybenzotriazole (DCC/ HOBt). All the coupling reactions were performed at ambient temperature

(25^{o}C) conditions unless specifically mentioned. The racemization at C^{α} is the major problem in peptide synthesis. Thus, HOBt reacts with acyl urea and form less reactive ester which is less sensitive toward racemization. The possibility of diastereomers formation due to racemization was confirmed by NMR. Normally no diastereomers could be detected. The ter-butyloxycarbonyl (Boc) and Naphthalene-2-methoxycarbonyl groups were used for amino N-terminal protection, while C-terminal was protected with methyl ester[5] or benzyl ester. The *N*-terminal deprotection was done by saponification of Boc group in trifluoroacetic acid solution. The C- terminal deprotections were performed by saponification for the ester groups in alkaline methanolic solution.

2.2.5 Characterization and Purification of Peptides

The column chromatography can be regarded as the heart of the chromatographic system. Peptide fragments were routinely checked for monitoring the reactions and homogeneity by thin layer chrmomatography (TLC) before subjecting to column chromatographic purification. The thin layer chromatography was performed on pre-coated silica gel plates (Kieselgel 60F254, Merck) using either $CHCl_3$: MeOH (9:1) or ethyl acetate: hexane (3:1) as eluent. Detailed characterization was done at every stage by an analysis of 400 MHz ^{1}H NMR spectra. All the peptides and their fragments were purified by column chromatography using silica gel (100-200 mesh size) as stationary phase and $CHCl_3$-MeOH, ethylacetate-hexane as eluents.

2.3 Spectroscopic Measurements

2.3.1 ^{1}H NMR Spectroscopy

All NMR spectra were recorded at 400 MHz Bruker AV 400 NMR spectrometer. TMS was used an internal reference in the NMR spectra.

Peptide concentrations were in the range of 1-10 mmol in $(CD_3)_2SO$ and $CDCl_3$.

2.3.2 FT-IR Spectroscopy

The reported FT-IR spectra were taken using Bruker (Tensor 27) FT-IR spectrophotometer. The solid state measurements were performed using the KBr pallet technique. The gel samples were done using crystal Zn-Se windows and scanned between 900 and 4000 cm^{-1} over 64 scans at a resolution of 4 cm^{-1} and an interval of 1 cm^{-1}.

2.3.3 Polarimeter

Specific rotations of the synthesized peptides were measured on an Autopol V automatic polarimeter (Rudolph research analytical). The cell (length =100 mm, capacity = 2 mL) was used for this study at 25 ^oC.

2.3.4 Mass Spectrometry

Mass spectra of peptides were recorded on Bruker micrOTOF-Q II by positive and negative mode electrospray ionizations.

2.3.5 High Performance Liquid Chromatography

A Dionex HPLC-Ultimate 3000 (High Performance Liquid Chromatography) pump was used to analyse products. A 20 µL of sample was injected onto a Dionex Acclaim ® 120 C18 column of 250 mm length with an internal diameter of 4.6 mm and 5 µm fused silica particles at a flow rate of 1 mL min^{-1} (linear gradient of 40 % v/v acetonitrile in water for 35 min, gradually rising to 100 % (v/v) acetonitrile in water at 35 min). This concentration was kept constant until 40 min when the gradient was decreased to 40 % (v/v) acetonitrile in water at 42 min. The sample preparation involved mixing of 100 µL gel in 900 µL acetonitrile-water

(50: 50 mixture) solution containing 0.1 % trifluroacetic acid. The samples were then filtered through a 0.45 µm syringe filter (Whatman, 150 units, 13 mm diameter, 2.7 mm pore size) prior to injection. The products were identified by using Ultimate 3000 RS Variable Wavelength Detector at 280 nm.

2.3.6 UV-Vis Spectroscopy

UV-Vis absorption spectra of self-assembled gel were recorded using a Varian Cary100 Bio UV-Vis spectrophotometer at a concentration of 20 mmol L^{-1}.

2.3.7 Fluorescence Spectroscopy

Fluorescence emission spectra were recorded upon specific excitation wavelength for self-assembled gel with medium sensitivity on a Horiba Scientific Fluoromax-4 spectrophotometer. The slit width for the excitation and emission was set at 2 nm and 1 nm data pitch. Samples were prepared in 1 cm^2 quartz cuvette at room temperature.

2.3.8 Time-Correlated Single Photon Counting Technique

Time Correlated Single Photon Counting (TCSPC) is based on the detection of single photons of the periodic light signal,[6] measurement of the detection times of the individual photons and the reconstruction of the waveform from the individual time measurements. 2 mL gel was prepared in a 1 cm^2 quartz cuvette and time resolved studies were done by a time correlated single photon counting (TCSPC) system from Horiba Yovin (Model: Fluorocube-01-NL). Samples were excited at 376 nm using a picosecond diode laser (Model: Pico Brite-375L). The signals were collected at magic angle (54.70) polarization using a photomultiplier tube (TBX-07C) as detector, which has a dark counts less than 20 cps. The instrument response function was typically 140 ps. The data analysis was

performed using IBH DAS (version 6, HORIBA Scientific, Edison, NJ) decay analysis software. The amplitude-weighted lifetime was estimated by

$$\langle \tau \rangle = \sum_{i=1}^{n} a_i \, \tau_i$$

where τ_1 is the fluorescence lifetime of various fluorescent species and the a_1 normalized pre-exponential factors. To gain the best fitting in all cases, the χ^2 was kept near to unity.

2.3.9 Circular Dichroism

Circular dichroism (CD) spectra were measured at 25^{o}C on a Jasco J-815 spectropolarimeter. Spectra were measured between 300 and 190 nm with a data pitch of 0.1 nm. The bandwidth was set to 1 nm with a scanning speed of 20 nm min^{-1} and a response time of 1 s. The path length was 1 mm quartz cell. Samples were prepared at a concentration of 2 mmol L^{-1}. Experimental data were acquired in thrice and the average data is shown.

2.3.10 Rheology

Rheological study was performed to determine the mechanical properties[7] of hydrogels. These properties were assessed using an Anton Paar Physica Rheometer (MCR 301, Austria) with cone plate geometry (20 mm in diameter, 50 µm gap and 1° angle) and temperature was controlled at 25 °C. The dynamic moduli of the hydrogel were measured as a function of frequency in the range of 0.1-100 rad s^{-1} with a constant strain value 0.05 %. To determine the exact strain for frequency sweep experiments, the linear viscoelastic (LVE) regime was performed at constant frequency of 10 rad s^{-1}. Experimental data was acquired in thrice and the average data is shown. Every time 200 µL of gel was prepared in glass vial and transferred it over the plate using microspatula to proceed for rheological measurements.

2.4 Microscopic Studies

2.4.1 Atomic Force Microscopic Study

Morphological studies of self-assembled peptides were investigated using a tapping mode atomic force microscopy. A very dilute solution of gel was placed (200 μL of gel was dissolved in 800 μL of milii-Q water) on mica and allowed it dry in air for 2 days at room temperature. Nanostructural images were colleted by using scanning probe microscope AIST-NT instrument (model no. smart SPM-1000).

2.4.2 Scanning Electron Microscopic Study

Field-emission Gun-scanning electron microscopic study was done by using Jeol Scanning Microscope-JSM-7600F. The gel samples were dried on a glass cover slip and coated with platinum. Interesting nanostructural morphology was observed in each sample of self-assembled gel.

2.4.3 Transmission Electron Microscopic Study

Transmission electron microscopy was used to determine the nanofibrillar[8] architectures of self-assembled gel. Sample was prepared by adding a drop of pre-formed gel over the carbon-coated copper grids (200 or 300 mesh). Excess gel was blotted with filter paper and sample was allowed dry under an infrared lamp for 30 min. The measurements of gels were acquired using a PHILIPS electron microscope (model: CM 200), operated at an accelerating voltage of 200 kV and JEM-2100 electron microscope operated at an accelerating voltage of 200 kV.

2.5 References

1. Marcus Y., Glikberg S. (1985), Recommended methods for the purification of solvents and tests for impurities: methanol and ethanol, *Pure & App. Chem.*, 57, 855-864 (DOI:10.1351/ pac198557060855).
2. Brenner M., Hubber W. (1953), Herstellung von α-mminosäureestern durch alkoholyse der methylester, *Helve. Chem. Acta*, 36, 1109-1115.
3. Schnabel E. (1967), *Ann. Chem.* 702, 188.
4. Bodanszky M., Bodanszky A. (1984), *The Practice of peptide synthesis*, Springer-Verlag, Berlin, Heidelberg, New York, Tokyo, PP.1-282.
5. Li J., Sha, Y. (2008), A convenient synthesis of amino acid methyl esters, *Molecules*, 13, 1111-1119 (DOI: 10.3390/ molecules13051111).
6. Lakowicz J. R., (2006), *Principles of fluorescence spectroscopy*, Third ed. Springer Science, Business Media, New York, pp. 1255.
7. Yin H., Akasaki T., Lin Sun T., Nakajima T., Kurokawa, T., Nonoyama, T., Taira T., Saruwatari Y., Gong J. P. (2013), Double network hydrogels from polyzwitterions: high mechanical strength and excellent anti-biofouling properties, *J. Mater. Chem. B*, 1, 3685-3693 (DOI: 10.1039/c3tb20324g).
8. Sagawa T., Chowdhury S., Takafuji M., Ihara H. (2006), Self-assembled nanofibrillar aggregates with amphiphilic and lipophilic molecules, *Macromol. Symp.* 237, 28-38, (DOI: 10.1002/masy.200650504).

Chapter 3

Peptide Self-Assembly Driven By Oxo-Ester Mediated Native Chemical Ligation

3.1 Introduction

Self-assembly[1] is a spontaneous process in nature which plays crucial roles in constructing various nanostructures. Self-assembled nanostructures of small molecules have attracted researchers for their potential applications in tissue engineering,[2] drug delivery[3] and biosensing.[4] Supramolecular gels[5] rely on non-covalent interactions, including hydrogen bonding, π-stacking and hydrophobic interactions which are exploited in nanostructures.[6] The study of designed short peptide based supramolecular gels is of interest due to their drug delivery and biomedical applications.[7] In recent years, different kinds of stimuli have been used to develop supramolecular gels. Our objective is to exploit chemical reactions towards the formation of soft materials as well as the formation of new kinds of peptide nanostructures.

Self-assembly through oxo-ester directed native chemical ligation remains unexplored. Since its discovery by Kent and co-workers in 1994, native chemical ligation (NCL) has revolutionized the total or semi-synthesis[8] of medium sized proteins. Typically, NCL involves the coupling of two unprotected peptides including a thioester peptide and an N-terminal cysteinyl peptide.[9] To achieve an efficient and simple method, our intention was to exploit oxo-ester[10] mediated native chemical ligation in peptide coupling and the subsequent formation of self-assembled peptide gels. The potential application in the self-assembly process of oxo-ester mediated NCL has not been investigated. The modified *p*-nitrophenyl (*p*-NP) ester could be a more effective acyl donor than the complex S-S acyl transfer of the corresponding thioester. Here, we have synthesized Nmoc-protected

amino acids/peptides having C-terminal *p*-NP esters. The modified ligation precursors undergo self-assembly via NCL with N-terminal cysteine residues. Self-assembly via NCL was studied with Nmoc-protected amino acid and peptide *p*-NP esters. Five compounds **1-5** (Figure 3.1) were synthesized by conventional solution phase methodology.

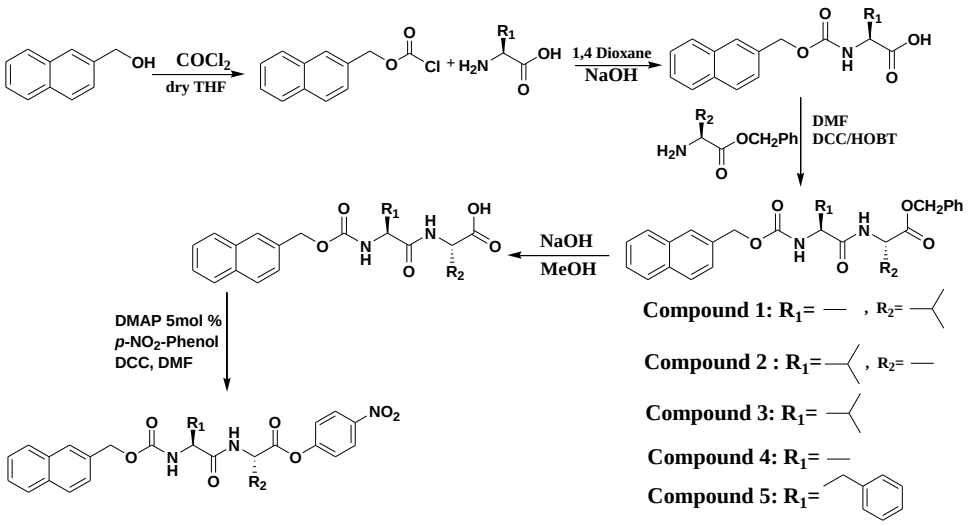

Figure 3.1. *Synthesis of Nmoc-protected active ester(compounds **1**, **2**, **3**, **4** and **5**) for NCL reactions.*

3.2 Experimental

*3.2.(1) Synthesis of compounds **1-5***

The Nmoc-protected peptides were synthesized by conventional solution phase peptide synthesis. Nmoc-protected amino acids coupled with corresponding methyl ester protected amino acid using dicyclohexylcarbodiimde/1-hydroxybenzotriazole (DCC/HOBt) as coupling reagents. The deprotection of methyl ester was done by saponification in acid medium. The active esters were synthesized using *p*-nitrophenol by DCC/HOBt method.

*3.2.1 Synthesis of compound **1:***

a) Synthesis of Nmoc-Cl **6**: To a stirred solution of naphthalene methanol (5g, 31.6 mmol) in dry THF (143.3 mL),

phosgene (39.2 mL, 75.5 mmol) was added at 0°C. The stirring was continued at ambient temperature for 24h. The reaction was monitored by thin layer chromatography (TLC). After completion of reaction, excess phosgene was removed under low vacuum and trapped with aqueous NaOH. Reaction mixture was concentrated and oily product was obtained. Then it was dissolved in hot hexane to get crystalline product **6**. Yield = 6.8 g (30 mmol, 94.93 %).

FT-IR (KBr): 3066 (m), 1777 (s), 1601 (m), 1168 (s) cm^{-1}.^{1}H NMR (400 MHz, $CDCl_3$): 7.89 (m, 4H), 7.56 (m, 3H), 5.48 (s, 2H).^{13}C NMR (100 MHz, $CDCl_3$) δ 71.82, 125.7, 126.6, 126.8, 127.8, 128.6, 130.6, 133.0, 133.5, 140.9, 147.9, 150.7 ppm.

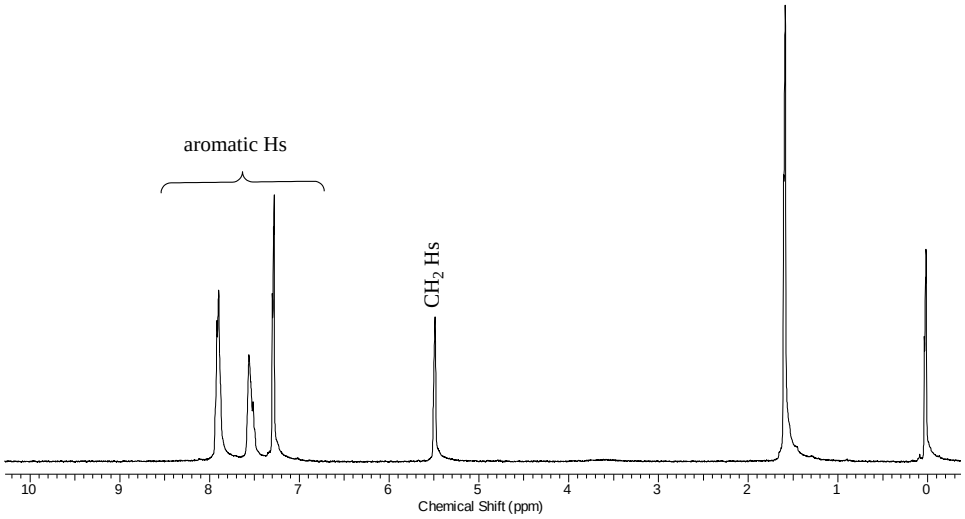

Figure 3.2. *400 MHz ^{1}H NMR spectrum of Nmoc-Cl **6** in $CDCl_3$.*

b) Synthesis of Nmoc-Ala **7**: A solution of L-alanine (0.445 g, 5 mmol) in a mixture of 1, 4 dioxane (10 mL) and 1 M sodium hydroxide (15 mL) was stirred and cooled in an ice-water bath. Naphthalene-2- methyloxychloroformate **6** (1.102 g, 5 mmol) was added and stirring was continued at room temperature for 12 h. Reaction mixture was diluted with 200 mL of water and dioxane was evaporated under vaccum. Aqueous layer was washed with diethyl ether and the pH of aqueous layer was adjusted to 2 with 2N hydrochloric acid. The aqueous phase was extracted with ethyl acetate

(3 x 50 mL) and dried with Na_2SO_4 and concentrated in vacuo to give **7** as colorless oil. Yield= 0.890 mg (3.2 mmol, 64%)
$[\alpha]_D^{25}$ -13° (*c* = 1, MeOH). ^{1}H NMR (400 MHz, DMSO-d_6): 12.51 (s, 1H, COO<u>H</u>), 7.98 (t, 4H, Nph), 7.65 (d, *J* = 7.6 Hz, 1H), 7.53 (t, 2H, Nph), 7.46 (d, 1H, NH), 5.15 (s, 2H, CH_2 of Nph), 4.09 (m, 1H, C^{α} H of Ala), 1.34 (d, *J*=7.6 Hz, 3H, C^{β} Hs of Ala). MS (ESI) m/z for $C_{15}H_{15}NO_4$ $(M+Na)^+$ calcd.: 296.0893, found: 296.0911. Elemental Analysis calculated for $C_{15}H_{15}NO_4$: C, 65.95; H, 5.53; N, 5.13; Found: C, 65.82; H, 5.52; N, 5.11.

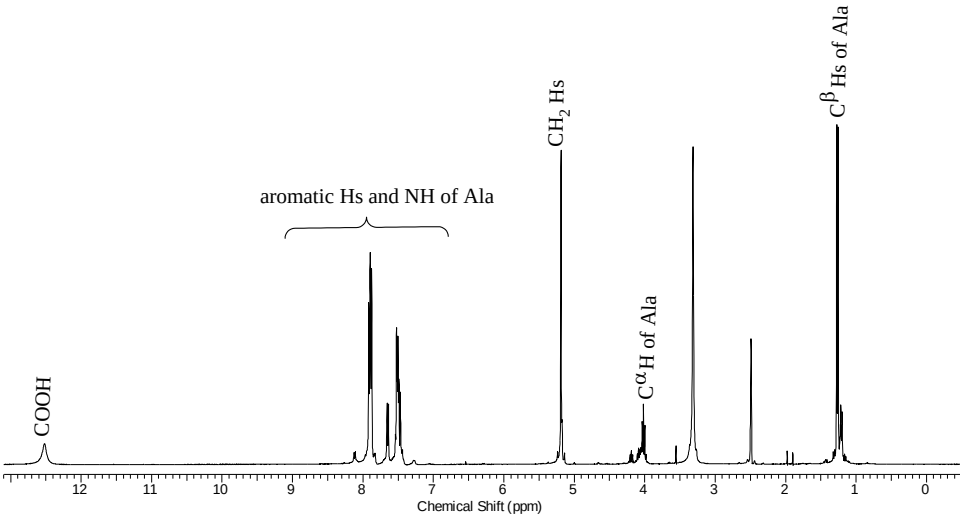

Figure 3.3. *400 MHz ^{1}H NMR spectrum of **7** in DMSO-d_6.*

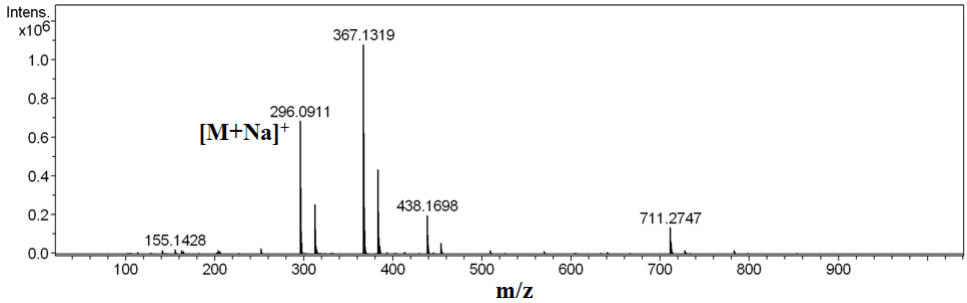

Figure 3.4. *ESI-MS spectrum of **7**.*

c) Synthesis of Nmoc-Ala(1)-Val(2)-OBn **8**: A solution of Nmoc-Ala-OH **7** (3.1 mmol, 0.846 g) and HOBt (3.1 mmol, 0.418 g) was stirred in 2 mL of DMF. A neutralized solution of valine benzyl ester (6.2 mmol, 2.349 g) was extracted from its corresponding *p*-toluene sulfonate salt and concentrated to add to the reaction mixture followed by dicyclohexylcarbodiimde (3.2 mmol, 0.659 g) at 0^{o}C and

allowed to stirred at room temperature for 12 hours. The mixture was diluted with ethyl acetate and organic layer was washed with 1M HCl (2 x 30 mL), brine solution, 1M Na_2CO_3 (3 x 30 mL) and brine solution. Ethyl acetate layer was dried over Na_2SO_4 and evaporated under vacuum to yield **8** as white powder. Purification was done by silica gel column (100-200 mesh) using ethyl acetate-toluene as eluent. Yield = 1.219 g (2.6 mmol, 83.87 %).

$[\alpha]_D^{25}$ -30° (c = 1, MeOH). ^{1}H NMR (400 MHz, $CDCl_3$): 7.83 (d, 4H, Nph), 7.51 (m, 3H, Nph), 7.48 (d 1H, NH), 7.45 (d 1H, NH), 7.37 (m,5H, Ph), 5.29 (s, 2H, CH_2 of Nph), 5.20 (dd, 2H, CH_2 of OBn), 4.61 (m, 1H, C^{α}H of Val), 4.31 (m, 1H, C^{α}H of Ala), 2.20 (m, 1H, C^{β}H of Val), 1.41 (d, 3H, C^{β}H of Ala), 0.88 (d, *J*=6.8 Hz, 6H, C^{γ}Hs of Val). MS (ESI) m/z for $C_{27}H_{30}N_2O_5$ $(M+Na)^+$ calcd.: 485.2047, found: 485.2123. Elemental Analysis calculated for $C_{27}H_{30}N_2O_5$: C, 70.11; H, 6.54; N, 6.06; Found: C, 70.14; H, 6.51; N, 6.04.

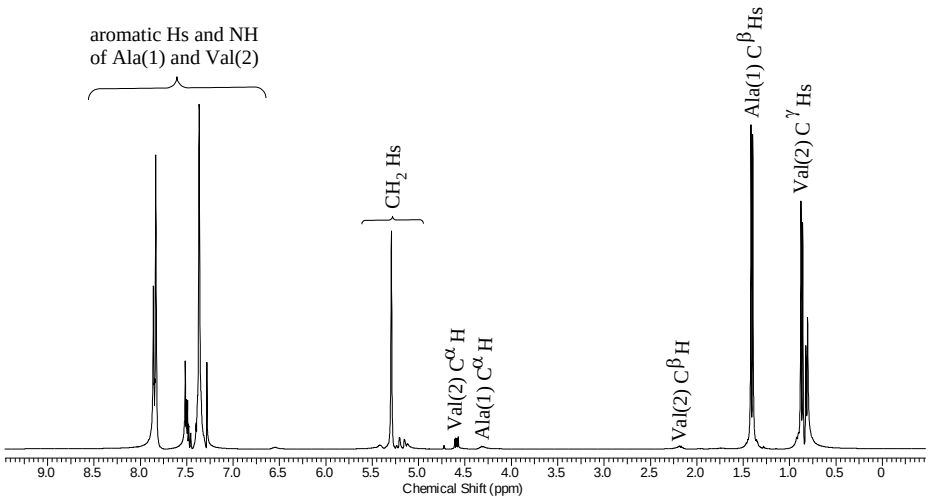

Figure 3.5. *400 MHz ^{1}H NMR spectrum of **8** in $CDCl_3$.*

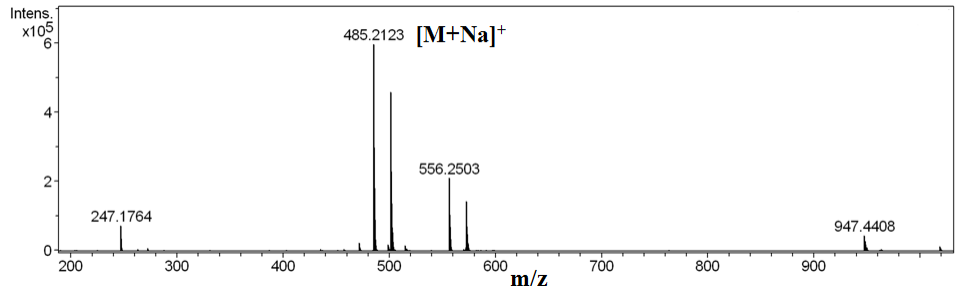

Figure 3.6. *ESI-MS spectrum of **8**.*

d) Synthesis of Nmoc-Ala(1)-Val(2)-OH **9**: A solution of Nmoc-Ala-Val-OBn **8** (1.180 g, 2.5 mmol) in 20 mL of dry MeOH was allowed to react with a solution of 10 mL 2M NaOH solution. The progress of reaction was monitored by thin layer chromatography (TLC). The reaction mixture was stirred upto 10 h. Then, methanol was removed under vacuum, residue was taken in 100 mL of water and washed with diethyl ether (2 x 20 mL). Then the pH of aqueous layer was adjusted to 2 using 2 M HCl and it was extracted with ethyl acetate (3 x 30 mL) and dried over anhydrous sodium sulfate and evaporated in vacuo to yield **9** as white powder and used further without purification. Yield = 0.716 g (1.9 mmol, 76 %).

$[\alpha]_D^{25}$ -14° (*c* = 1, MeOH). ^{1}H NMR (400 MHz, DMSO-d_6): 7.98 (t, 4H, Nph), 7.48 (d, 3H, *J* = 6.8 Hz Nph), 7.32 (d, 1H, NH of Val (2)), 7.09 (d, 1H, NH of Ala (1)), 5.19 (s, 2H), 4.18 (m, 2H, C^{α} H of Val(2) and Ala(1)), 2.06 (m, 1H, C^{β} H of Val (2)), 1.23 (d, *J* = 7.2 Hz, 3H, C^{β} Hs of Ala (1)), 1.1 (d, 6H C^{β} Hs of Val (2)). MS (ESI) m/z for $C_{20}H_{24}N_2O_5$ $(M+Na)^+$ calcd.: 395.1577, found: 395.1821. Elemental Analysis calculated for $C_{20}H_{24}N_2O_5$: C, 64.50; H, 6.50; N, 7.52; Found: C, 64.74; H, 6.53; N, 7.51.

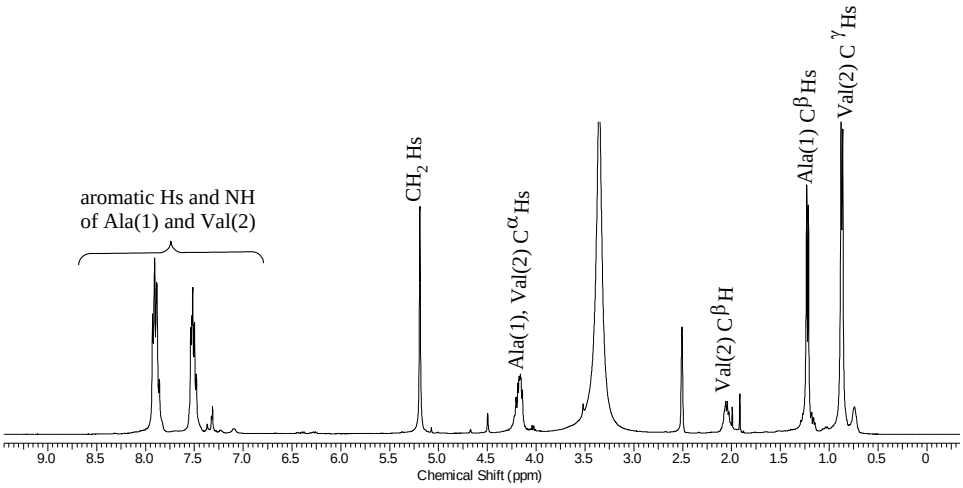

Figure 3.7. *400 MHz ^{1}H NMR spectrum of **9** in DMSO-d_6.*

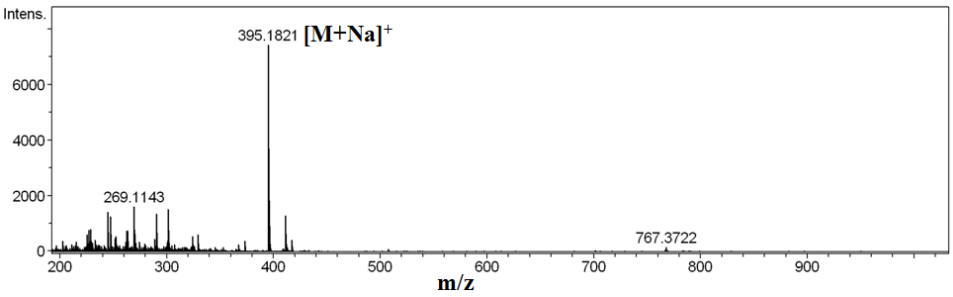

Figure 3.8. *ESI-MS spectrum of* ***9****.*

e) Synthesis of Nmoc-Ala(1)-Val(2)-*p*-Nitrophenol **1**: A solution of Nmoc-Ala-Val-OH **9** (0.690 g, 1.8 mmol) and 4-dimethyl amino pyridine (DMAP) (10 Mol %, 21.9 mg) was stirred in 2 mL of DMF. A *p*-Nitrophenol (0.264 g, 1.9 mmol) was added to the reaction mixture followed by DCC (2 mmol, 0.412 g) at 0 ^{o}C. The mixture was allowed to stir at room temperature for 12 h. The mixture was diluted with ethyl acetate and organic layer was washed with 0.1M HCl (2 x 30 mL), 1M $NaHCO_3$ (3 x 30 mL) and brine solution. The ethyl acetate layer was dried over Na_2SO_4 and evaporated under vacuum to yield **1** as yellow solid. Purification was done by silica gel column (100-200 mesh) using ethyl acetate-toluene as eluent. Yield= 751 g (1.5 mmol, 83.33 %).

$[\alpha]_D^{25}$ -12° (c = 1, MeOH). FT-IR (KBr): 3306(s), 3062 (m), 2965 (m), 1765 (s), 1694 (w), 1654 (m), 1525(s), 1451(w), 1344 (s), 1245(s) cm^{-1}. ^{1}H NMR (400 MHz, $CDCl_3$): 8.24 (d, 2H, *J*= 8.52 Hz, Ph), 8.14 (d, 1H, *J*=8.52 Hz, NH), 7.82 (d, 4H, Nph), 7.51 (d, 3H, Nph), 7.35 (s, 1H, NH), 7.24 (d, 2H, *J*= 8.56 Hz, Ph), 5.31 (s, 2H, CH_2 of Nph), 4.72 (m, 1H, C^{α} H of Val (2)), 4.39 (m, 1H, C^{α} H of Ala (1)), 2.33 (m, 1H, C^{β} H of Val (2)), 1.45 (d, 3H, C^{β} Hs of Ala (1)), 0.99 (d, 6H, C^{γ} Hs of Val (2)). ^{13}C NMR (100 MHz, $CDCl_3$): δ 188.17, 172.87, 169.59, 156.33, 154.95, 145.56, 133.41, 133.16, 128.40, 127.97, 127.23, 126.34, 126.11, 125.70, 125.27, 122.27, 115.65, 67.42, 57.55, 50.52, 33.84, 30.91, 25.19, 24.89, 19.05, 17.76. HRMS (ESI) m/z for $C_{26}H_{27}N_3O_7$ $(M+Na)^+$ calcd.: 516.1741, found: 516.2159. Elemental Analysis calculated for $C_{26}H_{27}N_3O_7$: C, 63.28; H, 5.51; N, 8.51; Found: C, 63.42; H, 5.53; N, 8.55.

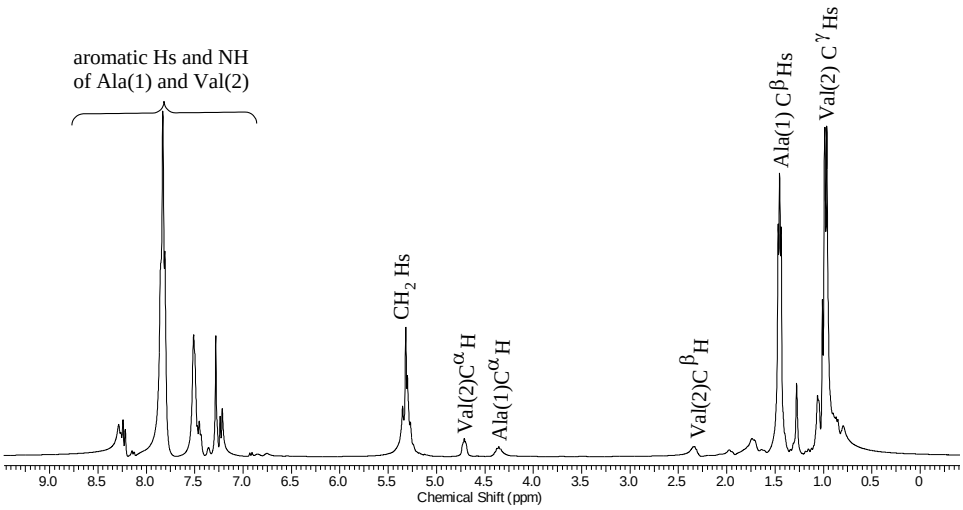

Figure 3.9. *400 MHz ^{1}H NMR spectrum of **1** in $CDCl_3$.*

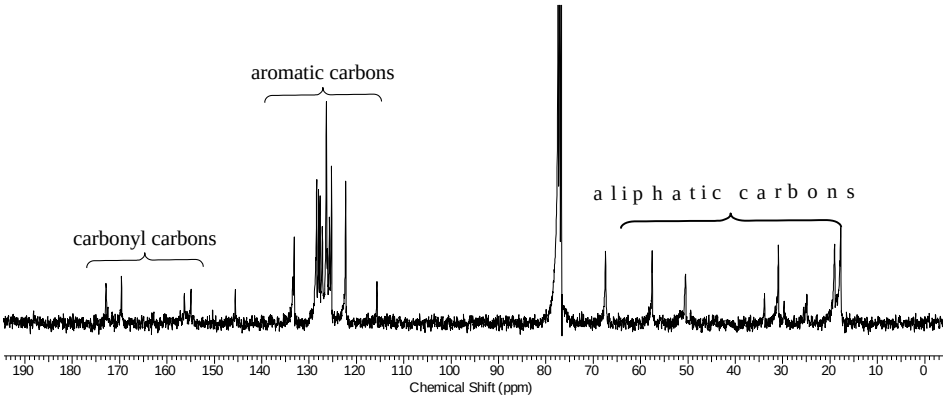

Figure 3.10. *100 MHz ^{13}C NMR spectrum of **1** in $CDCl_3$.*

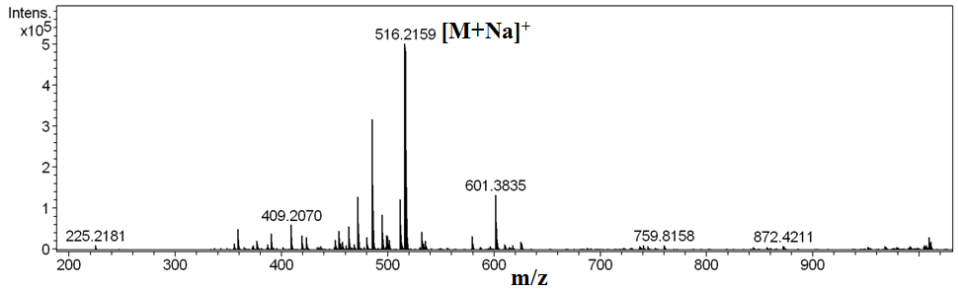

Figure 3.11. *ESI-MS spectrum of **1**.*

*3.2.2 Synthesis of Compound **2**:*

a) Synthesis of Nmoc-Val-OH **10**: A solution of valine (0.468 g, 4 mmol) in a mixture of 1, 4 dioxane (10 mL) and 1M sodium hydroxide (15 ml) was stirred and cooled in an ice-water bath. Naphthalene-2-methoxychloroformate **6** (0.882 g, 4 mmol) was added

and stirring was continued at room temperature for 12 h. Reaction mixture was diluted with 200 mL of water and dioxane was evaporated under vaccum. Aqueous layer was washed with diethyl ether and the pH of aqueous layer was adjusted to 2 with 2N hydrochloric acid. The aqueous phase was extracted with ethyl acetate (3 x 50 mL) and dried over Na_2SO_4 concentrated in vacuo to give **10** as colorless oil. Yield=0.863 g (2.8 mmol, 70 %).

$[\alpha]_D^{25}$ -5° (c = 1, MeOH). ^{1}H NMR (400 MHz, $CDCl_3$): 12.56 (s,1H, COOH), 7.90 (t, 4H, Nph), 7.53 (d, 3H, Nph), 7.37 (s, 1H), 5.22 (s, 2H, CH_2 of Nph), 4.02 (m, 1H, C^{α} H of Val), 2.08 (m, 1H, C^{β} H of Val), 0.92 (d, 6H, C^{γ} Hs of Val). MS (ESI) m/z for $C_{17}H_{19}NO_4$ $(M+Na)^+$ calcd.: 324.1206, found: 324.1228. Elemental Analysis calculated for $C_{17}H_{19}NO_4$: C, 67.76; H, 6.36; N, 4.65; Found: C, 67.65; H, 6.38, N, 4.63.

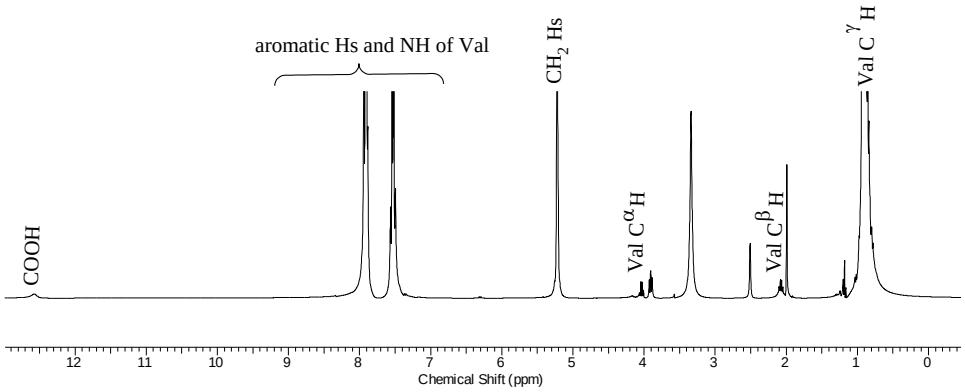

Figure 3.12. *400 MHz ^{1}H NMR spectrum of **10** in DMSO-d_6.*

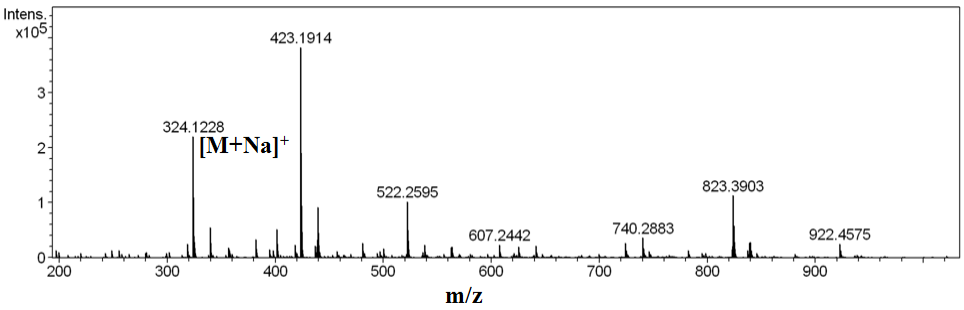

Figure 3.13. *ESI-MS spectrum of **10**.*

b) Synthesis of Nmoc-Val(1)-Ala(2)-OMe **11**: A solution of Nmoc-Val-OH **10** (0.602 g, 2.2 mmol) and HOBt (0.297 g, 2.2 mmol) was stirred in 2 mL of DMF. A neutralized solution of Alanine methyl ester (1.223 g, 8.8 mmol) was extracted from its corresponding hydrochloride salt and concentrated to add to the reaction mixture followed by dicyclohexylcarbodiimde (0.474 g, 2.2 mmol) at 0^{o}C and allowed to stirred at room temperature for 12 hours. The mixture was diluted with ethyl acetate and organic layer was washed with 1M HCl (2 x 30 mL), brine solution, 1M Na_2CO_3 (3 x 30 mL) and brine solution. Ethyl acetate layer was dried over Na_2SO_4 and evaporated under vacuum to yield **11** as white powder. Yield= 0.676 g, (1.6 mmol, 72.72 %).

$[\alpha]_D^{25}$ -41° (*c* = 1, MeOH). ^{1}H NMR (400 MHz, $CDCl_3$): 7.82 (d, 4H, *J*= 10.28 Hz, Nph), 7.49 (t, 3H, Nph), 7.44 (s, 1H, NH), 5.27 (s, CH_2 of Nph), 4.57 (t, 1H, C^{α} H of Ala (1)), 4.03(m,1H, C^{α} H of Val (2)), 3.73 (s, 3H, OCH_3), 2.13 (m, 1H, C^{β} H of Val (1)), 1.39 (d, 3H, *J*=7.8 Hz, C^{β} Hs of Ala (2)), 0.97 (d, 6H, *J*=7.28 Hz, C^{γ} Hs of Val (1)). HRMS (ESI) m/z for $C_{21}H_{26}N_2O_5$ $(M+Na)^+$ calcd.: 409.1734, found: 409.1694. Elemental Analysis calculated for $C_{21}H_{26}N_2O_5$: C, 65.27; H, 6.78; N, 7.25; Found: C, 65.08; H, 6.37; N, 7.49.

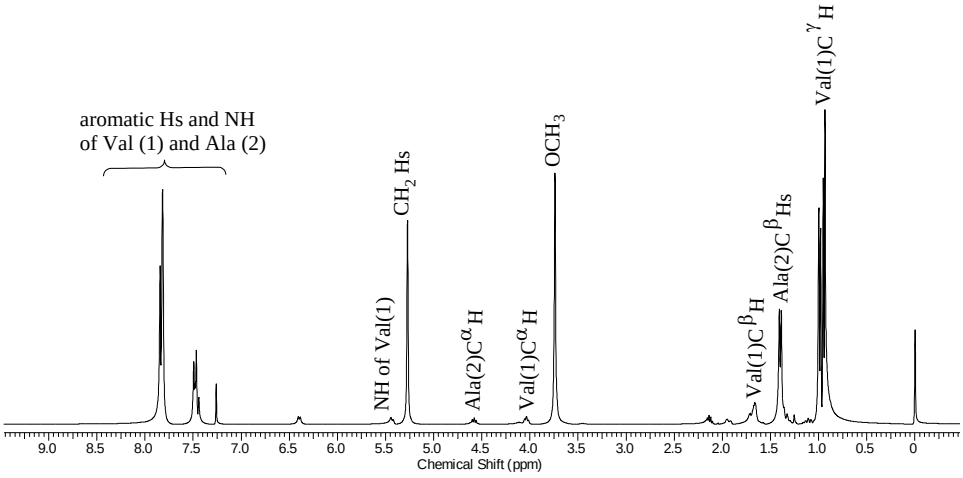

Figure 3.14. *400 MHz ^{1}H NMR spectrum of **11** in $CDCl_3$.*

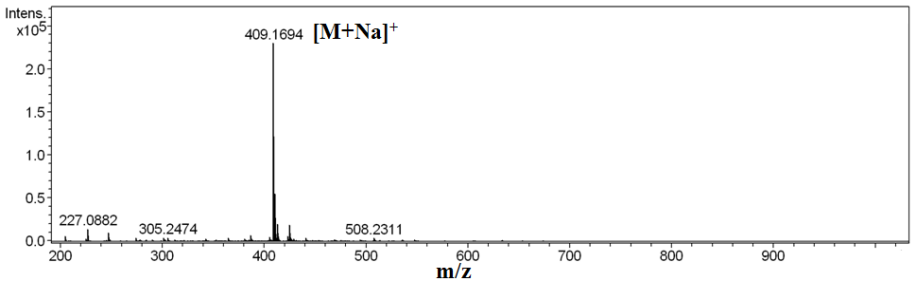

Figure 3.15. *ESI-MS spectrum of* ***11****.*

c) Synthesis of Nmoc-Val(1)-Ala(2)-OH **12**: A solution of Nmoc-Val-Ala methyl ester **11** (0.630 g, 1.5 mmol) in 20 mL of dry MeOH was allowed to react with a solution of 15 mL 2M NaOH solution. The progress of reaction was monitored by thin layer chromatography (TLC). The reaction mixture was stirred up to 10 h. Then, methanol was removed under vacuum, residue was taken in 100 mL of water and washed with diethyl ether (2 x 20 mL). Then the pH of aqueous layer was adjusted to 2 using 2 M HCL and it was extracted with ethyl acetate (3 x 30 mL) and dried over anhydrous sodium sulfate and evaporated in vacuo to yield **12** as white powder and used further without purification. Yield= 0.538 g (1.4 mmol, 93.33 %) $[\alpha]_D^{25}$ -36° (c = 1, MeOH). ^{1}H NMR (400 MHz, DMSO-d_6): 8.22 (d, 1H, J=7.76 Hz, NH), 7.91 (t, 4H, Nph), 7.51 (t, 3H, Nph), 7.31(d, 1H, NH), 5.20 (s, CH_2 of Nph), 4.21 (t, 1H, C^{α} H of Ala (2)), 3.92 (m, 1H, C^{α} H of Val (1)), 1.91 (m, 1H, C^{β} H of Val (1)), 1.26 (d, 3H, C^{β} Hs of Ala (2)), 0.91 (d, 6H, *J*=7.52 Hz, C^{γ} Hs of Val(1)). HRMS (ESI) m/z for $C_{20}H_{24}N_2O_5$ $(M+Na)^+$ calcd.: 395.1611, found: 395.1698. Elemental analysis calculated for $C_{20}H_{24}N_2O_5$: C, 64.50; H, 6.50; N, 7.52; Found: C, 64.36; H, 6.53; N, 7.53.

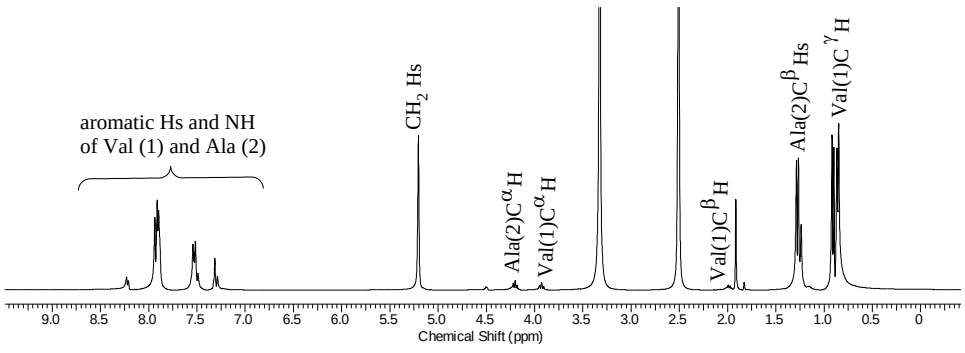

Figure 3.16. *400 MHz ^{1}H NMR spectrum of* ***12*** *in DMSO-d_6.*

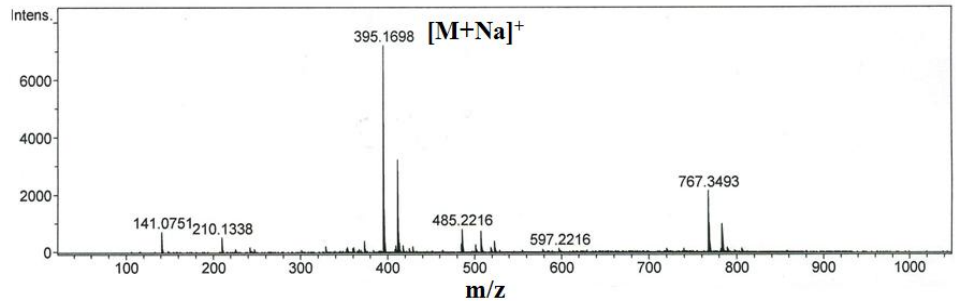

Figure 3.17. *ESI-MS mass spectrum of* ***12****.*

d) Synthesis of Nmoc-Val-Ala-*p*-nitrophenol **2**: A solution of Nmoc-Val-Ala-OH **12** (0.508 g, 1.3 mmol) and 4-Dimethyl amino pyridine (DMAP) (5 mol%, 8 mg) was stirred in 2 mL of DMF. A *p*-Nitrophenol (0.217 g, 1.5 mmol) was added to the reaction mixture followed by DCC (0.288 g, 1.4 mmol) at 0 °C. The mixture was allowed to stir at room temperature for 12 h. The mixture was diluted with ethyl acetate and organic layer was washed with 0.1M HCl (2 x 30 mL), 1M $NaHCO_3$ (3 x 30 mL) and brine solution. The ethyl acetate layer was dried over Na_2SO_4 and evaporated under vacuum to yield **2** as yellow solid. Purification was done by silica gel column (100-200 mesh) using ethyl acetate-toluene as eluent. Yield = 0.545 g (1.1 mmol, 84.61%).

$[\alpha]_D^{25}$ -33° (*c* = 1, MeOH). FT-IR (KBr): 3321(s), 3058 (w), 2930 (s), 2851(m), 1760 (s), 1688 (s), 1627 (s), 1528 (s), 1450 (m), 1381 (s), 1245 (m) cm^{-1}. ^1H NMR (100 MHz, $CDCl_3$): δ 8.23 (d, 2H, Ph), 8.12 (d, 1H, NH), 7.81 (d, 4H, Nph), 7.49 (d, 3H, Nph), 7.18 (d, 2H, *J*= 7 Hz, Ph), 5.27 (s, 2H, CH_2 of Nph), 4.75 (t, 1H, C^{α} H of Ala (2)), 4.10 (m, 1H, C^{α} H of Val (1)), 2.17 (m, 1H, C^{β} H of Val (1)), 1.93 (d, 3H, C^{β} Hs of Ala (2)), 0.95 (d, 6H, *J*=5.28 Hz, C^{α} Hs of Val (1)). ^{13}C NMR (100 MHz, $CDCl_3$) δ 171.32, 170.44, 156.75, 155.03, 133.53, 133.16, 128.38, 127.95, 127.70, 126.32, 125.66, 125.28, 122.22, 67.35, 60.35, 60.14, 49.18, 48.43, 33.92, 31.00, 30.99, 25.58, 24.92, 19.13, 17.84, 17.57. HRMS (ESI) m/z for $C_{26}H_{27}N_3O_7$ $(M+Na)^+$ calcd.: 516.1741, found: 516.1630; Elemental analysis calculated for $C_{26}H_{27}N_3O_7$: C, 63.28; H, 5.51; N, 8.51; Found: C, 63.55; H, 5.54; N, 8.50.

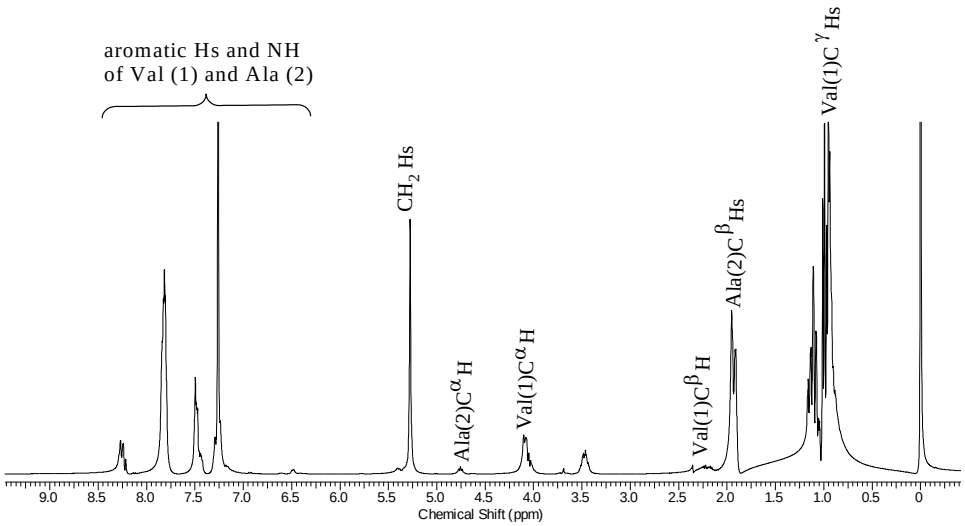

Figure 3.18. *400 MHz ^{1}H NMR spectrum of **2** in $CDCl_3$.*

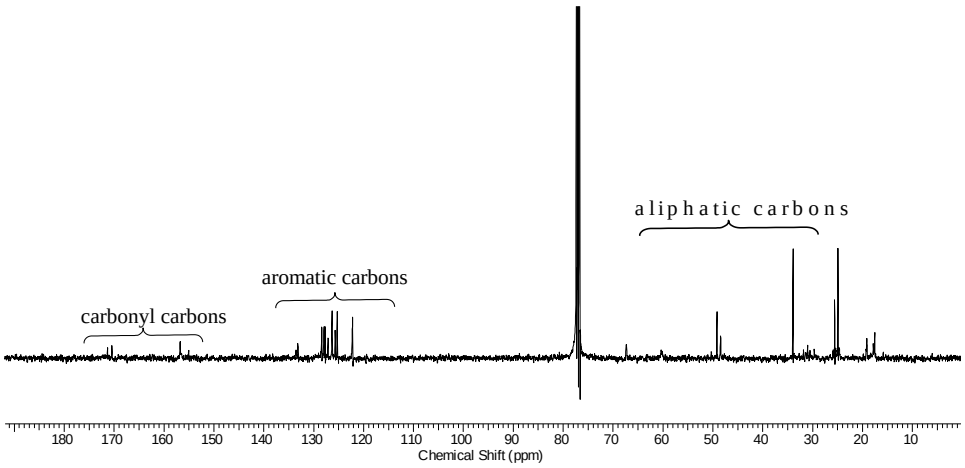

Figure 3.19. *100 MHz ^{13}C NMR spectrum of **2** in $CDCl_3$.*

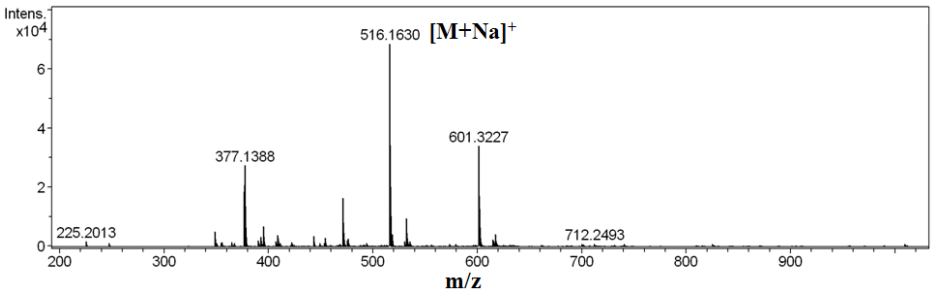

Figure 3.20. *ESI-MS spectrum of **2**.*

*3.2.3 <u>Synthesis of Compound **3**</u>:*

a) Synthesis of Nmoc-Val-*p*-nitrophenol **3**: A solution of Nmoc-Val-OH **10** (0.820 g, 2.7 mmol) and 4-dimethyl amino pyridine

(DMAP) (5 mol%, 15.8 mg) was stirred in 2 mL of DMF. *p*-Nitrophenol (0.393 g, 2.83 mmol) was added to the reaction mixture followed by DCC (0.598 g, 2.9 mmol) at 0°C. The mixture was allowed to stir at room temperature for 12 h. The mixture was diluted with ethyl acetate and organic layer was washed with 0.1M HCl (2 x 30 mL), 1M $NaHCO_3$ (3 x 30 mL) and brine solution. The ethyl acetate layer was dried over Na_2SO_4 and evaporated under vacuum to yield **3** as yellow solid. Purification was done by silica gel column (100-200 mesh) using ethyl acetate-toluene as eluent. Yield= 0.832 g (1.9 mmol, 70.37%).

$[\alpha]_D^{25}$ -11° (*c* = 1, MeOH). FT-IR (KBr): 3299(s), 3055 (m), 2966 (s), 2893(sm), 1762 (s), 1685 (w), 1614 (m), 1520(s), 1488(m), 1341 (s), 1245(w) cm^{-1}; ^1H NMR (400 MHz, $CDCl_3$): 8.15 (d, 2H, *J*= 9.04 Hz, Ph), 7.75 (d, 4H, Nph), 7.40 (t, 3H, Nph), 7.14 (d, 2H, J=9.04 Hz, Ph) 7.28 (d, 1H, NH), 5.23 (s, 2H, CH_2 of Nph), 4.46 (t, 1H, C^{α} H of Val), 2.26 (m, 1H, C^{β} H of Val), 0.97 (d, 6H, C^{γ} Hs of Val). ^{13}C NMR (100 MHz, $CDCl_3$) δ 170.05, 156.36, 154.97, 145.56, 133.44, 133.17, 128.43, 127.98, 127.72, 127.35, 126.36, 126.13, 125.81, 125.26, 122.28, 121.94, 72.12, 67.53, 59.46, 31.67, 19.14, 17.76. MS (ESI) m/z for $C_{23}H_{22}N_2O_6$ $(M+Na)^+$ calcd.: 445.1370, found: 445.1458; Elemental Analysis calculated for $C_{23}H_{22}N_2O_6$: C, 65.39; H, 5.25; N, 6.63; Found: C, 65.59; H, 5.26; N, 6.60.

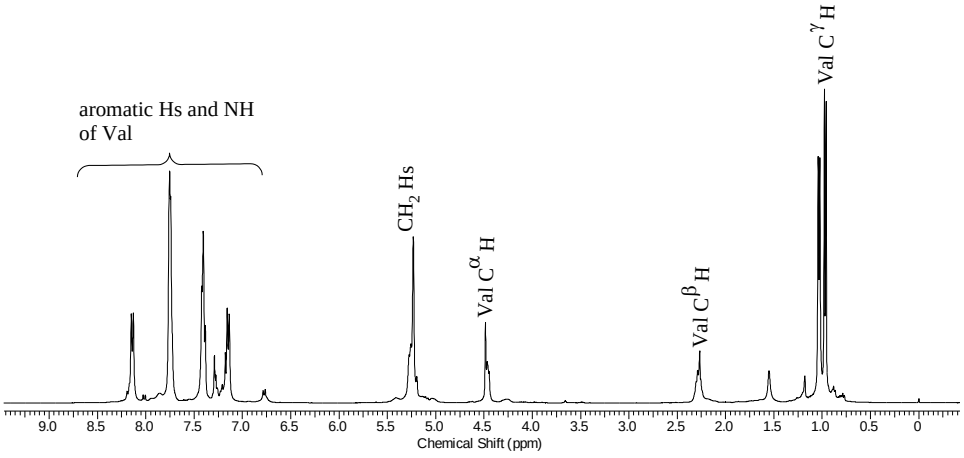

Figure 3.21. *400 MHz ^1H NMR spectrum of **3** in $CDCl_3$.*

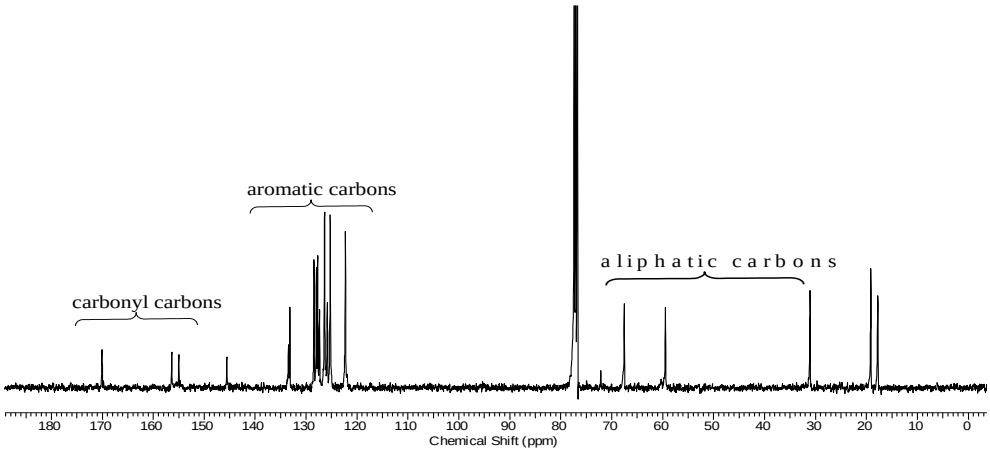

Figure 3.22. *100 MHz ^{13}C NMR spectrum of **3** in $CDCl_3$.*

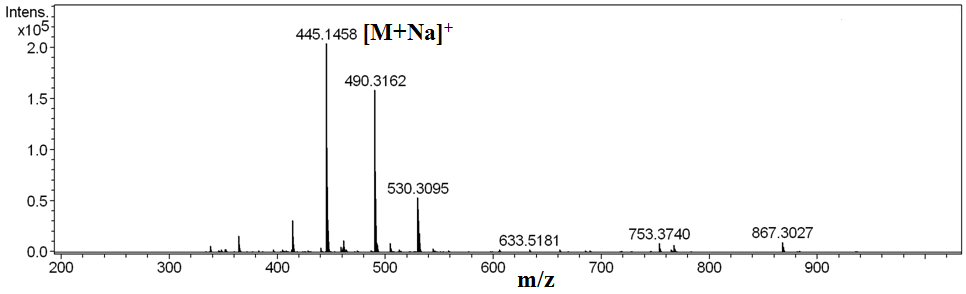

Figure 3.23. *ESI-MS spectrum of **3**.*

*3.2.4 Synthesis of Compound **4**:*

a) Synthesis of Nmoc-Ala-*p*-nitrophenol **4**: A solution of Nmoc-Ala-OH **7** (0.529 g, 1.9 mmol) and 4-dimethyl amino pyridine (DMAP) (5 Mol %, 11.5 mg) was stirred in 2 mL of DMF. A *p*-Nitrophenol (0.278 g, 2 mmol) was added to the reaction mixture followed by DCC (2 mmol, 0.412 g) at 0^oC. The mixture was allowed to stir at room temperature for 12 h. The mixture was diluted with ethyl acetate and organic layer was washed with 0.1M HCl (2 x 30 mL), 1M $NaHCO_3$ (3 x 30 mL) and brine solution. The ethyl acetate layer was dried over Na_2SO_4 and evaporated under vacuum to yield **4** as yellow solid. Purification was done by silica gel column (100-200 mesh) using ethyl acetate-toluene as eluent. Yield = 0.618 g (1.5 mmol, 78.94%).

$[\alpha]_D^{25}$ -17° (*c* = 1, MeOH). FT-IR (KBr): 3381(s), 3056 (m), 2920 (m), 1763 (s), 1617 (m), 1592(m), 1513(m), 1345 (s), 1291(m) cm^{-1}. ^1H NMR (400 MHz, $CDCl_3$): 8.23 (d,1H, *J*= 8.28 Hz, Ph), 7.85 (d, 4H,

Nph), 7.51 (t, 3H, Nph), 7.47 (s, 1H, NH), 7.25 (d, 2H, *J*= 8 Hz, Ph), 5.33 (s, 2H, CH_2 of Nph), 4.65 (m, 1H C^{α} H of Ala), 1.63 (d, 3H, C^{β} Hs of Ala); ^{13}C NMR (100 MHz, $CDCl_3$) δ 170.86, 161.57, 155.80, 155.00, 145.54, 133.40, 133.14, 128.41, 127.96, 127.69, 126.36, 126.18, 125.76, 125.21, 122.18, 115.58, 67.45, 50.01, 34.99, 26.69, 18.02. MS (ESI) m/z for $C_{21}H_{18}N_2O_6$ $(M+Na)^+$ calcd.:417.1057, found: 417.4989. Elemental Analysis calculated for $C_{21}H_{18}N_2O_6$: C, 63.96; H, 4.60; N, 7.01; Found: C, 64.13; H, 4.62; N, 6.98.

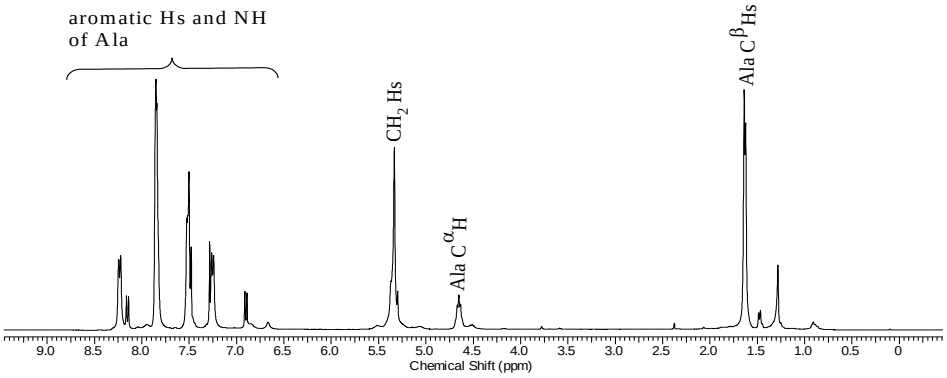

Figure 3.24. *400 MHz ^1H NMR spectrum of **4** in $CDCl_3$.*

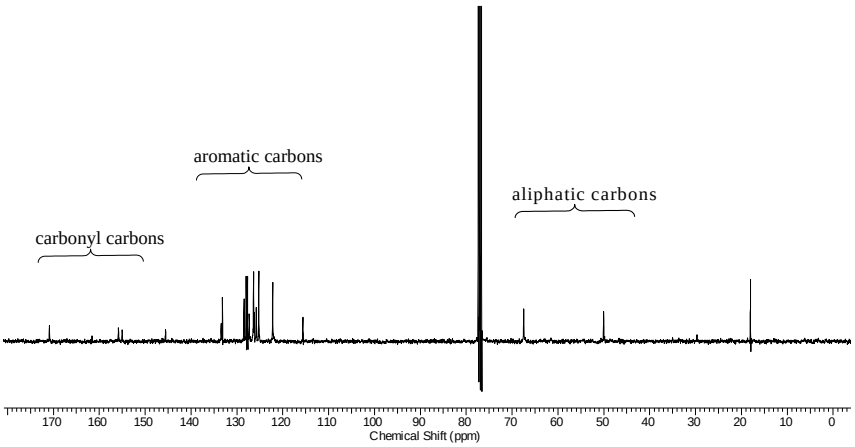

Figure 3.25. *100 MHz ^{13}C NMR spectrum of **4** in $CDCl_3$.*

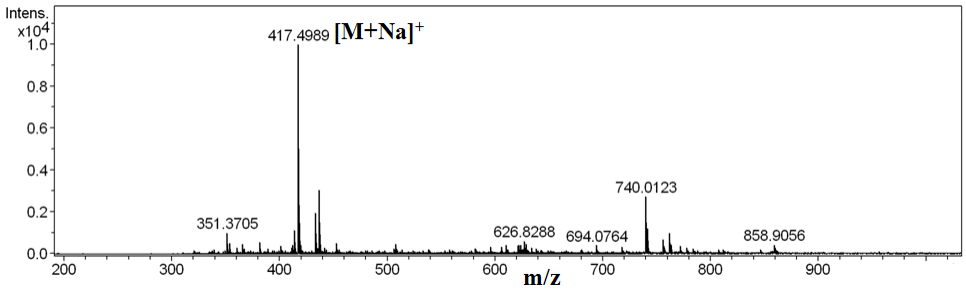

Figure 3.26. *ESI-MS spectrum of **4**.*

*3.2.5 Synthesis of Compound **5**:*

a) Synthesis of Nmoc-Phe-OH **13**: A solution of L-phenylalanine (0.825 g, 5 mmol) in a mixture of 1, 4 dioxane (10 mL) and 1M sodium hydroxide (15 mL) was stirred and cooled in an ice-water bath. Napthalene-2-methoxychloroformate **6** (1.102 g, 5 mmol) was added and stirring was continued at room temperature for 12 h. Reaction mixture was diluted with 200 mL of water and dioxane was evaporated under vaccum. Aqueous layer was washed with diethyl ether and the pH of aqueous layer was adjusted to 2 with 2N hydrochloric acid. The aqueous phase was extracted with ethyl acetate (3 x 50 mL) and dried with Na_2SO_4 and concentrated in vacuo to give **13** as colorless oil. Yield= 1.46 g, (4.1 mmol, 82 %)

$[\alpha]_D^{25}$: -7° (*c* = 1, MeOH). ^{1}H NMR (400 MHz, DMSO-d_6): 12.75 (s, 1H, COOH), 7.88 (d, 4H, Nph), 7.73 (d, 1H, *J*=8.04 Hz, Nph), 7.53 (t, 2H, Nph), 7.41 (d, 1H, *J*= 8.28, NH), 7.21 (m, 5H, Phe), 5.16 (s, 2H CH_2 of Nph), 4.21 (q, 1H, C^{α} H of Phe), 3.11 (d, 1H, *J*=11.2 Hz, C^{β} H of Phe), 2.86 (t, 1H, C^{β} H of Phe). HRMS (ESI) m/z for $C_{21}H_{19}NO_4$ $(M+Na)^+$ calcd.: 372.1212, found: 372.1206. Elemental Analysis calculated for $C_{21}H_{19}NO_4$: C, 72.19; H, 5.48; N, 4.01; Found: C, 72.21; H, 5.53; N, 4.11.

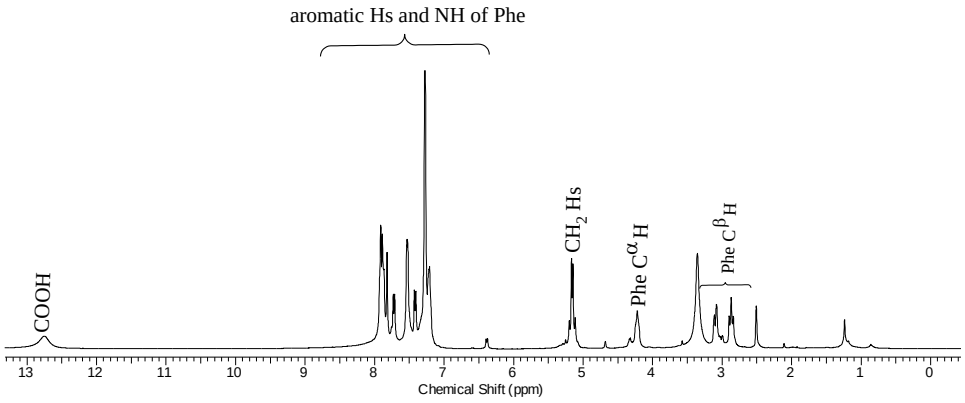

Figure 3.27. *400 MHz ^{1}H NMR spectrum of **13** in DMSO-d_6.*

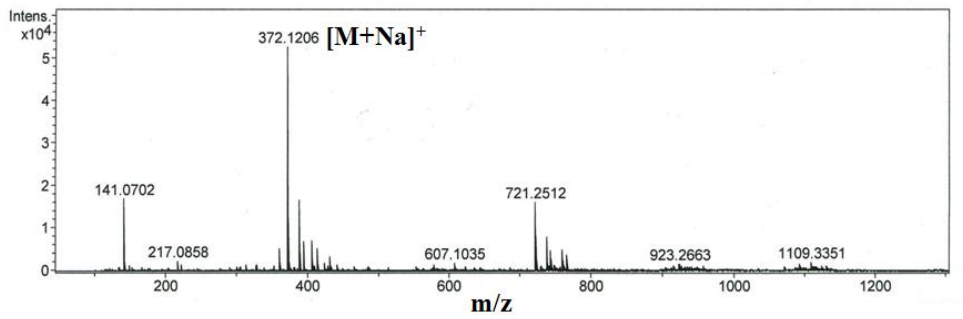

Figure 3.28. *ESI-MS spectrum of* ***13****.*

b) Synthesis of Nmoc-Phe-*p*-nitrophenol: A solution of Nmoc-F-OH (1.25 g, 3.5 mmol) and 4-Dimethyl amino pyridine (DMAP) (10 Mol %, 42.7 mg) was stirred in 2 mL of DMF. A *p*-Nitrophenol (0.264 g, 1.9 mmol) was added to the reaction mixture followed by DCC (4.2 mmol, 0.583 g) at 0^{o}C. The mixture was allowed to stir at room temperature for 12 h. The mixture was diluted with ethyl acetate and organic layer was washed with 0.1M HCl (2 x 30 mL), 1M $NaHCO_3$ (3 x 30 mL) and brine solution. The ethyl acetate layer was dried over Na_2SO_4 and evaporated under vacuum to yield as yellow solid. Purification was done by silica gel column (100-200 mesh) using ethyl acetate-toluene as eluent Yield= 1.50 g (3.1 mmol, 85.57 %).

$[\alpha]_D^{25}$: -40° (c = 1, MeOH). FT-IR (KBr): 3322 (s), 3057 (m), 2924 (m), 2857 (m), 1763 (s), 1686 (s), 1594 (s), 1510 (m), 1453 (m), 1347 (s), 1301 (m), 1252(s) cm^{-1}. ^{1}H NMR (400 MHz, $CDCl_3$): 8.17 (d, 2H, *J*= 8.28 Hz, Ph), 7.79 (d, 4H, Nph), 7.48 (d, 3H, *J*= 3.52 Hz, Nph), 7.44 (d, 1H, *J*=8.52 Hz, Nph), 7.21 (d, 2H, *J*= 6.52 Hz, Nph), 7.30 (m, 5H, Phe), 7.21 (d, 1H, *J*= 6.52 Hz, NH), 7.02 (d, 2H, *J*= 8.28 Hz, Ph), 5.28 (s, 2H, CH_2 of Nph), 4.88 (t, 1H, C^{α}H of Phe), 3.24 (d, 2H, C^{β}Hs of Phe). ^{13}C NMR (100 MHz, $CDCl_3$) δ 169.60, 161.92, 155.92, 154.78, 145.56, 135.04, 133.33, 133.17, 129.29, 128.98, 128.44, 127.97, 127.72, 127.67, 127.35, 126.39, 126.16, 125.76, 125.20, 122.18, 115.59, 67.59, 55.28, 38.08, 29.70. MS (ESI) m/z for $C_{27}H_{22}N_2O_6$ $(M+Na)^+$ calcd.: 493.1376, found: 493.1683. Elemental Analysis calculated for $C_{27}H_{22}N_2O_6$: C, 68.93; H, 4.71; N, 5.95; Found: C, 67.97; H, 4.84; N, 6.07.

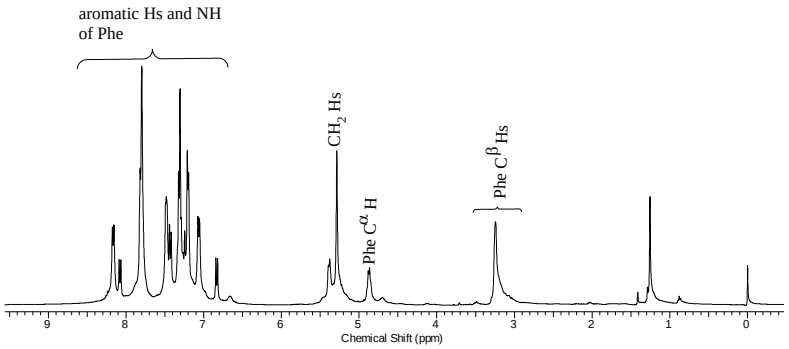

Figure 3.29. *400 MHz ^{1}H NMR spectrum of **5** in $CDCl_3$.*

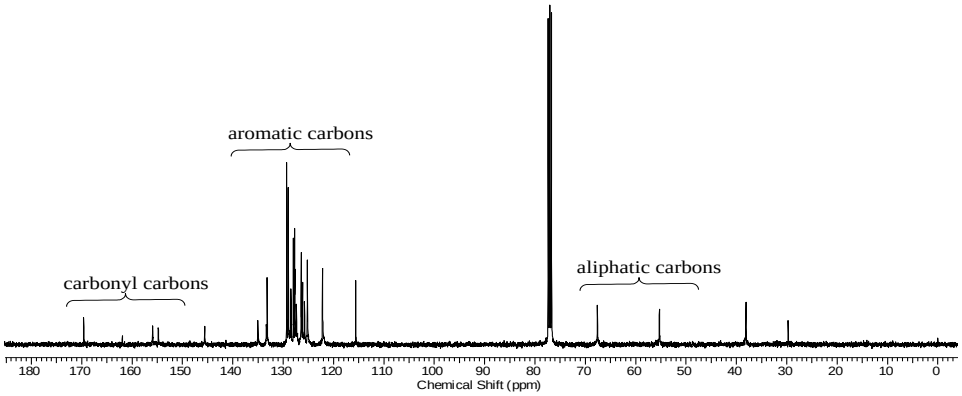

Figure 3.30. *100 MHz $^{13}CNMR$ spectrum of **5** in $CDCl_3$.*

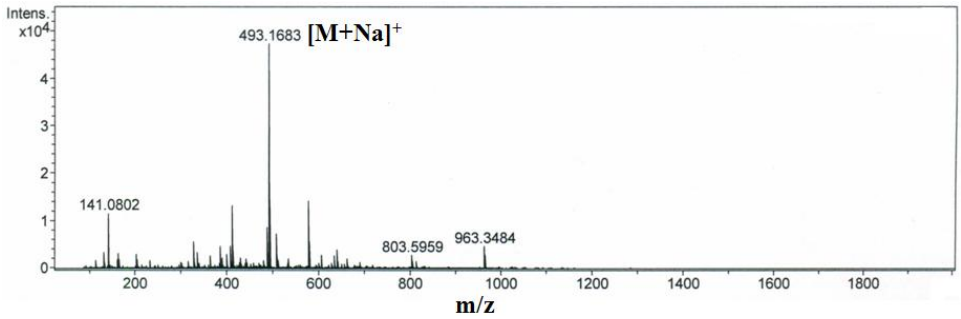

Figure 3.31. *ESI-MS spectrum of **5**.*

3.3 Gel Preparation and Characterization Techniques

3.3.1 Gel Preparation

A compound **1** Nmoc-AV-*p*NP (20 mmol L^{-1}, 9.8 mg) was dissolved in 100 µL of methanol. A solution of cysteine (80 mmol L^{-1}, 9.6 mg) in phosphate buffer 900 µL (pH 8) was mixed together to homogeneous followed by incubation for 15 min at 80 °C. Self-assembly of ligated

product **1b** was observed after 6h of native chemical ligation reaction. Formation of Nmoc-AVC and Nmoc-AVC-CVA-Nmoc were confirmed by HPLC and ESI-MS. Similarly, compound **5** Nmoc-F-*p*NP (20 mmol L^{-1}, 9.4 mg) was ligated to cysteine at same reaction condition. Self-assembly of ligated product **5b** was observed after 3h of native chemical reatcion. Synthesized products Nmoc-FC **5a** and Nmoc-FC-CF-Nmoc **5b** were confirmed by HPLC and ESI-MS.

3.3.2 Gel-Sol Transition

Self-assembly and dis-assembly were observed for gelators **1b** and **5b** as described in the text. **1a** transforms into **1b** upon exposure to air resulting into the formation of self-supporting strong gel. Gel-sol transition occurred after 3h after addition of reductant Tris(2-carboxyethyl)phosphine (TCEP) 40 mmol/L to **1b** gel at pH 5.2. However, quick gel-sol transition was observed for compound **5b** (1.5 h) at pH 4.8. TCEP is an effective reductant which can cleave disulfide linkage.

3.3.3 ^{1}H NMR Spectroscopy

All NMR spectra were recorded at 400 MHz Bruker AV 400 NMR spectrometer. TMS was used a internal reference in the NMR spectra. Peptides concentrations were in the range of 1-10 mmol in $(CD_3)_2SO$ and $CDCl_3$.

3.3.4 Polarimeter

Specific rotations of the synthesized peptides were measured on an Autopol V automatic polarimeter (Rudolph research analytical). The cell (length =100 mm, capacity = 2 mL) was used for this study at 25 ^{o}C.

3.3.5 Mass Spectrometry

Mass spectra of peptides were recorded on Bruker micrOTOF-Q II by positive and negative mode electrospray ionizations.

3.3.6 High Performance Liquid Chromatograpy Analysis

A Dionex HPLC-Ultimate 3000 (High Performance Liquid Chromatography) pump was used to analyze native chemical ligated products. A 20 μL of sample was injected onto a Dionex Acclaim ® 120 C 18 column of 250 mm length with an internal diameter 4.6 mm and 5 μm fused silica particles at a flow rate of 1 mL min^{-1} (linear gradient of 40 % v/v) acetonitrile in water for 35 min, gradually rising to 100 % (v/v) acetonitrile in water at 35 min). This concentration was kept constant until 40 min when the gradient was decreased to 40 % (v/v) acetonitrile in water at 42 min. The sample preparation involved mixing 100 μL of gel/solution with acetonitrile-water (900 μL, 50: 50 mixture) containing 0.1 % trifluoacetic acid. The samples were then filtered through a 0.45 μm syringe filter (Whatman, 150 units, 13 mm diameter, 2.7 mm pore size) prior to injection. The native chemical ligated products were identified by using Ultimate 3000 RS Variable Wavelength Detector at 280 nm.

3.3.7 Rheology

Rheological measurement was carried out using an Anton Paar Physica MCR 301 rheometer with parallel plate of geometry (25 mm in diameter, 0.200 μm gap). 200 μL of **1b** and **5b** gels were prepared in glass vials and transfered onto the plate of the instrument using microspatulla. The temperature was kept at 25°C by using an integrated temperature controller. Then dynamic frequency sweep of the gel Nmoc-AVC- CVA-Nmoc and Nmoc-FC-CF-Nmoc were measured as function of frequency in the range of 0.05-100 rad s^{-1} with constant strain value 0.05%. The time sweep was measured at constant strain of 0.05%. To determine the exact strain for frequency sweep and time sweep experiments the linear viscoelastic (LVE) regime were performed at constant frequency of 10 rad s^{-1}.

3.3.8 FT-IR Spectroscopy

Fourier transform infrared (FTIR) spectra were recorded using a bruker (Tensor 27) FTIR spectrophotometer for solid samples and wet gel material by using ZnSe windows. The gel samples were placed between crystal Zn-Se windows and scanned between 400 and 4000 cm^{-1} over 64 scans at a resolution of 4 cm^{-1} and an interval of 1 cm^{-1}.

3.3.9 Circular Dichroism

Circular dichroism (CD) spectra were measured at 25°C on a Jasco J-815 spectropolarimeter. Spectra were measured between 300 and 190 nm with a data pitch of 0.1 nm. The bandwidth was set to 1 nm with a scanning speed of 20 nm min^{-1} and a response time of 1 s. The path length was 1 mm quartz cell (Starna Scientific Ltd. Hainault, UK). Samples were prepared at concentration of 20 mmol L^{-1}. Experimental data were acquired in thrice and the average data is shown.

3.3.10 Fluorescence Spectroscopy

Fluorescence spectra of gel **1b** as well as solution **1** were recorded from 275-650 nm, exciting at 265 nm, using slit settings of 2 nm, with medium sensitivity on a Horiba Scientific Fluoromax-4 spectrophotometer. Samples were prepared in path length 1 cm quartz cuvettes at room temperature.

3.3. 11 Microscopic Study

Transmission electron microscopic images were taken using a PHILIPS electron microscope (model: CM 200), operated at an accelerating voltage of 200 kV. Dilute solution of the gel was dried on carbon-coated copper grids (300 mesh) by slow evaporation in air, then allowed to dry separately in a vacuum at room temperature.

Field-emission Gun-scanning electron microscopic study was done by using Jeol Scanning Microscope-JSM-7600F. The gel samples were dried on a glass cover slip and coated with platinum. Finally the morphology of gels was investigated using a tapping- mode atomic force microscope (AFM). AFM study was done by placing very dilute solution of gel (200 µL of gel was dissolved in 800 µL of milii-Q water) on mica and allowed it dry in air for 2 days at room temperature. Images were recorded by using scanning probe microscope AIST-NT instrument (model no. smart SPM-1000).

3.4 Results and Discussion

In this chapter a chemoselective native chemical ligation has been used to drive peptide self-assembly at sterically hindered amino acids. We anticipated that steric crowding at the C-terminal ligation site would not give full conversion to ligated products. Here, Nmoc-AV-*p*-NP ester **1** and Nmoc-F-*p*-NP ester **5** ligated with cysteine (Figure 3.32). In this procedure, peptides Nmoc-AVC **1a** and Nmoc-FC **5a** were obtained in 99% yield via an intermediate state under an inert atmosphere.

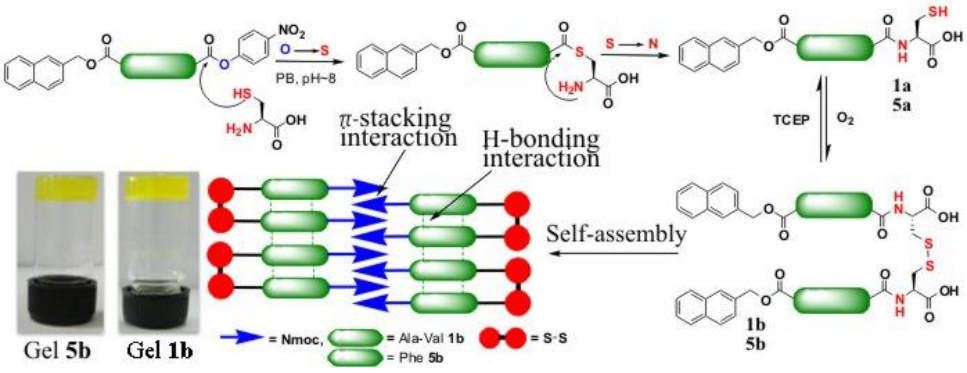

Figure 3.32. *Native chemical ligation at Nmoc-protected-p-NP esters. The cysteine amino acid induces O→S exchange with Nmoc-protected-p-NP* ***1*** *or* ***5*** *(step I) to form a thioester intermediate. Subsequent S →N acyl transfer furnishes the peptide bond* ***1a*** *or* ***5a*** *(step II). Air oxidation provides the formation of ligated disulfide* ***1b*** *or* ***5b*** *(step III) resulting in supramolecular peptide gels.*

3.4.1 Ligation Study

Compound **1** (0.9 wt%) was dissolved in 100 mL of methanol followed by a solution of cysteine in phosphate buffer (900 mL, pH 7.5–8) slowly and incubated up to 80°C for 15 min under an inert atmosphere (Figure 3.33A). The HPLC analysis showed 99% NCL prior to air exposure. Interestingly, the HPLC data revealed the formation of two products.[11] Two parallel peaks appeared in the HPLC chromatogram with 49% and 50% conversion, which were further analyzed with ESI-MS (Figure 3.33B and C). ESI-MS data support ligated product mass only, which confirms the dual product mass for the intermediate state and ligated product.

The ligated products were left undisturbed in atmospheric air. Strong self-supporting gels of **1**/**1b** and **5**/**5b** were observed after 6 h and 3 h of reaction. However, compounds **2**, **3** and **4** could not form gels under similar conditions. Precipitation was observed after 6 h of reaction for compounds **2**, **3** and **4**. All the ligated products were characterized by HPLC and ESI-MS.

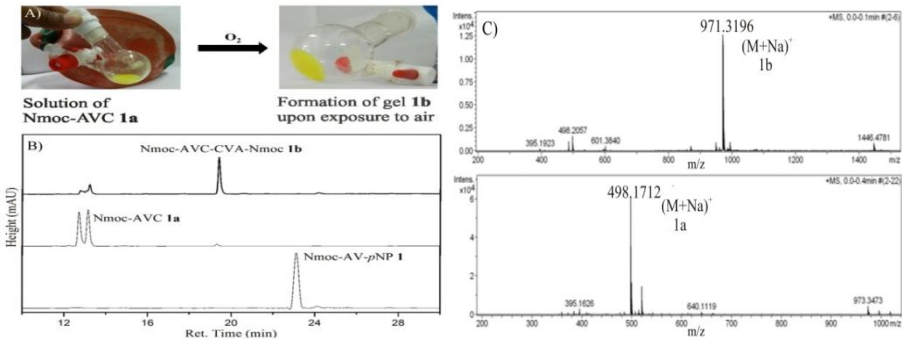

Figure 3.33. *(A) NCL reaction carried out in argon atmosphere. A solution of Nmoc-AVC turns to gel upon exposure to air. (B) Results of HPLC analysis represent the formation of ligated product **1a** and its corresponding disulfide **1b** upon reaction of **1** with cysteine. (C) Mass spectra for Nmoc-AVC **1a** and Nmoc-AVC-CVA-Nmoc **1b**.*

*Table 3.1. Gelation properties of ligated products obtained from compounds **1-5**.*

Entry	Starting material[a]	Yield (%) (Inert atm.)	Yield (%) (disulfide)	Gel formation[b]
1.	Nmoc-AV-*p*NP **1**	99 (biphasic) **1a**	84.51 **1b**	G
2.	Nmoc-VA-*p*NP **2**	85.86 **2a**	83.31 **2b**	P
3.	Nmoc-V-*p*NP **3**	69.13 **3a**	98 **3b**	P
4.	Nmoc-A-*p*NP **4**	99 **4a**	35.11 **4b**	P
5.	Nmoc-F-*p*NP **5**	99.2 **5a**	99 **5b**	G

[a] *p*NP = *p*-nitro phenol, [b]G = gelation, P = precipitation

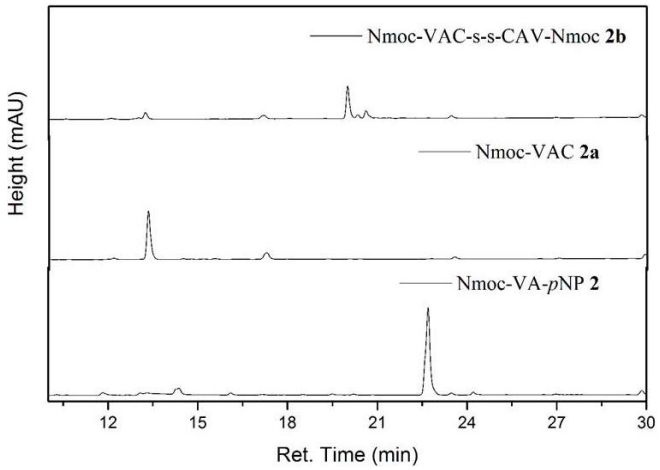

***Figure 3.34.** Overlaid HPLC chromatographs for compound **2** showing peak **2a** after native chemical ligation and peak **2b** for its corresponding disulfide.*

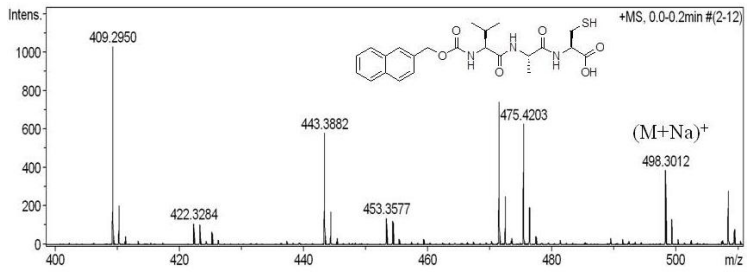

***Figure 3.35.** ESI-MS spectrum of compound **2a**.*

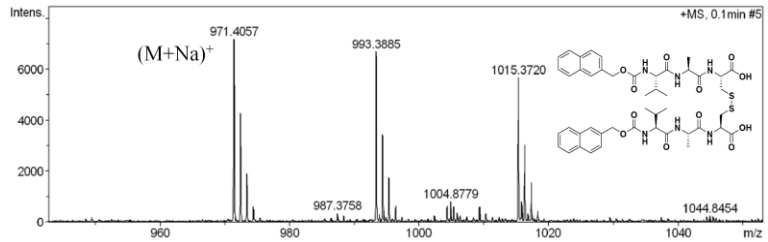

***Figure 3.36.** ESI-MS spectrum of compound **2b**.*

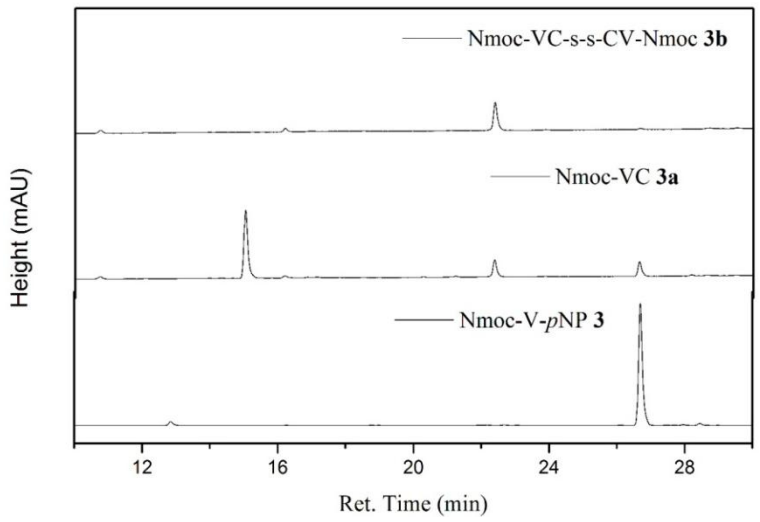

Figure 3.37. *Overlaid HPLC chromatographs for compound **3** showing peak **3a** after native chemical ligation and peak **3b** for its corresponding disulfide.*

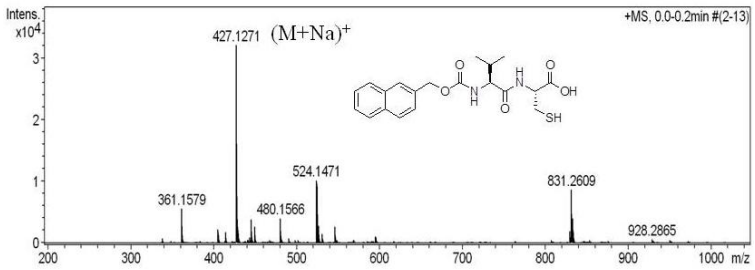

Figure 3.38. *ESI-MS spectrum of compound **3a**.*

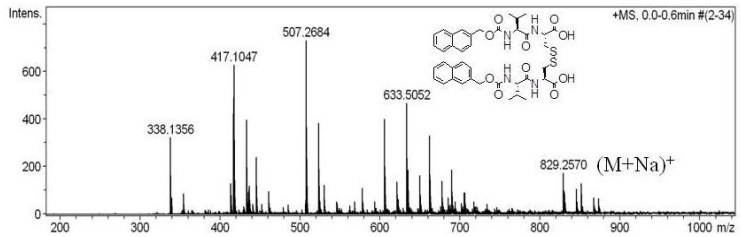

Figure 3.39. *ESI-MS spectrum of compound **3b**.*

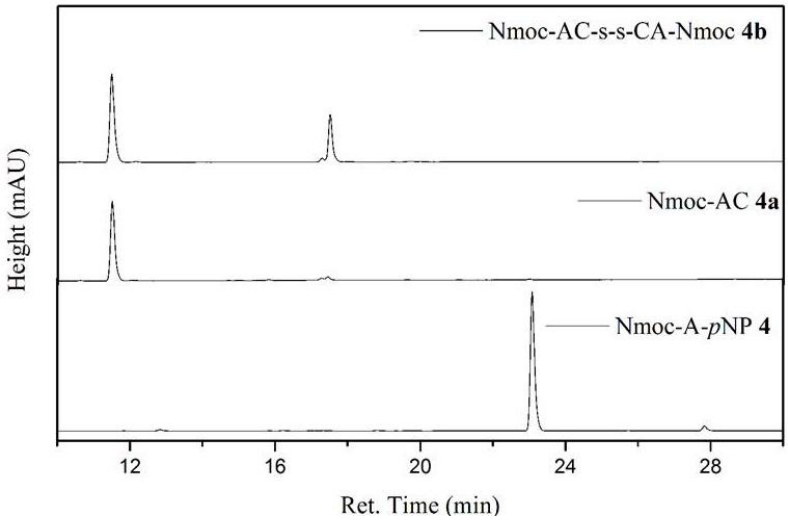

Figure 3.40. *Overlaid HPLC chromatographs for compound* ***4*** *showing peak* ***4a*** *after native chemical ligation and peak* ***4b*** *for its corresponding disulfide.*

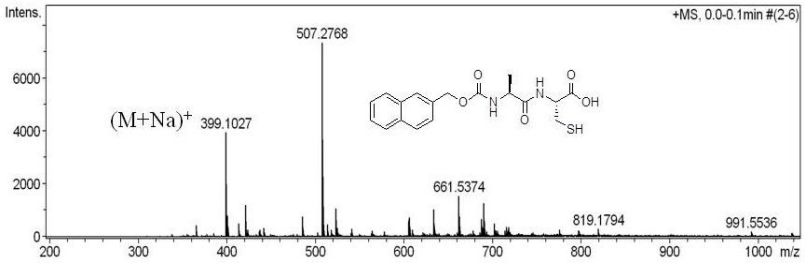

Figure 3.41. *ESI-MS spectrum of compound* ***4a****.*

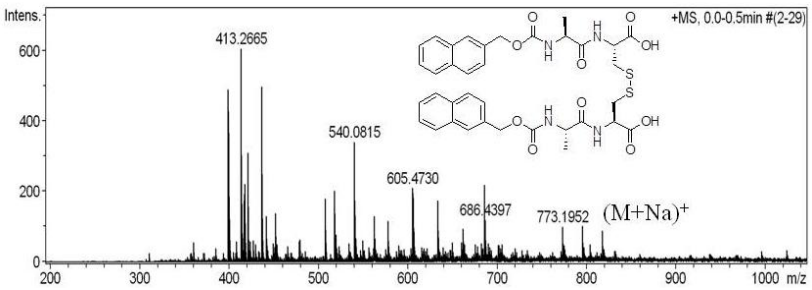

Figure 3.42. *ESI-MS spectrum of compound* ***4b****.*

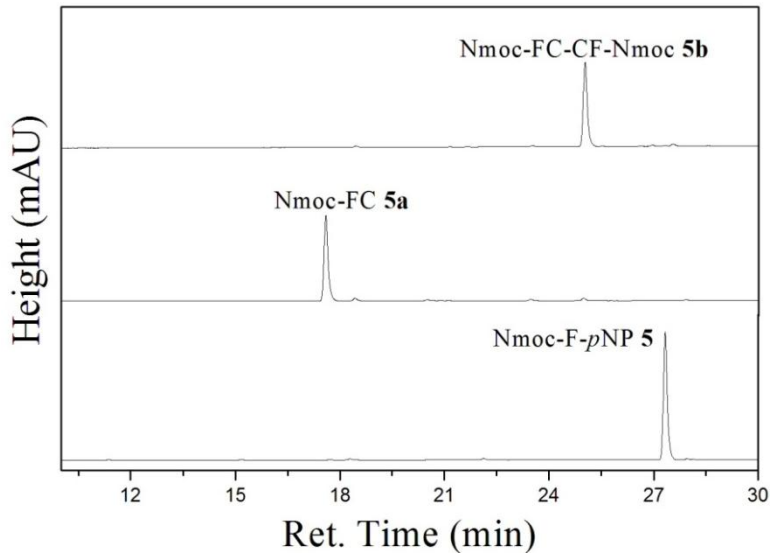

Figure 3.43. *Overlaid HPLC chromatographs for compound* ***5*** *showing peak* ***5a*** *after native chemical ligation and peak* ***5b*** *for its corresponding disulfide.*

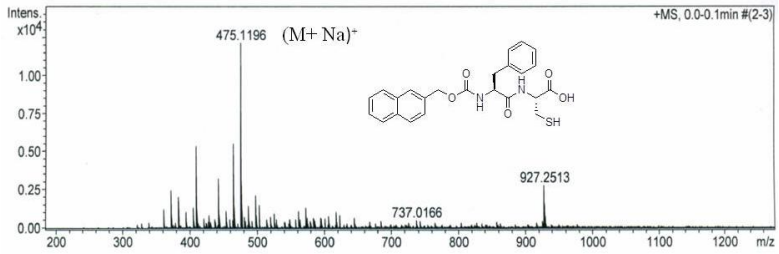

Figure 3.44. *ESI-MS spectrum of compound* ***5a****.*

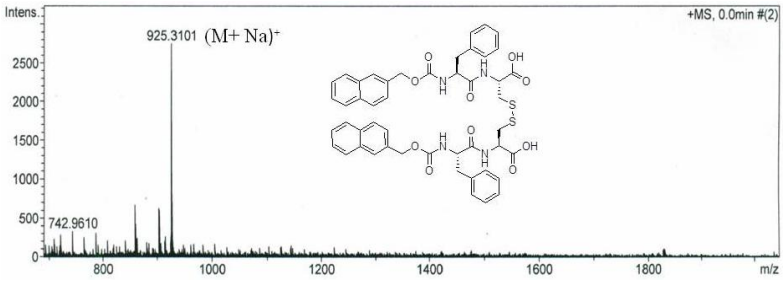

Figure 3.45. *ESI-MS spectrum of compound* ***5b****.*

3.4.2 Self-assembly Study

Self-assembly of compounds **1a** and **5b** were observed upon exposure to atmospheric air. The dis-assembly phenomenon was observed after 3 h for gelator **1b** and 1.5 h for **5b** upon treatment with reducing agent tris(2 carboxyethyl)phosphine (TCEP). The product conversion of gel reversal was analysed by HPLC.

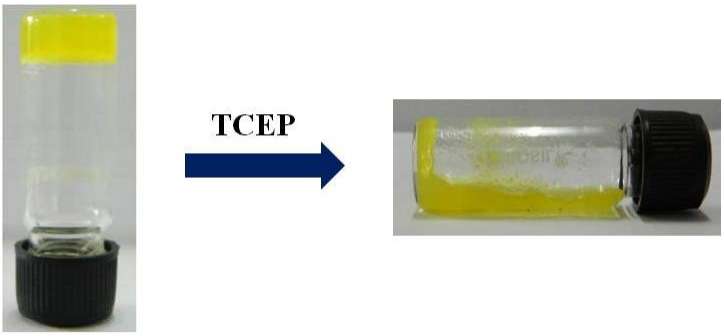

Figure 3.46. *Optical images showing gel transform into solution upon treatment with Tris(2-carboxyethyl)phosphine (TCEP) after 3h.*

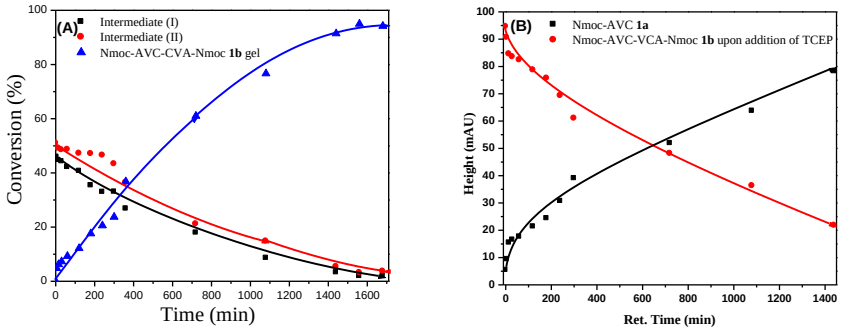

Figure 3.47. *A) HPLC analysis for product* ***1b*** *formation as function of time upon exposure to air (intermediates I and II Nmoc-AVC* ***1a****) and B)* ***1a*** *formation as function of time upon addition of TCEP 40 mmol/L to* ***1b.***

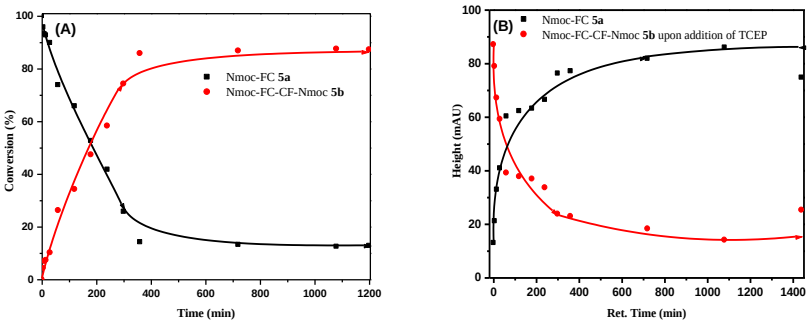

Figure 3.48. *A) HPLC analysis for product* ***5b*** *formation as function of time upon exposure to air and B)* ***5a*** *formation as function of time upon addition of TCEP 40 mmol/L to* ***5b****.*

3.4.3 Rheological Study

Rheological measurements (Figures 3.49A and 3.50B) demonstrate the viscoelastic properties of gels **1b** and **5b**. The values of the storage moduli (G') exceeded those of the loss moduli (G'') by an order of

magnitude, which indicates the formation of strong and solid like gels. Rheological experiments show that the gelation process started at 32 min for **1b** (Figure 3.49B) and 22 min for **5b** (Figure 3.51A) after exposure to air. The disassembly behaviour of gels **1b** (Figure 3.50A) and **5b** (Figure 3.51B) upon treatment with TCEP was also analysed by rheological experiments.

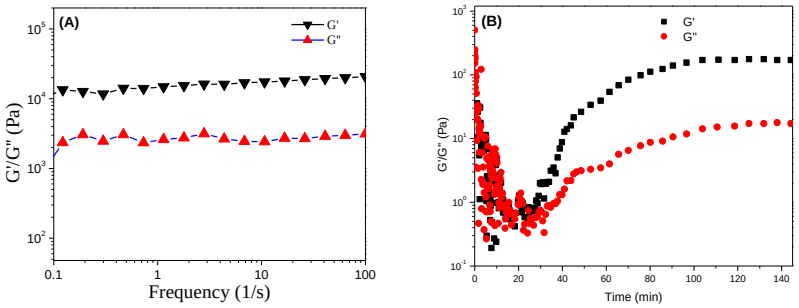

Figure 3.49. *A) Dynamic frequency sweep of Nmoc-AVC-CVA-Nmoc* ***1b*** *gel at constant strain 0.05% and B) Oscillatory rheology of a solution containing 20 mmol of* ***1b*** *at 25°C.*

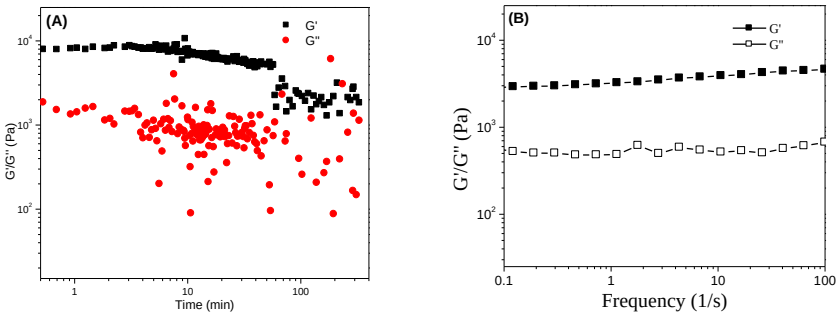

Figure 3.50. *A) Oscillatory rheology of a gel containing 20 mmol of* ***1b*** *and solution of TCEP 40 mmol at 25°C and B) Dynamic frequency sweep of Nmoc-FC-CF-Nmoc* ***5b*** *gel at constant strain 0.05%.*

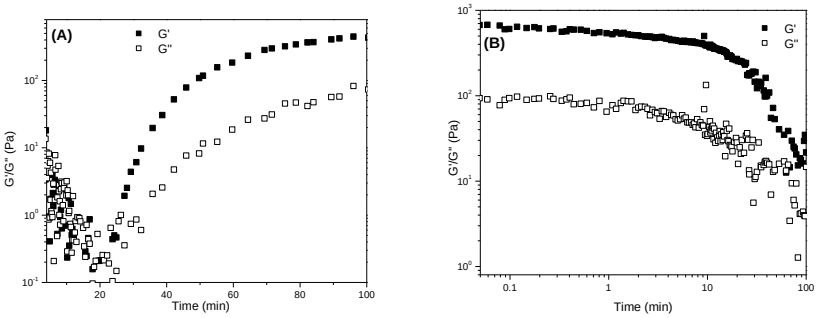

Figure 3.51. *A) Oscillatory rheology of a solution containing 20 mmol of* ***5b*** *at 25°C and B) gel containing 20 mmol of* ***5b*** *and solution of TCEP 40 mmol at 25°C.*

3.4.4 FTIR and Circular Dichroism Study

To discover more about the molecular interactions of gelators **1b** and **5b** in the gel phase, FT-IR (Figures 3.52 and 3.53) and circular dichroism (CD) (Figure 54) spectra were recorded. A gel of **1b** exhibits well defined amide I bands centered at 1639 and 1687 cm^{-1} and gel **5b** exhibits bands at 1636 and 1686 cm^{-1}. This indicates that the peptides self-assemble in a β-sheet fashion.[12] A broad peak appeared at 3287-3350 cm^{-1}, which indicates hydrogen bonded N–H stretching vibrations for both cases. Dis-assembly of gels **1b** and **5b** was also analyzed by FT-IR, which showed new peaks in the amide I region centred at 1650 and 1651 cm^{-1}. This corresponds to a β-turn conformation. The CD spectrum of gel **1b** showed the presence of a negative peak at 217 nm, which confirms the β-sheet[13] conformation. Similarly, a positive peak at 196 nm and negative peaks at 208 and 228 nm were observed for **5b**, which indicate a mixture of β-sheet and α-helical conformations. Structural changes were observed after the addition of TCEP to gels **1b** and **5b**.

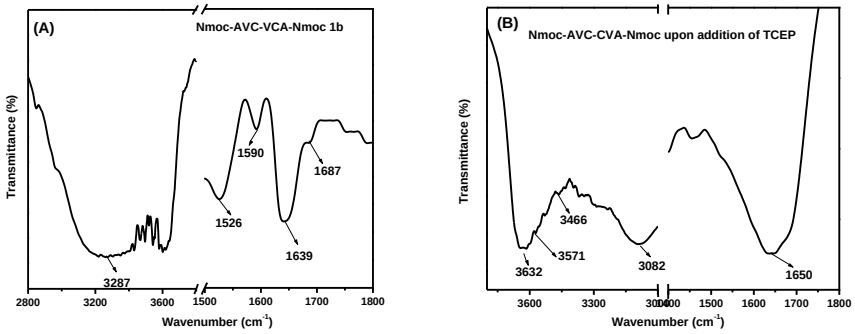

Figure 3.52. *FT-IR spectra of A) Nmoc-AVC-CVA-Nmoc **1b** gel and B) a solution of Nmoc-AVC formed after addition of TCEP.*

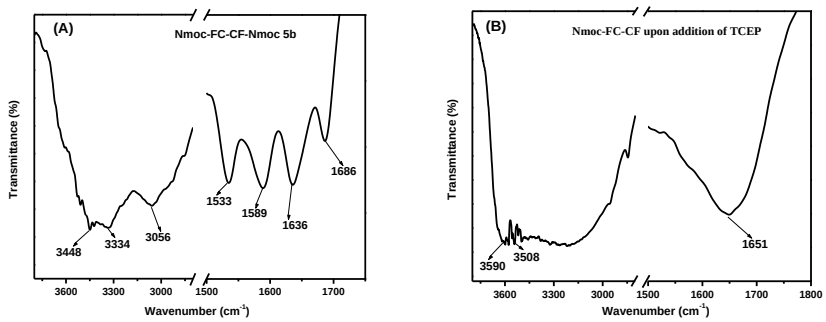

Figure 3.53. *FT-IR spectra of A) Nmoc-FC-CF-Nmoc* ***5b*** *gel and B) a solution of Nmoc-FC formed after addition of TCEP.*

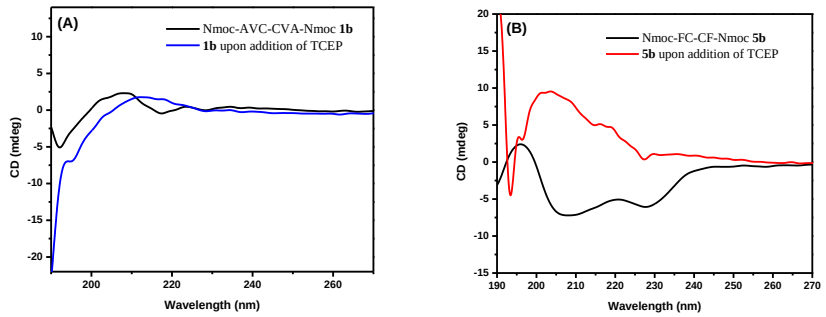

Figure 3.54. *CD spectra of* ***A)*** *Nmoc-AVC-AVC-Nmoc* ***1b*** *gel and Nmoc-AVC solution formed after addition of TCEP.* ***B)*** *Nmoc-FC-FC-Nmoc* ***5b*** *gel and Nmoc-FC solution formed after addition of TCEP.*

3.4.5 Fluorescence Study

An emission maximum at 334 nm for the naphthalene double ring and a small peak at 466 nm corresponding to the *p*-nitrophenyl ester appeared for Nmoc-AV-*p*-NP **1**. The pronounced emission for gel **1b** at 531 nm suggests π-π interactions between naphthalene groups and cleaved *p*-nitrophenolate anions (Figure 3.55). Yang *et al. (2006)* reported that a pronounced emission peak appeared above 400 nm for a naphthalene based dipeptide hydrogel.[14] Ikeda *et al. (2003)* showed that a caged excimer of a naphthalene group gives a broad emission peak between 400-550 nm.[15] This result clearly suggests that π-π stacking interactions also drive the self-assembly process.

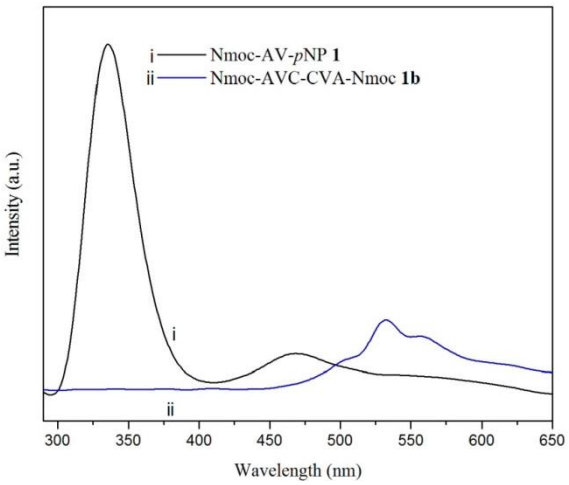

Figure 3.55. *Fluorescence emission spectra of Nmoc-AV-pNP* ***1*** *before and Nmoc-AVC-CVA-Nmoc* ***1b*** *gel after NCL reaction ($\lambda_{ex.}$ = 265 nm).*

3.4.6 Microscopic Study

Gels **1b** and **5b** were deposited on mica for AFM studies which showed fibrous nanostructures with height ranging from 1.75 nm to 14 nm (Figure 3.56). Nanofibrous dense network structures were observed for gels **1b** and **5b**, as is evident from SEM images. These results are consistent with AFM and TEM images. Nanofibrillar morphology was observed for gels **1b** and **5b** on SEM imaging, with width ranging from 25 to 60 nm (Figure 3.57). TEM analysis of gel **1b** shows highly entangled nanofibrous networks with fiber diameter ranging from 23 nm to 46 nm. These entangled nanofibrillar network structures are responsible for the stable gel.

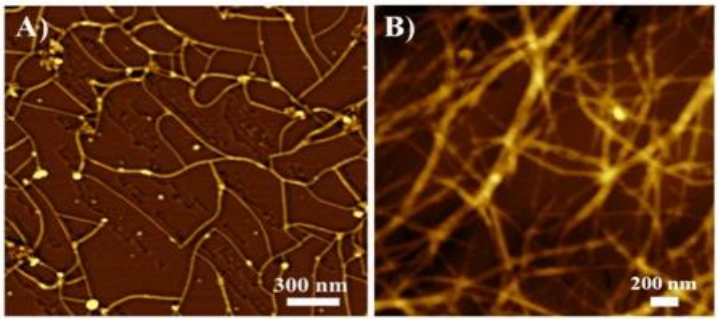

Figure 3.56. *AFM images of gels A)* ***1b*** *and B)* ***5b****.*

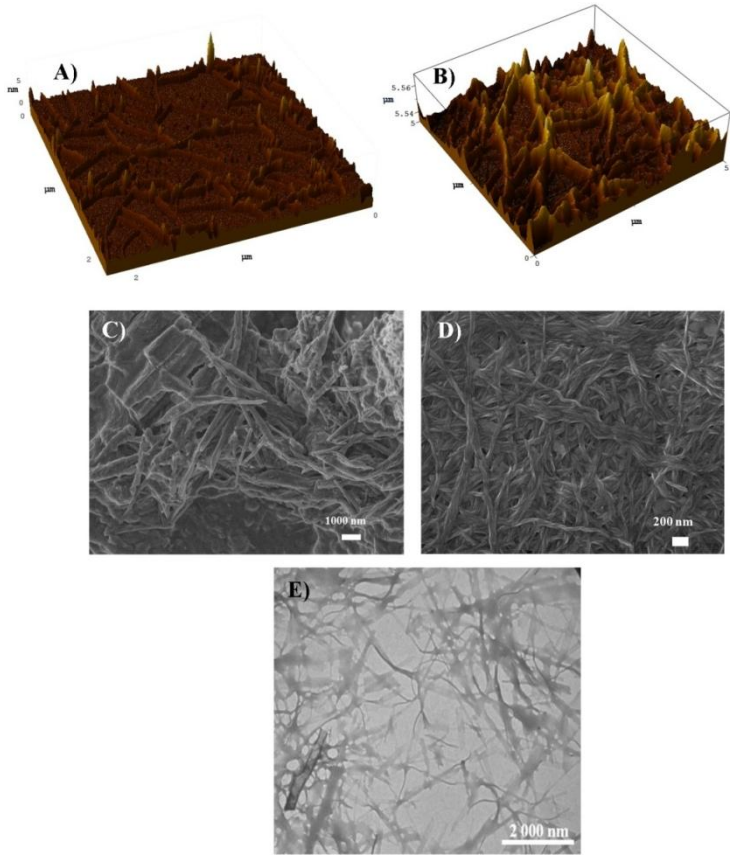

Figure 3.57. *A) and B) AFM height images for* ***1b*** *and* ***5b*** *gels. C) and D) SEM images for* ***1b*** *and* ***5b*** *gels. E) TEM image of* ***1b*** *gel.*

3.5 Conclusion

The present study has described oxo-ester mediated NCL for peptide self-assembly. N-terminal cysteines can be efficiently coupled with Nmoc protected peptide oxo-esters through amide bond formation via NCL reaction. Self-assembled dynamic peptide gels are formed via oxidation of the Nmoc-protected peptides synthesized via the NCL reaction. Similarly, enzyme catalysed reactions, thio-ester mediated native chemical reactions and redox as well as photoresponsive chemical reactions were used to make nanostructured peptide gels. A number of peptides with N-capped aromatic moieties including naphthalene, Fmoc, pyrene and anthracene groups have been shown to be suitable for the preparation of gels. Here, self-assembly and dis-assembly phenomena are highly dependent on the oxidation and reduction of cysteine and cystine based peptides. Here, NCL reactions

allow the formation of nanofibrillar structures. The entangled nanofibrillar[16] structures are responsible for the formation of self supporting gels. Peptides are self-assembled via disulfide bonds, hydrogen bonding and π-π stacking interactions. These kinds of soft biomaterials can be used for cell culture, tissue engineering and supramolecular electronics applications.

3.6 References

1. Fry H. C., Garcia J. M., Medina M. J., Ricoy U. M., Gosztola D. J., Nikiforov M. P., Palmer L. C., Stupp S. I. (2012), Self-assembly of highly ordered peptide amphiphile metalloporphyrin arrays, *J. Am. Chem. Soc.*, 134, 14646-14649 (DOI: 10.1021/ja304674d).
2. (a) Lee K. Y., Mooney D. J. (2001), Hydrogels for tissue engineering, *Chem. Rev.*, 101, 1869-1880 (DOI: 10.1021/ cr000108x); (b) Tsitsilianis C. (2010), Responsive reversible hydrogels from associative "smart" macromolecules, *Soft Matter,* 6, 2372- 2388 (DOI: 10.1039/B923947B) ; (c) Zhao X. B., Pan F., Xu H., Yaseen M., Shan H., Hauser C. A. E., Zhang S. Lu J. R. (2010), Molecular self-assembly and applications of designer peptide amphiphiles, *Chem. Soc. Rev*., 39, 3480-3498 (DOI: 10.1039/B915923C).
3. (a) Ma D., Tu K., Zhang L. M. (2010), Bioactive supramolecular hydrogel with controlled dual drug release characteristics, *Biomacromolecules,* 11, 2204-2212 (DOI: 10.1021/bm100676a); (b) Naskar J., Palui G., Banerjee A. (2009), Tetrapeptide-based hydrogels: For encapsulation and slow release of an anticancer drug at physiological pH, *J. Phys. Chem. B,* 113, 11787-11792 (DOI: 10.1021/jp904251j); (c) Li J. R., Sculley J., Zhou H. C (2012), Metal-organic frameworks for separations, *Chem. Rev.,* 112, 869-932 (DOI: 10.1021/cr200190s); (d) Ma L., Abney C., Lin W. (2009), Enantioselective catalysis with homochiral metal–

organic frameworks, *Chem. Soc. Rev.*, 38, 1248-1256 (DOI: 10.1039/B807083K); (e) Koley P., Pramanik A. (2012), Multilayer vesicles, tubes, various porous structures and organo gels through thesolvent-assisted self-assembly of two modified tripeptides and their different applications, *Soft Matter*, 8, 5364-5374 (DOI: 10.1039/C2SM25205H).

4. (a) Wada A., Tamaru S., Ikeda M., Hamachi I. (2009), MCM-enzyme-supramolecular hydrogel hybrid as a fluorescence sensing material for polyanions of biological significance, *J. Am. Chem. Soc.*, 131, 5321-5330 (DOI: 10.1021/ja900500j); (b) Yemini M., Reches M., Rishpon J., Gazit E. (2005), Novel electrochemical biosensing platform using self-assembled peptide nanotubes, *Nano Lett.*, 5, 183-186 (DOI: 10.1021/nl0484189).

5. (a) Tang C., Ulijn R. V., Saiani A. (2011), Effect of glycine substitution on Fmoc-diphenylalanine self-assembly and gelation properties, *Langmuir*, 27, 14438-14449 (DOI: 10.1021/la202113j); (b) Morris K. L., Chen L., Raeburn J., Sellick O. R., Cotanda P., Paul A., Griffiths P. C., King S. M., Reilly R. K. O., Serpell L. C., Adams D. J. (2013), Chemically programmed self-sorting of gelator networks, *Nat. Commun.*, 4, 1480 (DOI:10.1038/ncomms2499).

6. (a) Maity I., Rasale D. B., Das A. K. (2012), Sonication induced peptide-appended bolaamphiphile hydrogels for *in situ* generation and catalytic activity of Pt nanoparticles, *Soft Matter*, 8, 5301- 5308 (DOI: 10.1039/C2SM25126D); (b) Rasale D. B., Maity I., Das A. K. (2012), Emerging π-stacked dynamic nanostructured library, *RSC Adv.*, 2, 9791-9794 (DOI: 10.1039/ C2RA21334F).

7. (a) Li X., Kuang Y., Lin H., Gao Y., Shi J., Xu B. (2011), Supramolecular nanofibers and hydrogels of nucleopeptides, *Angew. Chem., Int. Ed.*, 50, 9365-9369 (DOI: 10.1002/ anie.201103641); (b) Liang G., Ren H., Rao J. (2010), A biocompatible condensation reaction for controlled assembly of

nanostructures in living cells, *Nat. Chem.*, 2, 54-60 (DOI: 10.1038/nchem.480).

8. Dawson P. E., Muir T. W., Clark-Lewis I., Kent S. B. (1994), Synthesis of proteins by native chemical ligation, *Science,* 266, 776-779 (DOI: 10.1126/science.7973629).
9. Kent S. B. (2009), Total chemical synthesis of proteins, *Chem. Soc. Rev.*, 38, 338-351(DOI: 10.1039/B700141J).
10. (a) Wan Q., Chen J., Yuan Y., Danishefsky S. J. (2008), Oxo-ester mediated native chemical ligation: concept and applications, *J. Am. Chem. Soc.*, 130, 15814-15816 (DOI:10.1021/ja804993y); (b) Weissenborn M. J., Castangia R., Wehner J. W., Sardzik R., Lindhorst T. K., Flitsch S. L. (2012), Oxo-ester mediated native chemical ligation on microarrays: an efficient and chemoselective coupling methodology, *Chem. Commun.*, 48, 4444-4446 (DOI: 10.1039/c2cc30844d).
11. Durek T., Alewood P. F. (2011), Preformed selenoesters enable rapid native chemical ligation at intractable sites, *Angew. Chem., Int. Ed.*, 50,12042-12045 (DOI: 10.1002/anie. 201105512).
12. (a)Yan X., Su Y., Li J., Fruh J., Mchwald H. (2011), Uniaxially oriented peptide crystals for active optical waveguiding, *Angew. Chem., Int. Ed.,* 50, 11186-11191 (DOI: 10.1002/anie.201103941); (b) Yan X., Zhu P., Li J. (2010), Self-assembly and application of diphenylalanine-based nanostructures, *Chem. Soc. Rev.*, 39, 1877-1890 (DOI: 10.1039/b915765b); (c) Zhu P., Yan X., Su Y., Yang Y., Li J. (2010), Solvent-induced structural transition of self-assembled dipeptide: from organogels to microcrystals, *Chem.-Eur. J.*, 16, 3176-3183 (DOI: 10.1002/chem.200902139).
13. Yan X., Cui Y., He Q., Wang K., Li J. (2008) Organogels based on self-Assembly of diphenylalanine peptide and their application to immobilize quantum dots, *Chem. Mater.,* 20, 1522-1526 (DOI: 10.1021/cm702931b).

14. Yang Z., Liang G., Xu B. (2006) Supramolecular hydrogels based on β-amino acid derivatives, *Chem. Commun.*, 738-740 (DOI: 10.1039/B516133A).

15. Ikeda H., Lidaka Y., Ueno A. (2003) Remarkably enhanced excimer formation of naphthylacetate in cation-charged γ-cyclodextrin, *Org. Lett.*, 5, 1625-1627 (DOI: 10.1021/ ol0342608).

16. (a) Chen L., Revel S., Morris K., Serpell L. C., Adams D. J. (2010) Effect of molecular structure on the properties of naphthalene-dipeptide hydrogelators, *Langmuir*, 26, 13466-13471 (DOI: 10.1021/la102059x); (b) Maity I., Rasale D. B., Das A. K. (2013), Exploiting a self-assembly driven dynamic nanostructured library, *RSC Adv.*, 3**,** 6395-6400 (DOI: 10.1039/c3ra22401e).

Chapter 4

In Situ Generation of Redox Active Peptides Driven By Selenoester Mediated Native Chemical Ligation

4.1 Introduction

In nature, complex soft materials are created through hierarchical self-assembly of nanoscale biomolecules.[1] Low molecular weight organic molecules are used in directed self-assembly, which further forms three dimensional network structures. Various functional groups can be incorporated into the molecular structure[2] to mimic and develop the biological processes in the laboratory. However, rational and universal molecular design remained challenge to fit them for biomaterial applications. Self-assembly of short peptides has sought great attention due to their vast applications in drug delivery,[3] tissue engineering[4] and supramolecular electronics.[5] Several physical stimuli[6] such as pH, temperature, light and enzymes are used to exploit the peptide self-assembly.[7] Redox active peptide self-assembly is still remained area of interest due to their potential applications in drug delivery. Redox reactions are prevalent in nature to regulate various biological functions. Redox active[8] nature mimicking dynamic self-assembly could be achieved using chemoselective native chemical ligation (NCL) reactions. Peptide self-assembly could be exploited through native chemical ligation reaction because (i) this method is orthogonal, (ii) self-assembly through NCL reaction is particularly interesting for the development of controlled dynamic self-assembly and (iii) the presence of free sulfhydryl group in peptides which can offer multiple applications after NCL reactions.

NCL reactions are the most revolutionary method for the total or semi synthesis of proteins.[9] Beside its useful applications in protein synthesis, NCL reactions can be used as effective and efficient methods

for the development of soft biomaterials. Collier and coworkers *(2008)* reported a novel method for the stiffing of a hydrogel via thioester mediated NCL reaction.[10] Messersmith group *(2009)* described a strategy, which forms covalently cross-linked polymer hydrogels.[11] In general, the conceptual approach for NCL is based on the reaction between two unprotected peptides one bearing C-terminal thioester and another N-terminal cysteine residue based peptide. The sulfhydryl group of N-terminal cysteine residue undergoes trans-thioesterification with C-terminal thioester[12] and forms thioester-linked intermediate. Thioester-linked intermediate simultaneously and rapidly undergoes intramolecular S→N acyl transfer to form native amide bond.[13] Inspired by this chemoselective ligation reaction,[14] our objective was to develop a simple and efficient approach which can direct dynamic peptide self-assembly. In order to reach our goal, we have synthesized compounds **1-4** with N-terminal capped with aromatic naphthalene-2-methoxycarbonyl (Nmoc) group. The C-terminals of **1-4** is protected with phenyl selenoester which can readily undergo NCL reaction at room temperature with N-terminal cysteine and N- terminal cysteine based peptide Cys-Gly.

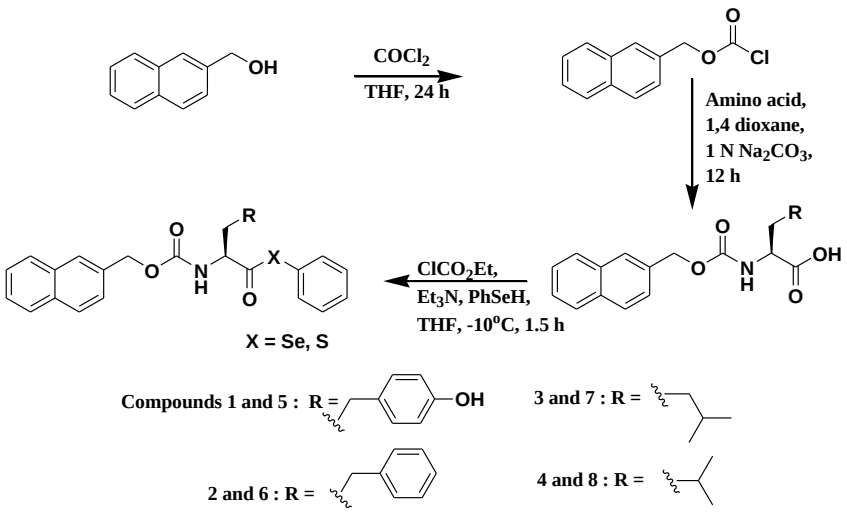

Figure 4.1. *Synthesis of Nmoc-protected seleno and thio-esters for NCL reactions.*

4.2 Experimental

*4.2.(1) Synthesis of compounds **1-8***

The Nmoc-protected amino acids were synthesized by reaction of Nmoc-Cl with amino acid. The corresponding active esters were synthesized by conventional acid activation methodology with ethyl chloroformate.

a) Synthesis of Compound **9:** To a stirred solution of naphthalene methanol (5 g, 31.6 mmol) in dry THF (140 mL), phosgene (39.2 mL, 75.5 mmol) was added at 0^{o} C. The stirring was continued at ambient temperature for 24 h. The reaction was monitored by thin layer chromatography (TLC). After completion of reaction, excess phosgene was removed under low vacuum and trapped with aqueous NaOH. Reaction mixture was concentrated and oily product was obtained. Then it was dissolved in hot hexane to get crystalline product **9.**

Yield = 6.8 g (30 mmol, 94.93 %); mp: 62 ^{o}C; FT-IR (KBr): 3066 (m), 1777 (s), 1601 (ms), 1168 (s) cm^{-1} ; ^{1}H NMR (400 MHz, $CDCl_3$): δ 7.90 (d, 4H), 7.56 (m, 2H), 7.29 (s, 1H), 5.48 (s, 2H) ppm; ^{13}C NMR (100 MHz, $CDCl_3$): δ 71.82, 125.7, 126.6, 127.8, 128.1, 128.6, 130.6, 133.5, 140.9, 147.9, 150.7 ppm.

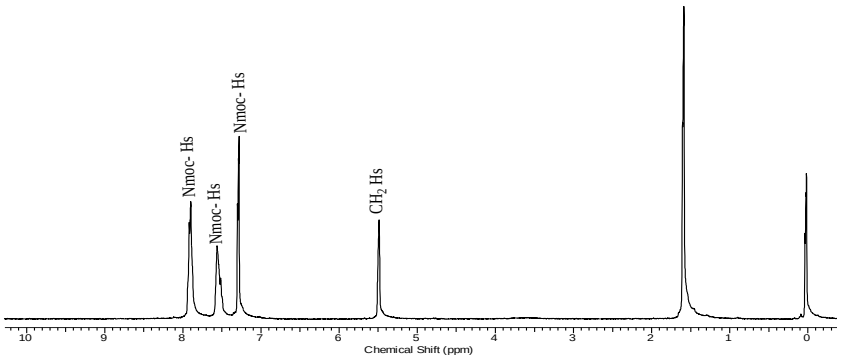

Figure 4.2. *400 MHz ^{1}H NMR spectrum of Nmoc-Cl **9** in $CDCl_3$.*

b) Synthesis of Nmoc-Tyr-OH **10:** A solution of tyrosine (0.724 g, 4 mmol) in a mixture of 1,4 dioxane (10 mL) and 2M sodium hydroxide (15 mL) was stirred and cooled in an ice-water bath. Naphthalene-2-methoxychloroformate (0.882 g, 4 mmol) was added and stirring was continued at room temperature for 12 h. Reaction mixture was diluted with 200 mL of water and dioxane was evaporated under vaccum. Aqueous layer was washed with diethyl ether and the pH of aqueous layer was adjusted to 2 with 2N hydrochloric acid. The aqueous phase was extracted with ethyl acetate (3 x 50 mL) and dried over Na_2SO_4. It was concentrated in vacuo to give **10** as colorless solid.

Yield= 1.124 g (3 mmol, 75 %). mp: 111°C. $[\alpha]_D^{25}$ = -7 (c = 1, MeOH); FT-IR (KBr): 3331 (br), 3055 (br), 2928 (ms), 1709 (s), 1612 (ms), 1513 (s), 1445 (s), 1367 (ms), 1336 (ms), 1225 (s) cm^{-1}; ^1H NMR (400 MHz, DMSO-d_6): δ 9.21 (s, 1H, O<u>H</u> of Tyr), 7.89 (d, 4H, Nph), 7.52 (t, 3H, Nph), 7.42 (s, 1H, *J*= 7.52 Hz, NH), 7.05(d, 2H, *J*= 8.28 Hz, Tyr), 6.66 (d, 2H, *J*= 8 Hz, Tyr), 5.17 (q, 2H, CH_2 of Nph), 4.25 (m, 1H, C^{α} H of Tyr), 2.95 (dd, 1H, *J*= 4.52 and 4 Hz, C^{β} H of Tyr), 2.87 (dd, 1H, *J*= 5 and 5 Hz, C^{β} H of Tyr) ppm; MS (ESI) m/z for $C_{21}H_{19}NO_5$ $(M+H)^+$ calcd.: 366.1341 found: 366.4131; Elemental Analysis calculated for $C_{21}H_{19}NO_5$: C, 69.03; H, 5.24; N, 3.83; Found: C, 66.53; H, 5.46, N, 3.32.

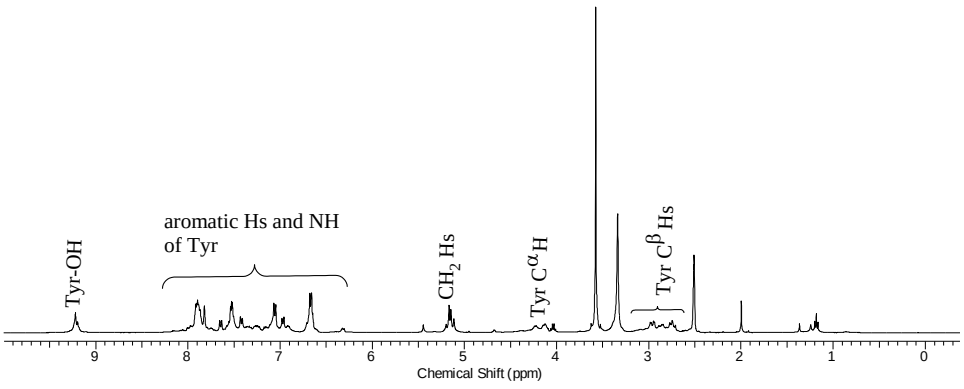

Figure 4.3. *400 MHz ^1H NMR spectrum of Nmoc-Tyr-OH **10** in DMSO-d_6.*

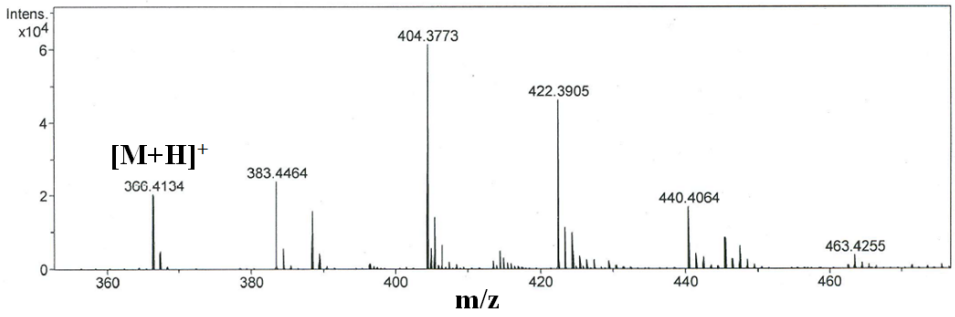

Figure 4.4. *ESI-MS spectrum of Nmoc-Tyr-OH* ***10****.*

*4.2.1 Synthesis of Nmoc-Tyr-SePh **1**:*

c) Nmoc-Tyrosine (0.500 gm, 1.36 mmol) in 50 mL THF was added with (1.36 mmol, 0.189 mL) Et_3N. 1.36 mmol (0.129 mL) of $ClCO_2Et$ was added to the reaction mixture at -15 ^oC and stirred it for 10 min. The benzeneselenol (1.36 mmol, 0.144 mL) which was easily prepared from C_6H_5MgBr and Se was added to the reaction mixture. The solution was kept for 30 min at 10 ^oC with stirring. The reaction mixture was stirred for 1h at room temperature. 20 mL water was added. THF was evaporated in vacuo and the residue was dissolved in ethyl acetate. The solution was washed with saturated $NaHCO_3$ solution and water. The ethyl acetate layer was extracted and dried over Na_2SO_4. It was concentrated in vacuo and covered with a layer of petroleum ether. The compound **1** was obtained as white solid. Purification was done by silica gel column (100-200 mesh) using hexane-ethylacetate (9:1) as eluent.

Yield= 0.520 g (1 mmol, 73.52 %). mp: 161^oC; $[\alpha]_D^{25}$ = -36 (c = 1, MeOH); FT-IR (KBr): 3316 (br), 3053 (ms), 2922 (s), 2852 (ms), 1696 (s), 1606 (ms), 1517 (s), 1471 (ms), 1369 (ms) 1260 (s) cm^{-1}; ^1H NMR (400 MHz, $CDCl_3$): δ 7.82 (d, 4H, *J*= 8 Hz, Nph), 7.48 (t 3H, Nph), 7.38 (m, 5H, Ph), 7.25 (s, 1H, NH), 6.97 (d, 2H, *J* = 7.28 Hz, Tyr), 6.68 (d, 2H, *J* = 7.56 Hz, Tyr), 5.28 (q, 2H, CH_2 oh Nph), 4.72 (m, 1H, C^α H of Tyr), 3.09 (dd, 1H, *J*= 4.24 and 4.24 Hz, C^β H of Tyr), 3.00 (dd, 1H, C^β of Tyr) ppm ; ^{13}C NMR (100 MHz, $CDCl_3$): δ 203.5, 155.9, 135.9, 133.1, 132.0, 130.5, 130.3, 129.4, 129.0, 128.6, 128.4,

128.0, 127.7, 127.3, 126.9,126.5, 126.4, 126.3, 125.7, 121.3, 115.7, 70.6, 67.6, 64.2, 36.9 ppm; MS (ESI) m/z for $C_{27}H_{23}NO_4Se$ $(M+Na)^+$ calcd.: 528.0690, found: 528.0686; Elemental Analysis calculated for $C_{27}H_{23}NO_4Se$: C, 64.29; H, 4.60; N, 2.78; Found: C, 65.69; H, 5.17, N, 2.29.

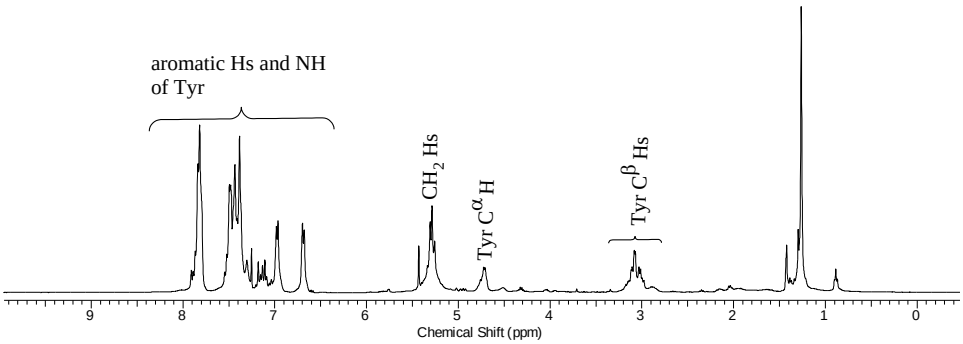

Figure 4.5. *400 MHz ^1H NMR spectrum of Nmoc-Tyr-SePh **1** in $CDCl_3$.*

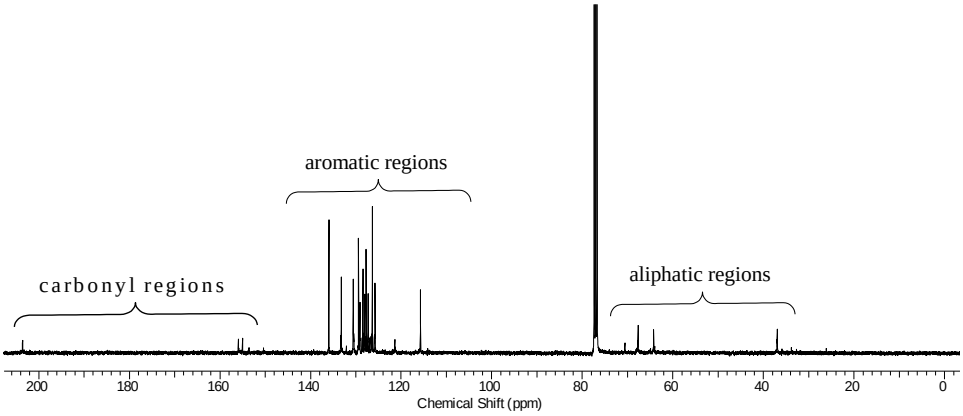

Figure 4.6. *100 MHz ^{13}C NMR spectrum of Nmoc-Tyr-SePh **1** in $CDCl_3$.*

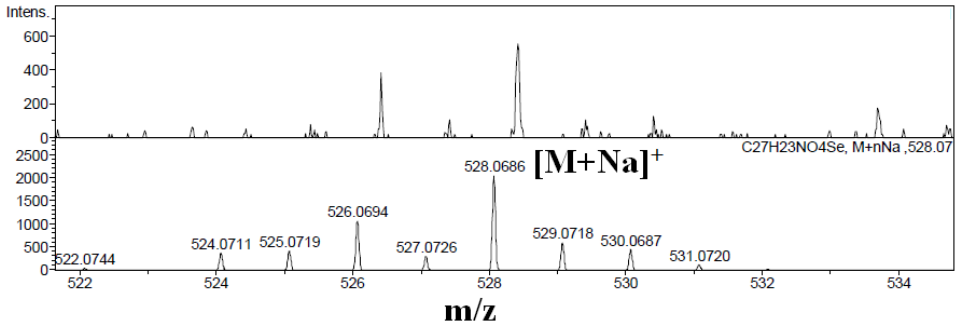

Figure 4.7. *ESI-MS spectrum of Nmoc-Tyr-SePh **1**.*

a) Synthesis of Nmoc-Phe-OH **11**: A solution of phenylalanine (0.660 g, 4 mmol) in a mixture of 1, 4 dioxane (10 mL) and 2M sodium hydroxide (15 mL) was stirred and cooled in an ice-water bath. Naphthalene-2-methoxychloroformate (0.882 g, 4 mmol) was added and stirring was continued at room temperature for 12 h. Reaction mixture was diluted with 200 mL of water and dioxane was evaporated under vaccum. Aqueous layer was washed with diethyl ether and the pH of aqueous layer was adjusted to 2 with 2N hydrochloric acid. The aqueous phase was extracted with ethyl acetate (3 x 50 mL) and dried over Na_2SO_4. The organic layer was concentrated in vacuo to give **11** as white solid.

Yield = 1.12 g (3.2 mmol, 80 %). mp: 102 ^oC; $[\alpha]_D^{25}$ = -7 (*c* = 1, MeOH); FT-IR (KBr): 3340 (s), 3030 (br), 2930 (br), 2884 (br), 1692 (s), 1529 (s), 1450 (m), 1338 (m), 1258 (s) cm^{-1}; 12.75 (s, 1H, COOH), 7.88 (d, 4H, Nph), 7.73 (d, 1H, *J*=8.04 Hz, Nph), 7.53 (t, 2H, Nph), 7.41 (d, 1H, *J*= 8.28, NH), 7.21 (m, 5H, Phe), 5.16 (s, 2H CH_2 of Nph), 4.21 (q, 1H, C^{α} H of Phe), 3.11 (d, 1H, C^{β}H of Phe), 2.86 (m, 1H, C^{β}H of Phe) ppm; MS (ESI) m/z for $C_{21}H_{19}NO_4$ $(M+Na)^+$ calcd.: 372.1212, found: 372.1206; Elemental Analysis calculated for $C_{21}H_{19}NO_4$: C, 72.19; H, 5.48; N, 4.01; Found: C, 72.21; H, 5.53; N, 4.11.

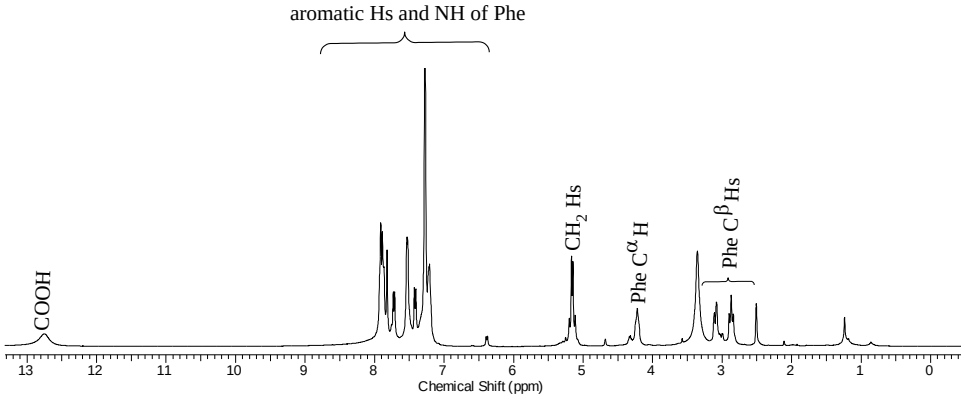

Figure 4.8. *400 MHz ^1H NMR spectrum of Nmoc-Phe-OH **11** in DMSO-d_6.*

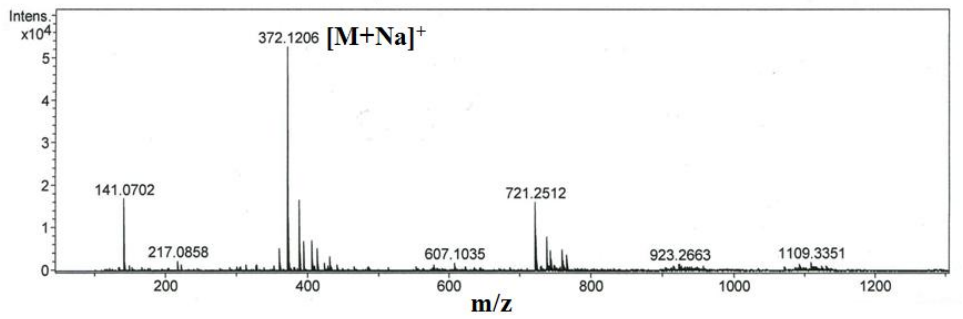

Figure 4.9. *ESI-MS spectrum of Nmoc-Phe* ***11.***

*4.2.2 Synthesis of Nmoc-Phe-SePh **2**:*

b) Nmoc-Phenylalanine (0.526 gm, 1.5 mmol) in 50 mL THF was added with (1.5 mmol, 0.208 mL) Et_3N. 1.5 mmol (0.142 mL) $ClCO_2Et$ was added to the reaction mixture at -15 ^oC and stirred it for 10 min. The benzeneselenol (1.36 mmol, 0.158 mL) which was easily prepared from C_6H_5MgBr and Se was added to the reaction mixture. The solution was kept for 30 min at 10 ^oC with stirring. The reaction mixture was stirred for 1h at room temperature. 20 mL water was added. THF was evaporated in vacuo and the residue was dissolved in ethyl acetate. The solution was washed with saturated $NaHCO_3$ solution and water. The ethyl acetate layer was extracted and dried over Na_2SO_4. It was concentrated in vacuo and covered with a layer of petroleum ether. The compound **2** was obtained as white solid. Purification was done by silica gel column (100-200 mesh) using hexane-ethylacetate (9:1) as eluent.

Yield=0.45g (0.92 mmol, 61.33 %). mp: 123^oC; $[\alpha]_D^{25}$ = -38 (c = 1, MeOH); FT-IR (KBr): 3299 (s), 3058 (ms), 3029 (ms), 2963 (ms), 1693 (s), 1578 (s), 1530 (ms), 1444 (ms), 1368 (ms), 1315 (ms), 1257 (s) cm^{-1}; ^1H NMR (400 MHz, $CDCl_3$): δ 7.84 (t, 4H, Nph), 7.48 (m, 3H, Nph), 7.41 (m, 5H, Ph), 7.24 (m, 5H, Phe), 7.15 (d, 1H, *J*= 7.52 Hz, NH), 5.30 (q, 2H, CH_2 of Nph), 4.75 (m, 1H, C^α H of Phe), 3.15 (d, 1H, C^β H of Phe), 3.12 (d, 1H, C^β H of Phe) ppm; ^{13}C NMR (100 MHz, $CDCl_3$): δ 203.5, 155.8, 135.9, 135.0, 133.3, 133.1, 130.5, 129.5, 129.3, 129.0, 128.8, 128.7, 128.4, 128.2,128.0, 127.7, 127.3, 127.2, 126.3, 125.8, 125.7, 67.6, 66.6, 65.0, 64.0, 62.0, 37.7; MS (ESI)

m/z for $C_{27}H_{23}NO_3Se$ $(M+Na)^+$ calcd.: 512.0741, found: 512.0728; Elemental Analysis calculated for $C_{27}H_{23}NO_3Se$: C, 66.39; H, 4.75; N, 2.87; Found: C, 66.03; H, 4.72, N, 2.68.

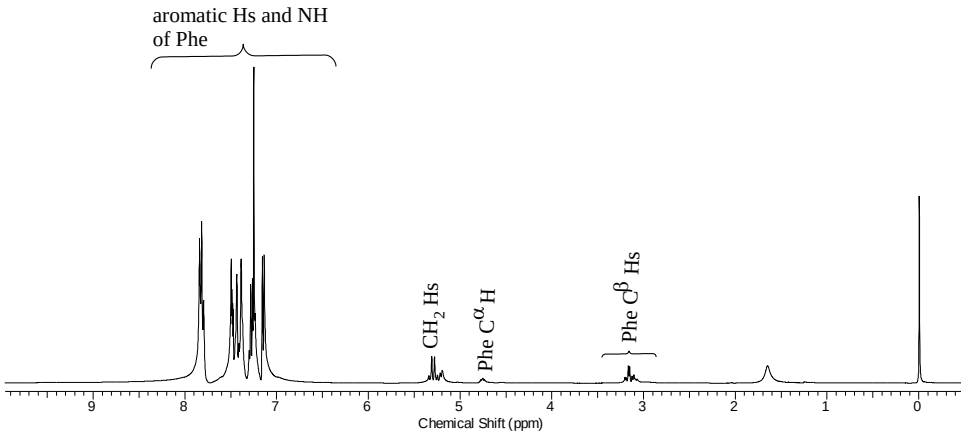

Figure 4.10. *400 MHz ^1H NMR spectrum of Nmoc-Phe-SePh **2** in $CDCl_3$.*

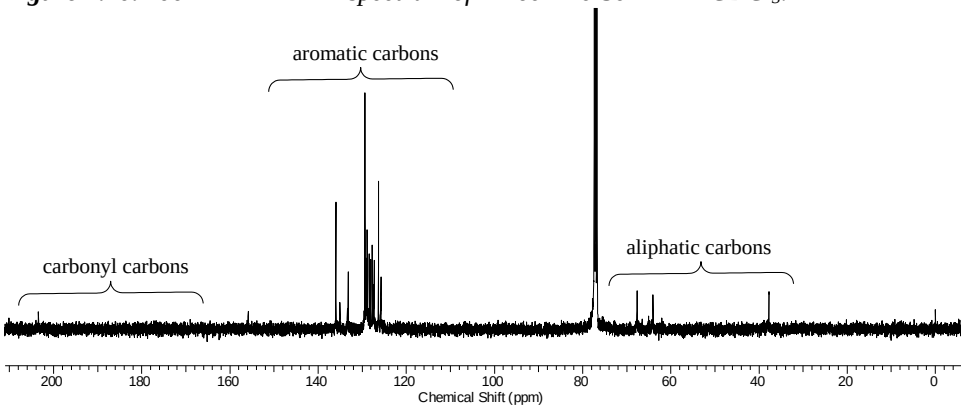

Figure 4.11. *100 MHz ^{13}C NMR spectrum of Nmoc-Phe-SePh **2** in $CDCl_3$.*

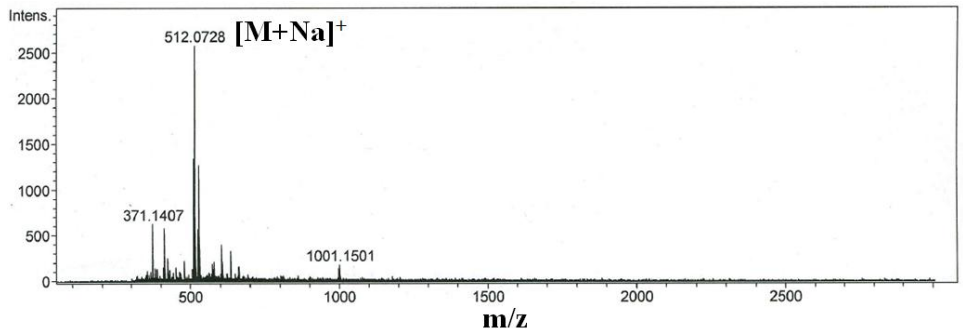

Figure 4.12. *ESI-MS spectrum of Nmoc-Phe-SePh **2**.*

a) Synthesis of Nmoc-Leu-OH **12**: A solution of leucine (0.524 g, 4 mmol) in a mixture of 1, 4 dioxane (10 mL) and 1M sodium hydroxide (15 mL) was stirred and cooled in an ice-water bath.

Naphthalene-2-methoxychloroformate (0.882 g, 4 mmol) was added and stirring was continued at room temperature for 12 h. Reaction mixture was diluted with 200 ml of water and dioxane was evaporated under vaccum. Aqueous layer was washed with diethyl ether and the pH of aqueous layer was adjusted to 2 with 2N hydrochloric acid. The aqueous phase was extracted with ethyl acetate (3 x 50 mL) and dried over Na_2SO_4. The organic layer was concentrated in vacuo to give **12** as white solid.

Yield =0.954 g (3 mmol, 75 %). mp: 79 °C; $[\alpha]_D^{25}$ = -12 (*c* = 1, MeOH); FT-IR (KBr): 3418 (br), 3380 (br), 3053 (ms), 2960 (s), 2874 (ms), 1700 (s), 1604 (ms), 1517 (s), 1462 (ms), 1363 (ms), 1321 (ms), 1239 (s) cm^{-1}; ^1H NMR (400 MHz, $CDCl_3$): δ 7.91 (t, 4H, Nph), 7.63 (d, 1H, J= 7.84 Hz, NH), 7.53 (t, 3H, Nph), 5.20 (s, 2H, CH_2 of Nph), 4.00 (m, 1H, C^{α} H of Leu), 1.66 (m, 1H C^{γ}H, of Leu), 1.53 (m, 1H, C^{β}H of Leu), 1.49 (m, 1H, C^{β}H of Leu), 0.88 (d, 6H, C^{δ}Hs of Leu) ppm; MS (ESI) m/z for $C_{18}H_{21}NO_4$ $(M+Na)^+$ calcd.: 338.1368, found: 338.1378; Elemental Analysis calculated for $C_{18}H_{21}NO_4$: C, 68.55; H, 6.71; N, 4.44; Found: C, 67.06; H, 6.84, N, 4.04.

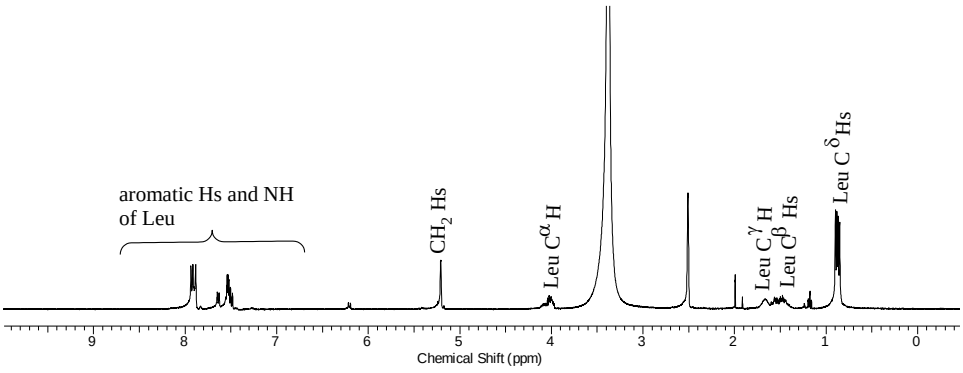

Figure 4.13. *400 MHz ^1H NMR spectrum of Nmoc-Leu-OH* ***12*** *in DMSO-d_6.*

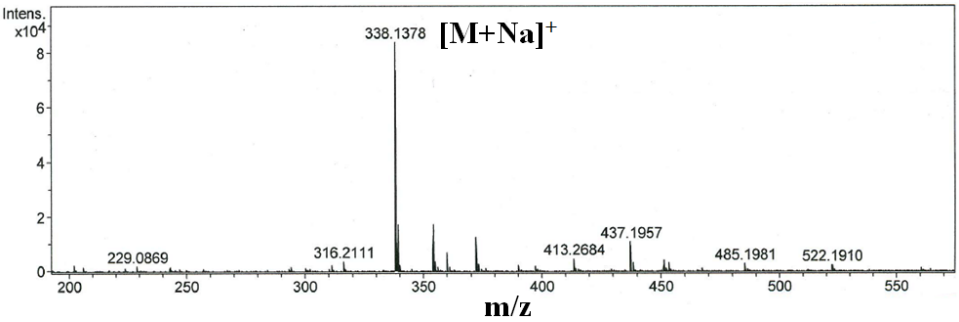

Figure 4.14. *ESI-MS spectrum of Nmoc-Leu-OH* ***12.***

*4.2.3 Synthesis of Nmoc-Leu-SePh **3**:*

b) Nmoc-Leucine (0.392gm, 1.24 mmol) in 50 mL THF was added with (1.24 mmol, 0.172 mL) Et_3N. 1.24 mmol (0.117 mL) $ClCO_2Et$ was added to the reaction mixture at -15 ^oC and stirred it for 10 min. The benzeneselenol (1.24 mmol, 0.131 mL) which was easily prepared from C_6H_5MgBr and Se was added to the reaction mixture. The solution was kept for 30 min at 10 ^oC with stirring. The reaction mixture was stirred for 1h at room temperature. 20 mL water was added. THF was evaporated in vacuo and the residue was dissolved in ethyl acetate. The solution was washed with saturated $NaHCO_3$ solution and water. The ethyl acetate layer was extracted and dried over Na_2SO_4. It was concentrated in vacuo and covered with a layer of petroleum ether. The compound **3** was obtained as white solid. Purification was done by silica gel column (100-200 mesh) using hexane-ethyl acetate (9:1) as eluent.

Yield =0.321g (0.7 mmol, 56.45 %). mp: 91^oC; $[\alpha]_D^{25}$ = -30 (*c* = 1, MeOH); FT-IR (KBr): 3382 (s), 3059 (ms), 2955 (s), 2872 (ms), 1718 (s), 1701 (s), 1600 (ms), 1576 (s), 1465 (ms), 1386 (ms), 1336 (ms), 1250 (s) cm^{-1}; ^1H NMR (400 MHz, $CDCl_3$): δ 7.84 (d, 4H, *J*= 7.76 Hz, Nph), 7.48 (m, 5H, Ph), 7.37 (d, 3H, Nph), 7.27 (s, 1H, NH), 5.35 (m, 2H, CH_2 of Nph), 4.51 (m, 1H, C^{α} H of Leu), 1.73 (d, 2H, C^{β}Hs of Leu), 1.52 (m, 1H, C^{γ}H of Leu), 0.93 (d, 6H, *J* = 6.04 Hz, C^{δ}Hs of Leu) ppm; ^{13}C NMR (100 MHz, $CDCl_3$): δ 203.9, 155.9, 136.01, 133.4, 133.2, 133.1, 131.5, 129.3, 129.1, 128.9, 128.4, 128.01, 127.7,

127.5, 127.2, 126.3, 125.7, 67.6, 62.4, 41.0, 24.7, 23.0, 22.6, 21.4 ppm; MS (ESI) m/z for $C_{24}H_{25}NO_3Se$ $(M+Na)^+$ calcd.: 478.0897, found: 478.0890; Elemental Analysis calculated for $C_{24}H_{25}NO_3Se$: C, 63.43; H, 5.55; N, 3.08; Found: C, 63.60; H, 5.62, N, 2.98.

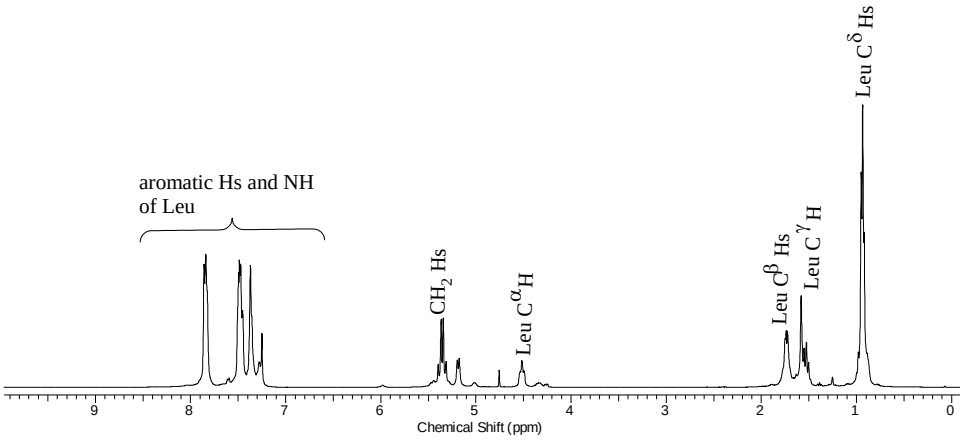

Figure 4.15. *400 MHz ^1H NMR spectrum of Nmoc-Leu-SePh **3** in $CDCl_3$.*

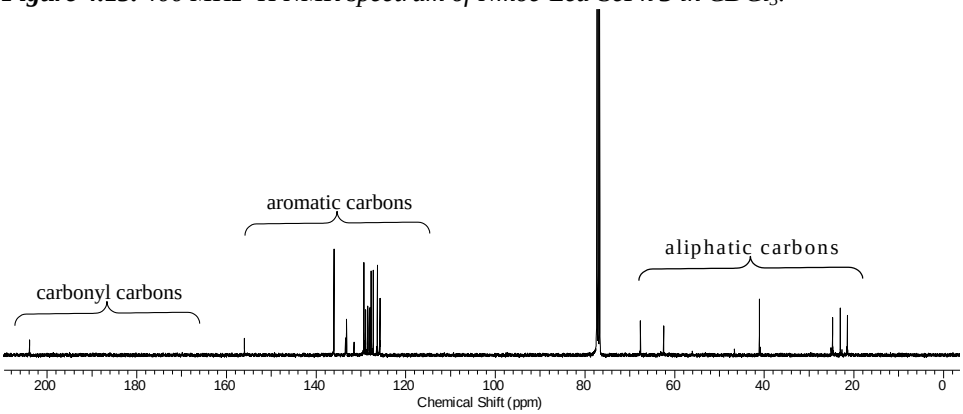

Figure 4.16. *100 MHz ^{13}CNMR spectrum of Nmoc-Leu-SePh **3** in $CDCl_3$.*

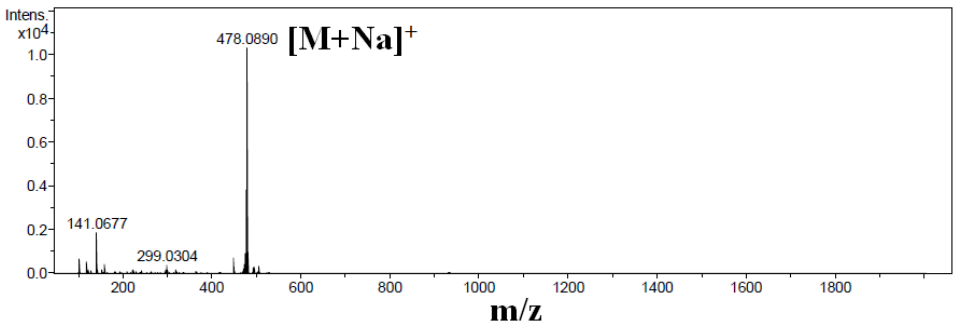

Figure 4.17. *ESI-MS spectrum of Nmoc-Leu-SePh **3**.*

a) Synthesis of Nmoc-Val-OH **13**: A solution of Valine (0.468 g, 4 mmol) in a mixture of 1, 4 dioxane (10 mL) and 1M sodium hydroxide (15 mL) was stirred and cooled in an ice-water bath. Naphthalene-2-

methoxychloroformate (0.882 g, 4 mmol) was added and stirring was continued at room temperature for 12 h. Reaction mixture was diluted with 200 mL of water and dioxane was evaporated under vaccum. Aqueous layer was washed with diethyl ether and the pH of aqueous layer was adjusted to 2 with 2N hydrochloric acid. The aqueous phase was extracted with ethyl acetate (3 x 50 mL) and dried over Na_2SO_4 concentrated in vacuo to give **13** as white solid.

Yield=1.012 g (3.3 mmol, 82.5 %). mp: 99 ^oC; $[\alpha]_D^{25}$ = -5 (*c* = 1, MeOH); FT-IR (KBr): 3419 (s), 3055 (br), 2960 (br), 1739 (s), 1679 (m), 1545 (s), 1463 (m), 1399 (m), 1258 (s) cm^{-1}; ^1H NMR (400 MHz, $CDCl_3$): δ 12.56 (s,1H, COOH), 7.90 (t, 4H, Nph), 7.53 (d, 3H, Nph), 7.37 (s, 1H, NH), 5.22 (s, 2H, CH_2 of Nph), 4.02 (m, 1H, $C^{\alpha}H$ of Val), 2.08 (m, 1H, $C^{\beta}H$ of Val), 0.92 (d, 6H, $C^{\gamma}Hs$ of Val). ppm; MS (ESI) m/z for $C_{17}H_{19}NO_4$ $(M+Na)^+$ calcd.: 324.1206, found: 324.1228; Elemental Analysis calculated for $C_{17}H_{19}NO_4$: C, 67.76; H, 6.36; N, 4.65; Found: C, 67.65; H, 6.38, N, 4.63.

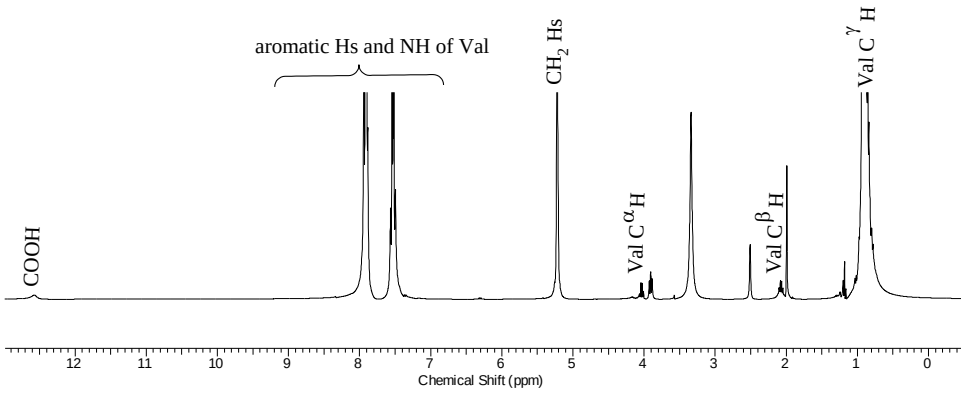

Figure 4.18. *400 MHz ^1H NMR spectrum of Nmoc-Val-OH* ***13*** *in DMSO-d_6.*

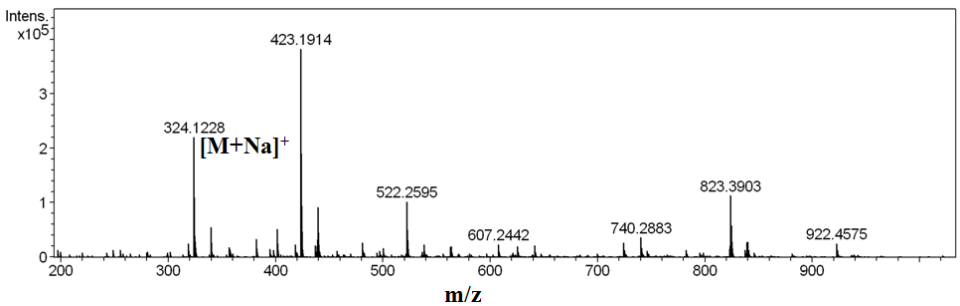

Figure 4.19. *ESI-MS spectrum of Nmoc-Val* ***13***.

*4.2.4 Synthesis of Nmoc-Val-SePh **4**:*

b) Nmoc-Valine (0.540 gm, 1.79 mmol) in 50 mL THF was added with (1.79 mmol, 0.248 mL) Et_3N. 1.79 mmol (0.169 mL) $ClCO_2Et$ was added to the reaction mixture at -15 ^oC and stirred it for 10 min. The benzeneselenol (1.79 mmol, 0.189 mL) which was easily prepared from C_6H_5MgBr and Se was added to the reaction mixture. The solution was kept for 30 min at 10 ^oC with stirring. The reaction mixture was stirred for 1h at room temperature. 20 mL water was added. THF was evaporated in vacuo and the residue was dissolved in ethyl acetate. The solution was washed with saturated $NaHCO_3$ solution and water. The ethyl acetate layer was extracted and dried over Na_2SO_4. It was concentrated in vacuo and covered with a layer of petroleum ether. The compound **4** was obtained as white solid.

Yield = 0.387 g (0.87 mmol, 48.99 %). mp: 99 ^oC; $[\alpha]_D^{25}$ = -42 (*c* = 1, MeOH); FT-IR (KBr): 3420 (s), 3054 (br), 2968 (br), 2868 (ms), 1723 (s), 1693 (s), 1602 (m), 1519 (s), 1466 (m), 1391 (ms), 1314 (ms), 1259 (s) cm^{-1}; ^1H NMR (400 MHz, $CDCl_3$): δ 7.88 (t, 4H, Nph), 7.53 (m, 5H, Ph), 7.41 (d, 3H, Nph), 7.34 (s, 1H, NH), 5.38 (q, 2H, CH_2 of Nph), 4.49 (q, 1H, $C^{\alpha}H$ of Val), 2.40 (m, 1H, $C^{\beta}H$ of Val), 0.97 (d, 6H, *J* = 6.76 Hz, $C^{\gamma}Hs$ of Val) ppm; ^{13}C NMR (100 MHz, $CDCl_3$): δ 203.2, 156.3, 135.9, 133.4, 133.2, 133.1, 131.5, 129.3, 129.2, 129.0, 128.4, 128.0, 127.7, 127.3, 126.3, 125.9, 125.7, 68.5, 67.7, 30.6, 19.5, 16.7 ppm; MS (ESI) m/z for $C_{23}H_{23}NO_3Se$ $(M+Na)^+$ calcd.: 464.0741, found: 464.0740; Elemental Analysis calculated for $C_{23}H_{23}NO_3Se$: C, 62.73; H, 5.26; N, 3.18; Found: C, 63.25; H, 5.33, N, 2.95.

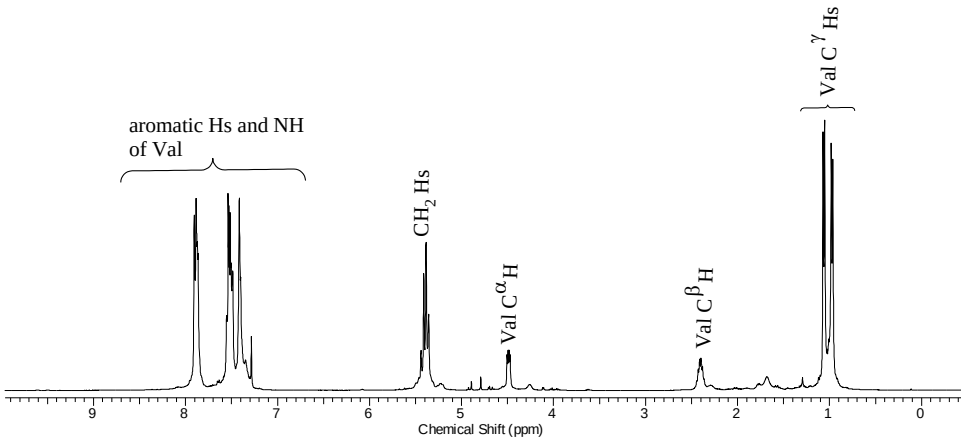

Figure 4.20. *400 MHz ^{1}H NMR spectrum of Nmoc-Val-SePh **4** in $CDCl_3$.*

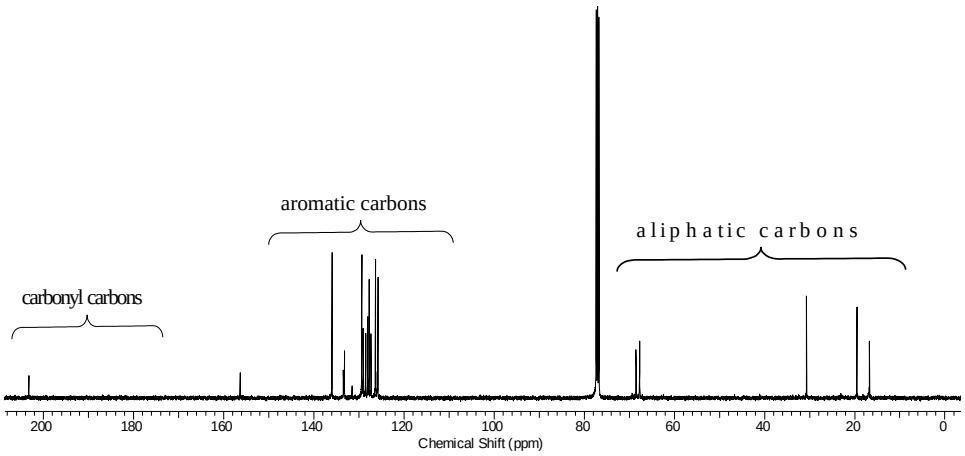

Figure 4.21. *100 MHz ^{13}C NMR spectrum of Nmoc-Val-SePh **4** in $CDCl_3$.*

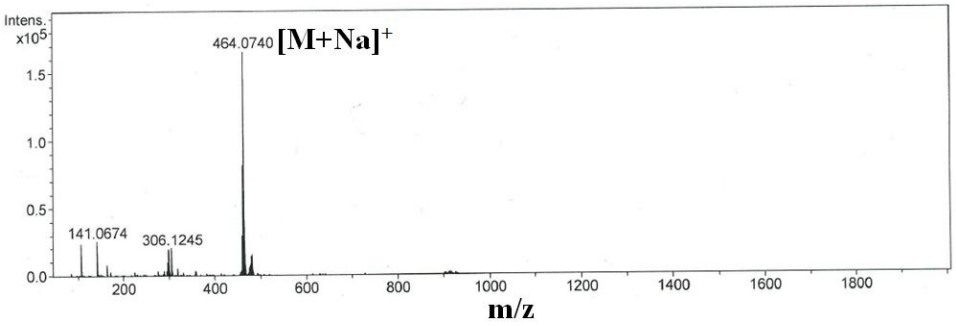

Figure 4.22. *ESI-MS spectrum of Nmoc-Val-SePh **4**.*

*4.2.5 Synthesis of Nmoc-Tyr-SPh **5**:*

a) Nmoc-Tyr-OH (0.358 gm, 0.98 mmol) in 25 mL THF was added with 0.98 mmol (0.137 mL) Et_3N. 0.98 mmol (0.093 mL) of $ClCO_2Et$ was added to the reaction mixture at -15 ^{o}C and stirred it for

10 min. Thiophenol (0.98 mmol, 0.1 mL) was added to the reaction mixture. The solution was kept for 30 min at 10 ^{o}C with stirring. The reaction mixture was stirred for 1h at room temperature. 20 mL water was added. THF was evaporated in vacuo and the residue was dissolved in ethyl acetate. The solution was washed with saturated $NaHCO_3$ solution and water. The ethyl acetate layer was extracted and dried over Na_2SO_4. It was concentrated in vacuo and covered with a layer of petroleum ether. The compound **5** was obtained as white solid. Yield= 0.324 g (0.71 mmol, 72.34 %). $[\alpha]_D^{25}$ = -30 (c = 1, MeOH); FT-IR (KBr): ῡ 3320 (br), 3050 (ms), 2955 (ms), 1689 (s), 1604 (ms), 1521 (s), 1440 (ms), 1340 (ms), 1310 (ms), 1264 (s); ^{1}H NMR (400 MHz, $CDCl_3$): δ 7.81 (t, 4H, Nph), 7.48 (m, 2H), 7.43 (s, 1H, Nph), 7.40 (m, 5H, Ph), 7.33 (d, 1H, NH), 7.01 (d, 2H, *J*= 8.8 Hz, Tyr), 6.71 (d, 2H, *J*= 8.8 Hz, Tyr), 5.28 (s, 2H of Nph), 4.77 (m, 1H, C^{α}H of Tyr), 3.08 (m, 2H, C^{β}Hs of Tyr) ppm; ^{13}C NMR (100 MHz, $CDCl_3$): δ 198.90, 155.7, 154.8, 134.6, 133.4, 133.1, 130.6, 129.6, 129.3, 128.4, 128.0, 127.7, 127.2, 127.1, 126.9, 126.3, 125.8, 115.6, 67.49, 61.51, 37.63 ppm; MS (ESI) m/z for $C_{27}H_{23}NO_4S$ $(M+Na)^+$ calcd.: 480.1240 found: 480.1305.

*4.2.6 Synthesis of Nmoc-Phe-SPh **6**:*

a) Nmoc-Phe-OH (0.522 gm, 1.5 mmol) in 50 mL THF was added with 1.5 mmol, 0.208 mL) Et_3N. 1.5mmol (0.142 mL) of $ClCO_2Et$ was added to the reaction mixture at -15 ^{o}C and stirred it for 10 min. Thiophenol (1.5 mmol, 0.152 mL) was added to the reaction mixture. The solution was kept for 30 min at 10 ^{o}C with stirring. The reaction mixture was stirred for 1h at room temperature. 20 mL water was added. THF was evaporated in vacuo and the residue was dissolved in ethyl acetate. The solution was washed with saturated $NaHCO_3$ solution and water. The ethyl acetate layer was extracted and dried over Na_2SO_4. It was concentrated in vacuo and covered with a layer of petroleum ether. The compound **6** was obtained as white solid. Yield= 0.580 g (1.31 mmol, 87%). $[\alpha]_D^{25}$ = -16 (c = 1, MeOH); FT-IR (KBr): ῡ 3305 (s), 3058 (ms), 2965 (ms), 1690 (s), 1533 (ms), 1446 (s),

1369 (ms), 1318 (ms), 1259 (s); ^{1}H NMR (400 MHz, $CDCl_3$): δ 7.76 (m, 4H, Nph), 7.41 (m, 2H, Nph), 7.31 (s, 1H, Nph), 7.21 (d, 1H, *J*= 7.28 Hz, NH), 7.18 (m, 5H, Ph), 7.10 (m, 5H, Phe), 5.22 (s, 2H, CH_2 of Nph), 4.78 (m, 1H, $C^{\alpha}H$ of Phe), 3.10 (m, 2H, $C^{\beta}Hs$ of Phe) ppm; ^{13}C NMR (100 MHz, $CDCl_3$): δ 198.7, 193.1, 135.2, 134.6, 133.4, 133.1, 131.7, 129.6, 129.4, 129.2, 128.7, 128.3, 127.7, 127.2, 126.2, 125.7, 67.45, 61.37, 38.43 ppm; MS (ESI) m/z for $C_{27}H_{23}NO_3S$ $(M+Na)^+$ calcd.: 464.1291 found: 464.1368.

*4.2.7 Synthesis of Nmoc-Leu-SPh **7**:*

Nmoc-Leu-OH (0.321 gm, 1 mmol) in 25 mL THF was added with 1 mmol (0.139 mL) Et_3N. 1 mmol (0.095 mL) of $ClCO_2Et$ was added to the reaction mixture at -15 °C and stirred it for 10 min. Thiophenol (1 mmol, 0.1 mL) was added to the reaction mixture. The solution was kept for 30 min at 10 °C with stirring. The reaction mixture was stirred for 1h at room temperature. 20 mL water was added. THF was evaporated in vacuo and the residue was dissolved in ethyl acetate. The solution was washed with saturated $NaHCO_3$ solution and water. The ethyl acetate layer was extracted and dried over Na_2SO_4. It was concentrated in vacuo and covered with a layer of petroleum ether. The compound **7** was obtained as white solid.

Yield= 0.262 g (0.64 mmol, 64%). $[\alpha]_D^{25}$ = -11 (c = 1, MeOH); FT-IR (KBr): ῡ 3380 (s), 3058 (ms), 2958 (ms), 2875 (ms), 1700 (s), 1506 (s), 1469 (ms), 1336 (ms), 1262 (s); ^{1}H NMR (400 MHz, $CDCl_3$): δ 7.84 (m, 4H, Nph), 7.49 (d, 2H, Nph), 7.46 (s, 1H, Nph), 7.39 (m, 5H, Ph), 5.32 (s, 2H, CH_2 of Nph), 4.62 (m, 1H, $C^{\alpha}H$ of Leu), 1.76 (m, 2H, $C^{\beta}Hs$ of Leu), 1.58 (m, 1H, $C^{\gamma}H$ of Leu), 0.96 (d, 6H, J= 5.28 Hz, $C^{\delta}Hs$ of Leu) ppm; ^{13}C NMR (100 MHz, $CDCl_3$): 199.5, 155.8, 134.6, 133.5, 133.2, 133.1, 129.5, 129.2, 128.4, 128.0, 127.7, 127.2, 127.0, 126.3, 126.2, 125.7, 67.45, 59.54, 41.79, 24.82, 23.06, 21.58 ppm; MS (ESI) m/z for $C_{24}H_{25}NO_3S$ $(M+Na)^+$ calcd.: 430.1447 found: 480.1446.

*4.2.8 Synthesis of Nmoc-Val-SPh **8**:*

Nmoc-Val-OH (0.311 gm, 1 mmol) in 25 mL THF was added with 1 mmol (0.139 mL) Et_3N. 1 mmol (0.1 mL) of $ClCO_2Et$ was added to the reaction mixture at -15 ^oC and stirred it for 10 min. Thiophenol (1 mmol, 0.1 mL) was added to the reaction mixture. The solution was kept for 30 min at 10 ^oC with stirring. The reaction mixture was stirred for 1h at room temperature. 20 mL water was added. THF was evaporated in vacuo and the residue was dissolved in ethyl acetate. The solution was washed with saturated $NaHCO_3$ solution and water. The ethyl acetate layer was extracted and dried over Na_2SO_4. It was concentrated in vacuo and covered with a layer of petroleum ether. The compound **8** was obtained as white solid.

Yield= 0.289 g (0.735 mmol, 73.66%). $[\alpha]_D^{25}$ = -9 (c = 1, MeOH); FT-IR (KBr): ῡ 3347 (s), 3051 (ms), 2960 (ms), 1723 (s), 1682 (s), 1529 (s), 1446 (ms), 1392 (ms), 1343 (ms), 1295 (s); ^1H NMR (400 MHz, $CDCl_3$): δ 7.84 (m, 4H, Nph), 7.49 (m, 3H, Nph), 7.39 (m, 5H, Ph), 5.32 (s, 2H, CH_2 of Nph), 4.51 (m, 1H, $C^{\alpha}H$ of Val), 2.36 (m, 1H, $C^{\beta}H$ of Val), 1.04 (d, 3H, *J*= 7.28 Hz, $C^{\gamma}Hs$ of Val), 0.93 (d, 3H, *J*= 7.28 Hz, $C^{\gamma}Hs$ of Val) ppm; ^{13}C NMR (100 MHz, $CDCl_3$): 198.7, 156.2, 134.6, 133.5, 133.2, 133.1, 131.7, 130.1, 129.5, 129.2, 128.4, 128.0, 127.7, 127.2, 127.0, 126.3, 126.2, 125.7, 67.52, 65.74, 31.23, 19.48, 16.87 ppm; MS (ESI) m/z for $C_{23}H_{23}NO_3S$ $(M+Na)^+$ calcd.: 416.2191 found: 416.1297.

4.3 Gel Preparation and Characterization Techniques

4.3.1 Gel Preparation

Compound **1** Nmoc-Y-SePh (20 mmol L^{-1}, 10.1 mg) was dissolved in 100 μL of ethanol. A solution of Cys-Gly (20 mmol L^{-1}, 3.5 mg) in phosphate buffer (900 μL, pH 7-8) was mixed together and left undisturbed at room temperature for 1h. Self-assembly of ligated

product **1a** was observed at 60 min after mixing with Cys-Gly dipeptide. Formation of Nmoc-YCG was confirmed by HPLC and ESI-MS. Similarly, compound **2** Nmoc-F-SePh (20 mmol L^{-1}, 9.7 mg) was ligated to Cys-Gly at same reaction condition. The **2c** is a ligated product which forms sulfur-selenium bond with cleaved phenyl selenol resulting into formation of self-supporting gel. The self-assembly of **2c** was observed at 15 min after NCL reaction. No self-assembly was observed for compounds **3** to **8** at same reaction condition. Similarly, compounds **1** to **4** were subjected to NCL reaction with cysteine at same reaction conditions and ligated products were characterized by HPLC and ESI-MS. None of them self-assembled in phosphate buffer except **6b** $(Nmoc\text{-}FC\text{-}OH)_2$ which is the disulfide of ligated product **6a**.

4.3.2 Dis-assembly Study

Dynamic self-assembly $(NmFC)_2$ was monitored upon NCL reaction under inert atmosphere. The NmFC is a ligated product formed upon NCL reaction which remained in solution phase until exposure to air. Self-supporting gel was observed when NmFC was exposed to air which turned into disulfide $(NmFC)_2$. The gel-sol reversal phenomenon was observed for $(NmFC)_2$ upon addition of a reductant Tris(2-carboxyethyl)phosphine (TCEP) 40 mmol/L at pH 5.8.

4.3.3 ^{1}H NMR Spectroscopy

All NMR spectra were recorded with 400 MHz Bruker AV 400 NMR spectrometer. TMS was used as internal reference in the NMR spectra. Compounds concentrations were in the range of 1-10 mmol in $(CD_3)_2SO$ and $CDCl_3$.

4.3.4 Polarimeter

Specific rotations of the synthesized compounds were measured on an Autopol V automatic polarimeter (Rudolph research analytical). The

cell (length =100 mm, capacity = 2 mL) was used for this study at 25 ^{o}C.

4.3.5 Mass Spectrometry

Mass spectra of peptides were recorded on Bruker micrOTOF-Q II by positive and negative mode electrospray ionizations.

4.3.6 High Performance Liquid Chromatograpy (HPLC) Analysis

A Dionex HPLC-Ultimate 3000 (High Performance Liquid Chromatography) pump was used to analyze native chemical ligated products. 20 μL of sample was injected onto a Dionex Acclaim ® 120 C 18 column of 250 mm length with an internal diameter 4.6 mm and 5 μm fused silica particles at a flow rate of 1 mL min^{-1} (linear gradient of 40 % v/v) acetonitrile in water for 35 min, gradually rising to 100 % (v/v) acetonitrile in water at 35 min). This concentration was kept constant until 40 min when the gradient was decreased to 40 % (v/v) acetonitrile in water at 42 min. The sample preparation was involved mixing of 100 μL of gel/solution with acetonitrile-water (900 μL, 50: 50 mixture) containing 0.1 % trifluoroacetic acid. The samples were then filtered through a 0.45 μm syringe filter (Whatman, 150 units, 13 mm diameter, 2.7 mm pore size) prior to injection. The native chemical ligated products were identified by using Ultimate 3000 RS Variable Wavelength Detector at 280 nm.

4.3.7 Rheology

Rheological measurements were carried out using an Anton Paar Physica MCR 301 rheometer with parallel plate of geometry (25 mm in diameter, 0.200 μm gap). 200 μL of NmYCG**,** NmF(SePh)CG and $(NmFC)_2$ gels were prepared in glass vials and transferred onto the plate of the instrument using microspatulla. The temperature was kept at 25°C by using an integrated temperature controller. Then dynamic

frequency sweep of the gel NmYCG**,** NmF(SePh)CG and $(NmFC)_2$ were measured as function of frequency in the range of 0.05-100 rad s^{-1} with constant strain value 0.05%. The time sweep was measured at constant strain of 0.05%. To determine the exact strain for frequency sweep and time sweep experiments the linear viscoelastic (LVE) regime were performed at constant frequency of 10 rad s^{-1}.

Dis-assembly behavior of gel was performed by adding Tris(2-carboxyethyl)phosphine (TCEP) (40 mmol/L, 10.6 µl) to a gel formed by $(NmFC)_2$ (20 mmol/L). The gels were transferred onto the plate of rheometer by using micro-spatula immediately after addition of TCEP. The time sweep measurement was done at constant strain of 0.05%. As time sweep experiment shows that the gel $(NmFC)_2$ started to break at 60 min, where the G' (storage modulus) and G'' (loss modulus) started to intermix with each other.

4.3.8 FT-IR Spectroscopy

Fourier transform infrared (FTIR) spectra were recorded using a bruker (Tensor 27) FTIR spectrophotometer for wet gel material by using ZnSe windows. The gel samples were placed between crystal Zn-Se windows and scanned between 900 and 4000 cm^{-1} over 64 scans at a resolution of 4 cm^{-1} and an interval of 1 cm^{-1}.

4.3.9 Circular Dichroism

Circular dichroism (CD) spectra were measured at 25°C on a Jasco J-815 spectropolarimeter. Spectra were measured between 300 and 190 nm with a data pitch of 0.1 nm. The bandwidth was set to 1 nm with a scanning speed of 20 nm min^{-1} and a response time of 1 s. The path length was 1 mm quartz cell (Starna Scientific Ltd. Hainault, UK). Samples were prepared at concentration of 2 mmol/L. Experimental data were acquired in thrice and the average data is shown.

4.3.10 Time Correlated Single Photon Counting Spectroscopy

A 2 mL of gel sample was prepared in a 1 cm^2 quartz cuvette and Time resolved studies were done by a time correlated single photon counting (TCSPC) system from Horiba Yovin (Model: Fluorocube-01-NL). Samples were excited at 376 nm using a picosecond diode laser (Model: Pico Brite-375L). The signals were collected at magic angle (54.70) polarization using a photomultiplier tube (TBX-07C) as detector, which has a dark counts less than 20 cps. The instrument response function was typically 140 ps. The data analysis was performed using IBH DAS (version 6, HORIBA Scientific, Edison, NJ) decay analysis software.

The amplitude weighted lifetime was estimated by

$$\langle \tau \rangle = \sum_{i=1}^{n} a_i \, \tau_i$$

where τ_i is the fluorescence lifetime of various fluorescent species and are the normalized pre-exponential factors. To gain the best fitting in all cases the χ^2 was kept near to unity.

4.3.11 Microscopic Techniques

Transmission electron microscopic images were taken using a PHILIPS electron microscope (model: CM 200), operated at an accelerating voltage of 200 kV. The 2 $mmolL^{-1}$ of dilute solution of the gel was dried on carbon-coated copper grids (300 mesh) by slow evaporation in air, then allowed to dry separately under vacuum at room temperature.

AFM study was done by placing very dilute solution of gel (200 µL of gel was dissolved in 800 µL of milii-Q water) on mica and allowed it to dry in air for 2 days at room temperature. Images were recorded by using scanning probe microscope AIST-NT instrument (model no. smart SPM-1000).

4.4 Results and Discussion

Native chemical ligation is a widely used method in proteins and peptide synthesis. In the chapter, we focused on the redox active peptides generated via selenoester mediated native chemical ligation. L-Cysteineglycine, a prooxidant generated from the extracellular glutathione through the catalytic activity of an enzyme γ-glutamyltransferase.[15] Cys-Gly is known as a highly reactive metabolite which is directly related to induce the oxidative stress in the cells. Lin *et al. (2007)* reported that higher cysteineglycine level were marginally associated with an increased risk of breast cancer in women.[16]

Here, we have exploited Cys-Gly dipeptide in the development of dynamic peptide self-assembly through NCL reaction (figure 4.23). The selenoester easily undergoes NCL reaction with Cys-Gly dipeptide which could be an assay in further clinical research.

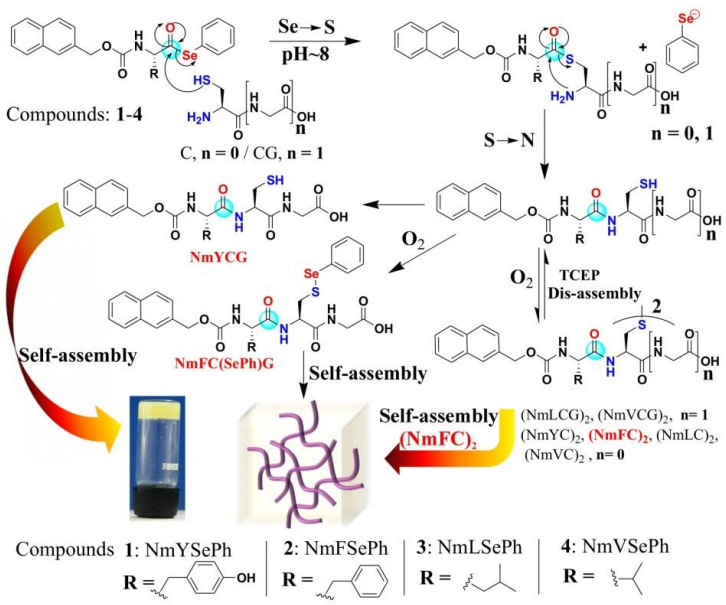

***Figure 4.23**. Selenoester mediated native chemical ligation. Ligated products were formed upon NCL of selenoesters with Cys-Gly and Cysteine at pH~8 and undergoes dynamic peptide self-assembly. Nmoc-YCG **1a** self-assembled in its reduced form while Nmoc-F(SePh)CG **2c** (sulfur linked with selenophenol) and (Nmoc-FC-OH)$_2$ **6b** oxidized in presence of atmospheric air to form self-supporting soft materials.*

4.4.1 Ligation Study

The NCL reaction proceeds through thioester linked intermediate where acyl transfers from Se→S[17] followed by intramolecular S→N acyl transfer to give a peptide bond (Figure 4.23). A compound **1** Nmoc-Y-SePh (20 $mmolL^{-1}$, 10.1 mg) was dissolved in 100 µL of ethanol. A solution of Cys-Gly (20 $mmolL^{-1}$, 3.5 mg) in phosphate buffer (900 µL, pH~8) was mixed together and left undisturbed at room temperature for 1h. Self-assembly of ligated product NmYCG was observed at 60 min after mixing with Cys-Gly dipeptide. Formation of Nmoc-YCG was confirmed by HPLC and ESI-MS. Similarly, compound **2** Nmoc-F-SePh (20 $mmolL^{-1}$, 9.7 mg) was ligated to Cys-Gly at same reaction condition. The NmF(SePh)CG is a ligated product which forms sulfur-selenium bond with cleaved phenyl selenol resulting into formation of self-supporting gel.

Table 4.1. *Native chemical ligation under inert as well as air conditions*
[a]Cys-Gly dipeptide, [b]Cysteine, [c]G = gel, S = solution

Entry	Substrate	CG[a] and C[b]	Conversion in inert atm.[c] [%]	Conversion in air[c] [%]	Gel[d]
1	**1**	CG	>99 NmYCG	>99 NmYCG	G
2	**2**	CG	22.64/76[e] NmFCG/ NmFC(SePh)G	77.36 NmFC(SePh)G	G
3	**3**	CG	>99 NmLCG	>99 $(NmLCG)_2$	S
4	**4**	CG	65.79 NmVCG	63.35 $(NmVCG)_2$	S
5	**1**	C	>99 NmYC	95.09 $(NmYC)_2$	S
6	**2**	C	94.31NmFC	84.90 $(NmFC)_2$	G
7	**3**	C	>99 NmLC	>99 $(NmLC)_2$	S
8	**4**	C	>99 NmVC	79.28 $(NmVC)_2$	S

The self-assembly of NmFC(SePh)G was observed at 15 min after NCL reaction. No self-assembly was observed for compounds **3** to **8** at same reaction condition. Similarly, compounds **1** to **8** were subjected to NCL reaction with cysteine at same reaction conditions and ligated products were characterized by HPLC and ESI-MS (Figure 4.24-4.42). None of them self-assembled in phosphate buffer except $(NmFC)_2$.

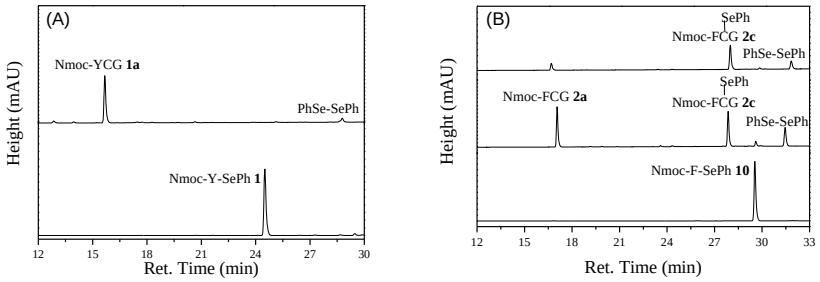

Figure 4.24. *A) Overlaid HPLC chromatograms for compound **1** showing peak **1a** after native chemical ligation in air as well as in inert atmosphere B) compound **2** showing peaks **2a** in inert condition after native chemical ligation and sulfur selenide bond of ligated product **2c** in air.*

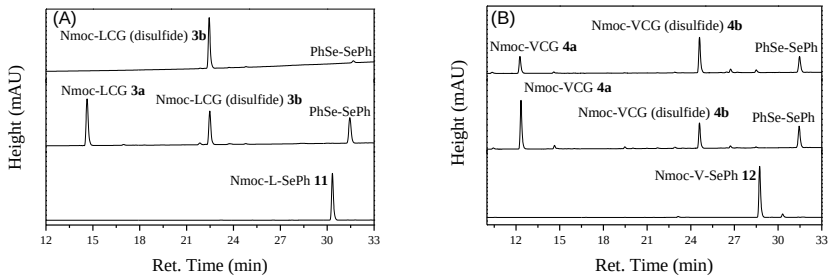

Figure 4.25. *A) Overlaid HPLC chromatograms for compound **3** showing peaks **3a** in inert condition after native chemical Ligation and **3b** disulfide of ligated product in air B) compound **4** showing peak **4a** in inert condition after native chemical ligation and **4b** disulfide of ligated product in air.*

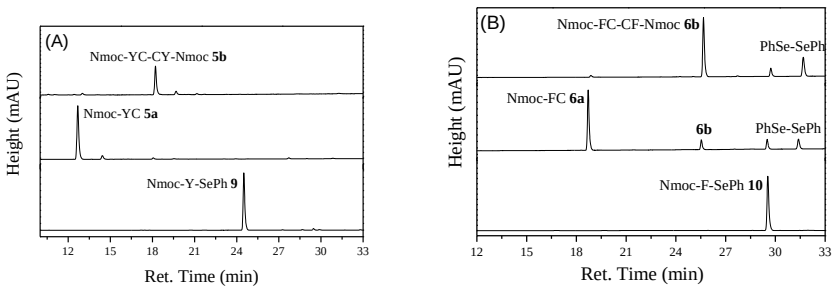

Figure 4.26. *A) Overlaid HPLC chromatograms for compound **1** showing peaks **5a** in inert condition after native chemical ligation and peak **5b** for its corresponding disulfide in air B) compound **2** showing peak **6a** in inert condition after native chemical ligation and peak **6b** for its corresponding disulfide in air.*

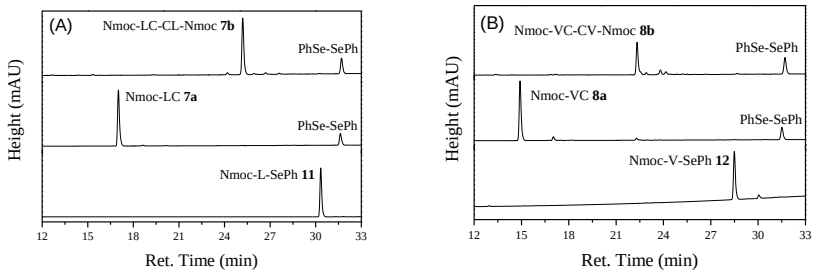

Figure 4.27. *A) Overlaid HPLC chromatograms for compound **3** showing peak **7a** in inert condition after native chemical ligation and peak **7b** for its corresponding disulfide in air B) compound **4** showing peak **8a** in inert condition after native chemical ligation and peak **8b** for its corresponding disulfide in air.*

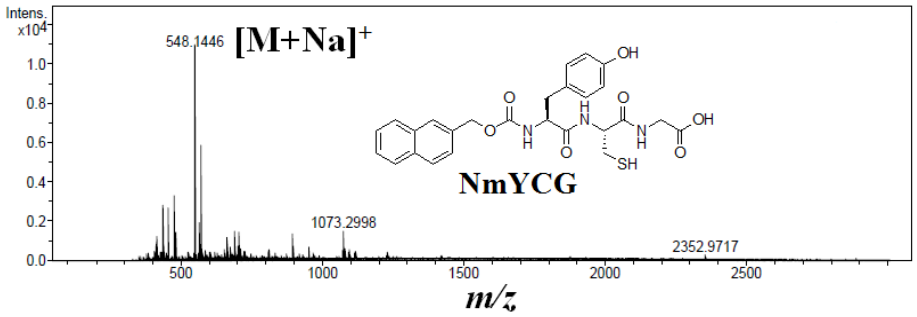

Figure 4.28. *ESI-MS spectrum of ligated product **NmYCG**.*

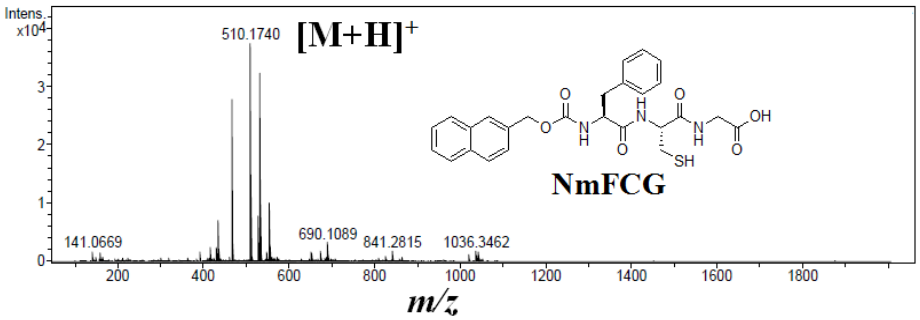

Figure 4.29. *ESI-MS spectrum of ligated product **NmFCG**.*

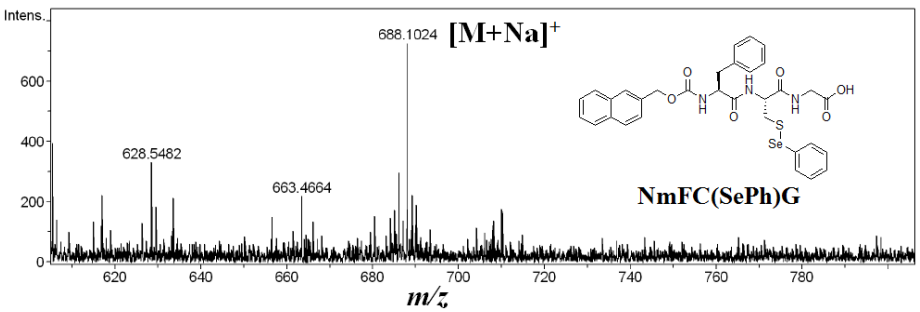

Figure 4.30. *ESI-MS spectrum of ligated product **NmF(SePh)CG**.*

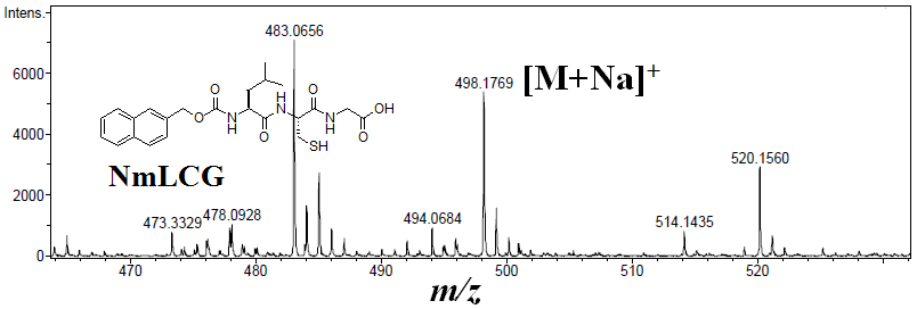

Figure 4.31. *ESI-MS spectrum of ligated product* ***NmLCG****.*

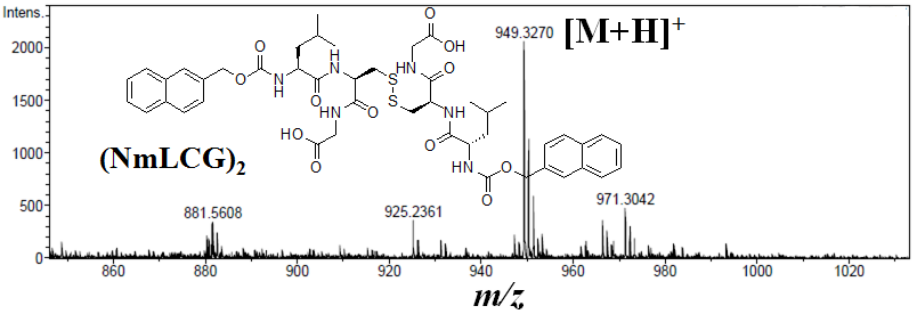

Figure 4.32. *ESI-MS spectrum of ligated produ t (****NmLCG)$_2$****.*

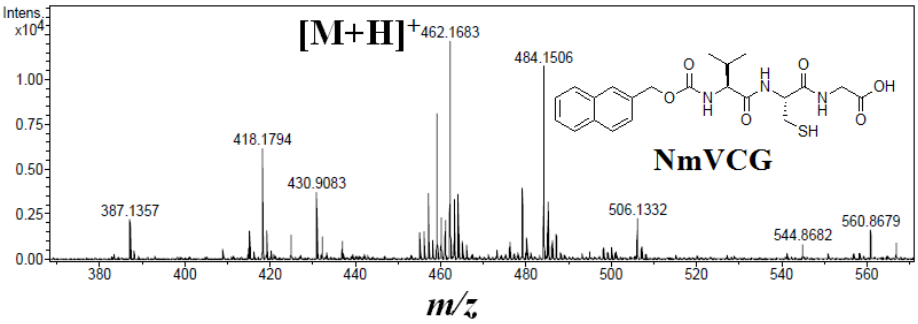

Figure 4.33. *ESI-MS spectrum of ligated product* ***NmVCG****.*

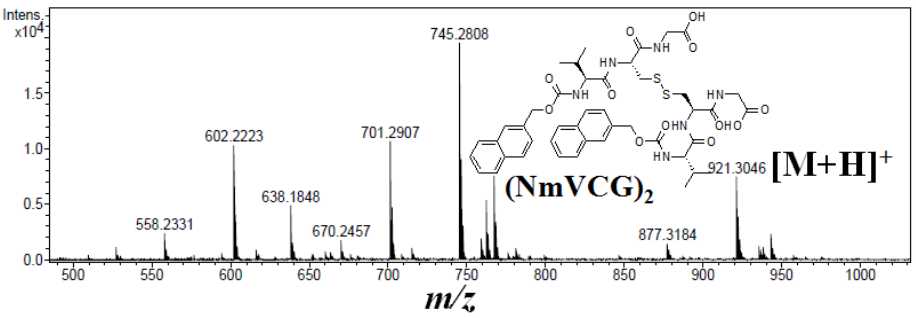

Figure 4.34. *ESI-MS spectrum of ligated product* ***(NmVCG)$_2$****.*

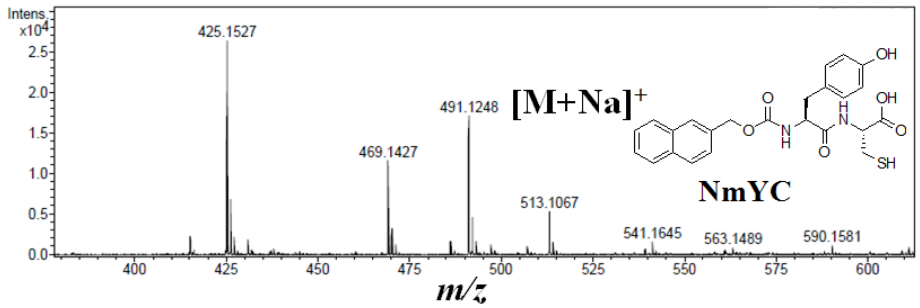

Figure 4.35. *ESI-MS spectrum of ligated product* ***NmYC****.*

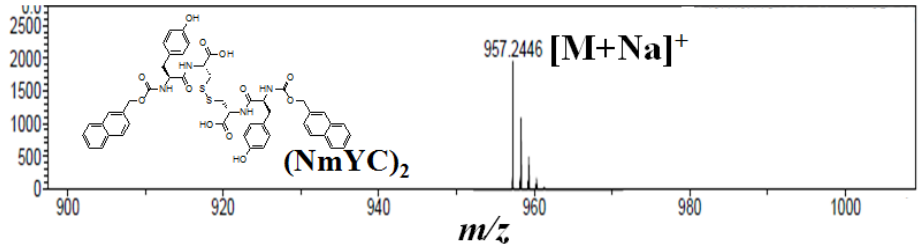

Figure 4.26. *ESI-MS spectrum of ligated product* ***(NmYC)$_2$****.*

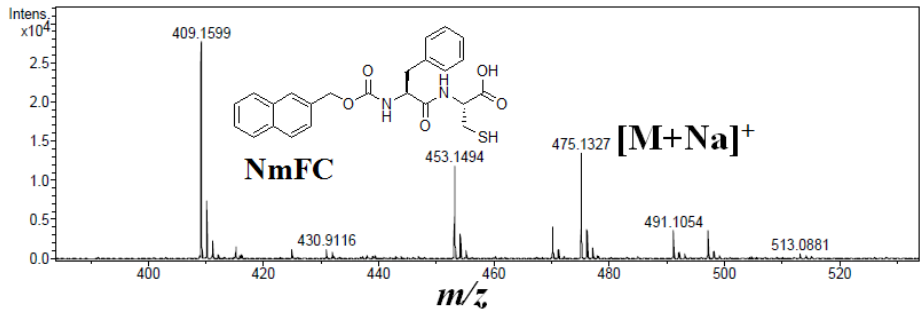

Figure 4.37. *ESI-MS spectrum of ligated product* ***NmFC****.*

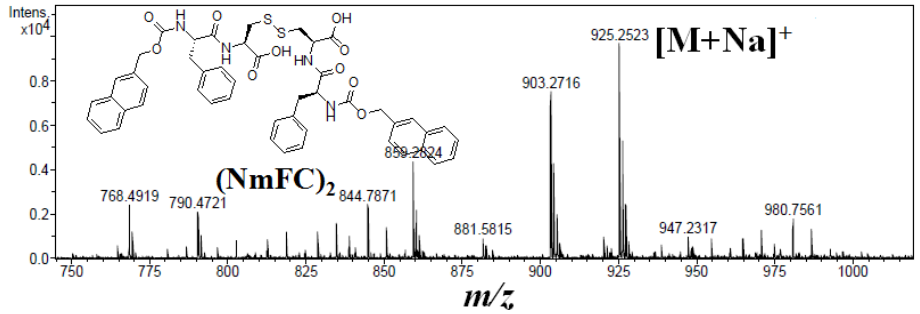

Figure 4.38. *ESI-MS spectrum of ligated product* ***(NmFC)$_2$****.*

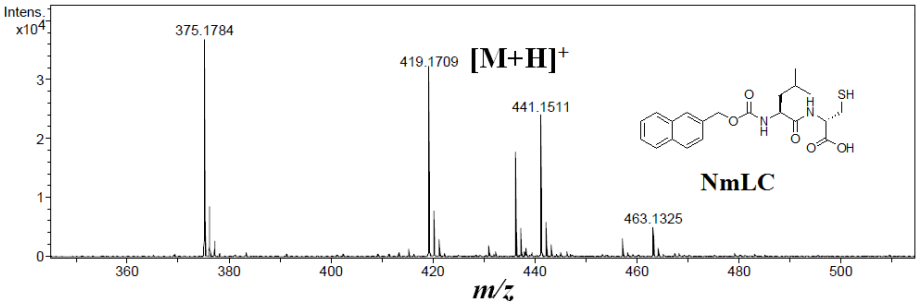

Figure 4.39. *ESI-MS spectrum of ligated product* ***NmLC.***

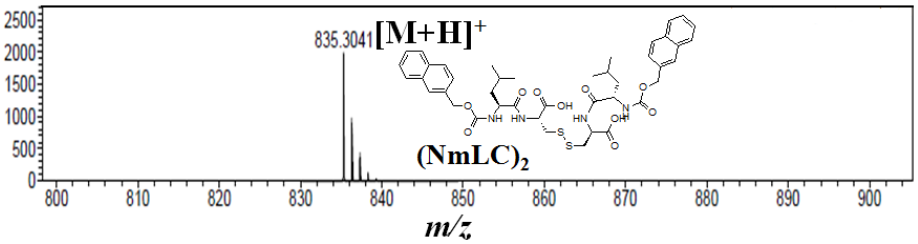

Figure 4.40. *ESI-MS spectrum of ligated product* ***(NmLC)₂.***

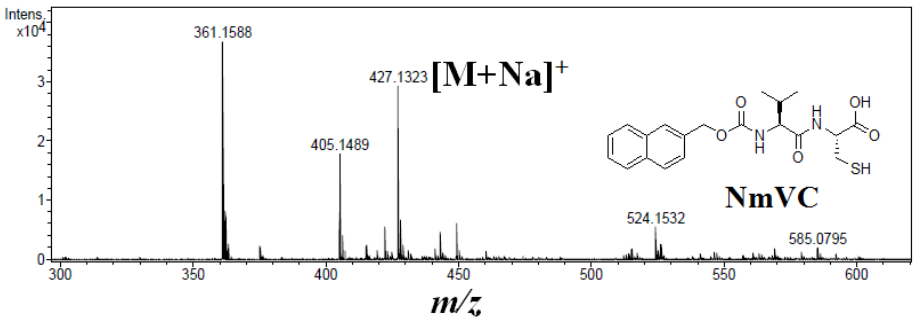

Figure 4. 41. *ESI-MS spectrum of ligated product* ***NmVC.***

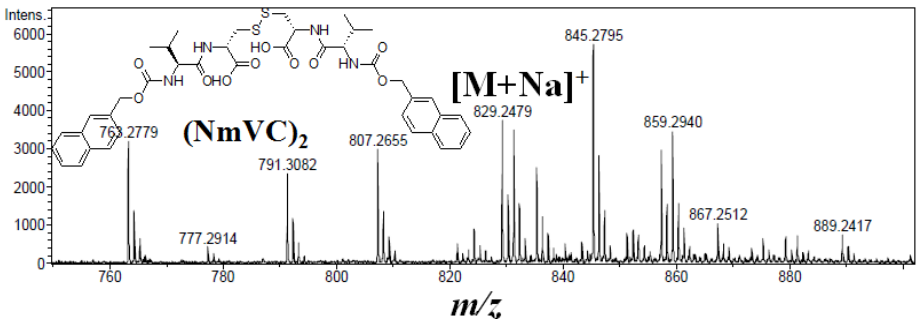

Figure 4.42. *ESI-MS spectrum of ligated product* ***(NmVC)₂.***

4.4.2 Self-Assembly Study

Compounds **1-4** (20 mmol/L) were dissolved in 100 µL of ethanol and Cys or Cys-Gly (20 mmol/L) was dissolved in 900 µL of phosphate

buffer (pH = 7-8, 100 mmol/L). 900 µL of Cys or Cys-Gly was added to the reaction vial containing compounds **1** to **4** (entries 1-8, Table 4.1). The reaction vial was allowed to leave undisturbed and self-supporting gels were observed after 1 h of reaction for entries **1**, **2** and **6**. The ligation reactions of Nmoc capped amino acid based selenoesters with Cys or Cys-Gly was monitored with reverse phase high performance liquid chromatography (HPLC) and the corresponding products were analyzed by ESI-MS (Figure 4.43C and 4.23-4.41). We also monitored the visual changes of solution **1** upon mixing with dipeptide Cys-Gly in phosphate buffer. Initially milky white solution was observed in 5 min which turned turbid to colorless after 15 min. The colorless viscous solution was observed after 30 min which turned into self-supporting gel after 60 min (Figure 4.44B). The compound **1** gives >99 % ligated peptide with Cys-Gly and similarly gives >99 % with cysteine (Table 4.1). Thus, NCL reaction with selenoester is the easiest and simplest way to synthesis peptides. However, the thioesters with similar amino acid sequences (compounds **5**-**8**) yielded poor conversion of peptides (Table Anx. **1**) and were unable to form gel under similar conditions.

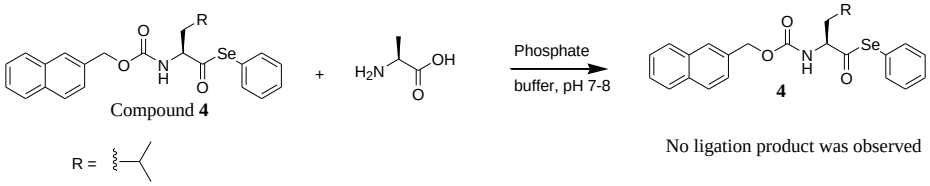

Figure 4.43. *Control experiment with Nmoc-V-SePh and alanine*

The control experiment with Nmoc capped Valine selenoester **3** with alanine confirms the requirement of C-terminal cysteine group in ligation reaction with selenoester (Figure 4.43). The free sulfhydryl group plays an important role in biology such as in glutathione, which regulates the oxidative stress in cell[18] and also acts as an antioxidant. Generally, it is oxidized to glutathione disulfide by donating its electron to the reactive oxygen species. The enzyme glutathione reductase converts glutathione glutathione disulfide to glutathione,

which performs normal functions in cell. Typically, NCL reactions are carried out in presence of reductant such as *tris* (2-carboxyethyl) phosphine (TCEP) and dithiothreitol (DTT). TCEP or DTT helps to avoid the formation of disulfides. Surprisingly, we have not used any reductant for the reaction of compound **1** with Cys-Gly (entry **1**). The reduced form of Nmoc-Tyr-Cys-Gly was observed after 16 h in aerobic condition.[19] However, entries 3-8 showed exactly reverse behavior to entry **1**. Oxidized form of NCL products were observed for entries 3-8 in similar conditions to NCL reaction of entry **1** (Table 4.1).

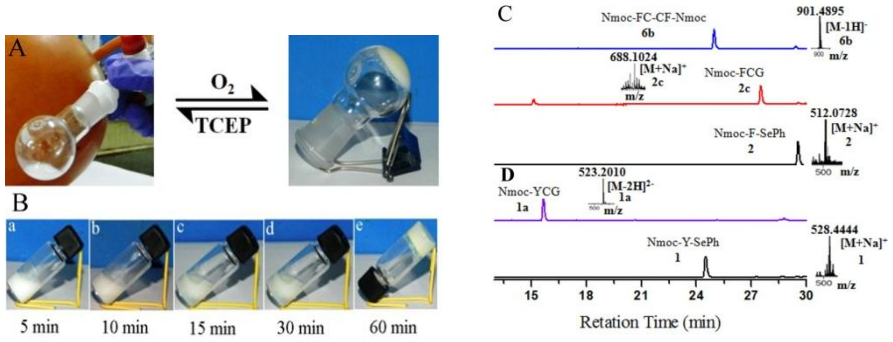

F*igure 4.44.* *A) Dynamic self-assembly of 6b formed upon NCL reaction of compound **2** with cysteine. NCL reation of compound **2** with cysteine gives NmFC **6a** under inert atmosphere and subsequently formed dynamic gel $(NmFC)_2$ **6b** upon exposure to air. B) Visual indication of reaction progress initially mixing of compound **1** (20 $mmolL^{-1}$) with Cys-Gly (20 mmol/L) in phosphate buffer at pH 7-8. a) Milky white solution at 5 min, (b) turbid at 10 min, (c) colorless solution at 15 min, (d) colorless viscous solution at 30 min and (e) self-supporting gel formed after 60 min. C) HPLC trace analysis of a representative ligation of compound **2** with Cys-Gly and Cysteine after 1 h with corresponding ESI-MS of ligated products. D) HPLC traces of representative NCL reaction of compound **1** with Cys-Gly with corresponding ESI-MS of ligated product.*

A self-supporting gel for entry **1** was observed with 99% synthesized peptide Nmoc-YCG. Another self-supporting gel for entry **6** was also observed for the newly synthesized 84.9 % oxidized peptide $(Nmoc\text{-}Phe\text{-}Cys\text{-}OH)_2$. However, in case of entry **2**, a dipeptide Cys-Gly reacted with compound **2** and formed the corresponding tripeptide Nmoc-FCG. Nmoc-FCG further reacted with cleaved selenophenol and formed sulfer-selenium bond (Figure 4.22). The resulting product

NmF(SePh)CG turned to a self-supporting gel. Our data indicates that reduced and oxidized form of ligated peptides can self-assemble and lead to self-supporting gels.[20] The self-assembly of ligated products drives self-selection and self-organization into reduced and oxidized form of peptides. The dis-assembly phenomenon of **6** was observed using a reductant TCEP (40 mmol/L) after 2 h which further explores gelators as versatile candidates for drug delivery (Figure 4.44A).

4.4.3 Rheological Study

The relative rigidity of soft materials formed upon NCL reactions was analyzed using oscillatory rheology. The viscoelastic nature of self-assembled gel was confirmed when storage modulus (G') found higher by an order of magnitude than loss modulus (G'') which indicates elastic nature of a gel. The self-assembly of $(Nmoc\text{-}FC)_2$ exhibits higher value of G' than the gel formed by NmYCG and NmF(SePh)CG **2c** (Figure 4.45B, 4.46A and B). The time sweep experiment was performed for $(NmFC)_2$ gel which undergoes gelation upon disulfide formation. The gelation process started at 12 min after NCL reaction which was indicated by time sweep experiment (Figure 4.47A). The disulfide reduction leads to gel-sol transition of $(Nmoc\text{-}FC)_2$ which was monitored with oscillatory time sweep experiment after addition of TCEP (Figure 4.47B).

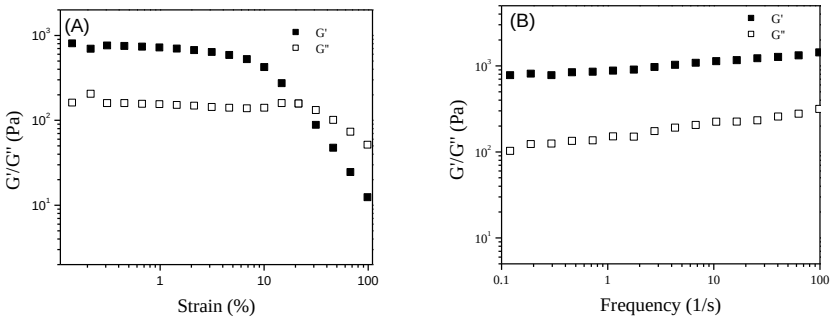

Figure 4.45. *A) Rheological measurement of LVE at constant frequency 10 rad s^{-1} for gel* ***1a.*** *B) Dynamic frequency sweep of self-assembled peptide NmYCG* ***1a*** *at constant strain 0.05%.*

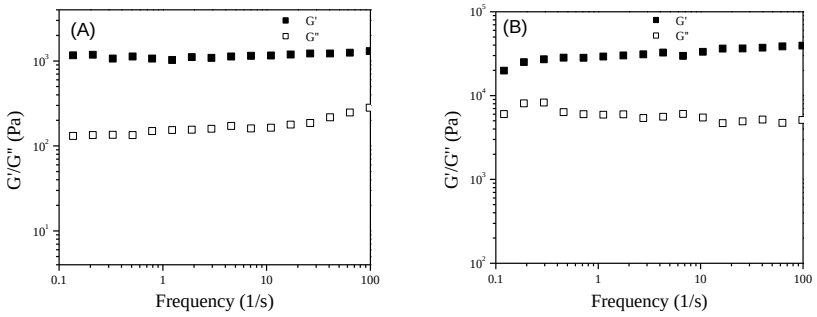

Figure 4.46. *A) Dynamic frequency sweep of self-assembled peptide NmF(SePh)CG* ***2c*** *and B) (NmFC)$_2$* ***6b*** *at constant strain 0.05%.*

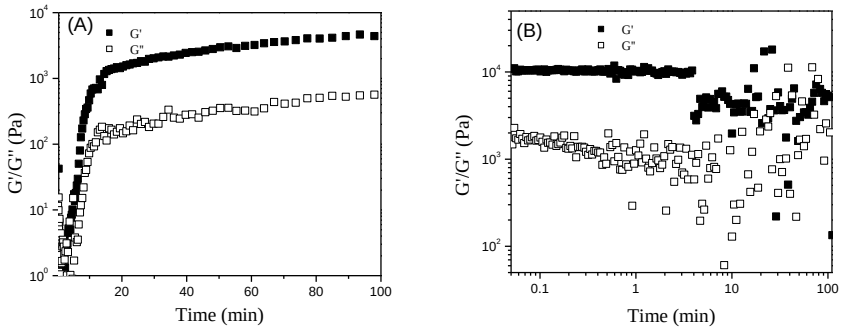

Figure 4.47. *Oscillatory rheology of a solution containing 20 mmol/L of (NmFC)$_2$ at 25 ^{o}C shows that (NmFC)$_2$ started gaining gelation property at 12 min B) a gel containing 20 mmol/L of (NmFC)$_2$ and solution of TCEP 40 mmol/L at 25 ^{o}C indicates that the gel started breaking at 60 min.*

4.4.4 Circular Dichroism and FTIR study

Circular dichroism is used to elucidate the secondary structure of proteins and peptides. It also provides useful information about the self-assembled architectures. We used CD to observe peptide conformations in gel phase medium (Figure 4.48A). The selenoester **1** in NCL reaction with Cys-Gly peptide self-assembled in ethanolic phosphate buffer solution. The CD spectrum of Nmoc-YCG (entry 1, Table 4.1) shows a positive peak at 208 nm and a negative peak at 221 nm corresponding to the co-existence of random-coil and β-sheet conformation.[21] However, CD spectra of **2** and **6** in gel state show characteristic twisted conformation. The two negative peaks at 222 nm and 205 nm indicate twisted conformation of self-assembled peptides.[22] The CD spectrum of gel (NmFC)$_2$ upon treatment with

TCEP indicates the change in conformation of the reduced dis-assembled peptide (Figure 4.48B). Fourier transform infrared spectroscopy (FTIR) was also used to support the secondary structures of self-assembled peptides (Table 4.2). The ligated peptide Nmoc-YCG shows peaks at 1640 cm^{-1} and 1688 cm^{-1} which correspond to turn type structures.

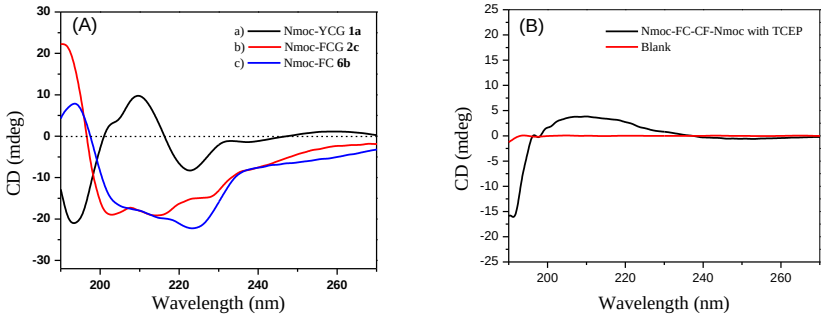

Figure 4.48. *CD spectra of self-assembled peptides (a) Nmoc-YCG **1a**, (b) Nmoc-FCG **2c** and (c) $(NmFC)_2$ (concentration of **1a**, **2c**, **6b** = 2 mmol/L) formed upon NCL reaction at pH~8 B) $(NmFC)_2$ **6b** gel upon treatment with TCEP which results into gel-sol transition.*

Table 4.2. *FTIR analysis of peptide gels obtained via NCL*

Sr. No.	Peptide gel	Amide-I (C=O stretching)	Amide-II (C-N stretching, N-H bending)
1	**1a**	1640/1688 cm^{-1}	1580/1534 cm^{-1}
2	**2c**	1610/1680 cm^{-1}	1551/1504 cm^{-1}
3	**6b**	1685 cm^{-1}	1589/1526 cm^{-1}

4.4.5 Time Correlated Single Photon Counting Study

A time resolved fluorescence study was acquired to investigate the higher order aggregation of the fluorophore groups (Nmoc) of the NmYCG, NmF(SePh)CG and $(NmFC)_2$ gels. We measured fluorescence decay traces of the gels at an excitation of 376 nm and the emission was monitored at 470 nm. The average lifetime 1.14 ns of Nmoc-YCG **1a**, 3.39 ns of Nmoc-F(SePh)CG **2c** and 1.06 ns of $(Nmoc\text{-}FC)_2$ **6b** were observed (Table 4.3, Figure 4.49). The average

fluorescence lifetime of the gel samples indicates a more dense aggregated nanofibrous network in the gel state.

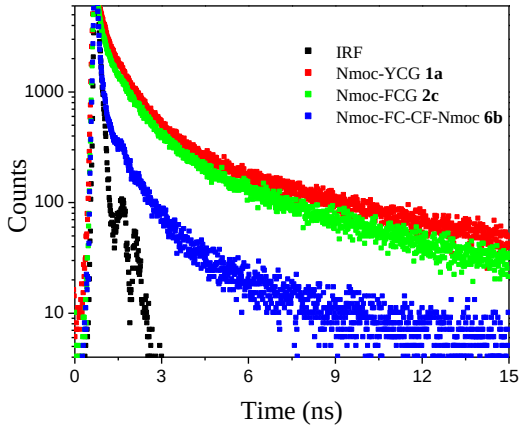

Figure 4.49. *Emission decay curves for self-supproting gels of Nmoc-YCG, Nmoc-F(SePh)CG* ***2c*** *and Nmoc-FC-CF-Nmoc monitored at 470 nm (IRF: instrument response function).*

Table 4.3. *Decay parameters for NmYCG, NmF(SePh)CG and* $(NmFC)_2$ *gels.*

Entry	α_1	α_2	τ_1(ns)	τ_2(ns)	τ^a(ns)	χ^2
Nmoc-YCG (gel)	0.91	0.09	0.70	5.59	1.14	1.67
Nmoc-F(SePh)CG (gel)	0.71	0.29	1.31	7.04	3.39	1.10
$(Nmoc-FC)_2$ (gel)	0.94	0.06	0.84	4.78	1.06	1.26

4.4.6 Microscopic Study

The presence of secondary structures with viscoelastic properties make it more curious about the structural morphology of the self-assembled materials. We used transmission electron microscopy (TEM) to characterize the morphology of the self-assembled architectures in gel phase. The nanotubular[23] structures were observed for a gel formed by Nmoc-YCG (entry 1) with average diameter of 150 nm. However, gels formed by Nmoc-FCG (entry 2) and $(Nmoc-FC-OH)_2$ (entry 6) showed entangled nanofibrillar networks with the diameter ranging from 10 to 60 nm (Figure 4.50).

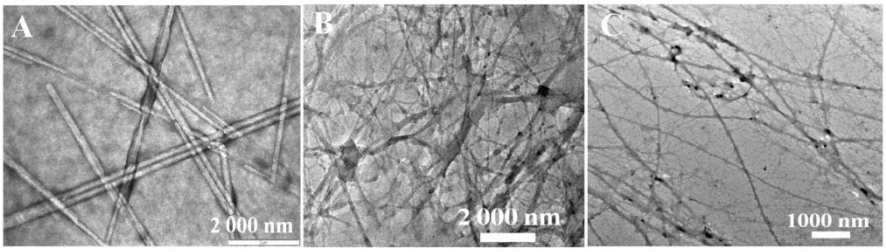

Figure 4.50. *TEM images indicating nanotubular to nanofibrillar structures of self-assembled gels A) Nmoc-YCG* ***1a*** *B) Nmoc-F(SePh)CG* ***2c*** *C)* $(NmFC)_2$ ***6b.***

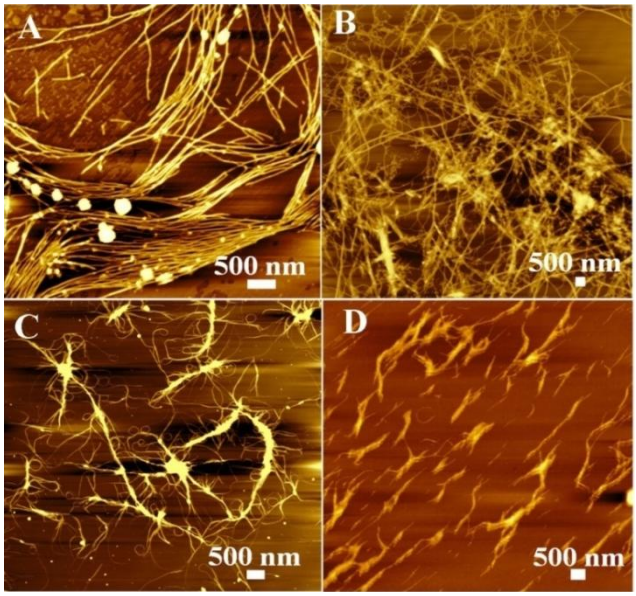

Figure 4.51. *AFM images indicating nanofibrillar structures of self-assembled gels A) NmYCG* ***1a****, B) NmF(SePh)CG* ***2c****, C)* $(NmFC)_2$ ***6b****, D) AFM image of dis-assembled peptide gel* $(NmFC)_2$ ***6b*** *(20 mmol*L^{-1}*) upon addition of TCEP (40 mmol*L^{-1}*) which converts to NmFC* ***6a*** *indicating disruption of nanofibrillar structures.*

The atomic force microscopy (AFM) studies of gels also showed nanofibrillar morphology (Figure 4.51). The gel **1** exhibited highly aligned nanostructures in gel phase medium with the height of 3 to 6 nm (Figure 4.51A). However, the gel formed by **2** showed elongated thin nanofibrous morphology with average width of 2 nm. The AFM analysis of **6** indicated that nanofibers originated from thick fibers. The AFM result for gel-sol transition indicates the breaking of nanofibers which leads to dis-assembly of self-assembled gel **6** (Figure 4.51D).

4.5 Conclusion

In summary, we showed a novel method based on selenoester mediated native chemical ligation for the exploitation of peptide self-assembly.

Cysteine and Cys-Gly peptide have provided mechanistic insight into the NCL driven self-assembly process. We have also shown the redox active dynamic peptide gels which are formed via oxidation and reduction of the Nmoc-protected peptide synthesized via NCL reactions. Here, gel-sol transition is highly dependent on the oxidation and reduction of cysteine and cystine based peptides. Peptides are self-assembled via hydrogen bonding and π-π stacking interactions and peptides are redox active in nature. Here, selenoester mediated NCL reaction are responsible for nanofibrillar structure. There are several reports about the anchoring of peptides and polypeptides over maleimide-functionalized lipids via thiol reactions. Our method can be used to design desired peptides to anchor over such a biological membrane. Such novel system will be useful to develop functional biomaterials.

4.6 References

1. Whitesides G. M., Grzybowski B. (2002), Self-assembly at all scales, *Science,* 295, 2418-2421 (DOI: 10.1126/ science. 1070821).
2. Cengiz N.; Rao J., Sanyal A., Khan A. (2013), Designing functinalizable hydrogel through thiol-epoxy coupling chemistry, *Chem.Commun.,* 49, 11191-11193 (DOI: 10.1039/C3CC45859H).
3. Stevens M. M., George J. H. (2005), Exploring and engineering the cell surface interface, *Science*, 310, 1135-1138 (DOI: 10.1126/science.1106587).
4. Kopecek J., Yang J. (2012), Smart self-assembled hybrid hydrogel biomaterials, *Angew. Chem. Int. Ed.*, 51, 7396-7417 (DOI: 10.1002/anie.201201040).
5. Sasso L., Vedarethinam I., Emnéus J., Svendsen W. E., Castillo-León J. (2012), Self-assembled diphenylalanine nanowires for cellular studies and sensor applications, *J.*

Nanosci. Nanotechnol., 12, 3077-3083 (DOI:10.1166/jnn. 2012.4534).

6. (a) Ghosh A., Haverick M., Stump K., Yang X., Tweedle M. F., Goldberger J. E. (2012), Fine-tuning the pH trigger of self-assembly, *J. Am. Chem. Soc.*, 134, 3647-3650 (DOI: 10.1021/ja211113n); (b) Nagarkar R. P., Hule R. A., Pochan D. J., Schneider J. P. (2008), De novo design of strand-swapped β-hairpin hydrogels, *J. Am. Chem. Soc.*, *130*, 4466-4474 (DOI: 10.1021/ja710295t); (c) Hwang I., Jeon W. S. Kim H. J., Kim D., Kim H., Selvapalam N., Fujita, N., Shinkai S., Kim K. (2007), Cucurbit[7]uril: A simple macrocyclic, pH-triggered hydrogelator exhibiting guest-induced stimuli-responsive behavior, *Angew. Chem. Int. Ed.*, 119, 214-217 (DOI: 10.1002/ange.200603149); (d) Kloxin A. M., Kasko A. M., Salinas C. N., Anseth K. S. (2009), Photodegradable hydrogels for dynamic tuning of physical and chemical properties, *Science*, 324, 59-63 (DOI: 10.1126/science.1169494); (e) Guler M. O., Stupp S. I. (2007), A self-assembled nanofiber catalyst for ester hydrolysis, *J. Am. Chem. Soc.*, 129, 12082-12083 (DOI: 10.1021/ja075044n).

7. Gazit E. (2007), Self-assembled peptide nanostructures: The design of molecular building blocks and their technological utilization, *Chem. Soc. Rev.*, 36, 1263-1269, (DOI: 10.1039/ B605536M).

8. (a) Ikeda M., Tanida T., Yoshii T., Hamachi I. (2011), Rational molecular design of stimulus-responsive supramolecular hydrogels based on dipeptides, *Adv. Mater.*, 23, 2819-2822 (DOI: 10.1002/adma.201004658); (b) Wain A. J., Do H. N. L., Mandal H.S., Kraatz F., Zhou H.-B. (2008), Influence of molecular dipole moment on the redox-induced reorganization of α-helical peptide self-assembled monolayers: An electrochemical SPR investigation, *J. Phys. Chem. C.*, 112, 14513-14519 (DOI: 10.1021/jp804643c).

9. (a) Johnson E. C. B., Kent S. B. H. (2006), Insights into the mechanism and catalysis of the native chemical ligation reaction, *J. Am. Chem. Soc.*,128, 6640-6646 (DOI: 10.1021/ ja058344i); (b) Dawson P. E., Muir T. W., Clark-Lewis I., Kent S. B. H. (1994), Synthesis of proteins by native chemical ligation, *Science*, 266, 776-779 (DOI: 10.1126/science. 7973629); (c) Kent S. B. H. (2009), Total chemical synthesis of proteins, *Chem. Soc. Rev*., 38, 338-351 (DOI: 10.1039/B700141J); (d) Wan Q., Chen J., Yuan Y., Danishefsky S. J. J. (2008), Oxo-ester mediated native chemical ligation: Concept and applications, *J. Am. Chem. Soc*. 130, 15814-15816 (DOI: 10.1021/ja804993y).

10. Jung J. P., Jones J. L., Cronier S. A., Collier J. H. (2008), Modulating the mechanical properties of self-assembled peptide hydrogels via native chemical ligation, *Biomaterials*, 29, 2143-2151 (DOI:10.1016/j.biomaterials.2008.01.008).

11. Hu B. H., Su J., Messersmith, P. B. (2009), Hydrogels cross-linked by native chemical ligation, *Biomacromol.*, 10, 2194-2200 (DOI: 10.1021/bm900366e).

12. Shin Y., Winans K. A., Backes B. J., Kent S. B. H. Ellman J. A., Bertozzi C. R. (1999), Fmoc-based synthesis of peptide-αthioesters: Application to the total chemical synthesis of a glycoprotein by native chemical ligation, *J. Am. Chem. Soc.*, 121, 11684-11689 (DOI: 10.1021/ja992881j); (b) Batjargal S., Wang Y. J., Goldberg J. M., Wissner R.F., Petersson E. J. (2012), Native chemical ligation of thioamide-containing peptides: Development and application to the synthesis of labeled α-synuclein for misfolding studies, *J. Am. Chem. Soc.*, 134, 9172−9182 (DOI: 10.1021/ja2113245); (c) Shmilovici M. A., Mandal K., Gates Z. P., Phillips N. B., Weiss M. A., Kent S. B. H. (2013), Fully convergent chemical synthesis of sster insulin: Determination of the high resolution X-ray structure by racemic protein crystallography, *J. Am. Chem. Soc.*, 135, 3173-3185 (DOI: 10.1021/ja311408y).

13. (a) Chen J., Wan Q., Yuan Y., Zhu J., Danishefsky S. J. (2008), Native chemical ligation at valine: A contribution to peptide and glycopeptide synthesis, *Angew. Chem. Int. Ed.*, 47, 8521-8524 (DOI:10.1002/anie.200803523); (b) Hentschel J., Krause E., Borner H. G. (2006), Switch-peptides to trigger the peptide guided assembly of poly(ethylene oxide)-peptide conjugates into tape structures, *J. Am. Chem. Soc.*, 128, 7722-7723 (DOI: 10.1021/ja060759w); (c) Cergol K. M., Thompson R. E., Malins L. R., Turner P., Payne R. J. (2014), One-pot peptide ligation-desulfurization at glutamate, *Org. Lett.*, 16, 290-293 (DOI: 10.1021/ol403288n.); (d) Dheur J., Ollivier N., Vallin A. Melnyk O. (2011), Synthesis of peptide alkylthioesters using the intramolecular *N,S*-Acyl shift properties of bis(2-sulfanylethyl)amido peptides, *J. Org. Chem.* 76, 3194-3202 (DOI: 10.1021/jo200029e); (e) Siman P., Karthikeyan S. V., Brik A. (2012), Native chemical ligation at glutamine, *Org. Lett.*, 14, 1520-1523 (DOI: 10.1021/ol300254y).

14. (a) Lemieux G. A., Bertozzi C. R. (1998), Chemoselective ligation reactions with proteins, oligosaccharides and cells, Trends Biotech. 16, 506-513 (DOI: 10.1016/S0167-7799(98)01230-X); (b) Rodriguez E. C., Winans K. A., King D. S., Bertozzi C. R. (1997), A strategy for the chemoselective synthesis of O-Linked glycopeptides with native sugar-peptide linkages, *J. Am. Chem. Soc.*, 119, 9905-9906 (DOI: 10.1021/ja971633p); (c) Weissenborn M. J., Castangia R., Wehner J. W., Sardzik R., Lindhorst T. K., Flitsch S. L. (2012), Oxo-ester mediated native chemical ligation on microarrays: An efficient and chemoselective coupling methodology, *Chem. Commun.* 48, 4444-4446 (DOI: 10.1039/c2cc30844d); (d) Fang G.-M., Wang J. -X., Liu L. (2012), Convergent chemical synthesis of proteins by ligation of peptide hydrazides, *Angew. Chem. Int. Ed.*, 124, 10493-10496 (DOI: 10.1002/ange. 201203843).

15. Dirx M. J., Van den Brandt P. A. Goldbohm R. A. Lumey L. H. (2003), Energy restriction early in life and colon carcinoma risk, *Cancer*, 97, 46-55 (DOI: 10.1002/cncr.11052).

16. Lin J., Manson J. E., Selhub J., Buring J. E., Zhang S. M. (2007), Plasma cysteinylglycine levels and breast cancer risk in women, *Cancer Res.*, 67, 11123-11127 (DOI:10.1158/0008-5472).

17. Durek T., Alewood P. F. (2011), Preformed selenoesters enable rapid native chemical ligation at intractable sites, *Angew.Chem. Int. Ed.*, 50, 12042-12045 (DOI: 10.1002/anie.201105512).

18. Couto N., Malys N., Gaskell S. J. Barber J. (2013), Partition and turnover of glutathione reductase from *saccharomyces cerevisiae*: A proteomic approach, *J. Proteome Res.* 12, 2885-2894 (DOI: 10.1021/pr4001948).

19. Singh S., Topuz F., Hahn K., Albrecht K., Groll J. (2013), Embedding of active proteins and living cells in redox-sensitive hydrogels and nanogels through enzymatic cross-linking, *Angew. Chem. Int. Ed*., 52, 3000 –3003 (DOI: 10.1002/anie. 201206266).

20. Miao X., Cao W., Zheng W., Wang J., Zhang X., Gao J., Yang C., Kong D., Xu H., Wang L. Yang Z. (2013), Switchable catalytic activity: selenium-containing peptides with redox-controllable self-assembly properties, *Angew. Chem. Int. Ed.*, 52, 7781-7785 (DOI: 10.1002/anie.201303199).

21. Chen C. S., Ji T. -J., Xu X. -D., Zhang X.-Z., Zhuo R. -X. (2010), Nanofibers self-assembled from structural complementary borono-decapeptides, *Macromol. Rapid Commun.*, 31, 1903-1908 (DOI: 10.1002/marc.201000292).

22. (a) Banwell E. F., Abelardo E. S., Adams D. J., Birchall M. A., Corrigan A., Donald A. M., Kirkland M., Serpell L. C., ButlerM. F., Woolfson D. N. (2009), Rational design and application of responsive α-helical peptide hydrogels, *Nature Mater.*, 8, 596-600 (DOI:10.1038/nmat2479); (b) Tarasov S. G.,

Gaponenko V., Howard O. M. Z., Chen Y., Oppenheim J. J., Dyba M. A., Subramaniam S., Lee Y., Michejda C., Tarasova N. I. (2011), Structural plasticity of a transmembrane peptide allows self-assembly into biologically active nanoparticles *Proc. Natl. Acad. Sci. U. S. A.*, 108, 9798-9803 (DOI: 10.1073/pnas.1014598108) (c) Qin L., Duan P., Xie F., Zhang L., Liu M. (2013), A metal ion triggered shrinkable supramolecular hydrogel and controlled release by an amphiphilic peptide dendron, *Chem. Commun*., 49, 10823-10825 (DOI: 10.1039/C3CC47004K).

23. Tu S., Kim S.H., Joseph J., Modarelli D. A., Parquette J. R. (2011), Self-assembly of a donor-acceptor nanotube. A strategy to create bicontinuous arrays, *J. Am. Chem. Soc.*, 133, 19125-19130 (DOI: 10.1021/ja205868b).

Chapter 5

Emerging π-Stacked Dynamic Nanostructured Peptide Library

5.1 Introduction

Self-assembly[1] plays a vital role in constructing complex functional materials for applications in biosensing,[2] 3D matrices for cell culture,[3] drug delivery[4] and wound healing[5] treatment. Various small molecules, including amino acids [6] carbohydrates[7] and antibiotics[8] have been used in the development of supramolecular hydrogels. Peptide self-assembly leading to supramolecular hydrogels has been reported in response to external stimuli including pH, ionic strength, temperature, light and enzyme catalyzed reactions.[9] Enzyme catalyzed peptide hydrogels have shown promise in biomedical applications.[10] It has been reported that enzymatic conversion promotes the formation of more ordered nanostructures in supramolecular hydrogels.[11] Xu and co-workers *(2007)* reported that intracellular enzymatic formation of nanofibers results in hydrogelation.[12] Dynamic covalent chemistry exploits the reversibility of chemicalreactions for the generation of library molecules under thermodynamic control. In recent years, dynamic combinatorial libraries (DCLs)[13] are envisaged to build precise molecular architectures. Sanders et al. reported one of the most successful hydrazone exchange reactions for the generation of a dynamic combinatorial library.[14] In addition to host–guest relationships, covalent and noncovalent interactions alter the distribution of library members. Lehn and co-worker *(2005)* developed constitutional dynamic libraries based on supramolecular and reversible connections which involve selforganization and component selection to

generate dynamic hydrogels.[15] Das *et al.* (2009) have shown the construction of a dynamic library of building blocks of self-assembled hydrogelators.[16] Few principles need to be designed for the successful generation of dynamic libraries where self-assembly facilitates towards the most preferred component. Enzyme catalyzed peptide hydrolysis reactions are close to equilibrium in aqueous medium and are thermodynamically favoured.[17] Our objective is to exploit reversible breaking/making of peptide bonds and non-covalent interactions that lead to theformation of a single predominating product among the library members. The self-assembly of molecules is based on the formation of hydrogen bonding as well as π–π stacking interactions of highly conjugated aromatic moieties.[18] Here, we report the generation of a dynamic library of small peptides with an N-terminal aromatic protecting group *i.e.* naphthalene-2-methoxycarbonyl (Nmoc) that self-assemble to form self-supporting hydrogels and ultimately lead to a nanostructured predominating product via hydrogen bonding and π-stacking interactions (Figure 5.1).

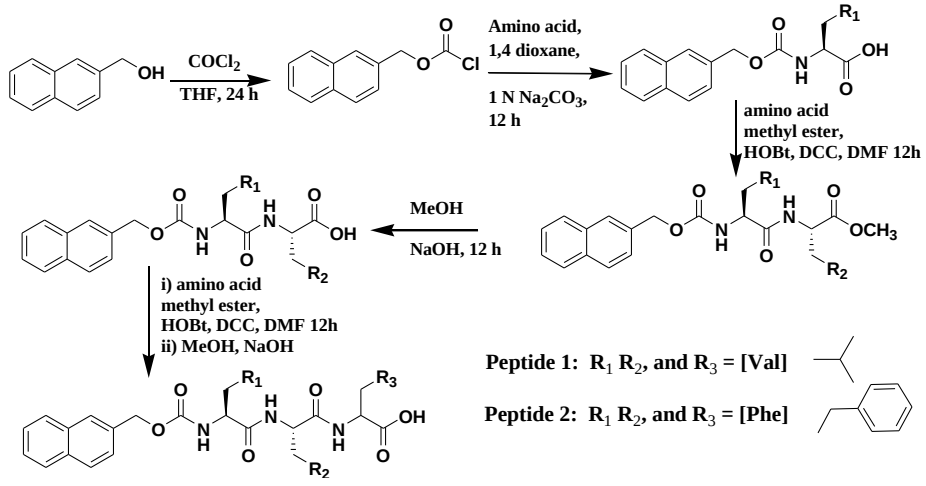

Figure 5.1. *Synthesis of Nmoc-protected tripeptides.*

5.2 Experimental

*2.2.(1) Synthesis of compounds **1** and **2***

The Nmoc-protected amino acids were synthesized by reaction of Nmoc-Cl with amino acid. The subsequent coupling of amino acids in tri-peptides was achieved by conventional solution phase methodology.

5.2.1 Synthesis of Compound **1**:

a) Synthesis of Nmoc-Cl **3**: To a stirred solution of naphthalene methanol (5 g, 31.6 mmol) in dry THF (140 mL), phosgene (39.2 ml, 75.5 mmol) was added at 0^{o} C. The stirring was continued at ambient temperature for 24 h. The reaction was monitored by thin layer chromatography (TLC). After completion of reaction, excess phosgene was removed under low vacuum and trapped with aqueous NaOH. Reaction mixture was concentrated and oily product was obtained. Then, it was dissolved in hot hexane to get crystalline product **3.**

Yield = 6.8 g (30 mmol, 94.93 %). mp: 62 ^{o}C; FT-IR (KBr): ῡ 3066 (m), 1777 (s), 1601 (ms), 1168 (s) cm^{-1} ; ^{1}H NMR (400 MHz, $CDCl_3$): δ 7.90 (d, 4H), 7.56 (m, 2H), 7.29 (s, 1H), 5.48 (s, 2H) ppm; ^{13}C NMR (100 MHz, $CDCl_3$): δ 71.82, 125.7, 126.6, 127.8, 128.1, 128.6, 130.6, 133.5, 140.9, 147.9, 150.7 ppm.

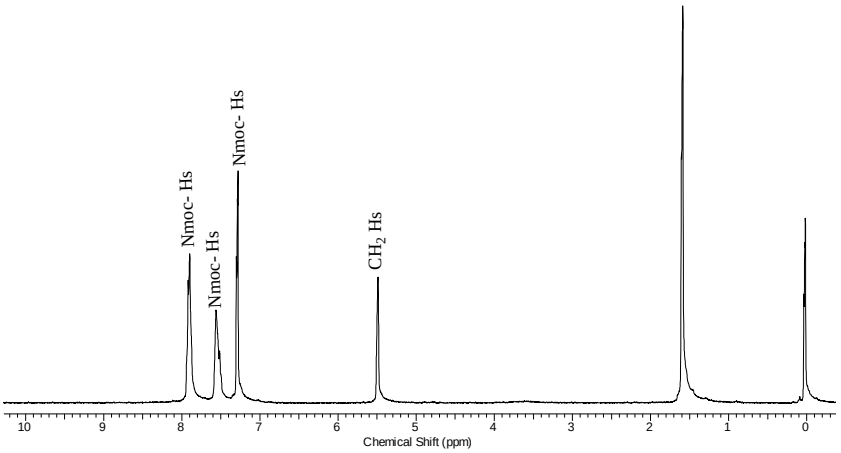

Figure 5.2. *400 MHz ^{1}H NMR spectrum of Nmoc-Cl **3** in $CDCl_3$.*

b) Synthesis of Nmoc-Val-OH **4:** A solution of valine (0.585 g, 5 mmol) in a mixture of 1, 4 dioxane (10 mL) and 1M sodium hydroxide (15 mL) was stirred and cooled in an ice-water bath. Naphthalene-2-methyloxychloroformate (1.102 g, 5 mmol) was added and stirring was continued at room temperature for 12 h. Reaction mixture was diluted with 200 mL of water and dioxane was evaporated under vaccum. Aqueous layer was washed with diethyl ether and the pH of aqueous layer was adjusted to 2 with 2N hydrochloric acid. The aqueous phase was extracted with ethyl acetate (3 x 50 mL) and dried over Na_2SO_4 and concentrated in vacuo to give **4** as colorless oil.

Yield= 1.05 g, (3.5 mmol, 70 %); ^{1}H NMR (400 MHz, $CDCl_3$): 7.93 (m, 4H, Nph), 7.54 (m, 3H, Nph), 7.35 (d, 1H, NH), 5.22 (s, 2H, CH_2 of Nph), 4.12 (m, 1H, $C^{\alpha}H$ of Val), 2.18 (m, 1H, $C^{\beta}H$ of Val), 0.92 (d, 6H, $C^{\gamma}H$ of Val) ppm; MS (ESI) m/z for $C_{17}H_{19}NO_4$ $(M+Na)^+$ calcd.: 324.1212, found: 324.1238

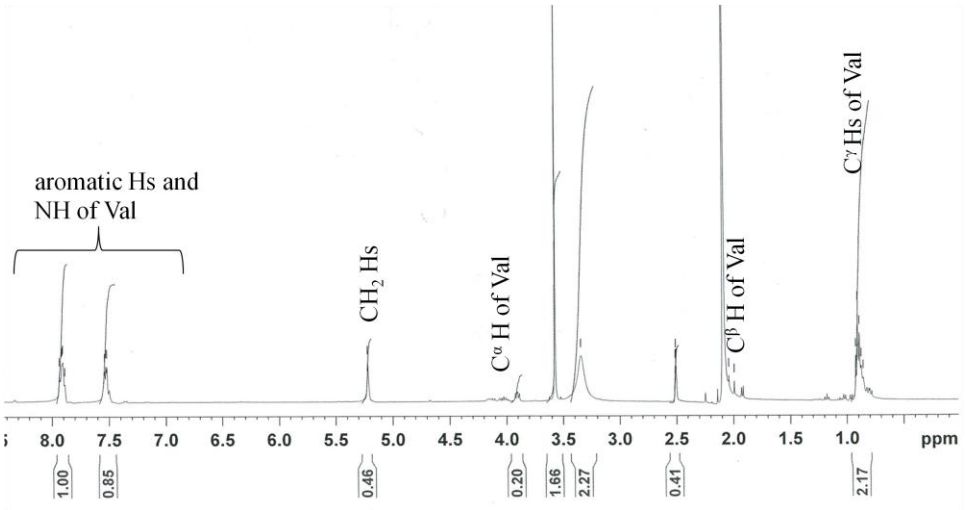

Figure 5.1. *400 MHz ^{1}H NMR spectrum of Nmoc-Val **4** in DMSO-d_6.*

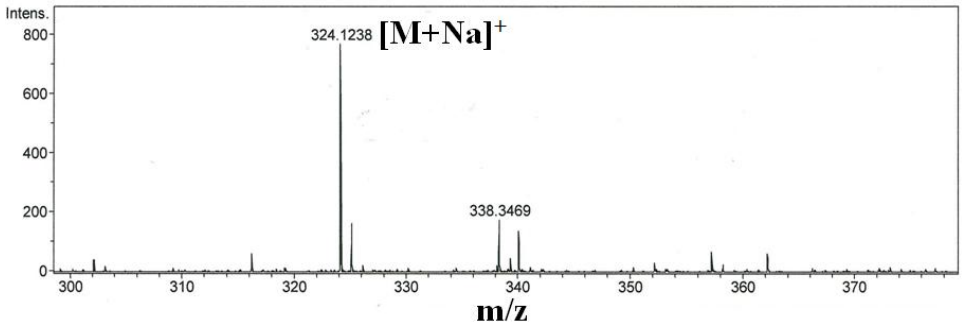

Figure 5.4. *ESI-MS spectrum of Nmoc-Val* ***4****.*

c) Synthesis of Nmoc-Val(1)-Val(2)-OBn **5:** A solution of Nmoc-Val-OH **4** (3.2 mmol, 0.980 g) and HOBt (3.2 mmol, 0.432 g) was stirred in 2 mL of DMF. A neutralized solution of valine benzyl ester (6.4 mmol, 2.425 g) was extracted from its corresponding *p*-toluene sulfonate salt and concentrated to add to the reaction mixture followed by di-isopropylcarbodiimde (3.2 mmol, 0.403g) at 0^{o}C and allowed to stirr at room temperature for 12 hours. The mixture was diluted with ethyl acetate and organic layer was washed with 1M HCl (2 x 30 mL), brine solution, 1M Na_2CO_3 (3 x 30 mL) and brine solution. Ethyl acetate layer was dried over Na_2SO_4 and evaporated under vacuum to yield **5** as white powder.

Yield= 1.56 g, (3.1 mmol, 96.87 %); ^{1}H NMR (400 MHz, $CDCl_3$): δ 7.86 (d, 4H, Nph), 7.46 (m, 3H, Nph), 7.33 (m, 5H, Ph), 7.28, (m, 1H, NH), 5.32 (s, 2H, CH_2 of Nph), 5.24 (s, 2H, CH_2 of Ph), 4.62 (m, 1H, $C^{\alpha}H$ of Val(2)), 4.06 (m, 1H, $C^{\alpha}H$ of Val(1)), 2.13 (m, 2H, $C^{\beta}H$ of Val(1) and (2)), 0.99 (d, 6H, $C^{\gamma}H$ of Val(2)), 0.88 (d, 6H, $C^{\gamma}H$ of Val(1)) ppm. HRMS (ESI) m/z for $C_{29}H_{34}N_2O_5$ $(M+Na)^{+}$ calcd.: 513.2366, found: 513.2360.

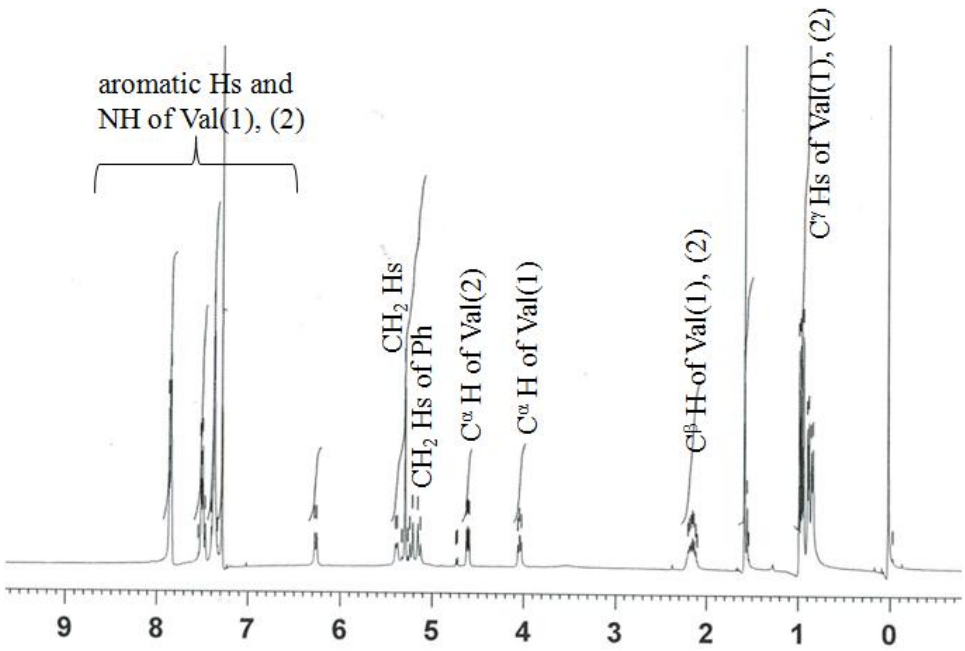

Figure 5.52. *400 MHz ^{1}H NMR spectrum of Nmoc-Val-Val-OBn* ***5*** *in $CDCl_3$.*

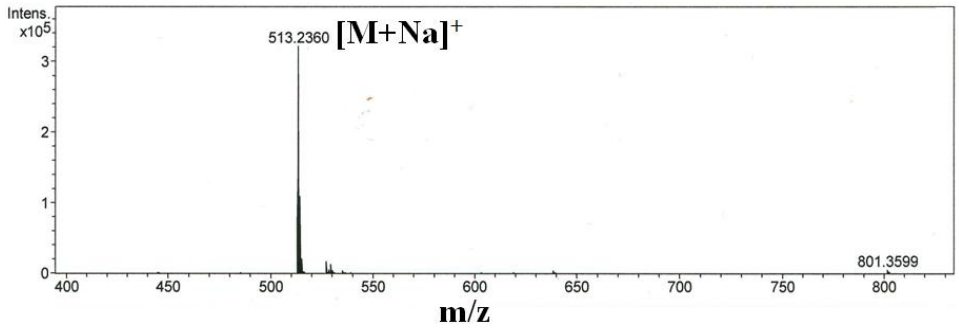

Figure 5.3. *ESI-MS spectrum of Nmoc-Val-Val-OBn* ***5.***

d) Synthesis of Nmoc-Val (1)-Val (2)-OH **6:** A solution of Nmoc-Val (1)-Val (2)-OBn **5** (1.46 g, 2.9 mmol) in 20 mL of dry MeOH was allowed to react with a solution of 17 mL 2M NaOH solution. The progress of the reaction was monitored by thin layer chromatography (TLC). The reaction mixture was stirred upto 10 h. Then, methanol was removed under vacuum, residue was taken in 100 mL of water and washed with diethyl ether (2 x 20 mL). Then, the pH of aqueous layer was adusted to 2 using 2 M HCl and it was extracted with ethyl acetate (3 x 30 mL) and dried over anhydrous sodium sulfate and evaporated in vacuo to yield **6** as white powder and used further without purification.

Yield = 1.10 g, (2.7 mmol, 93.1 %). ^{1}H NMR (400 MHz, DMSO-d_6): δ 12.6 (s, 1H, COOH), 7.92 (m, 4H, Nph), 7.53 (m, 3H, Nph), 7.36 (d, 1H, *J*= 8 Hz, NH), 7.31 (d, 1H, NH), 5.20 (s, 2H, CH_2 of Nph), 4.14 (m, 1H, CH of Val(2)), 4.00 (m, 1H, $C^{\alpha}H$ of Val(1)), 1.99 (m, 2H, $C^{\beta}H$ of Val(1) and (2)), 0.90 (d, 12H, $C^{\gamma}H$ of Val (1) and (2)) ppm. MS (ESI) m/z for $C_{22}H_{28}N_2O_5$ $(M+Na)^+$ calcd.: 423.1998, found: 423.1911

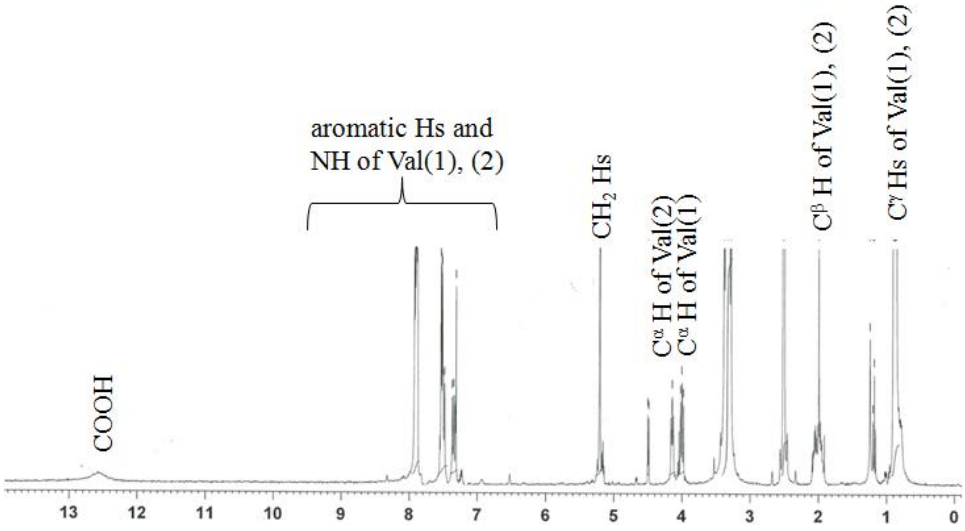

Figure 5.4. *400 MHz ^{1}H NMR spectrum of Nmoc-Val-Val-OH* ***6*** *in DMSO-d_6.*

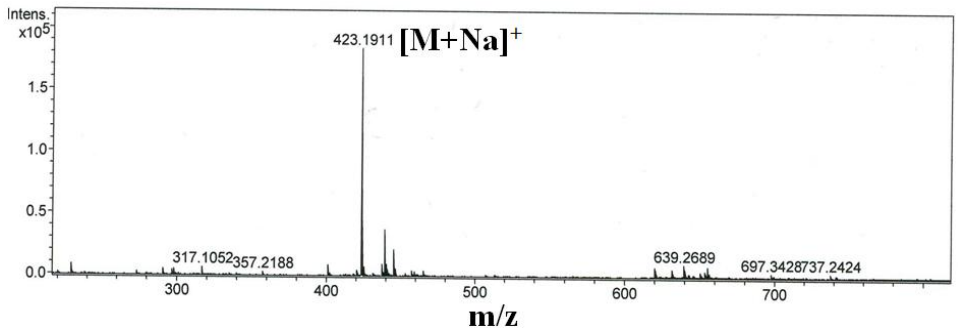

Figure 5.8. *ESI-MS spectrum of Nmoc-Val-Val-OH* ***6****.*

e) Synthesis of Nmoc-Val(1)-Val(2)-Val(3)-OBn **7:** A solution of Nmoc-Val(1)-Val(2)-OH **6** (1.00 g, 2.5 mmol) and HOBt (2.5 mmol, 0.337 g) was stirred in 2 mL of DMF. A neutralized solution of valine benzyl ester was extracted from its corresponding *p*-toluene sulfonate salt and concentrated to add to the reaction mixture followed by DIC (2.5 mmol, 0.315 g) at 0°C. The mixture was allowed to stir at room

temperature for 12 h. The mixture was diluted with ethyl acetate and organic layer was washed with 1M HCl (2 x 30 mL), brine solution, 1M Na_2CO_3 (3 x 30 mL) and brine solution. The ethyl acetate layer was dried over Na_2SO_4 and evaporated under vacuum to yield **7** as white solid. Purification was done by silica gel column (100-200 mesh) using ethyl acetate-toluene as eluent.

Yield= 1.12 g, (1.9 mmol, 76%). ^{1}H NMR (400 MHz, $CDCl_3$): δ 7.84 (d, 4H, *J*= 8 Hz, Nph), 7.49 (m, 3H, Nph), 7.45 (d, 1H, NH), 7.41 (d, 1H, NH), 7.35 (m, 5H, Ph), 7.21 (d, 1H, NH), 5.28 (s, 2H, CH_2 of Nph), 5.14 (s, 2H, CH_2 of Ph), 4.63 (m, 1H, $C^{\alpha}H$ of Val(3)), 4.36 (m, 1H, $C^{\alpha}H$ of Val(2)), 4.07 (m, 1H, $C^{\alpha}H$ of Val(1)), 2.19 (m, 3H, $C^{\beta}Hs$ of Val(1), (2), and (3)), 0.93 (d, 18H, $C^{\gamma}Hs$ of Val Val(1), (2), and (3)) ppm; MS (ESI) m/z for $C_{34}H_{43}N_3O_6$ $(M+Na)^+$ calcd.: 612.3152, found: 612.3127

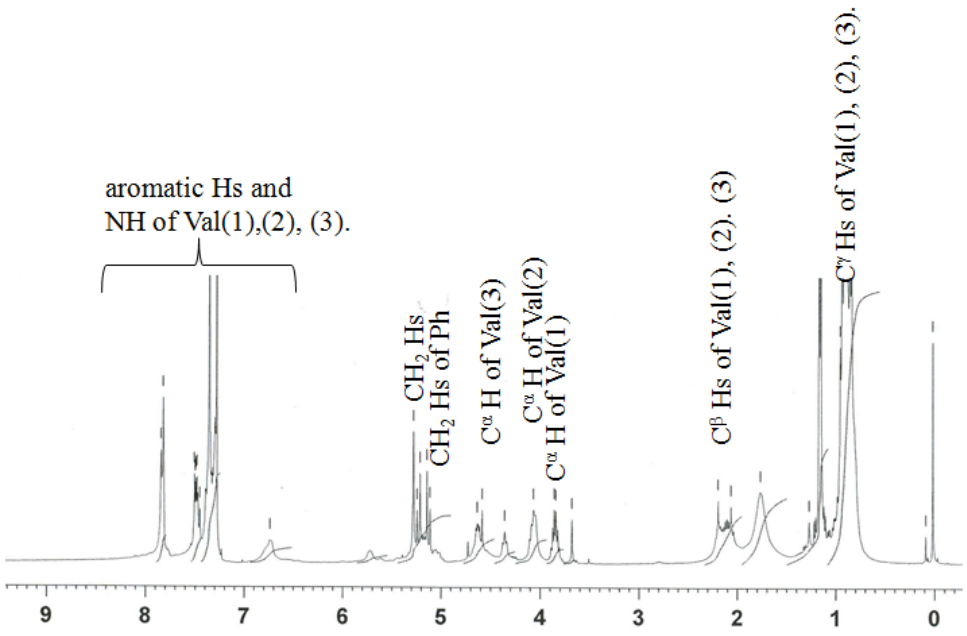

Figure 5.9. *400 MHz ^{1}H NMR spectrum of Nmoc-Val-Val-Val-OBn **7** in $CDCl_3$.*

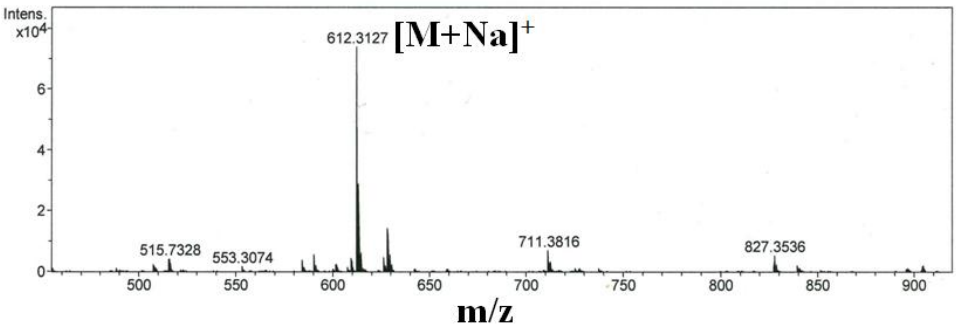

Figure 5.10. *ESI-MS spectrum of Nmoc-Val-Val-Val-OBn* ***7.***

f) Synthesis of Nmoc-Val(1)-Val(2)-Val(3)-OH **1:** A solution of Nmoc-Val(1)-Val(2)-Val(3)-OBn **7** (1.02g, 1.7 mmol) in 50 mL of dry MeOH allowed to react with a solution of 25 mL (2M) NaOH solution. The progress of the reaction was monitored by thin layer chromatography (TLC). The reaction mixture was stirred upto 12 h. Then, methanol was removed under vacuum, residue was taken in 100 mL of water and washed with diethyl ether (2 x 20 mL). Then, the pH of aqueous layer was adusted to 2 using 2M HCl and it was extracted with ethyl acetate (3 x 30 mL) and the ethyl acetate layer was dried over anhydrous sodium sulfate and evaporated in vacuo to yield **1** as white solid and used further without purification.

Yield= 0.618 g (1.2 mmol, 70.58 %). FT-IR (KBr): 3388 (s), 3065(m), 1711 (ms), 1640 (s), 1542 (s), 1462 (m) cm^{-1} ; 1H NMR (400 MHz, DMSO-d_6): δ 7.89 (m, 4H, Nph), 7.54 (m, 3H, Nph), 7.50 (d, 1H, NH), 7.42 (d, 1H, NH), 5.75 (m, 2H, CH_2 of Nph), 4.32 (m,1H, $C^{\alpha}H$ of Val(3)), 4.12 (m, 1H, $C^{\alpha}H$ of Val(2)), 3.95 (m, 1H, $C^{\alpha}H$ of Val(1)), 2,09 (m, 3H,$C^{\beta}Hs$ of Val(1), (2), and (3)), 0.86 (d, 18H, $C^{\gamma}Hs$ of Val(1), (2), and (3)); ^{13}C NMR (100 MHz, DMSO-d_6) δ 17.4, 17.9, 18.1, 18.9, 19.0, 19.1, 29.6, 30.1, 30.7, 60.3, 62.8, 65.3, 125.5, 125.9, 126.3, 126.5, 127.5, 127.9, 132.4, 132.7, 134.7, 142.4, 156.0, 171.0, 172.0, 172.6, 174.0 ppm. MS

ESI) m/z for $C_{27}H_{37}N_3O_6$ $(M+Na)^+$ calcd.: 522.2580, found: 522.2559.

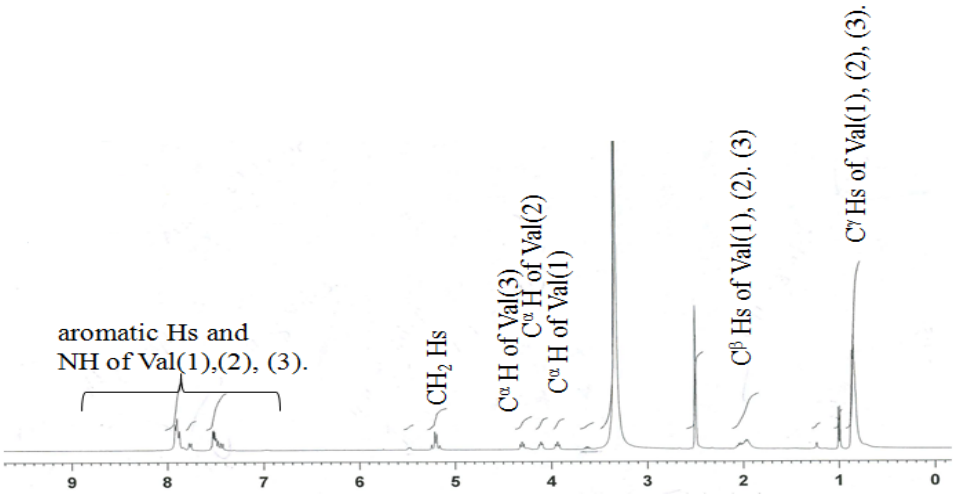

Figure 5.11. *400 MHz ^{1}H NMR spectrum of Nmoc-Val-Val-Val-OH **1** in DMSO-d_6.*

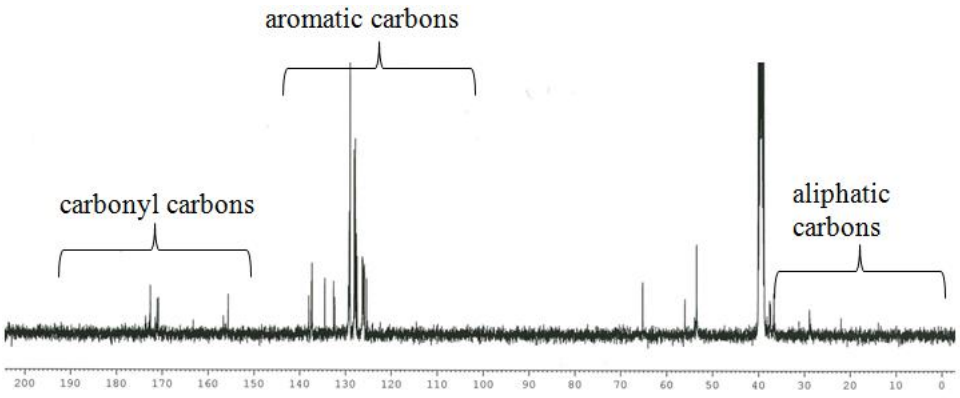

Figure 5.125. *100 MHz ^{13}C spectrum of Nmoc-Val-Val-Val-OH **1** in DMSO-d_6.*

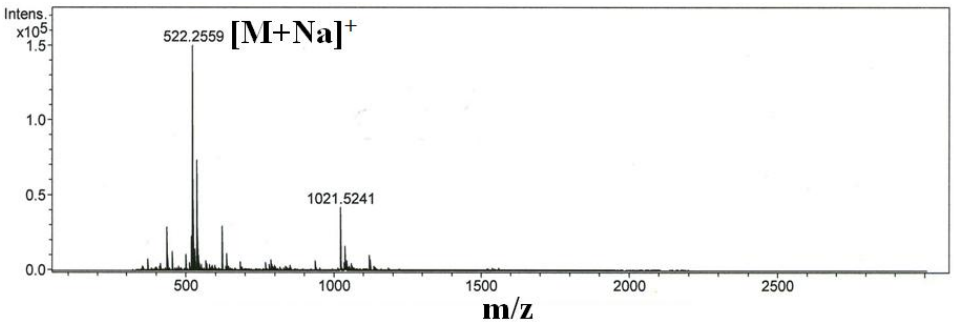

Figure 5.136. *ESI-MS spectrum of Nmoc-Val-Val-Val-OH **1.***

*5.2.2 Synthesis of Compound **2**:*

a) Synthesis of Boc-Phe-OH **8:** A solution of phenylalanine (3.3 g, 20 mmol) in a mixture of 1, 4 dioxane (40 mL), 1N sodium hydroxide (20

mL) and water (20 mL) was stirred and cooled in an ice-water bath. Boc-anhydride (4.8 mL, 21 mmol) was added and stirring was continued at room temperature for 12 h. Reaction mixture was diluted with 200 mL of water and dioxane was evaporated under vaccum. Aqueous layer was washed with diethyl ether and the pH of aqueous layer was adjusted to 2 with 2N hydrochloric acid. The aqueous phase was extracted with ethyl acetate (3 x 50 mL) and dried with Na_2SO_4 and concentrated in vacuo to obtain product **8** as colorless oil.

Yield= 5.105 g (19.2 mmol, 96 %) ^{1}H NMR (400 MHz, DMSO-d_6): δ 12.59 (s, 1H, COOH), 7.25 (m, 5H, Phe), 7.10 (d, 1H, *J*= 8.52, NH), 4.09 (q, 1H, C^{α}H of Phe), 3.04 (dd, 1H, *J*= 4.52 Hz and 4.52 Hz, C^{β} H of Phe), 2.81 (dd, 1H, C^{β} H of Phe), 1.32 (s, 9H, Boc), ppm; MS (ESI) m/z for $C_{14}H_{19}NO_4$ $(M+Na)^+$ calcd.: 288.1212, found: 288.1223

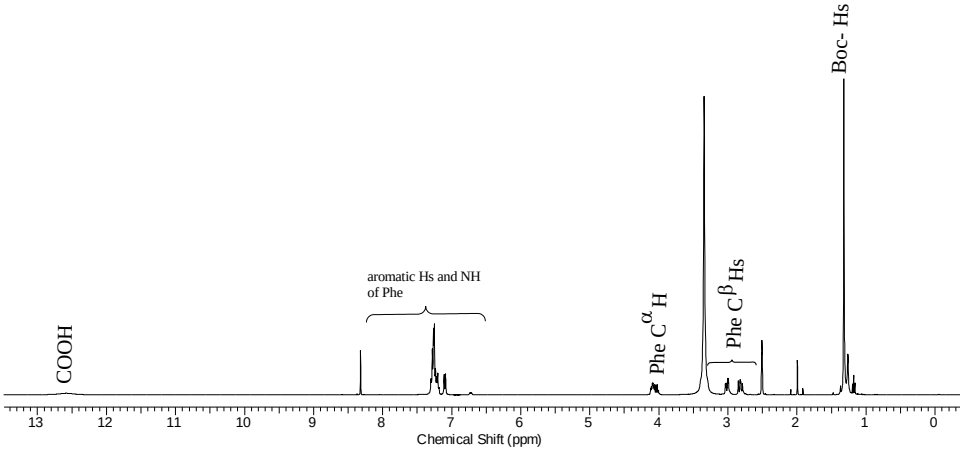

Figure 5.14. *400 MHz ^{1}H NMR spectrum of Boc-Phe-OH **8** in DMSO-d_6.*

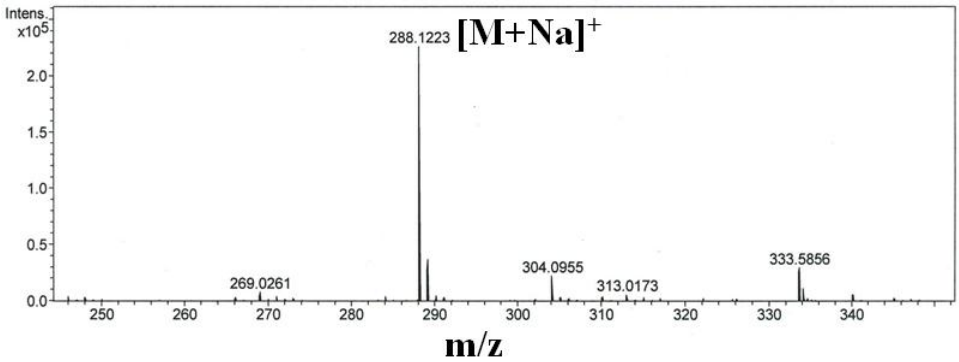

Figure 5.15. *ESI-MS spectrum of Boc-Phe-OH **8.***

b) Synthesis of Boc-Phe(1)-Phe(2)-OCH_3 **9:** A solution of Boc-Phe-OH (1.32 g, 5 mmol) and HOBt (5 mmol, 0.677 g) was stirred in 2 mL of DMF. A neutralized solution of phenyalanine methyl ester was extracted from its corresponding hydrochloride salt and concentrated to add to the reaction mixture followed by DCC (5.1 mmol, 1.052 g) at 0°C. The mixture was allowed to stir at room temperature for 12 h. The mixture was diluted with ethyl acetate and organic layer was washed with 1M HCl (2 x 30 mL), brine solution, 1M Na_2CO_3 (3 x 30 mL) and brine solution. The ethyl acetate layer was dried over Na_2SO_4 and evaporated under vacuum to yield white solid product **9**. Purification was done by silica gel column (100-200 mesh) using ethyl acetate- toluene as eluent.

Yield= 1.85g, (4.6mmol, 92 %). ^{1}H NMR (400 MHz, $CDCl_3$): δ 7.24 (m, 10H, Phe (1) and (2)), 7.00 (d, 1H, NH), 6.28 (d, 1H, *J*= 7.76 Hz, NH), 4.81(q, 1H C^{α} H of Phe(2)), 4.34 (q, 1H of C^{α} H of Phe (1)), 3.69 (s, 3H, OCH^3), 3.06 (d, 4H, *J*= 6.04 Hz, C^{β} H of Phe (1) and (2)), 1.47 (s, 9H, Boc Hs)) ppm. HRMS (ESI) m/z for $C_{24}H_{30}N_2O_5$ $(M+Na)^+$ calcd.: 449.2052, found: 449.2086

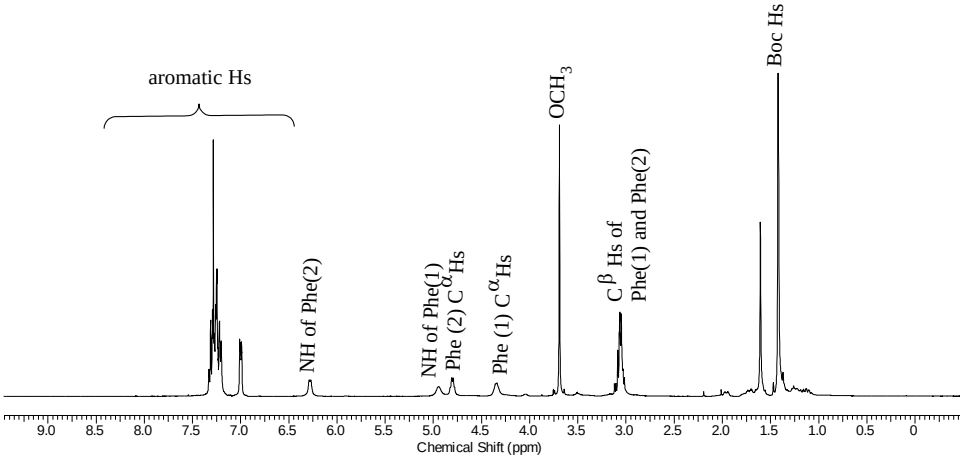

Figure 5.16. *400 MHz ^{1}H NMR spectrum of Boc-Phe-Phe-OCH_3 **9** in $CDCl_3$.*

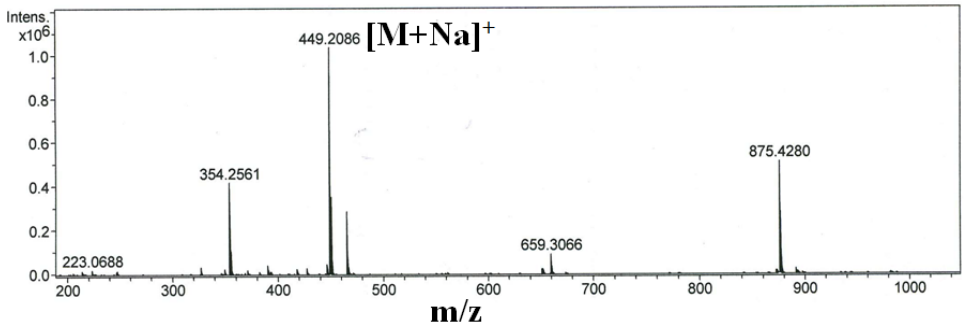

Figure 5.17. *ESI-MS spectrum of Boc-Phe-Phe-OCH_3* ***9.***

c) Synthesis of NH_2-Phe-Phe-OCH_3 **10:** A solution of Boc-Phe-Phe-OMe **9** (1.6 g, 3.7 mmol) in TFA stirred for 12 h under argon at room temperature. The excess TFA was removed under vaccum. Oily residue was taken in 100 mL of water and washed with diethyl ether (2 x 20 mL). White product **10** was obtained after lypholization and used further for the reactions.

Yield= 1.18 g (3.6 mmol, 97.29 %) ^{1}H NMR (400 MHz, DMSO-d_6): δ 9.02 (d, 1H, *J*= 9.64 Hz, NH), 8.13 (s, 3H, NH_2), 7.29 (m, 10H, Phe (1) and (2)), 4.60 (m, 1H, $C^{\alpha}H$ of Phe (2)),4.03 (m, 1H, $C^{\alpha}H$ of Phe (1)), 3.61 (s, 3H, OCH_3), 3.08 (d, 2H, C^{β} Hs of Phe (2)), 2.94 (d, 2H, C^{β} Hs of Phe(1)) ppm; MS (ESI) m/z for $C_{19}H_{23}N_2O_3$ $(M+H)^+$ calcd.: 327.1709, found: 327.1717

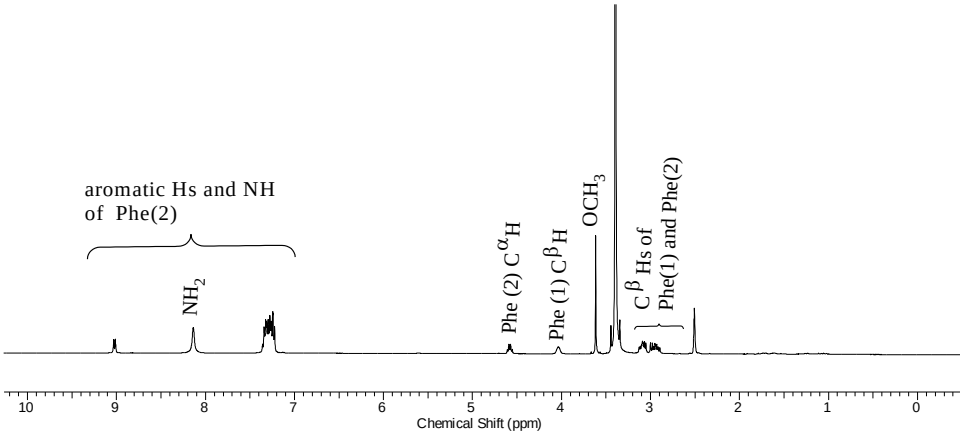

Figure 5.18. *400 MHz ^{1}H NMR spectrum of NH_2-Phe-Phe-OCH_3* ***10*** *in DMSO-d_6.*

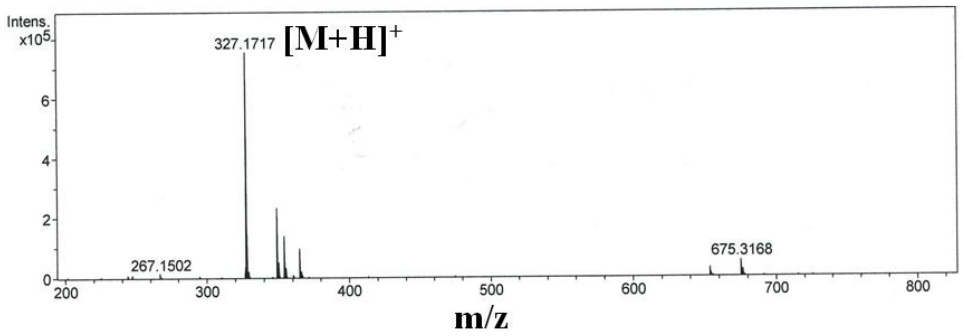

Figure 5.19. *ESI-MS spectrum of NH_2-Phe-Phe-OCH_3* ***10****.*

d) Synthesis of Nmoc-Phe-OH **11:** A solution of phenylalanine (0.825 g, 5 mmol) in a mixture of 1,4 dioxane (10 mL) and 1M sodium hydroxide (15 mL) was stirred and cooled in an ice-water bath. Naphthalene-2-methoxychloroformate (1.102 g, 5 mmol) was added and stirring was continued at room temperature for 12 h. Reaction mixture was diluted with 200 mL of water and dioxane was evaporated under vaccum. Aqueous layer was washed with diethyl ether and the pH of aqueous layer was adjusted to 2 with 2N hydrochloric acid. The aqueous phase was extracted with ethyl acetate (3 x 50 mL) and dried over Na_2SO_4 and concentrated in vacuo to give product **11** as colorless oil.

Yield= 1.568 (4.4 mmol, 88 %) ^{1}H NMR (400 MHz, DMSO-d_6): δ 12.8 (s, 1H, COOH), 7.90 (d, 4H, *J*=7.6 Hz, Nph), 7.53 (t, 3H, Nph), 7.40 (d, 1H, *J*= 8.52 Hz, NH), 7.23 (m, 5H, Ph), 5.15 (s, 2H, CH_2 of Nph), 4.19 (t, 1H, C^{α} H of Phe), 3.07 (d, 2H, C^{β} H of Phe) ppm. MS (ESI) m/z for $C_{21}H_{19}NO_4$ $(M+Na)^+$ calcd.: 372.1212, found: 372.1206

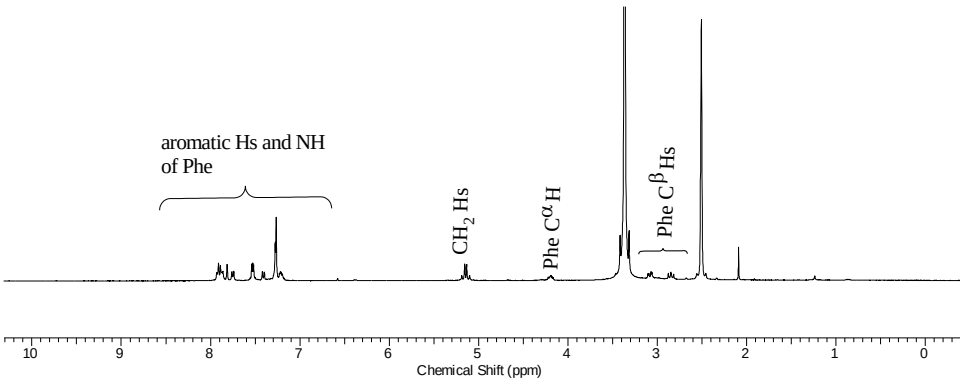

Figure 5.20. *400 MHz ^{1}H NMR spectrum of Nmoc-Phe-OH* ***11*** *in DMSO-d_6.*

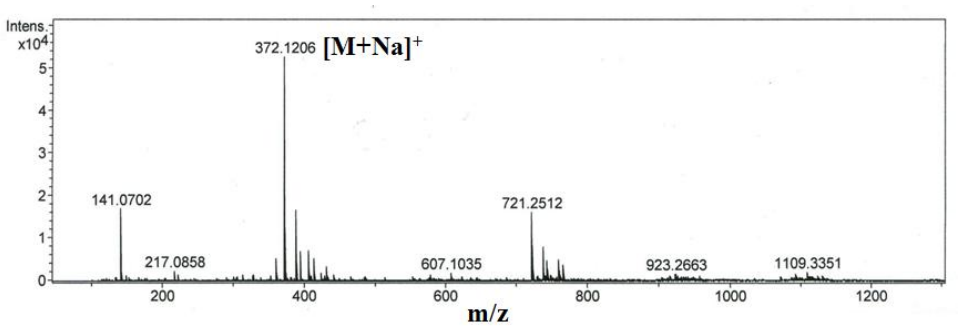

Figure 5.21. *ESI-MS spectrum of Nmoc-Phe-OH* ***11.***

e) Synthesis of Nmoc-Phe-Phe-Phe-OCH_3 **12:** A solution of Nmoc-Phe-OH (1.42 g, 4.1 mmol) and HOBt (0.555 g, 4.1mmol) was stirred in 2 mL of DMF. A neutralized solution of NH_2-Phe(1)-Phe(2)-OMe **11** (1.34 gm, 1 mmol) was added to the reaction mixture followed by DCC (0.866 g, 4.2 mmol) at 0^oC. The mixture was allowed to stir at room temperature for 12 h. The reaction mixture was diluted with ethyl acetate and organic layer was washed with 1M HCl (2 x 30 ml), brine solution, 1M Na_2CO_3 (3 x 30 mL) and brine solution, dried over Na_2SO_4 and evaporated under vacuum to yield white solid product **12**. Purification was done by silica gel column (100-200 mesh) using ethyl acetate- toluene as eluent.

Yield= 1.54 g (2.3 mmol, 56.09 %) ^{1}H NMR (400 MHz, $CDCl_3$): δ 7.85 (d, 4H, *J*= 8.04 Hz, Nph) 7.51 (dd 3H, Nph), 7.23 (m, 15H, Phe 1,2,3) 7.15 (d, 1H, *J*= 6.5 Hz, NH), 7.07 (d, 1H, *J*= 7.04 Hz, NH), 7.01 (d, 1H, NH), 5.22 (s, 2H, CH_2 of Nph), 4.75 (m, 1H, $C^{\alpha}H$ of Phe(3)), 4.57 (m, 1H, $C^{\alpha}H$ of Phe(2)), 4.39 (m, 1H, $C^{\alpha}H$ of Phe (2)), 3.74 (s, 3H, OCH_3), 3.15 (d, 2H, C^{β} H of Phe (3)), 3.09 (d, 2H, C^{β} H of Phe (2)), 3.06 (d, 2H, C^{β} H of Phe (1)) ppm; HRMS (ESI) m/z for $C_{40}H_{39}N_3O_6$ (M+Na)+ calcd.: 680.2737, found: 680.2733

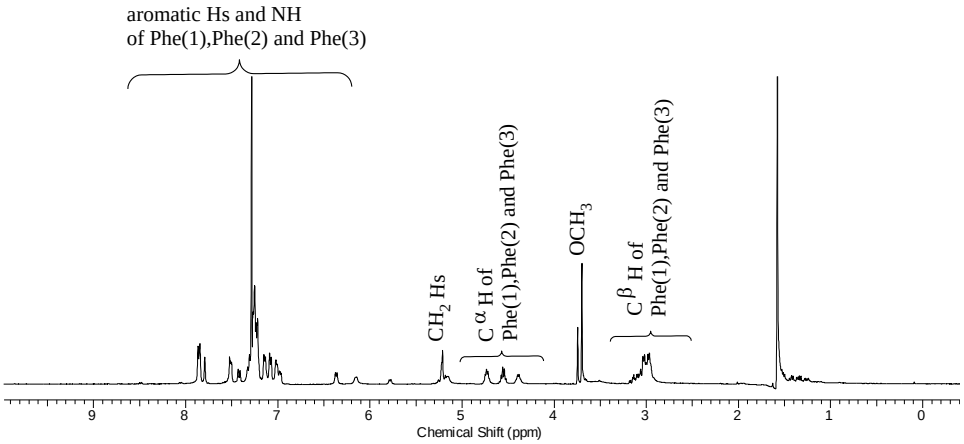

Figure 5.22. *400 MHz ^{1}H NMR spectrum of Nmoc-Phe-Phe-Phe-OCH_3* ***12*** *in $CDCl_3$.*

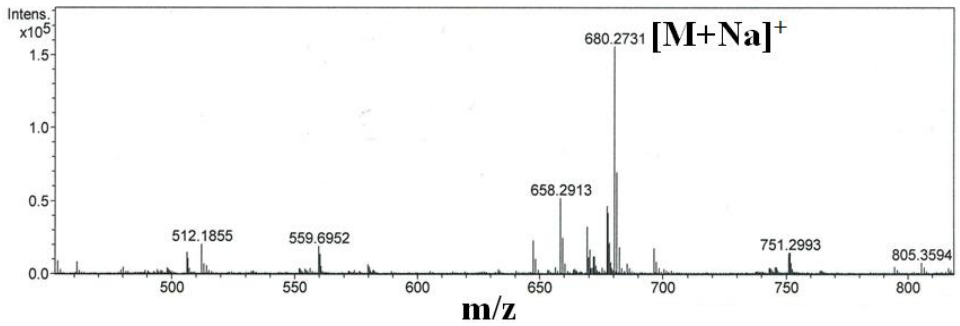

Figure 5.23. *ESI-MS spectrum of Nmoc-Phe-Phe-Phe-OCH_3* ***12****.*

f) Synthesis of Nmoc-Phe(1)-Phe(2)-Phe(3)-OH **2:** A solution Nmoc-Phe(1)-Phe(2)-Phe(3)-OCH_3 **12** (0.201 g, 0.3 mmol) in 100 mL of dry MeOH was allowed to react with a solution of 2M NaOH. The progress of the reaction was monitored by thin layer chromatography (TLC). The reaction mixture was stirred upto 12 h. Then, methanol was removed under vacuum, residue was taken in 100 mL of water and washed with diethyl ether (2 x 20 mL). Then, the pH of aqueous layer was adjusted to 2 using 2M HCl and it was extracted with ethyl acetate (3 x 30 mL) and ethyl acetate layer was dried over anhydrous sodium sulfate and evaporated in vacuo to yield **2** as white solid and used further without purification.

Yield= 0.18 g (0.27 mmol, 90 %) FT-IR (KBr): 3292 (s), 3061(m), 1707 (ms), 1647 (s), 1541 (s), 1444 (m) cm^{-1} ; ^{1}H NMR (400 MHz, DMSO-d_6):

δ 12.8 (s, 1H, COOH), 8.07 (d, 1H, *J*= 8.24 Hz, NH), 7.89 (m, 4H, Nph), 7.77 (s, 1H, Nph), 7.52 (d, 2H, Nph), 7.48 (d, 1H, *J*=8.8 Hz, NH), 7.36 (d 1H, *J*= 8 Hz, NH), 7.24 (m, 15H, Phe (1), (2) and (3)), 5.09 (s, 2H, CH_2 of Nph), 4.59 (q,1H, $C^{\alpha}H$ of Phe (3)), 4.46 (q, 1H, $C^{\alpha}H$ of Phe (2)), 4.23 (q, 1H, $C^{\alpha}H$ of Phe (1)), 3.03 (d, 2H, C^{β} Hs of Phe (3)), 2.94 (d, 2H, C^{β} Hs of Phe (2)), 2.84 (d, 2H, C^{β} Hs of Phe (1)) ppm; ^{13}C NMR (100 MHz, DMSO-d_6) δ 173.6, 172.6, 171.5, 171.1, 170.0, 163.3, 156.7, 155.6, 138.0, 137.5, 137.4, 137.3, 134.5, 132.6, 132.5, 132.3, 129.6, 129.4, 129.2, 129.0, 128.6, 127.9, 127.8, 127.6, 127.5, 126.3, 126.2, 126.1, 126.0, 125.9, 125.4, 65.2, 56.0, 53.4, 37.6, 37.4, 36.6, 28.9 ppm. MS (ESI) m/z for $C_{39}H_{37}N_3O_6$ $(M+Na)^+$ calcd.: 666.2580, found: 666.2580

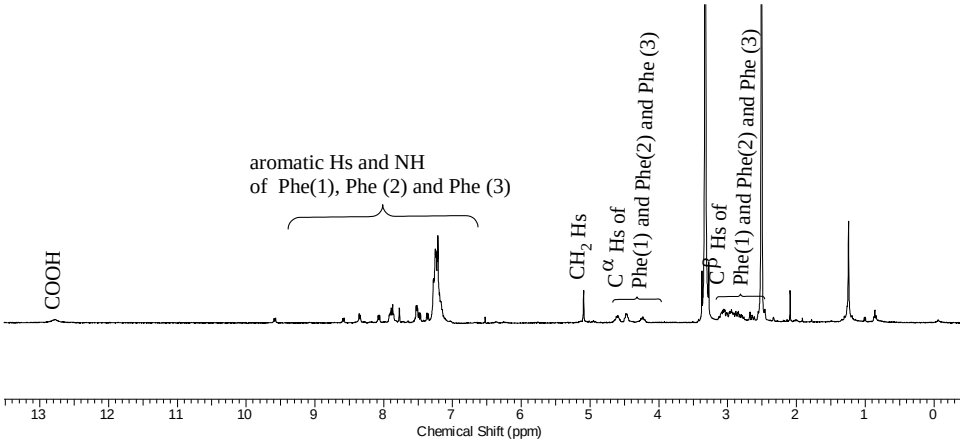

Figure 5.24. *400 MHz ^1H NMR spectrum of Nmoc-Phe-Phe-Phe-OH **2** in DMSO-d_6.*

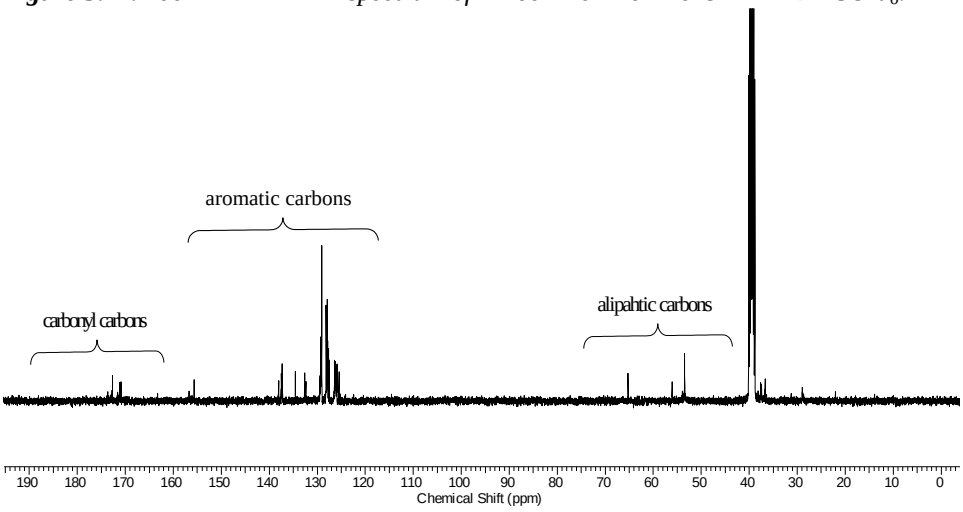

Figure 5.25. *100 MHz ^{13}C NMR spectrum of Nmoc-Phe-Phe-Phe-OH **2** in DMSO-d_6.*

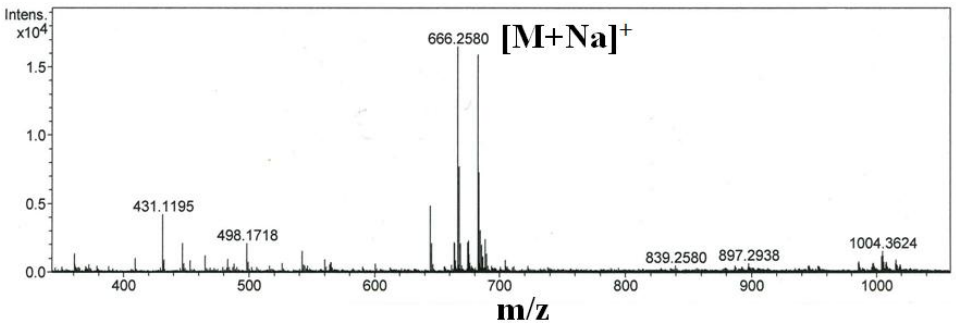

Figure 5.26. *ESI-MS spectrum of Nmoc-Phe-Phe-Phe-OH* ***2****.*

5.3 Gel Preparation and Characterization Techniques

5.3.1 Gel Preparation

Nmoc-VVV (20 mg, 20 mmol L^{-1}) was dispersed in 2 mL water. The pH of the peptide-water mixture was first increased to pH 10 by addition of 0.5 M NaOH, thereby solubilizing the peptide, and then gradually taken back to pH 6.5-7 by slow addition of 0.1 M HCl. Nmoc-VVV could not form a gel. 1 mg (~ 40 U mg^{-1}) thermolysin was added to the reaction vial. It turned to strong gel within 1 h of reaction time and was stable for two months. Nmoc-FFF solution was formed in a similar manner. 20 mmol Nmoc-amino acids (valine, V; phenylalanine, F) with a fourfold excess of nucleophile (VV, FF dipeptides) were solubilised in 2 mL water by the dropwise addition of 0.5 M NaOH and the pH was adjusted to 8 by addition of 0.1M HCl. Thermolysin (1 mg) was added to the reaction mixture and product formation was detected using HPLC.

5.3.2 ^{1}H NMR Spectroscopy

All NMR spectra were recorded at 400 MHz Bruker AV 400 NMR spectrometer. TMS was used an internal reference in the NMR spectra.

Peptide concentrations were in the range of 1-10 mmol in $(CD_3)_2SO$ and $CDCl_3$.

5.3.3 Mass Spectrometry

Mass spectra of peptides were recorded on Bruker micrOTOF-Q II by positive and negative mode electrospray ionizations.

5.3.4 High Performance Liquid Chromatograpy (HPLC) Analysis

A Dionex HPLC-Ultimate 3000 (High Performance Liquid Chromatography) pump was used to analyze library components. A 20 μL of sample was injected onto a Dionex Acclaim ® 120 C 18 column of 250 mm length with an internal diameter 4.6 mm and 5 μm fused silica particles at a flow rate of 1 mL min^{-1} (linear gradient of 40 % v/v) acetonitrile in water for 35 min, gradually rising to 100 % (v/v) acetonitrile in water at 35 min). This concentration was kept constant until 40 min when the gradient was decreased to 40 % (v/v) acetonitrile in water at 42 min. The sample preparation involved mixing of 100 μL of gel/solution with acetonitrile-water (900 μL, 50: 50 mixture) containing 0.1 % trifluoacetic acid. The samples were then filtered through a 0.45 μm syringe filter (Whatman, 150 units, 13 mm diameter, 2.7 mm pore size) prior to injection. The library components were identified by using Ultimate 3000 RS Variable Wavelength Detector at 280 nm.

5.3.5 Rheology

Rheological measurement was carried out using an Anton Paar Physica MCR 301 rheometer with cone plate of geometry (25 mm in diameter, 50 μm gap and 1^o cone). Nmoc-V hydrogel 200 μL poured onto the plate of the instrument, which was kept at 25^oC by using an integrated temperature

controller. Then dynamic frequency sweep of the hydrogel Nmoc-V were measured as function of frequency in the range of 0.1-100 rad s^{-1} with constant strain value. The stiffness of gel was determined when the value storage modulus G' exceed over the loss modulus G''. The value of G' for hydrogel is almost 20 times more than value G'' indicating very strong hydrogel.

5.3.6 Fluorescence Spectroscopy

Fluorescence spectra were recorded for a solution of Nmoc-VVV (20 mg mL^{-1}) prior to enzyme addition and hydrogel formed by Nmoc-V after addition of enzyme. Excitation wavelength was λ_{ex}=265. A small peak was observed at 463 nm which indicates excimer formation in higher order state. To get more significant about peak at 463 nm, we excited gel sample at 380 nm showed prominent peak at 463 nm.

5.3.7 Time Correlated Single Photon Counting Spectroscopy

A 2 mL of gel sample was prepared in a 1 cm^2 quartz cuvette and time resolved studies were done by a time correlated single photon counting (TCSPC) system from Horiba Yovin (Model: Fluorocube-01-NL). Samples were excited at 376 nm using a picosecond diode laser (Model: Pico Brite-375L). The signals were collected at magic angle (54.70) polarization using a photomultiplier tube (TBX-07C) as detector, which has a dark counts less than 20 cps. The instrument response function was typically 140 ps. The data analysis was performed using IBH DAS (version 6, HORIBA Scientific, Edison, NJ) decay analysis software.

The amplitude weighted lifetime was estimated by

$$\langle \tau \rangle = \sum_{i=1}^{n} a_i \, \tau_i$$

where τ_i is the fluorescence lifetime of various fluorescent species and are the normalized pre-exponential factors. To gain the best fitting in all cases, the χ^2 was kept near to unity.

5.3.8 Microscopy

The morphologies of the peptide nanofibers were characterized using a field-gun scanning electron microscope (Jeol JSM-7600F). The gel samples were dried on a glass cover slip and coated with platinum.

5.4 Results and Discussion

5.4.1 Self-assembly

DCLs are established when library components continuously exchange themselves via reversible reactions under thermodynamic control. A viscous solution of Nmoc-VVV **1** was observed in a pH dependent manner at pH 6.5-7 at a concentration of 0.9 wt% but it could not form gel rather than a viscous solution. Non-specific endoprotease enzyme thermolysin was added to the solution of Nmoc-VVV and was left at room temperature for about 3 h, resulting in the formation of a self-supporting rigid hydrogel. The hydrogel remained stable for two months. Thermolysin was chosen as the endoprotease to bring about peptide hydrolysis and reverse hydrolysis (Figure 5.27) of peptide **1** leading to the formation of a predominating product Nmoc-V at pH 7 driven by π-stacking interactions of aromatic Nmoc groups.

The HPLC results indicated that 87% of **1** was converted to Nmoc-V after 48 h (Figure 5.28A) and that self-assembly of this newly generated species leads to a self-supporting supramolecular hydrogel. Based on the above DCL concept, the synthesized compound Nmoc-FFF **2** was also tested for hydrogelation.

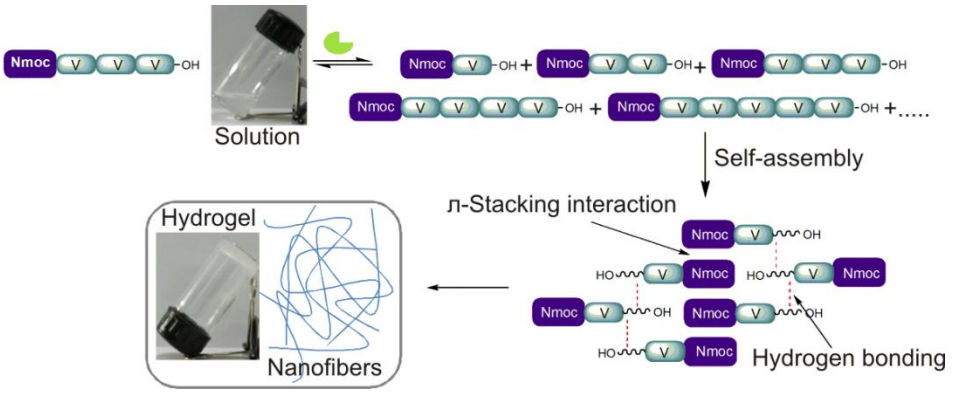

Figure 5.27. *Schematic representation showing enzymatic hydrolysis/reverse hydrolysis, self-assembly of a single predominating product and formation of a self-supporting hydrogel.*

Nmoc-FFF **2** was dispersed and solubilised in water at a concentration of 1.2 wt% by the dropwise addition of 0.5 M NaOH, then gradually decreased to pH 7 by the slow addition of 0.1 M HCl. This system turned into a self-supporting hydrogel.

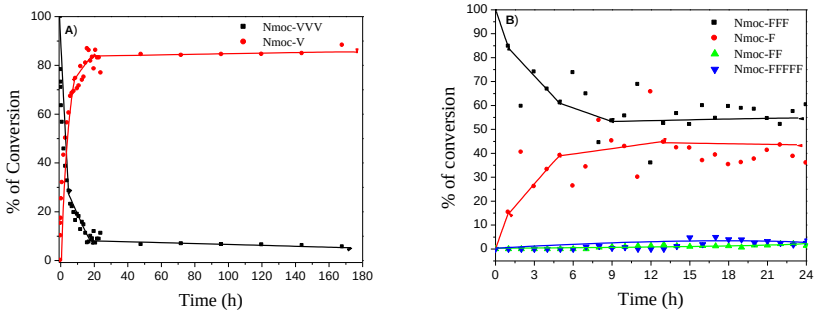

Figure 5.28. *A) Percentage of Nmoc-V conversion as a function of time followed by HPLC B) percentage of conversion for Nmoc-F, Nmoc-FF and Nmoc-FFFFF as function of time followed by HPLC. It was achieved from Nmoc-FFF after treatment with enzyme thermolysin.*

Compound **1** itself self-assembles in water and forms a hydrogel upon treatment with enzyme and generates a library of components with the single predominating product Nmoc-V. However, compound **2** showed exactly reverse behaviour to **1** on treatment with thermolysin.

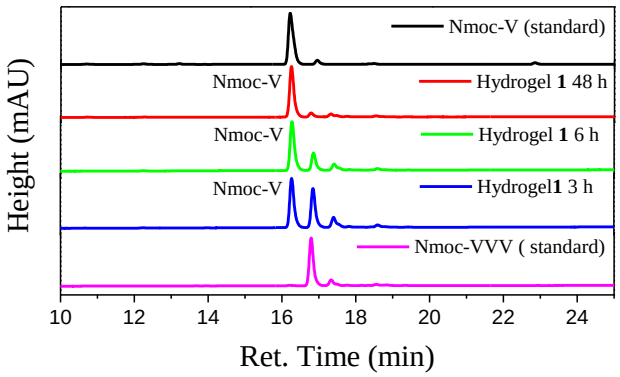

Figure 5.29. *HPLC chromatograms show conversion for Nmoc-V when a solution of Nmoc-VVV treated with thermolysin at different time*

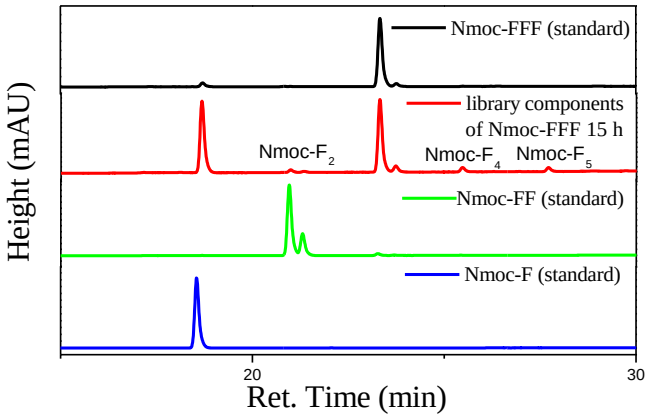

Figure 5.30. *HPLC chromatograms showing the library of components generated when Nmoc-FFF treated with thermolysin (Nmoc-F, Nmoc-FF, Nmoc-FFF, Nmoc-FFFF and Nmoc-FFFFF).*

It forms a library of four components with an uneven distribution and turns to liquid under similar conditions (Figure 5.30). All the newly synthesized products were characterized by reverse phase HPLC and ESI-MS (Figure 5.32-5.33). The hydrogel **1** starts breaking slowly when the pH is lowered below 5. It is entirely precipitated out at pH 4. At higher pH (>8) the gel also starts breaking slowly and at pH 11 the gel to sol transition occurs completely.

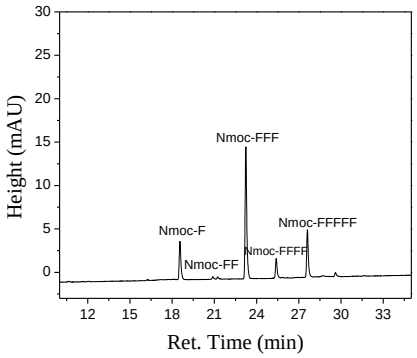

Figure 5.7. *HPLC chromatogram showing reverse hydrolysis for Nmoc-F and FF to obtain Nmoc-FFF.*

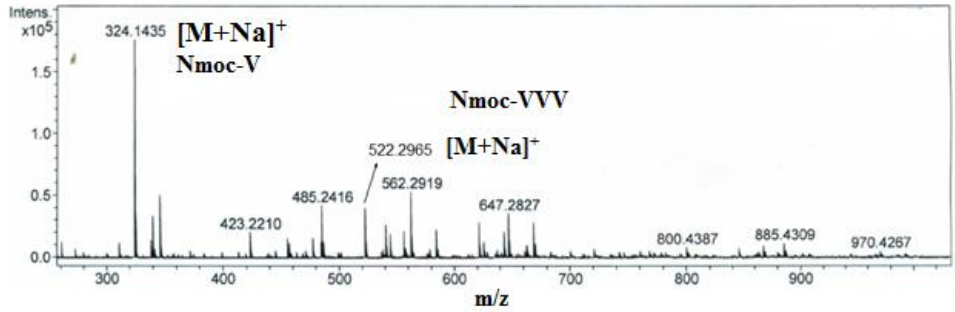

Figure 5.8. *ESI-MS spectrum confirms the formation of library members Nmoc-V and Nmoc-VVV*

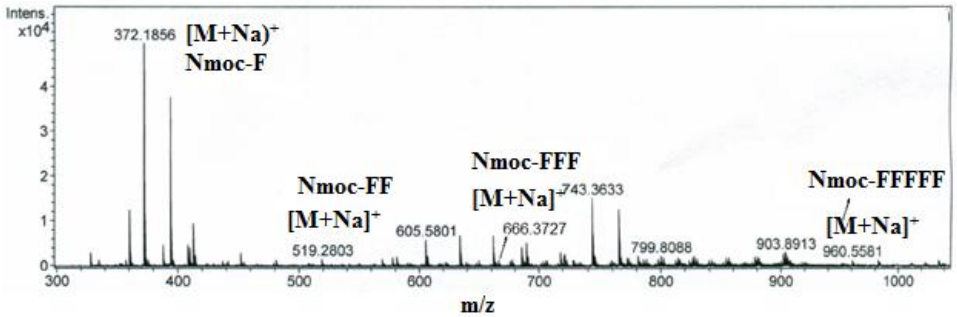

Figure 5.33. *ESI-MS spectrum confirms the generation library of components Nmoc-F, Nmoc-FF, Nmoc-FFF and Nmoc-FFFFF.*

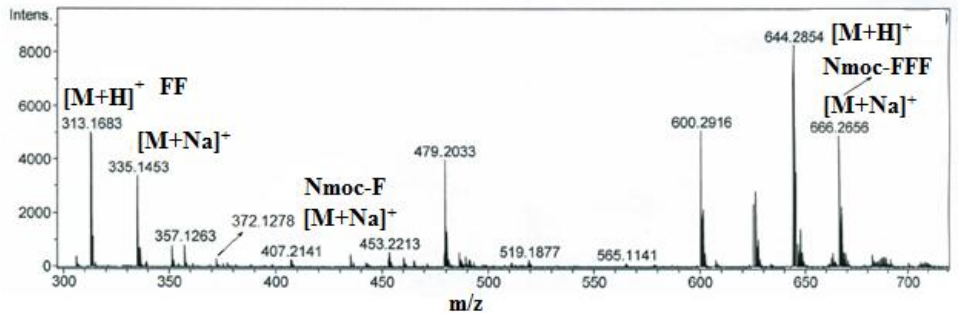

Figure 5.34. *ESI-MS spectrum confirms the formation Nmoc-FFF from Nmoc-F and FF upon enzymatic reverse hydrolysis.*

Nmoc-amino acids (valine, V; phenylalanine, F) with a fourfold excess of nucleophiles (VV, FF dipeptides) were solubilised in water and thermolysin was added to the reaction mixture at pH 8.16. Newly generated product was not obtained from the Nmoc-V/VV system. 72% Nmoc-FFF (Figure 5.31and 5.34) was formed from the Nmoc-F/FF system at 24 h and it turned into a hydrogel within 1 h of enzyme addition. Four fold excess of nucleophile is required for reverse hydrolysis reactions under similar conditions to peptide hydrolysis reactions. Nmoc-V is the predominating product obtained from parent Nmoc-VVV using enzyme catalyzed peptide hydrolysis reaction. These results clearly demonstrate that enzyme-catalyzed self-assembly (hydrogelation) facilitates the formation of the most stable predominating component.

5.4.2 Rheological Study

The viscoelastic properties of the hydrogel Nmoc-VVV/Nmoc-V system were characterized using oscillatory rheology. A rigid strong hydrogel has a storage modulus (G') value that exceeds the loss modulus (G'') value by an order of magnitude.[19] Dynamic frequency sweep testing was carried out to study the hydrogel formation on different time scales (figure 5.35-5.36).

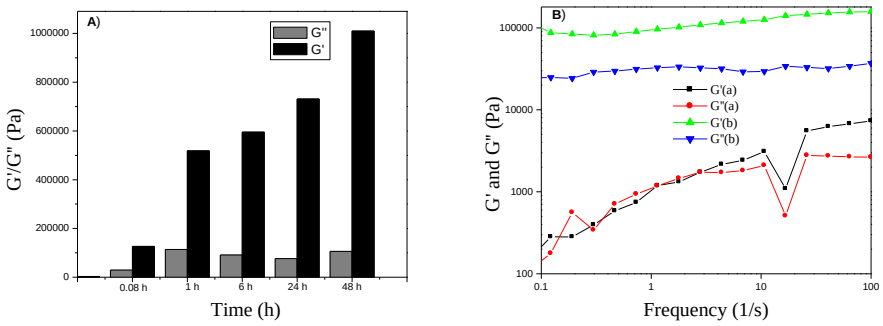

Figure 5.35. *A) Comparison between the storage modulus (G') and loss modulus (G'') at a particular point of angular frequency (10.7 s^{-1}) with the course of reaction time at a constant strain of 0.1%. B) Dynamic frequency sweep showing viscoelastic nature of Nmoc-V hydrogel a) a solution of Nmoc-VVV prior enzyme addition and b) hydrogel of Nmoc-V 5 min after addition of enzyme.*

G' overlaps with G'' (Figure 5.35 A) suggesting that the viscous solution of Nmoc-VVV is not fairly strong prior to enzyme addition. Thermolysin was added to the solution of 0.9 wt% of peptide Nmoc-VVV at pH 7 for rheological studies. However G' and G'' increased with time, the value of G' dominating over G'' about 5 min after addition of thermolysin (Figure 5.35A). As shown in Figure 5.35A, G' was much higher than G'' after about 1 h of reaction. After about 2 days of enzyme reaction the G' value for the hydrogel is almost 20 times that of G'', indicating the extensive 3D network in the hydrogel.

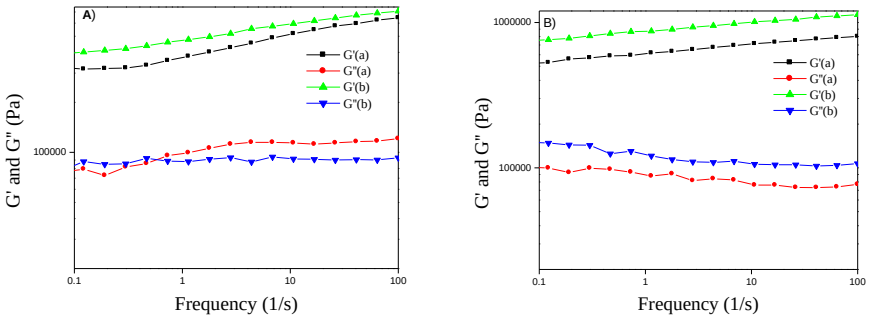

Figure 5.36. *A) Dynamic frequency sweep showing viscoelastic nature of Nmoc-V hydrogel a) Nmoc-V hydrogel after 1 h of enzyme reaction and b) Nmoc-V hydrogel after 6 h of enzyme reaction.B) Nmoc-V hydrogel 1 day after enzyme reaction and b) Nmoc-V 2 days after enzyme reaction.*

5.4.3 Fluorescence Study

Fluorescence emission spectra were recorded to gain more insight into the molecular arrangement of the gelator molecules in the gel phase.

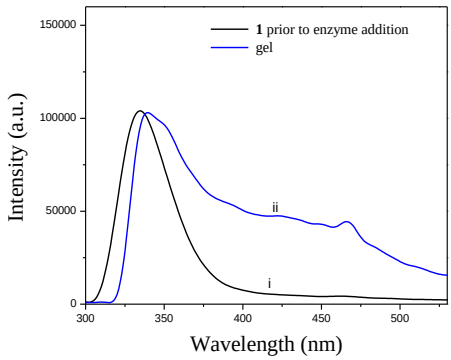

Figure 5.37. *Normalized fluorescence spectra taken during the self-assembly process: (i) solution of Nmoc-VVV prior to enzyme addition and (ii) gel of Nmoc-V after enzyme addition (λex = 265 nm).*

As peptide **1** formed a gel only upon enzyme addition, the emission peak originating from the naphthalene double ring centered at 334 nm (in solution) was red shifted to 340 nm (gel phase) (Figure 5.37). The hydrogel formed by self-assembly of a predominating library member Nmoc-V derived from peptide Nmoc-VVV which forms efficient π-π stacking interactions in the gel phase medium. An emission peak centered at 463 nm suggests excimer formation at a higher order aggregate state.

5.4.4 Time Correlated Single Photon Counting Study

A time resolved fluorescence study was acquired to investigate the higher order aggregated states of the fluorophore groups (Nmoc) of the Nmoc-V hydrogel. Time resolved fluorometry allows very keen discrimination between fluorophore species in different environments by contributing individual emissions at the same wavelength. The fluorescence decay time of the Nmoc-V hydrogel was measured at an excitation wavelength of 376

nm and the emission was monitored at 463 nm. Tri-exponential decay was fitted to measure the lifetime of Nmoc-V hydrogel at 1 day after enzyme addition (Figure 5.38). The average lifetime was 0.7755 ns of Nmoc-VVV prior to enzyme addition. The average lifetime of 1.108 ns of the Nmoc-V hydrogel was observed a day after enzyme addition at room temperature (Table 5.1).

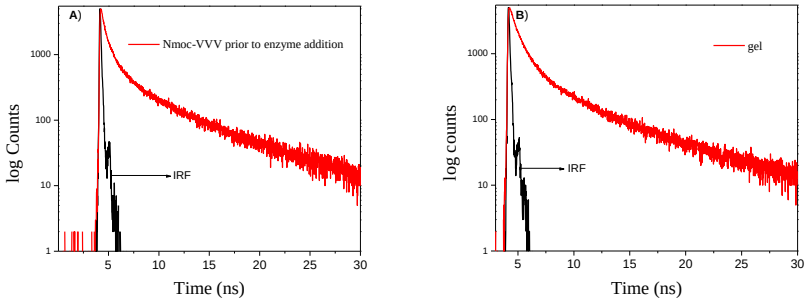

Figure 5.38. *A) Emission decay curves for a solution of Nmoc-VVV prior to enzyme addition monitored at 463 nm (IRF: instrument response function). B) gel Nmoc-VVV/ Nmoc-V system monitored at 463 nm after a day (IRF: instrument response function).*

Table 5.1. *Decay parameters for hydrogel of Nmoc-V after enzyme reaction at different time.*

Nmoc-VVV	α_1	α_2	α_3	τ_1 (ns)	τ_2(ns)	τ_3(ns)	τ^a(ns)	χ^2
Prior to enzyme addition	0.21	0.05	0.74	1.2374	7.0116	0.24230	0.7755	1.3455
6 h	0.27	0.06	0.67	1.4205	6.7926	0.4091	1.0436	1.1981
24 h	0.24	0.05	0.70	1.6119	7.1659	0.4615	1.1080	1.1488
36 h	0.26	0.06	0.68	1.5301	6.8341	0.4375	1.1140	1.2106
48 h	0.23	0.71	0.06	1.7070	0.4857	7.2150	1.1402	1.2374

τ^a The amplitude weighted average lifetime, Normalized amplitude of each component is given by α

This value, showing the fluorescence lifetime of the naphthalene groups of hydrogel samples with time scale, indicates a more dense aggregated nanofibrous network in the hydrogel.[20]

5.4.5 Microscopic Study

Field-emission scanning electron microscopy (SEM) was used to reveal the self-assembled nanostructures of the hydrogel in a time dependent manner that relate to the self-assembly kinetics of the system. As shown in Figure 5.39, the hydrogelator Nmoc-V self-assembled into nanofibers that cross-linked to form a fibrous network. The image (Figure 5.39) shows the dense mass of Nmoc-VVV prior to enzyme addition when the conversion of gelator was zero. However, there was an extreme change in morphology of the hydrogelator Nmoc-V after enzyme addition. Figure 5.39B shows a highly dense mass of gelator because of the inefficient self-assembly of the hydrogelator Nmoc-V when the conversion of Nmoc-V was only 10% up to 5 min after enzyme addition. As mentioned earlier, library member Nmoc-V forms a hydrogel but not its parent molecule Nmoc-VVV. The removal of two hydrophobic units from peptide Nmoc-VVV in response to enzyme hydrolysis forms a delicate balance of molecular interaction in the self-assembled nanofiber networks, which results in viscous sol-gel transition.

The SEM image Figure 5.39C reveals short entangled nanofibers with an average width of 30 nm at 1 h after enzyme addition. Figure 5.39D and 5.39E show a dense, aggregated nanofibrous network which appears quite random and exhibits ordered microstructure. However, the sample (Figure 5.39F) with one month long enzyme reaction interestingly exhibits quite elongated and thick nanofibers. HPLC analysis showed that the conversion of Nmoc-V after 6 h and 24 h was 67% and 76% respectively. These network structures of nanofibers[21] of a preferred library member are responsible for stable hydrogel formation.

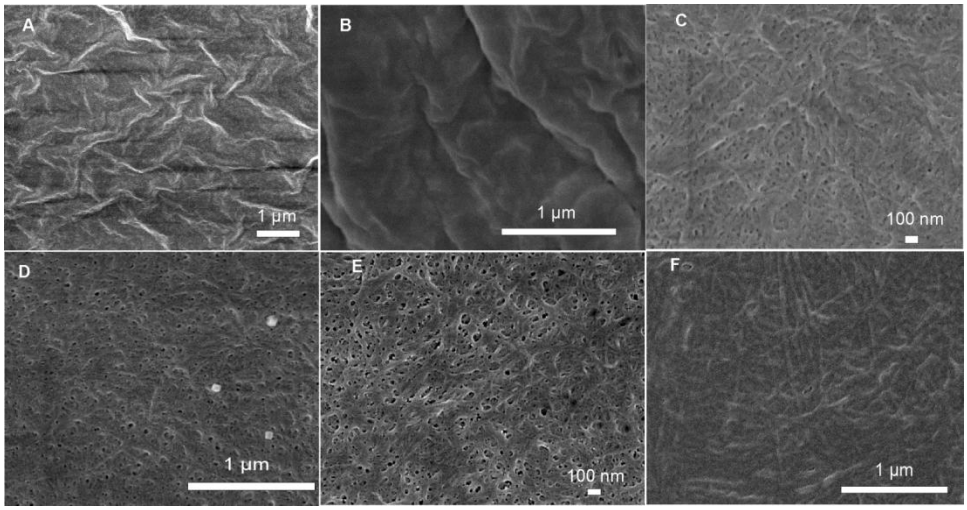

Figure 5.39. *FE-SEM images of the Nmoc-VVV/Nmoc-V system. SEM images of (A) Nmoc-VVV before addition of enzyme and after enzyme addition at (B) 5 min, (C) 1 h, (D) 6 h, (E) 1 day and (F) 1 month. (B) to (F) show the change of nanostructural morphology with subsequent formation of Nmoc-V leading to formation of a self-supporting hydrogel.*

5.5 Conclusion

In summary, we have demonstrated a new kind of dynamic supramolecular hydrogel by introducing an N-terminus protecting aromatic moiety *i.e.* the naphthalene-2-methoxycarbonyl (Nmoc) group. Enzyme catalyzed hydrogelation leads to the formation of a dynamic library. The dynamic peptide library generates a very simple nanostructured predominating product that self-assembles through π-π stacking interactions. A real-time morphological change was also described, which will be a powerful methodology for making biomaterials.

5.6 References

1. Lehn J. M. (1995), *Supramolecular chemistry*: concept and perspective, VCH, Weinheim.

2. (a) Kiyonaka S., Sada K, Yoshimura I., Shinkai S., Kato N., Hamachi I. (2004), Semi-wet peptide/protein array using supramolecular hydrogel, *Nat. Mater.*, 3, 58-64 (DOI:10.1038/ nmat1034); (b) Wada A., Tamaru S., Ikeda M., Hamachi I. (2009), MCM-enzyme-supramolecular hydrogel hybrid as a fluorescence sensing material for polyanions of biological significance, *J. Am. Chem. Soc.*, 131, 5321-5330 (DOI: 10.1021/ja900500j).

3. (a) Genove E., Shen C., Zhang S. G., Semino C. E. (2005), The effect of functionalized self-assembling peptide scaffolds on human aortic endothelial cell function, *Biomaterials*, 26, 3341-3351 (DOI: 10.1016/j.biomaterials.2004.08.012); (b) Jung J. P., Nagaraj A. K., Fox E. K., Rudra J. S., Devgun J. M., Collier J. H. (2009), Co-assembling peptides as defined matrices for endothelial cells, *Biomaterials*, 30, 2400-2410 (doi: 10.1016/ j.biomaterials. 2009.01.033.).

4. Bhuniya S., Park S. M. Kim B. H. (2005), Biotin-amino acid conjugates:α An approach toward self-assembled hydrogelation, *Org. Lett.*, 7, 1741-1744 (DOI: 10.1021/ol050300r).

5. Yang Z. M., Liang G. L., Ma M. L., Abbah A. S., Lu W. W., Xu B. (2007), D-glucosamine-based supramolecular hydrogels to improve wound healing, *Chem. Commun.*, 843-845 **(**DOI: 10. 1039/B616563J).

6. Yang Z. M., Gu H. W., Fu D. G., Gao P., Lam J. K., Xu B. (2004), Enzymatic formation of supramolecular hydrogels, *Adv. Mater.*, 16, 1440-1444 (DOI: 10.1002/adma.200400340).

7. John G., Zhu G., Li J., Dordick J. S. (2006), Enzymatically derived sugar-containing self-assembled organogels with nanostructured morphologies, *Angew. Chem., Int. Ed.*, 45, 4772-4775 (DOI: 10.1002/anie.200600989).

8. Xing B. G., Yu C. W., Chow K. H., Ho P. L., Fu D. G., Xu B. (2002), Hydrophobic interaction and hydrogen bonding

cooperatively confer a vancomycin hydrogel:α A potential candidate for biomaterials *J. Am. Chem. Soc.*, 124, 14846-14847 (DOI: 10.1021/ja028539f).

9. (a) Amdursky N., Gazit E., Rosenman G. (2010), Quantum confinement in self-assembled bioinspired peptide hydrogels, *Adv. Mater.*, 22, 2311-2315 (DOI: 10.1002/adma.200904034); (b) Orbach R., Adler-Abramovich L., Zigerson S., Mironi-Harpaz I., Seliktar D., Gazit E. (2009), Self-assembled Fmoc-peptides as a platform for the formation of nanostructures and hydrogels, *Biomacromolecules*, 10, 2646-2651 (DOI: 10.1021/bm900584m); (c) Guilbaud J.-B., Vey E., Boothroyd S., Smith A. M., Ulijn A. V., Saiani A., Miller A. F., (2010), Enzymatic catalyzed synthesis and triggered gelation of ionic peptides, *Langmuir*, 26, 11297-11303 (DOI: 10.1021/la100623y); (d) Nagarkar R. P., Hule R. A., Pochan D. J., Schneider J. P. (2008), De novo design of strand-swapped β-hairpin hydrogels, *J. Am. Chem. Soc.*, 130, 4466-4474 (DOI: 10.1021/ja710295t); (e) Banwell E. F., Abelardo E. S., Adams D. J., Birchall M. A., Corrigan A., Donald A. M., Kirkland M., Serpell L. C., Butler M. F., Woolfson D. N. (2009), Rational design and application of responsive α-helical peptide hydrogels, *Nat. Mater.*, 8, 596-600 (DOI:10.1038/nmat2479).

10. (a) Boyle A. L., Woolfson D. N., (2011), De novo designed peptides for biological applications, Chem. Soc. Rev., 40, 4295-4306 (DOI: 10.1039/c0cs00152j); (b) Gazit E. (2007), Self-assembled peptide nanostructures: the design of molecular building blocks and their technological utilization, *Chem. Soc. Rev.*, 36, 1263-1269 (DOI: 10.1039/b605536m).

11. Hirst A. R., Roy S., Arora M., Das A. K., Hodson N., Murray P., Marshall S., Javid N., Sefcik J., Boekhoven J., van Esch J. H., Santabarbara S., Hunt N. T., Ulijn R. V. (2010), Biocatalytic

induction of supramolecular order, *Nat. Chem.*, 2, 1089 (DOI: 10.1038/NCHEM.861).

12. Yang Z., Xu K., Guo Z., Guo Z., Xu B. (2007), Intracellular enzymatic formation of nanofibers results in hydrogelation and regulated Cell Death, *Adv. Mater.*, 19, 3152-3156 (DOI: 10.1002/adma.200701971).
13. (a) Corbett P. T., Leclaire J., Vial L., West K. R., Wietor J.-L., Sanders J. K. M., Otto S. (2006), Dynamic combinatorial chemistry, *Chem. Rev.*, 106, 3652-3711 (DOI: 10.1021/ cr020452p); (b) Boekhoven J., Brizard A. M., Kowlgi K. N. K., Koper G. J. M., Eelkema R., van Esch J. H. (2010), Dissipative self-assembly of a molecular gelator by using a chemical fuel, *Angew. Chem., Int. Ed.,* 49, 4825-4828 (DOI: 10.1002/ anie. 201001511).
14. Lam R. T. S., Belenguer A., Roberts S. L., Naumann C., Jarrosson T., Otto S., Sanders J. K. M. (2005), Amplification of acetylcholine-binding catenanes from dynamic combinatorial libraries, *Science*, 308, 667-669 (DOI: 10.1126/science.1109999).
15. Sreenivasachary N., Lehn J. M. (2005), Gelation-driven component selection in the generation of constitutional dynamic hydrogels based on guanine-quartet formation, *Proc. Natl. Acad. Sci. U.S.A.*, 102, 5938-5943 (DOI: 10.1073/pnas.0501663102).
16. Das A. K., Hirst A. R., Ulijn R. V. (2009), Evolving nanomaterials using enzyme-driven dynamic peptide libraries (eDPL), *Faraday Discuss.*, 143, 293-303 (DOI: 10.1039/ b902065a).
17. Carpenter F. H. (1960), The free energy change in hydrolytic reactions: The non-ionized compound convention, *J. Am. Chem. Soc.*, 82, 1111-1122 (DOI: 10.1021/ja01490a024).

18. Chen Y., Liang G. (2012), Enzymatic self-assembly of nanostructures for theranostics, *Theranostics,* 2, 139-147 (DOI: 10.7150/thno.3696).

19. Greenfield M. A., Hoffman J. R., de la Cruz M. O., Stupp S. I. (2010), Tunable mechanics of peptide nanofiber gels, *Langmuir,* 26, 3641-3647 (DOI: 10.1021/la9030969).

20. Mukhopadhyay S., Maitra U., Krishnamoorthy G., Schmidt J., Talmon Y. (2004), Structure and dynamics of a molecular hydrogel derived from a tripodal cholamide, *J. Am. Chem. Soc.*, 126, 15905-15914 **(**DOI: 10.1021/ja046788t).

21. Maity I., Rasale D. B., Das A. K. (2012), Sonication induced peptide-appended bolaamphiphile hydrogels for *in situ* generation and catalytic activity of Pt nanoparticles, *Soft Matter,* 8, 5301-5308 (DOI: 10.1039/C2SM25126D).

Chapter 6

Lipase Catalyzed Inclusion of Gastrodigenin for the Evolution of Blue Light Emitting Peptide Nanofibers

6.1 Introduction

Self-assembly[1] is a spontaneous process in which a number of components form an organized structure. Inspired from natural systems, several synthetic systems such as low molecular weight organic molecules have been adapted to develop nanoscale architectures.[2] In general, these self-assembling systems remain in a local thermodynamic minimal state due to minimization of energy or continuous influx of chemical energy. To date, various self-assembled architectures have been reported which are under thermodynamic equilibrium.[3] Recently, there has been growing interest to develop dissipative self-assembly (DSA) systems, which have potential to adapt themselves. These DSA systems consist of non-assembling entities, which can form different nanostructures depending on external stimuli through activation of an energy source. Despite a constant source of energy, the non-equilibrium counterpart of the DSA system leads to dis-assembly due to deactivation of the building blocks caused by energy dissipation. So far, few examples of dissipative selfassembly[4] have been reported. van Esch *et al*. reported an excellent example of dissipative self-assembly of a molecular gelator by using a chemical fuel.[5] Herein, we have used the enzyme lipase as an energy source to meet the requirement of dissipative self-assembly.

Ajayaghosh *et al*. exploited controlled donor self-assembly and energy transfer to form a white light emitting organogel.[6] However, biocatalytic evolution of blue light emitting biomaterials[7] in aqueous media is not yet

reported in the literature. Xu and Ulijn are the pioneers of enzyme catalysed peptide self-assembly.[8] The enzyme lipase is known to hydrolyze carboxylic acid ester[9] in aqueous medium but also undergoes esterification[10] or trans-esterification[11] reactions in organic solvents. The simple visual colorimetric assay that responds to enzymatic reactions is the area of biosensing applications.[12] Enzymatic conjugation of fluorophores with enhanced emission properties in aqueous medium is more promising for bioassay and imaging applications.[13]

In this chapter, we report lipase from candida rugosa (CRL) catalyzed incorporation of gastrodigenin *p*-hydroxybenzyl alcohol (HBA) in Nmoc-protected peptides (Nmoc = naphthalene-2-methoxy carbonyl) followed by evolution of blue light emitting hydrogel. Very recent study shows the use of HBA as a promising candidate for the establishment of anti-angiogenic treatment strategies in cancer therapy.[14]

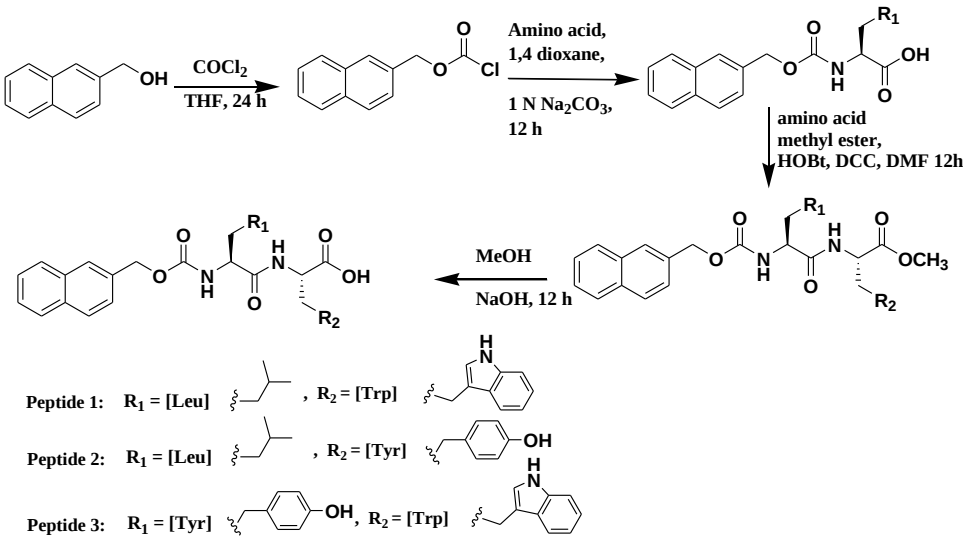

Figure 6.11. *Synthesis of Nmoc-protected dipeptides.*

6.2 Experimental

*6.2.(1) Synthesis of compounds **1**, **2** and **3***

The Nmoc-protected amino acids were synthesized by reaction of Nmoc-Cl with amino acid. The subsequent coupling of amino acids was achieved by conventional solution phase methododology.

*6.2.1 Synthesis of Compound **1**:*

a) Synthesis of Nmoc-Cl **4:** To a stirred solution of naphthalene methanol (5 g, 31.6 mmol) in dry THF (140 mL), phosgene (39.2 mL, 75.5 mmol) was added at 0 °C. The stirring was continued at ambient temperature for 24 h. The reaction was monitored by thin layer chromatography (TLC). After completion of reaction, excess phosgene was removed under low vacuum and trapped with aqueous NaOH. Reaction mixture was concentrated and oily product was obtained. Then, it was dissolved in hot hexane to get **4** as crystalline product**.**

Yield = 6.8 g (30 mmol, 94.93 %). mp: 62 °C; FT-IR (KBr): cm^{-1} 3066 (m), 1777 (s), 1601(ms), 1168 (s) cm^{-1}; ^{1}H NMR (400 MHz, $CDCl_3$): δ 7.90 (d, 4H), 7.56 (m, 2H), 7.29 (s, 1H), 5.48 (s, 2H) ppm; ^{13}C NMR (100 MHz, $CDCl_3$): δ 71.82, 125.7, 126.6, 127.8, 128.1, 128.6, 130.6, 133.5, 140.9, 147.9, 150.7 ppm.

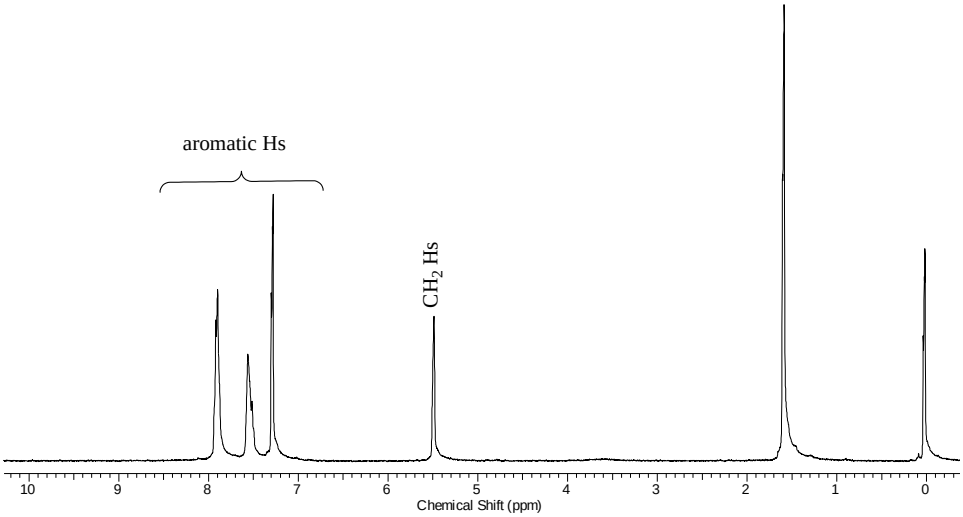

Figure 6.2. *400 MHz ^{1}H NMR spectrum of Nmoc-Cl **4** in $CDCl_3$.*

b) Synthesis of Nmoc-Leu-OH **5:** A solution of leucine (1.048 g, 8 mmol) in a mixture of 1, 4 dioxane (20 mL) and 1M sodium hydroxide (20 mL) was stirred and cooled in an ice-water bath. Naphthalene-2-methoxychloroformate **4** (1.764 g, 8 mmol) was added and stirring was continued at room temperature for 12 h. Reaction mixture was diluted with 200 mL of water and dioxane was evaporated under vaccum. Aqueous layer was washed with diethyl ether and the pH of aqueous layer was adjusted to 2 with 2M hydrochloric acid. The aqueous phase was extracted with ethyl acetate (3 x 50 mL) and dried over Na_2SO_4. The organic layer was concentrated under vacuum to give **5** as white solid.

Yield =1.962 g (6.2 mmol, 77.5 %). mp: 79 °C; $[\alpha]_D^{25}$ = -12 (*c* = 1, MeOH); FT-IR (KBr): cm^{-1} 3418 (br), 3380 (br), 3053 (ms), 2960 (s), 2874 (ms), 1700 (s), 1604 (ms), 1517 (s), 1462 (ms), 1363 (ms), 1321 (ms), 1239 (s) cm^{-1}; ^1H NMR (400 MHz, DMSO-d_6): δ 7.91 (d, 4H), 7.64 (d, 1H), 7.53 (d, 2H), 7.48 (d, 1H, NH), 5.20 (s, 2H, CH_2), 4.03 (m, 1H, $C^{\alpha}H$ of Leu), 1.47 (m, 2H, $C^{\beta}Hs$ of Leu), 1.17 (m, 1H, $C^{\gamma}H$ of Leu), 0.88 (d, 6H, $C^{\delta}Hs$ of Leu) ppm; MS (ESI) m/z for $C_{18}H_{21}NO_4$ $(M+Na)^+$ calcd.: 338.1368, found: 338.1378; Elemental Analysis calculated for $C_{18}H_{21}NO_4$: C, 68.55; H, 6.71; N, 4.44; Found: C, 67.06; H, 6.84, N, 4.04.

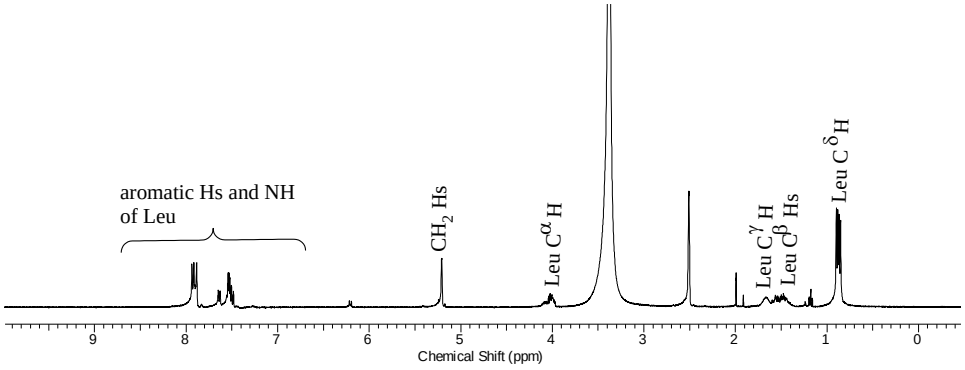

Figure 6.3. *400 MHz ^1H NMR spectrum of **5** in DMSO-d_6.*

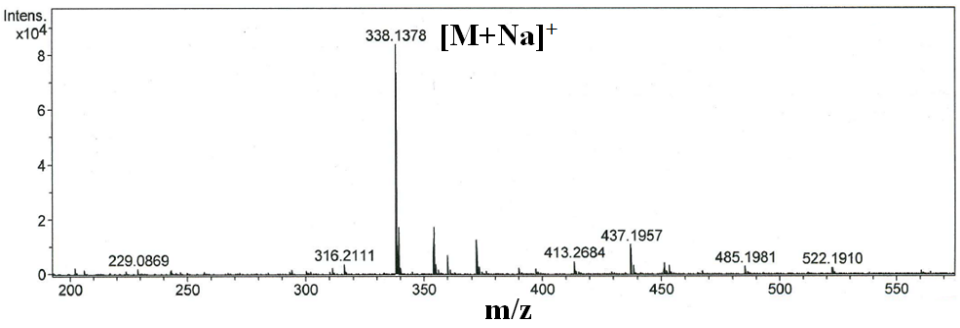

Figure 6.4. *ESI-MS spectrum of* ***5****.*

c) Synthesis of Nmoc-Leu-Trp-OCH_3 **6:** A solution of Nmoc-L (0.9 g, 2.8 mmol) and HOBt (0. 378 g, 2.8 mmol) was stirred in 2 mL of DMF. A neutralized solution of tryptophan methyl ester (1.42 g, 5.6 mmol) was extracted from its corresponding hydrochloride salt and concentrated to add to the reaction mixture followed by DCC (0.598 g, 2.9 mmol) at 0 °C. The mixture was allowed to stir at room temperature for 12 h. The mixture was diluted with ethyl acetate and organic layer was washed with 1 M HCl (2 x 30 mL), brine solution, 1 M Na_2CO_3 (3 x 30 mL) and brine solution. The ethyl acetate layer was dried over Na_2SO_4 and evaporated under vacuum to yield white solid product **6**. Purification was done by silica gel column (100-200 mesh) using chloroform-methanol as eluent.

Yield =1.23 g (2.38 mmol, 82.14 %); $[\alpha]_D^{25}$ = -16 (*c* = 1, MeOH); FT-IR (KBr): cm^{-1} 3315 (br), 3055(ms), 2954 (s), 2869 (ms), 1738 (ms), 1709 (ms), 1659 (s), 1528 (s), 1439 (ms), 1358 (ms), 1219 (s) cm^{-1}; ^1H NMR (400 MHz, $CDCl_3$): δ 7.77 (m, 4H, Nph), 7.42 (m, 3H, Nph), 7.37 (d, 1H, NH), 7.17 (d, 1H, *J* = 8.28 Hz, NH), 7.06 (t, 1H, Trp), 7.00 (t, 1H, Trp), 6.84 (d, 2H, Trp), 6.39 (d, 1H, *J* = 6.28 Hz, Trp), 5.16 (s, 2H, CH_2 of Nph), 4.81 (m, 1H, C^{α} H of Trp), 4.10 (m, 1H, C^{α} H of Leu), 3.59 (s, 3H, OCH_3), 3.22 (d, 2H, *J* = 4.76 Hz, C^{β} Hs of Trp), 1.87 (d, 1H, C^{β} H of Leu), 1.70 (d, 1H, C^{β} H of Leu), 1.28 (m, 1H, C^{γ} H of Leu), 0.82 (d, 6H, J = 5.24 Hz, C^{δ}Hs of Leu); MS (ESI) m/z for $C_{30}H_{33}N_3O_5$ $(M+H)^+$ calcd.: 516.2498, found: 516.2458; Elemental Analysis calculated for

$C_{30}H_{33}N_3O_5$: C, 69.88; H, 6.45; N, 8.15; Found: C, 69.38; H, 6.66, N, 8.12.

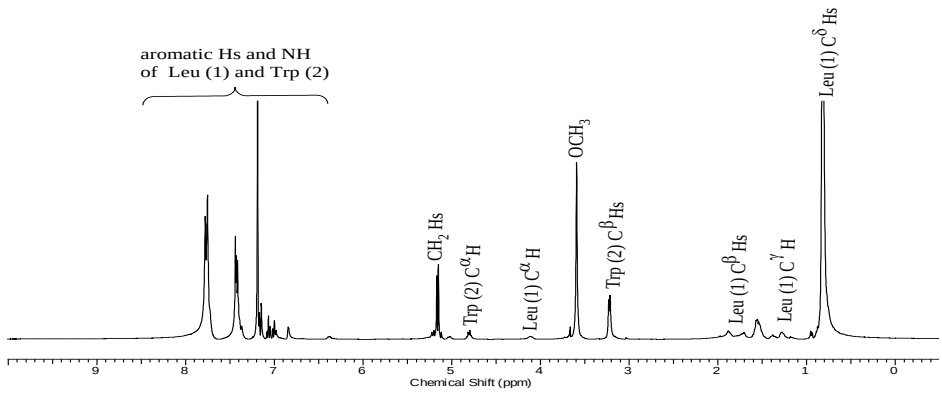

Figure 6.5. *400 MHz ^{1}H NMR spectrum of **6** in $CDCl_3$.*

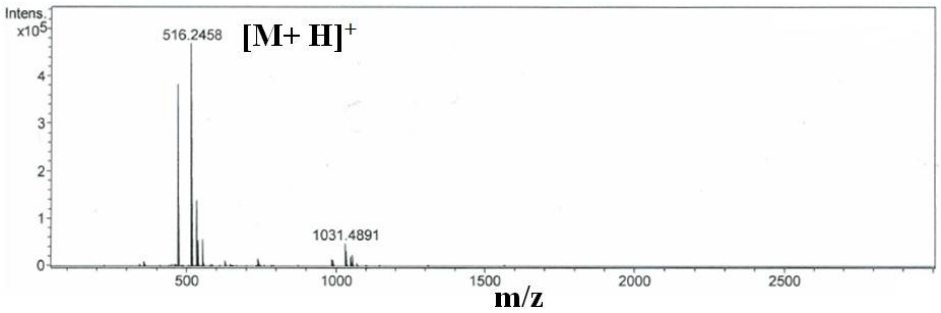

Figure 6.6. *ESI-MS spectrum of **6**.*

d) Synthesis of Nmoc-Leu-Trp-OH **1:** A solution of Nmoc-LW-OCH_3 **6** (0.980 g, 1.9 mmol) in 100 mL of dry MeOH was allowed to react with a solution of 2 M NaOH. The progress of the reaction was monitored by thin layer chromatography (TLC). The reaction mixture was stirred for 12 h. Then, methanol was removed under vacuum. The residue was taken in 100 mL of water and washed with diethyl ether (2 x 20 mL). The pH of aqueous layer was adjusted to 2 using 2 M HCl and it was extracted with ethyl acetate (3 x 30 mL). The ethyl acetate layer was dried over anhydrous sodium sulfate and evaporated in vacuum to yield **1** as white solid.

Yield =0.711 g (1.4 mmol, 73.68 %); $[\alpha]_D^{25}$ = -7 (*c* = 1, MeOH); FT-IR (KBr): 3321(br), 3056(ms), 2957 (s), 2870 (ms), 1712 (ms), 1660 (s), 1526 (s), 1457 (ms), 1337 (ms), 1255 (s) cm^{-1}; ^{1}H NMR (400 MHz,

DMSO-d_6): δ 10.7 (s, 1H, NH of Trp ring), 8.01 (d, 1H, *J* = 7.52 Hz, NH), 7.82 (t, 4H, Nph), 7.44 (m, 3H, Nph), 7.39 (d, 2H, *J* = 10.04 Hz, Trp), 7.26 (d, 1H, *J* = 8.04 Hz, NH), 7.08 (s, 1H, Trp), 6.98 (t, 1H, Trp), 6.90 (t, 1H, Trp), 5.12 (s, 2H, CH_2 of Nph), 4.41 (m, 1H, $C^{\alpha}H$ of Trp), 4.03 (m, 1H, $C^{\alpha}H$ of Leu), 3.09 (d, 1H, *J* = 5.28 Hz, C^{β} H of Trp), 3.02 (d, 1H, *J* = 7.80 Hz, C^{β} H of Trp), 1.54 (d, 1H, C^{γ}Hs of Leu), 1.36 (d, 2H, C^{β} H of Leu), 0.78 (d, 6H, *J* = 3.28 Hz, C^{δ}Hs of Leu); ^{13}C NMR (100 MHz, DMSO-d_6): δ 173.1, 172.2, 170.3, 155.8, 135.9, 134.6, 132.6, 132.4, 127.9, 127.6, 127.2, 126.2, 126.03, 125.6, 123.5, 120.8, 118.3, 111.2, 109.5, 65.44, 59.71, 53.01, 33.30, 26.90, 24.12, 23.02, 21.35, 20.72, 14.04; MS (ESI) m/z for $C_{29}H_{31}N_3O_5$ $(M+H)^+$ calcd.: 502.2342, found: 502.2376; Elemental Analysis calculated for $C_{29}H_{31}N_3O_5$: C, 69.44; H, 6.23; N, 8. 38; Found: C, 68.23; H, 6.50; N, 8.05.

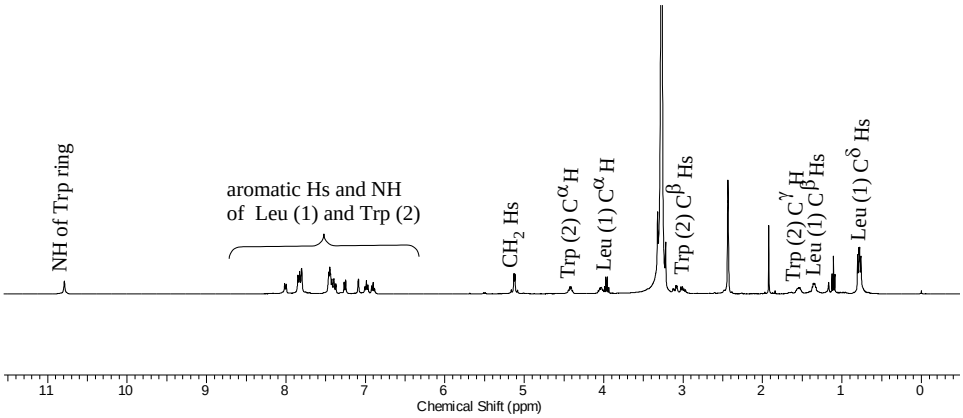

Figure 6.7. *400 MHz ^{1}H NMR spectrum of **1** in DMSO-d_6.*

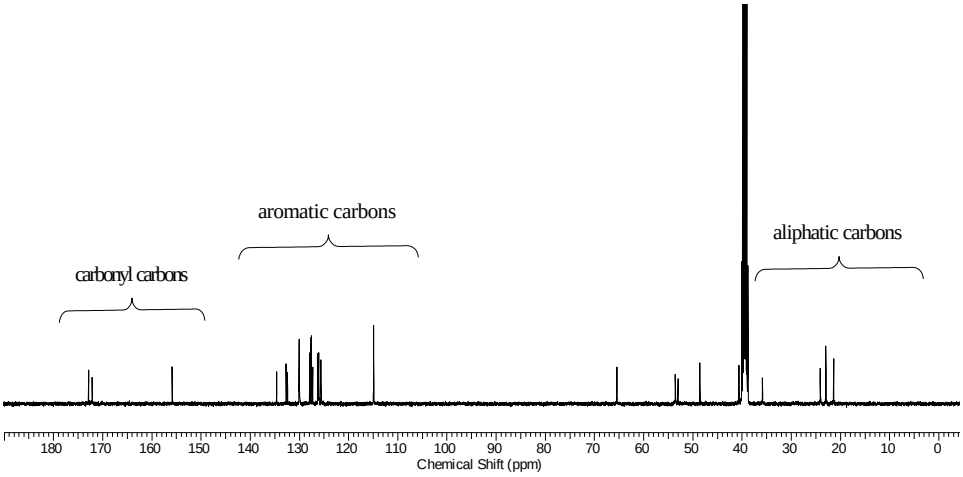

Figure 6.8. *100 MHz ^{13}C NMR spectrum of **1** in DMSO-d_6.*

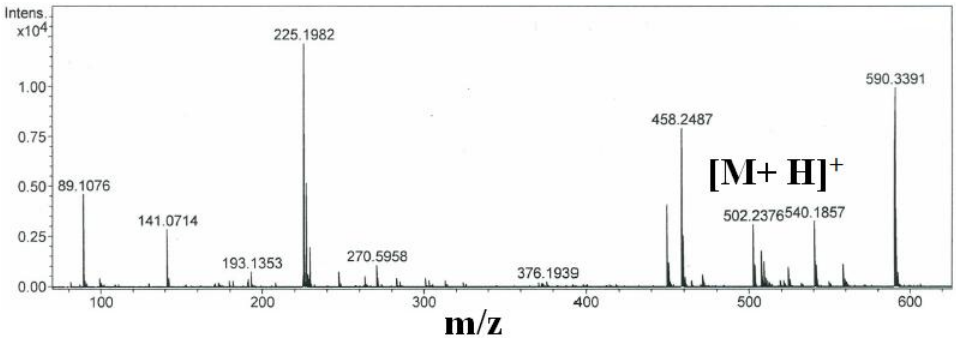

Figure 6.9. *ESI-MS spectrum of* ***1****.*

*6.2.2 Synthesis of Compound **2***:

a) Synthesis of Nmoc-Leu-Tyr-OCH_3 **7:** A solution of Nmoc-L **5** (0.958 g, 3 mmol) and HOBt (0.405 g, 3 mmol) was stirred in 2 mL of DMF. A neutralized solution of tyrosine methyl ester (1.17 g, 6 mmol) was extracted from its corresponding hydrochloride salt and concentrated to add to the reaction mixture followed by DCC (0.639 g, 3.1 mmol) at 0 °C. The mixture was allowed to stir at room temperature for 12 h. The mixture was diluted with ethyl acetate and organic layer was washed with 1 M HCl (2 x 30 mL), brine solution, 1 M Na_2CO_3 (3 x 30 mL) and brine solution. The ethyl acetate layer was dried over Na_2SO_4 and evaporated under vacuum to yield **7** white solid product. Purification was done by silica gel column (100-200 mesh) using chloroform- methanol as eluent.
Yield = 1.39 g (2.8 mmol, 93.33 %); $[\alpha]_D^{25}$ = -13 (*c* = 1, MeOH); FT-IR (KBr): 3313 (br), 3057(ms), 2955 (s), 2869 (ms), 17 39 (ms), 1706 (ms), 1658 (s), 1616 (ms), 1515 (s), 1443 (ms), 1365 (ms), 1227 (s) cm^{-1}; ^1H NMR (400 MHz, $CDCl_3$): δ 7.62 (d, 4H, Nph), 7.27 (d, 3H, Nph), 7.25 (d, 1H, NH), 7.05 (s, 1H, NH), 6.69 (d, 2H, *J* = 7.28 Hz, Tyr), 6.44 (d, 2H, *J* = 8.04 Hz, Tyr), 5.04 (s, 2H, CH_2 of Nph), 4.60 (m, 1H, C^{α} H of Tyr), 3.99 (m, 1H, C^{α}H of Leu), 3.50 (s, 3H, OCH_3), 2.83 (d, 1H, C^{β}H of Tyr), 2.78 (d, 1H, C^{β}H of Tyr), 1.39 (m, 1H, C^{γ}H of Leu), 1.11-1.04 (m, 2H, C^{β}Hs of Leu), 0.69 (d, 6H, J= 5.04 Hz, C^{δ} Hs of Leu); MS (ESI) m/z for $C_{28}H_{32}N_2O_6$ $(M+Na)^+$ calcd.: 515.2158, found: 515.2090; Elemental

Analysis calculated for $C_{28}H_{32}N_2O_6$: C, 68.28; H, 6.55; N, 5. 69; Found: C, 66.98; H, 6.77; N, 5.81.

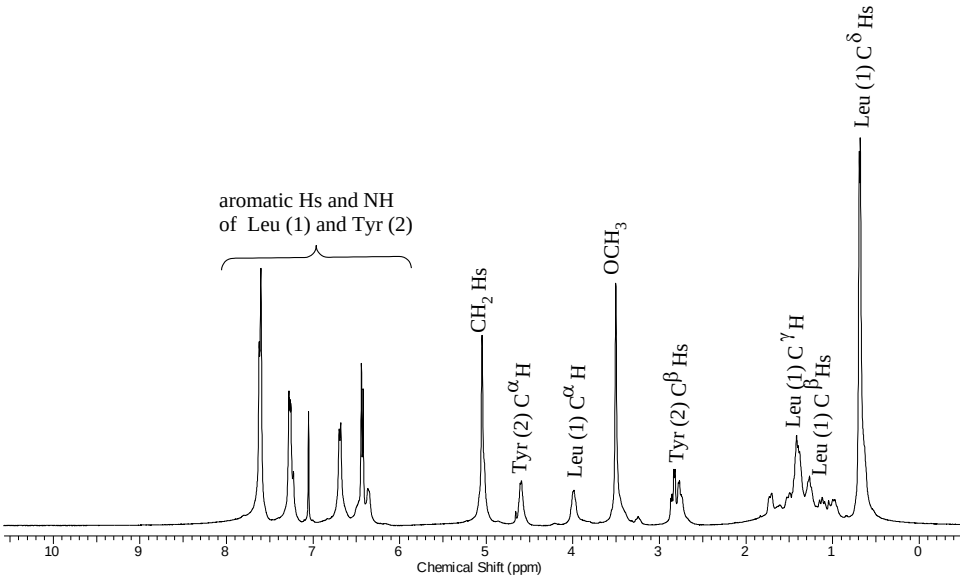

Figure 6.10. *400 MHz ^1H NMR spectrum of **7** in $CDCl_3$.*

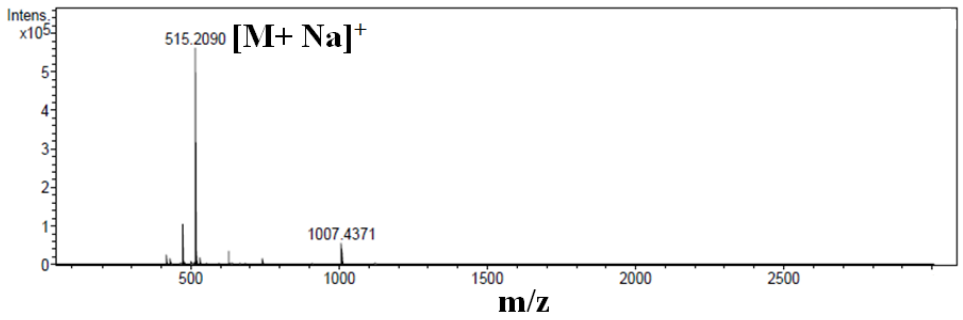

Figure 6.11. *ESI-MS spectrum of **7**.*

b) Synthesis of Nmoc-Leu-Tyr-OH **2:** A solution of Nmoc-LY-OCH_3 **7** (0.950 g, 1.9 mmol) in 100 mL of dry MeOH was allowed to react with a solution of 2M NaOH. The progress of the reaction was monitored by thin layer chromatography (TLC). The reaction mixture was stirred for 12 h. Then, methanol was removed under vacuum. The residue was taken in 100 mL of water and washed with diethyl ether (2 x 20 mL). The pH of aqueous layer was adjusted to 2 using 2 M HCl and it was extracted with ethyl acetate (3 x 30 mL). The ethyl acetate layer was dried over

anhydrous sodium sulfate and evaporated in vacuum to yield **2** as white solid.

Yield =0.788 g (1.6 mmol, 84.21 %); $[\alpha]_D^{25}$ = -3 (*c* = 1, MeOH); FT-IR (KBr): 3318 (br), 3058(ms), 2958 (s), 1711 (s), 1658 (s), 1515 (s), 1445 (ms), 1364 (ms), 1336 (ms), 1235 (s) cm^{-1}; ^1H NMR (400 MHz, DMSO-d_6): δ 9.14 (s, 1H), 7.92 (d, 1H, J= 7.8 Hz, Nph), 7.83 (t, 3H, Nph), 7.46 (t, 3H, Nph), 7.42 (d, 1H, *J* = 8.52 Hz, NH), 7.37 (d, 1H, *J* = 8.52 Hz, NH), 6.94 (d, 2H, *J* = 8.28 Hz, Tyr), 6.58 (d, 2H, *J* = 8.28 Hz, Tyr), 5.12 (s, 2H, CH_2 of Nph). 4.28 (m, 1H, $C^{\alpha}H$ of Tyr), 4.00 (m, 1H, $C^{\alpha}H$ of Leu), 2.84 (d, 1H, $C^{\beta}H$ of Tyr), 2.74 (d, 1H, $C^{\beta}H$ of Tyr), 1.52 (m, 1H, $C^{\gamma}H$ of Leu), 1.33 (d, 2H, $C^{\beta}Hs$ of Leu), 0.78 (d, 6H, *J*= 4 Hz, $C^{\delta}Hs$ of Leu); ^{13}C NMR (100 MHz, DMSO-d_6): δ 172.8, 172.1, 155.8, 134.6, 132.4, 130.6, 127.9, 127.6, 127.5, 126.2, 125.6, 114.9, 65.45, 53.57, 53.03, 48.56, 35.86, 24.10, 22.96, 21.39; MS (ESI) m/z for $C_{27}H_{30}N_2O_6$ $(M+Na)^+$ calcd.: 501.2002, found: 501.1873; Elemental Analysis calculated for $C_{27}H_{30}N_2O_6$: C, 67.77; H, 6.32; N, 5. 85; Found: C, 65.39; H, 6.70; N, 5.72.

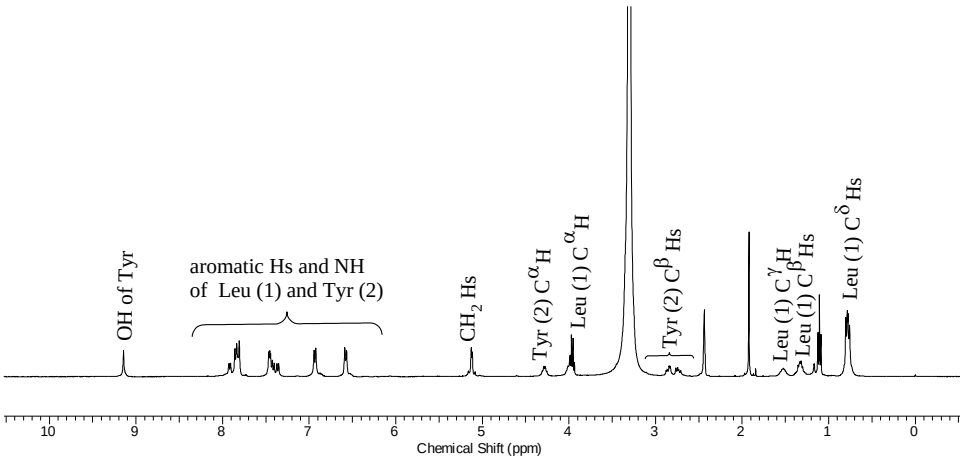

Figure 6.12. *400 MHz ^1H NMR spectrum of **2** in DMSO-d_6.*

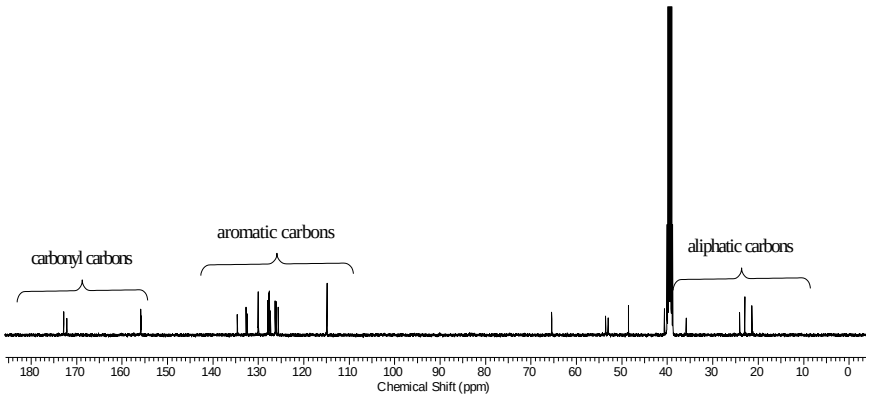

Figure 6.13. *100 MHz ^{13}C NMR spectrum of **2** in DMSO-d_6.*

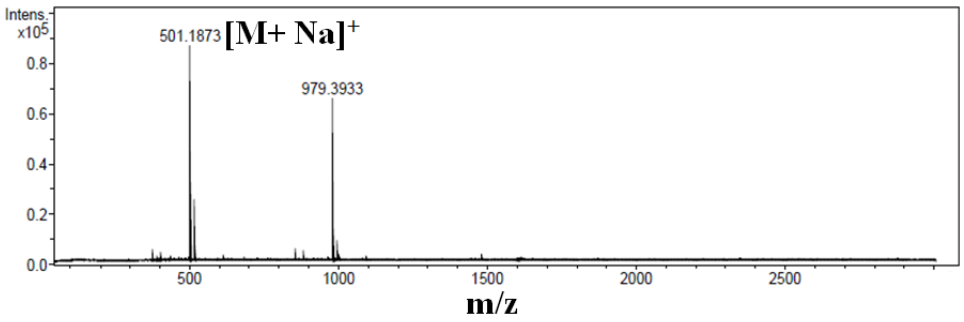

Figure 6.14. *ESI-MS spectrum of **2**.*

*6.2.3 Synthesis of Compound **3**:*

a) Synthesis of Nmoc-Tyr-OH **8:** A solution of Tyrosine (0.724 g, 4 mmol) in a mixture of 1,4 dioxane (10 mL) and 1M sodium hydroxide (13 mL) was stirred and cooled in an ice-water bath. Naphthalene-2-methoxychloroformate **4** (0.882 g, 4 mmol) was added and stirring was continued at room temperature for 12 h. Reaction mixture was diluted with 200 mL of water and dioxane was evaporated under vaccum. Aqueous layer was washed with diethyl ether and the pH of aqueous layer was adjusted to 2 with 2N hydrochloric acid. The aqueous phase was extracted with ethyl acetate (3 x 50 mL) and dried over Na_2SO_4. The organic layer was concentrated under vacuum to give **8** as colorless oil.

Yield= 1.124 g (3 mmol, 75 %). $[\alpha]_D^{25}$ = -7 (c = 1, MeOH); FT-IR (KBr): 3331 (br), 3055 (br), 2928 (ms), 1709 (s), 1612 (ms), 1513 (s), 1445 (s), 1367 (ms), 1336 (ms), 1225 (s) cm^{-1}; ^1H NMR (400 MHz, DMSO-d_6): δ

7.73 (d, 4H), 7.38 (d, 3H, Nph), 7.32 (d, 1H, NH), 6.86 (d, 2H, *J* = 8.04 Hz, Tyr), 6.57 (d, 2H, *J*= 8.04 Hz, Tyr), 5.17 (s, 2H, CH_2 of Nph), 4.57 (m, 1H, C^{α} H of Tyr), 2.95 (d, 2H, C^{β} Hs of Tyr) ppm; MS (ESI) m/z for $C_{21}H_{19}NO_5$ $(M+H)^+$ calcd.: 366.1341 found: 366.4134; Elemental Analysis calculated for $C_{21}H_{19}NO_5$: C, 69.03; H, 5.24; N, 3.83; Found: C, 66.53; H, 5.46, N, 3.32.

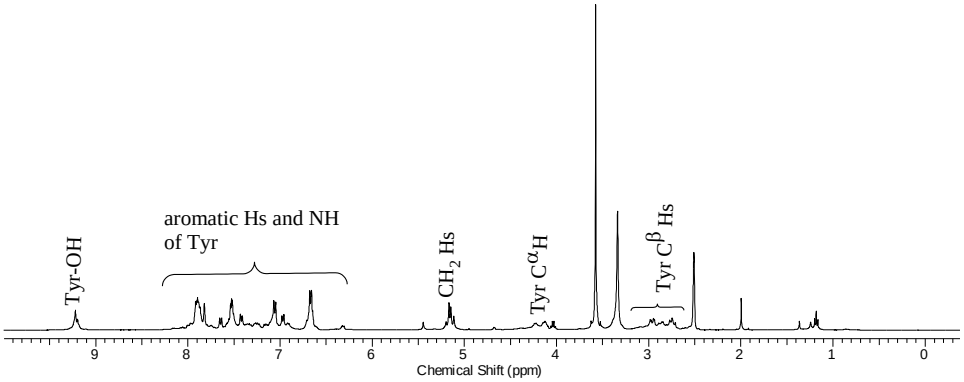

Figure 6.15. *400 MHz ^{1}H NMR spectrum of **8** in DMSO-d_6.*

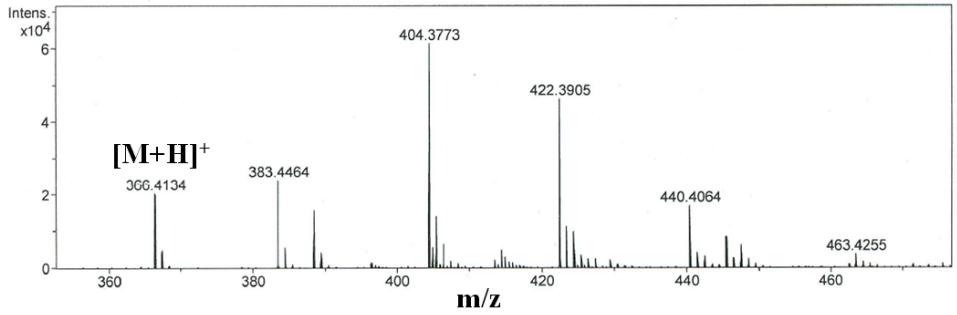

Figure 6.16. *ESI-MS spectrum of **8.***

b) Synthesis of Nmoc-Tyr-Trp-OCH_3 **9:** A solution of Nmoc-Y **8** (0.642 g, 1.75 mmol) and HOBt (0. 236 g, 1.75 mmol) was stirred in 2 mL of DMF. A neutralized solution of tryptophan methyl ester (0.889 g, 3.5 mmol) was extracted from its corresponding hydrochloride salt and concentrated to add to the reaction mixture followed by DCC (0.371 g, 1.77 mmol) at 0 °C. The mixture was allowed to stir at room temperature for 12 h. The mixture was diluted with ethyl acetate and organic layer was washed with 1 M HCl (2 x 30 mL), brine solution, 1 M Na_2CO_3 (3 x 30

mL) and brine solution. The ethyl acetate layer was dried over Na_2SO_4 and evaporated under vacuum to yield **9** as white solid product. Purification was done by silica gel column (100-200 mesh) using chloroform-methanol as eluent.

Yield = 0.500 g (0.88 mmol, 50.28 %). $[\alpha]_D^{25}$ = -18 (*c* = 1, MeOH); FT-IR (KBr): 3345(br), 3055(ms), 2951(s), 2852 (ms), 1729 (s), 1661 (s), 1515 (s), 1440 (ms), 1358 (ms), 1223 (s) cm^{-1}; ^1H NMR (400 MHz, $CDCl_3$): δ 8.46 (s, 1H), 8.87 (s, 1H), 7.75 (d, 4H, Nph), 7.69 (s, 1H, Nph), 7.42 (m, 2H, Nph), 7.31(d, 1H, *J* = 8 Hz), 7.16 (d, 2H, *J*= 9.04 Hz), 7.05 (t, 1H, Trp), 6.96 (t, 1H, Trp), 6.90 (d, 2H, *J*= 7.28 Hz), 6.68 (s, 1H, Trp), 6.16 (d, 2H, *J*= 7.52 Hz), 5.12 (s, CH_2 of Nph), 4.75 (m, 1H, $C^{\alpha}H$ of Trp), 4.27 (m, 1H, $C^{\alpha}H$ of Tyr), 3.54 (s, 3H, OCH_3), 3.15 (d, 2H, $C^{\beta}Hs$ of Trp), 2.85 (d, 2H, $C^{\beta}Hs$ of Tyr). MS (ESI) m/z for $C_{33}H_{31}N_3O_6$ $(M+Na)^+$ calcd.: 588.2111, found: 588.2080; Elemental Analysis calculated for $C_{33}H_{31}N_3O_6$: C, 70.07; H, 5.52; N, 7. 43; Found: C, 65.89; H, 5.28; N, 7.75.

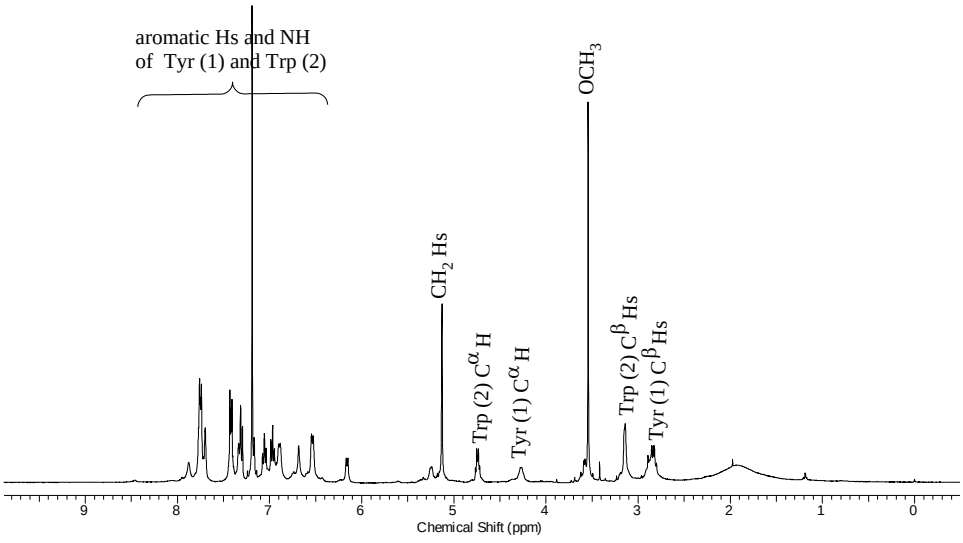

Figure 6.17. *400 MHz ^1H NMR spectrum of **9** in $CDCl_3$.*

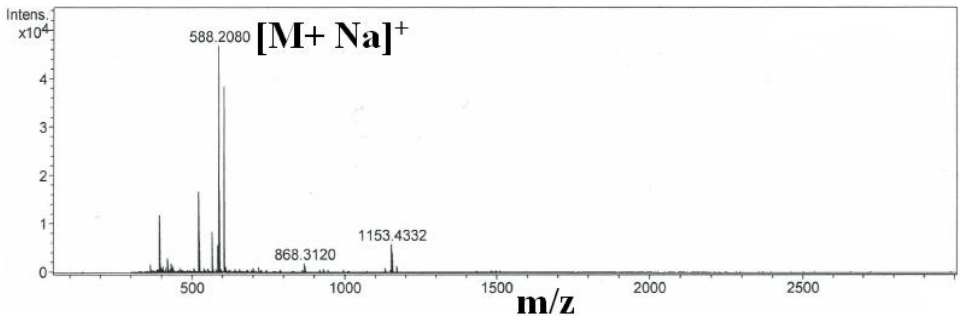

Figure 6.18. *ESI-MS spectrum of* ***9.***

c) Synthesis of Nmoc-Tyr-Trp-OH **3:** A solution of Nmoc-YW-OCH_3 (0.450 g, 0.79 mmol) in 100 mL of dry MeOH was allowed to react with a solution of 2 M NaOH. The progress of the reaction was monitored by thin layer chromatography (TLC). The reaction mixture was stirred for 12 h. Then, methanol was removed under vacuum. The residue was taken in 100 mL of water and washed with diethyl ether (2 x 20 mL). The pH of aqueous layer was adjusted to 2 using 2 M HCl and it was extracted with ethyl acetate (3 x 30 mL).The ethyl acetate layer was dried over anhydrous sodium sulfate and evaporated in vacuum to yield **3** as white solid.

Yield = 0.401 g (0.72 mmol, 91.13 %). $[\alpha]_D^{25}$ = - 6 (*c* = 1, MeOH); FT-IR (KBr): 3390 (br), 3056(ms), 2926 (s), 2854 (m), 1710 (s), 1659 (s), 1515 (s), 1441 (ms), 1358 (ms), 1339 (ms), 1234 (s) cm^{-1}; (400 MHz, DMSO-d_6): δ 10.80 (s, 1H, NH of Trp ring), 9.10 (s, 1H, OH of Tyr), 8.17 (d, 1H, J = 7.52 Hz), 7.82 (d, 4H, Nph), 7.71 (s, 1H, Nph), 7.45 (d, 2H, Nph), 7.38 (d, 1H, *J* =8.56 Hz, NH), 7.28 (m, 2H, *J* = 8.56 Hz, Trp), 7.11 (d, 1H, Trp), 6.99 (d, 2H, *J* = 8.28 Hz, Tyr), 6.91 (t, 1H, Trp), 6.75 (d, 1H, *J* = 8.28 Hz, Trp), 6.56 (d, 2H, *J* = 8.52 Hz, Tyr), 5.04 (s, 2H, CH_2 of Nph), 4.43 (m, 1H, $C^{\alpha}H$ of Trp), 4.17 (m, 1H, $C^{\alpha}H$ of Tyr), 3.12 (m, 1H, $C^{\beta}H$ of Trp), 3.01 (m, 1H, $C^{\beta}H$ of Trp), 2.82 (m, 2H, $C^{\beta}Hs$ of Tyr). (100 MHz, DMSO-d_6): δ 172.85, 172.13, 155.88, 155.82, 134.63, 132.69, 132.42, 130.04, 127.91, 127.65, 127.55, 127.31, 126.29, 126.10, 126.06, 125.63, 114.90, 65.45, 53.57, 53.03, 48.56, 40.46, 35.88, 24.10, 22.96, 21.39. MS (ESI) m/z for $C_{32}H_{29}N_3O_6$ $(M+Na)^+$ calcd.: 574.1854, found: 574.1865. ;

Elemental Analysis calculated for $C_{32}H_{29}N_3O_6$: C, 69.68; H, 5.30; N, 7.62; Found: C, 66.53; H, 5.57; N, 7.47.

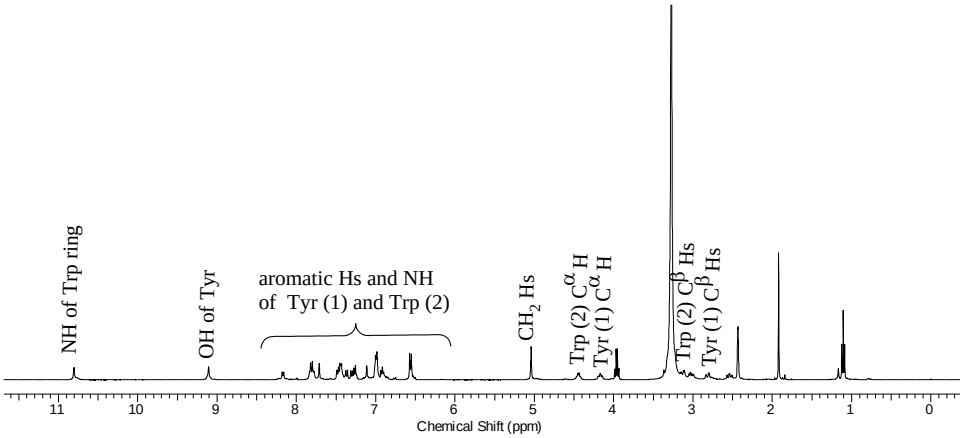

Figure 6.19. *400 MHz ^{1}H NMR spectrum of **3** in DMSO-d_6.*

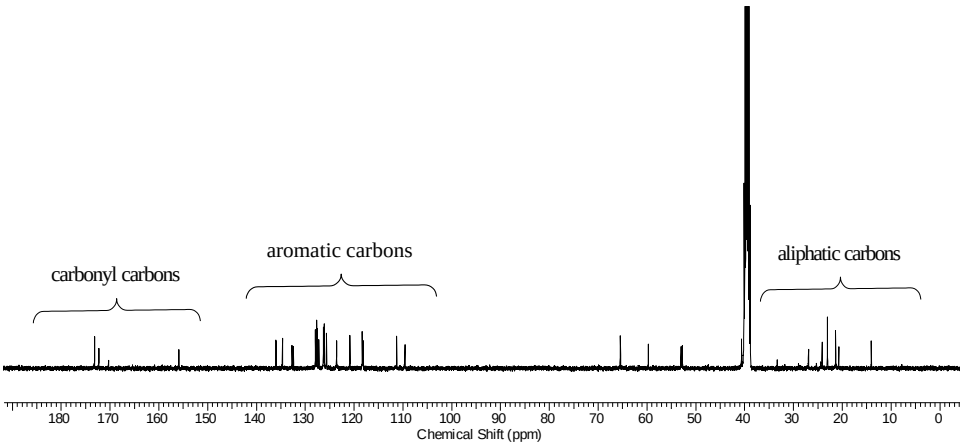

Figure 6.20. *100 MHz ^{13}C NMR spectrum of **3** in DMSO-d_6.*

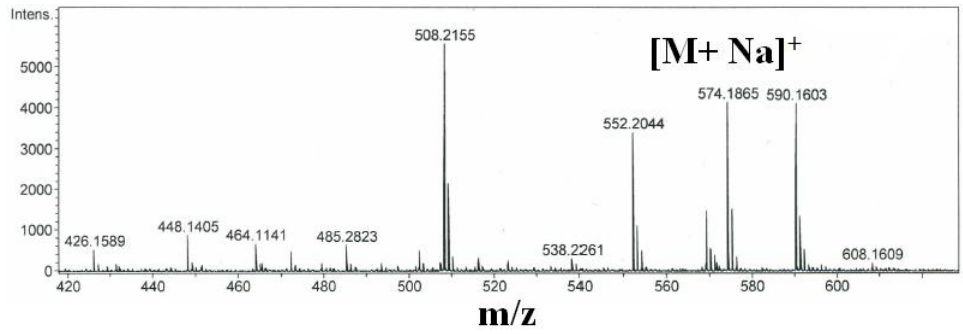

Figure 6.21. *ESI-MS spectrum of **3**.*

6.3 Hydrogel Preparation and Characterization Techniques

6.3.1 Hydrogel Preparation

The Nmoc-LW (20 mmol/L, 20.04 mg) and *p*-hydroxybenzyl alcohol (80 mmol/L, 19.84 mg) were dissolved in 2 mL of water at higher pH by adding 0.5 M sodium hydroxide and pH was adjusted to 7.4 by adding 0.1 M hydrochloric acid followed by 0.5 mg/mL *candida rugosa* lipase (CRL). The resulting colorless solution was incubated at 37 °C for 24 h.

6.3.2 ^{1}H NMR Spectroscopy

All NMR spectra were recorded at 400 MHz Bruker AV 400 NMR spectrometer. TMS was used an internal reference in the NMR spectra. Peptides concentrations were in the range of 1-10 mmol in $(CD_3)_2SO$ and $CDCl_3$.

6.3.3 Mass Spectrometry

Mass spectra of peptides were recorded on Bruker micrOTOF-Q II by positive and negative mode electrospray ionizations.

6.3.4 High Performance Liquid Chromatograpy (HPLC) Analysis

A Dionex HPLC-Ultimate 3000 (High Performance Liquid Chromatography) pump was used to analyse products. A 20 µL of sample was injected onto a Dionex Acclaim ® 120 C18 column of 250 mm length with an internal diameter of 4.6 mm and 5 µm fused silica particles at a flow rate of 1 mL min^{-1} (linear gradient of 40 % v/v acetonitrile in water for 35 min, gradually rising to 100 % (v/v) acetonitrile in water at 35 min). This concentration was kept constant until 40 min when the gradient was

decreased to 40 % (v/v) acetonitrile in water at 42 min. The sample preparation involved mixing of 100 µL gel in 900 µL acetonitrile-water (50: 50 mixture) solution containing 0.1 % trifluroacetic acid. The samples were then filtered through a 0.45 µm syringe filter (Whatman, 150 units, 13 mm diameter, 2.7 mm pore size) prior to injection. The products were identified by using Ultimate 3000 RS Variable Wavelength Detector at 280 nm.

6.3.5 Rheology

Rheological study was performed to determine the mechanical properties of hydrogels. These properties were assessed using an Anton Paar Physica Rheometer (MCR 301, Austria) with cone plate geometry (20 mm in diameter, 50 µm gap and 1° angle) and temperature was controlled at 25 °C. The dynamic moduli of the hydrogel were measured as a function of frequency in the range of 0.1-100 rad s^{-1} with a constant strain value 0.01 %. To determine the exact strain for frequency sweep experiments, the linear viscoelastic (LVE) regime was performed at constant frequency of 10 rad s^{-1}. Experimental data was acquired in thrice and the average data is shown. 200 µL of gel was prepared in glass vial and transferred it over the plate using microspatula to proceed for rheological measurements.

6.3.6 UV-Vis Spectroscopy

UV-vis absorption spectrum of the hydrogel **1** was recorded using a Varian Cary100 Bio UV-Vis spectrophotometer at a concentration of 20 mmol L^{-1}. Similarly, UV-vis absorption spectra of Nmoc-LW acids and *p*-hydroxybenzyl alcohol were recorded at concentration of 20 mmol L^{-1}.

6.3.7 Fluorescence Spectroscopy

Fluorescence emission spectra of hydrogel (20 mmol L^{-1}) as well as solution of Nmoc-LW and *p*-hydroxy benzyl alcohol were recorded at

different excitation wavelength 280 nm and 365 nm with medium sensitivity on a Horiba Scientific Fluoromax-4 spectrophotometer. The slit width for the excitation and emission was set at 2 nm and a 1 nm data pitch. Samples were prepared in 1 cm^2 quartz cuvette at room temperature.

6.3.8 Circular Dichroism

Circular dichroism (CD) spectra were measured at 25 °C on a Jasco J-815 spectropolarimeter. Spectra were measured between 300 and 190 nm with a data pitch of 0.1 nm. The bandwidth was set to 1 nm with a scanning speed of 20 nm min^{-1} and a response time of 1 s. The path length was 1 mm quartz cell. Samples were prepared at a concentration of 2 mmol/L. Experimental data were acquired in thrice and the average data is shown.

6.3.9 Time Correlated Single Photon Counting Spectroscopy

2 mL gel was prepared in a 1 cm^2 quartz cuvette and time resolved studies were done by a time correlated single photon counting (TCSPC) system from Horiba Yovin (Model: Fluorocube-01-NL). Samples were excited at 376 nm using a picosecond diode laser (Model: Pico Brite-375L). The signals were collected at magic angle (54.70) polarization using a photomultiplier tube (TBX-07C) as detector, which has a dark counts less than 20 cps. The instrument response function was typically 140 ps. The data analysis was performed using IBH DAS (version 6, HORIBA Scientific, Edison, NJ) decay analysis software.

The amplitude-weighted lifetime was estimated by

$$\langle \tau \rangle = \sum_{i=1}^{n} a_i \, \tau_i$$

where τ_1 is the fluorescence lifetime of various fluorescent species and the a_1 normalized pre-exponential factors. To gain the best fitting in all cases the χ^2 was kept near to unity.

6.3.10 Microscopic Techniques

Transmission electron microscopic images were taken using a PHILIPS electron microscope (model: CM 200), operated at an accelerating voltage of 200 kV. Dilute solution of the hydrogel was dried on carbon-coated copper grids (300 mesh) by slow evaporation in air and then allowed to dry separately under vacuum at room temperature.

The morphology of gels was investigated using tapping mode atomic force microscope (AFM). AFM study was done by placing very dilute solution of gel (200 µL of gel was dissolved in 800 µL of milli-Q water) on mica and allowed it dry in air for 2 days at room temperature. Images were recorded by using scanning probe microscope AIST-NT instrument (model: Smart SPM-1000).

Fluorescence Microscopy experiments were performed on a home-built epifluorescence microscopy setup. An air-cooled argon ion laser (Melles Griot, model 400-A03) with excitation wavelength of 457 nm was used to excite the hydrogel sample placed on an inverted microscope (Nikon, model Eclipse Ti-U). The images were analyzed with ImageJ (Version 1.46r) NIH. Dilute solution of the hydrogel was spin coated over glass cover slip before analysis.

6.4 Results and Discussion

6.4.1 Self-assembly

In this chapter, we exploit CRL for the inclusion of HBA regioselectively in the Nmoc based peptides via ester bond formation. Supramolecular chemistry presents the ability to drive the chemical processes reversibly through covalent and non-covalent interactions that evolve the stable entities under the pressure of self-organization.[15] Keeping this idea in mind, we forced reverse ester hydrolysis of Nmoc-dipeptide with HBA

using CRL in aqueous medium at physiological pH 7.4. We have successfully synthesized three dipeptides bearing N-terminal hydrophobic aromatic naphthalene-2-methoxy carbonyl moiety. The peptide Nmoc-LW **1** (20 mmol/L, 20.04 mg) (L: Leucine, W = Tryptophan) and *p*-hydroxybenzyl alcohol (HBA, 80 mmol/L, 19.84 mg) were dissolved in 2 mL of water at higher pH by adding 0.5 M sodium hydroxide. The pH was adjusted to 7.4 by adding 0.1 M hydrochloric acid followed by 0.5 mg/mL CRL. The resulting colorless solution was incubated at 37 °C for 24 h. The HPLC analysis showed 24% conversion of Nmoc-LW-HBA ester at 24 h upon enzyme treatment. However, the colorless solution turned to light pink, which later turned to dark pink self-supporting hydrogel when the conversion reached to 57% after 8 days (Figure 6.23B).

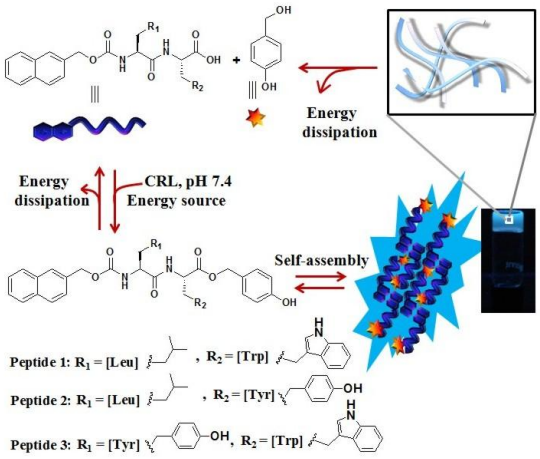

Figure 6.22. *Schematic representation of lipase (CRL) catalysed regioselective inclusion of HBA to Nmoc-peptides in aqueous medium. Lipase is used as a source of energy for the reaction cycle of the dissipative system. The corresponding ester evolves into a blue light emitting material upon the self-assembly process at pH 7.4.*

6.4.2 High Performance Liquide Chromatograpy (HPLC) Study

The self-assembly of small peptides bearing N-terminal hydrophobic moieties has been reported by several groups.[16] The HPLC kinetics showed that initial rate of esterification was faster which was relatively

slow after 8 days of enzyme reaction. The 91% conversion was observed after 28 days of enzyme reaction. The dipeptides Nmoc-LY **2** and Nmoc-YW **3** were unable to form self-supporting hydrogel. Moreover, the HPLC analysis showed poor conversion of Nmoc-LY-HBA (12.48 %) and Nmoc-YW-HBA (20 %) (Figure 6.24 A and B). The exceptional activity and higher yield by CRL towards regioselective incorporation of HBA to Nmoc-LW **1** in aqueous medium is driven by supramolecular ordering of peptides. In general, lipase favors ester hydrolysis reactions instead of esterification reactions in aqueous medium. This may be the reason for the poor yielding of esterification reactions of HBA with non-assembling peptides Nmoc-LY **2** and Nmoc-YW **3**.

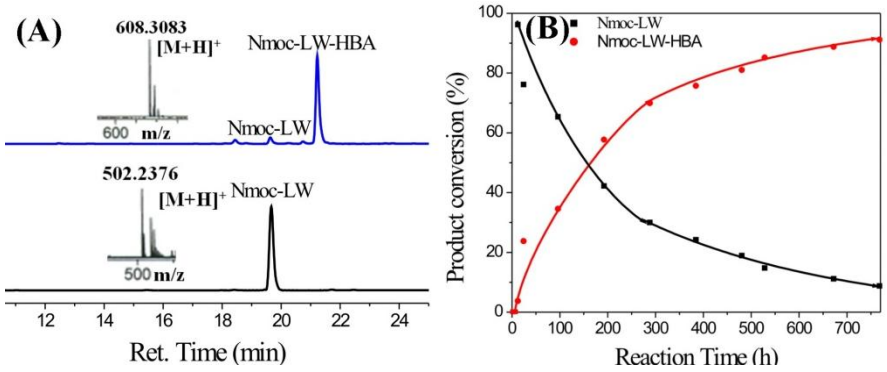

Figure 6.23. *(A) HPLC trace analysis of enzyme catalyzed esterification of Nmoc-LW **1** to Nmoc-LW-HBA with its corresponding ESI-MS. (B) Real time HPLC analysis for the formation of Nmoc-LW-HBA.*

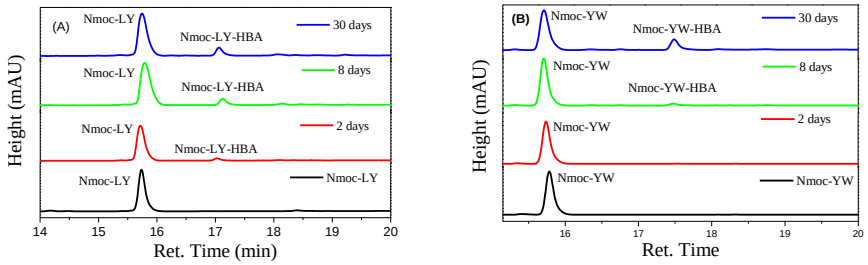

Figure 6.24. A) *HPLC chromatograms exihibit formation of Nmoc-LY-HBA from Nmoc-LY **2** upon lipase catalyzed inclusion of Gastrodigenin at different time B) Nmoc-YW-HBA from Nmoc-YW **3** upon lipase catalyzed inclusion of Gastrodigenin at different time.*

The chemically incorporation of HBA to Nmoc-peptides is quite difficult due to the presence of two hydroxyl groups on HBA which leads to the mixture of two products. Moreover, chemical incorporation of HBA with Nmoc-protected dipeptide having hydrophobic amino acids gives direct esterifies products which are poor soluble in aqueous medium. Hence, the biocatalytic method is more promising and highly selective. The CRL is an ideal biocatalyst that allows regioselective incorporation of HBA to Nmoc-LW **1** peptide in aqueous medium. The benzylic hydroxyl group of HBA is linked to carboxylic acid of Nmoc-LW *via* esterification reaction upon treatment with CRL. The CRL catalyzed regioselective ester product was confirmed by ^{1}H NMR which is further supported by ESI-MS and HPLC (Figure 6.25 and 6.23A).

Table 6.1. *Lipase catalyzed formation of peptide esters in aqueous medium*

Entry	Substrate [20 mmol L^{-1}]	HBA[a] [80 mmol L^{-1}]	Enzyme[b] [0.5 mg/mL]	Product Yield[c] [%]	Physical Characteristics[d]
1.	Nmoc-LW	HBA	CRL	91.29	G
2.	Nmoc-LY	HBA	CRL	12.48	S
3.	Nmoc-YW	HBA	CRL	19.66	S

[a]HBA = *p*-hydroxybenzyl alcohol, [b]Enzyme = Lipase from Candida Rugosa, [c]Analysed after 30 days, [d]G = gelation and S= solution

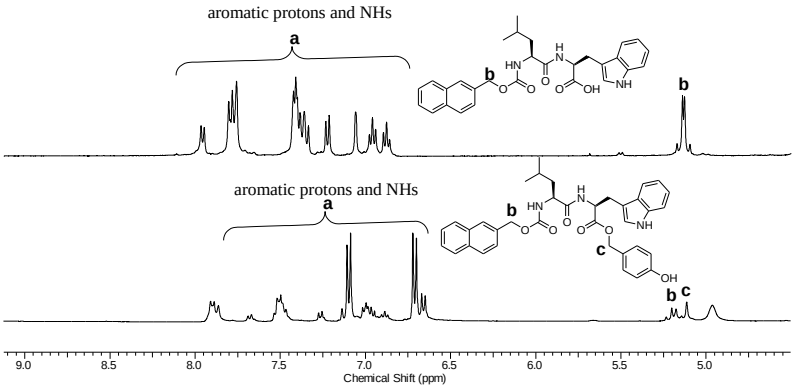

Figure 6.25. *^{1}H NMR of Nmoc-LW **1** and its corresponding Nmoc-LW-HBA synthesized via CRL catalyzed esterification reaction.*

6.4.3 Rheological Study

The flow behavior and rigidity of self-supporting hydrogel formed by Nmoc-LW-HBA ester was investigated by their rheological properties (Figure 6.26A and B). To evaluate the storage modulus (G') and loss modulus (G''), a typical frequency sweep experiment was carried out. The frequency sweep data shows that G' is higher than that of G'', which is an indication of viscoelastic nature of hydrogel. The viscoelastic nature of hydrogel **1** can be ascribed from the supramolecular ordering of peptide molecules in aqueous medium.

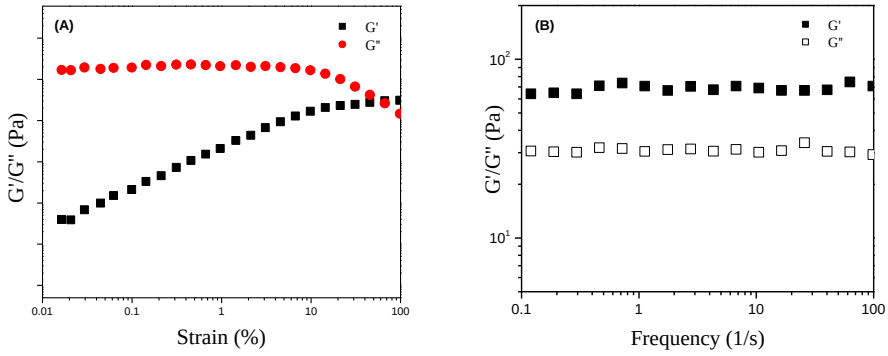

Figure 6.26. *A) Rheological measurement of LVE at constant frequency 10 rad* s^{-1} *B) Dynamic frequency sweep of Nmoc-LW-HBA hydrogel* ***1*** *at constant strain 0.01%.*

6.4.4 Circular Dichroism Study

The supramolecular ordering of peptides is driven by various non-covalent interactions including hydrogen bonding and π-π stacking interactions.[17] Circular dichroism spectra of the solution of Nmoc-LW **1** and corresponding gel Nmoc-LW-HBA help to evaluate the supramolecular ordering of **1a** in gel phase. The CD spectrum of Nmoc-LW-HBA ester hydrogel shows negative band near 193 nm and a positive band near 216 nm which are attributed from $\pi \rightarrow \pi^*$ and $n \rightarrow \pi^*$ transition of the CONH groups of the peptide backbone (Figure 6.27). The intense negative peak at

193 nm indicates the existence turn-type β-sheet conformation in hydrogel state.[18]

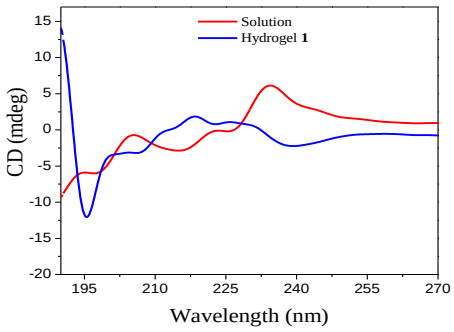

Figure 6.27. *CD spectrum of solution of Nmoc-LW* ***1*** *with HBA and hydrogel of Nmoc-LW-HBA.*

6.4.5 UV-Vis and Fluorescence Spectroscopic Study

The UV-vis and fluorescence study were performed to evaluate the supramolecular ordering of self-assembled hydrogel. The UV-vis spectra of HBA and Nmoc-LW **1** in aqueous solutions were recorded at 20 mmol L^{-1} concentration. Both the solutions exhibit UV-vis absorption spectra in the range of 250 to 300 nm (Figure 6.28A). However, UV-vis absorption spectrum of Nmoc-LW-HBA exhibits a broad peak at 372 nm along with a broad peak near 220-300 nm (Figure 6.28B).

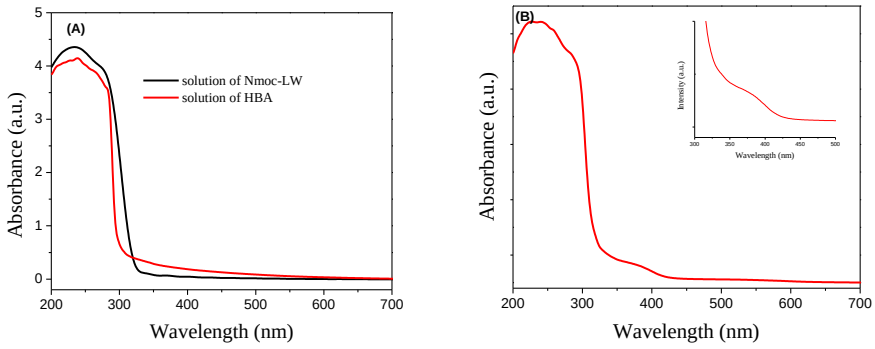

Figure 6.28. *A) Absorption spectra of Nmoc-LW and p-hydroxybenzyl alcohol in aqueous medium B) UV-vis absorption spectra of hydrogel* ***1*** *at 20 mmol* L^{-1} *concentration.*

The higher red shift in UV-vis spectrum is due to the self-organization of gelator molecules in hydrogel state. The self-supporting Nmoc-LW-HBA hydrogel emits blue fluorescence upon exposure to UV light (illuminated at 365 nm) (Figure 6.29). Self-assembly of Nmoc-LW-HBA was observed upon gradual conversion of Nmoc-LW **1** to Nmoc-LW-HBA via CRL catalyzed esterification reaction. The self-assembled dark pink hydrogel under day light showed bright blue fluorescence under UV light which is further examined by steady state fluorescence spectroscopy (Figure 6.30, 6.31).

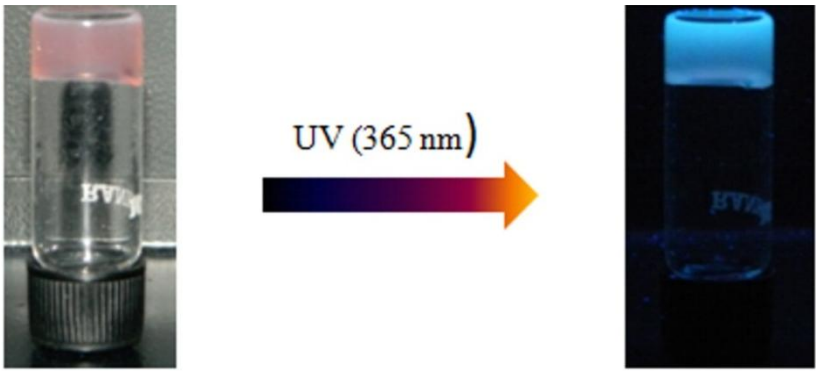

Figure 6.29. *Optical images of hydrogel Nmoc-LW-HBA 1 under day light and under UV light (365 nm).*

The self-assembled Nmoc-LW-HBA peptide is composed of three fluorophore moieties. In general, the assembled naphthalene double ring emits at 320 nm to 350 nm upon excitation at 280 nm.[19] However, the tryptophan moiety emits in the range of 300 nm to 350 nm, which depends upon the micro-environments. In this case, emission spectra were recorded upon excitation at 280 nm based on UV-vis absorption spectra. The emission maxima exhibit at 350 nm for the solution of Nmoc-LW with HBA, a characteristics peak of tryptophan and naphthalene chromophores. To further confirm the individual emission of HBA and Nmoc-LW solutions, emission spectra were recorded upon excitation at 280 nm.

HBA gives emission at 305 nm whereas Nmoc-LW **1** exhibits emission at 354 nm (Figure 6.30A) However, upon excitation at 280 nm, the self-assembled Nmoc-LW-HBA hydrogel shows a strong emission at 455 nm. While excitation at 365 nm, the hydrogel gives emission at 470 nm (Figure 6.30B).

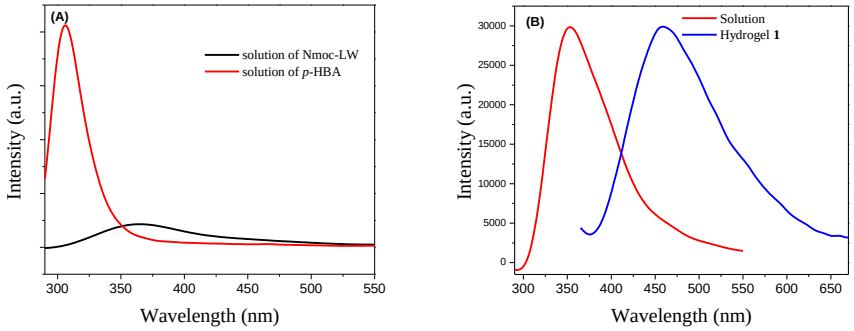

Figure 6.30. *A) Emission spectra of Nmoc-LW and p-hydroxybenzyl alcohol in aqueous medium B) Normalized emission spectra of solution of Nmoc-LW* ***1*** *with HBA (λ_{ex} = 280 nm) and hydrogel formed by Nmoc-LW-HBA (λ_{ex} = 365 nm).*

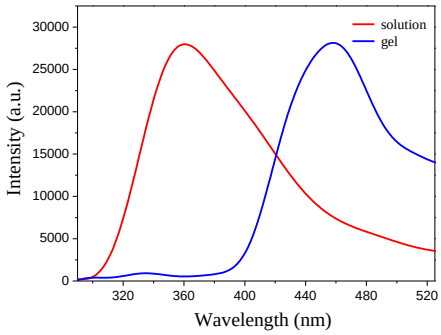

Figure 6.31. *Normalized emission spectra of solution of Nmoc-LW* ***1*** *with HBA (λ_{ex} = 280 nm) and hydrogel formed by Nmoc-LW-HBA (λ_{ex} = 280 nm).*

This happens due to strong π-π stacking interactions of the aromatic fluorophores in gel phase. The observed significant red shift of emission maxima is attributed from the strong supramolecular ordering of peptide molecules in gel phase. Moreover, the emission peak appeared at 455-470 nm corresponding to blue light in the visible region of electromagnetic spectrum.

6.4.6 Time Correlated Single Photon Counting Spectroscopic Study

The time resolved fluorescence study was acquired using our time correlated single photon counting (TCSPC) setup (Figure 6.32). The decay curve of Nmoc-LW-HBA hydrogel was recorded to investigate the higher order aggregates in gel phase medium (Table 6.2).

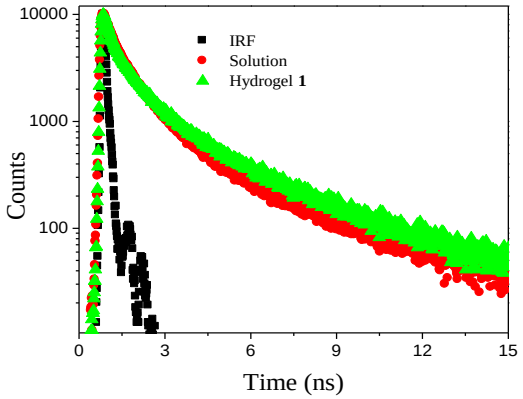

Figure 6.32. *Emission decay curves of solution of* ***1*** *and HBA and corresponding self-assembled hydrogel* ***1*** *monitored at 455 nm (IRF: instrument response function).*

The average lifetime of peptide hydrogel was exhibited as 1.39 ns with lifetime components of 0.84 ns (81%) and 3.77 ns (19%). However, the average lifetime of the solution of Nmoc-LW and HBA is 1.25 ns which shows fast biexponential decay with lifetime components of 0.90 ns (90%) and 4.44 ns (10%). Such difference in decay lifetime is an evidence of non-radiative energy transfer[20] in solution. However, such processes are hampered in self-assembled hydrogel state due to the rigid and close molecular packing through hydrogen bonding and π-π stacking interactions, which results in higher lifetime.

Table 6.2. *Decay parameters for Nmoc-LW and Nmoc-LW-HBA hydrogel.*

Entry	α_1	α_2	τ_1(ns)	τ_2(ns)	τ^a(ns)	χ^2
Nmoc-LW-OH solution	0.90	0.10	0.90	4.44	1.25	1.62
Nmoc-LW-HBA Hydrogel	0.81	0.19	0.84	3.77	1.39	1.49

τ^a The amplitude weighted average lifetime, Normalized amplitude of each component is given by α

6.4.7 Microscopic Study

Transmission electron microscopy (TEM) and atomic force microscopy (AFM) were used to reveal nanostructural morphology of blue light emitting self-assembled hydrogel. As shown in AFM image (Figure 6.33 B), the hydrogel gives interwoven nanofibrous network with average height 7 nm. The transmission electron microscopic study also exhibits the formation of nanofibrillar networks with average diameter 90 nm (Figure 6.33 A). The microscopic studies demonstrate that supramolecular ordering governed by formation of nanofibrillar networks in hydrogel state. Fluorescence microscopic study was carried out to directly visualize the fluorescent properties of self-assembled nanofibers (Figure 6.33C). Fluorescence microscopy image reveals that fluorescent hydrogel is composed of blue light emitting entangled self-assembled nanofibers.[21]

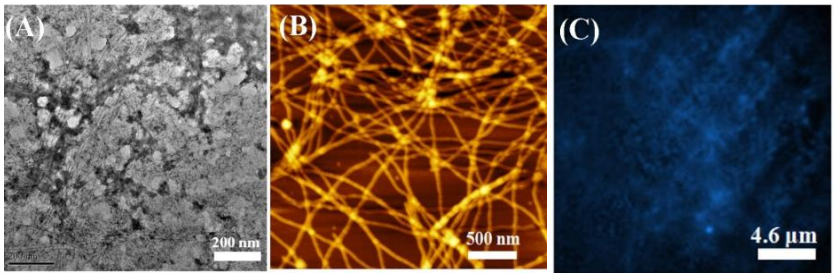

Figure 6.33. *A) TEM image of hydrogel of Nmoc-LW-HBA* ***1*** *indicating nanofibrillar network in gel phase medium. B) AFM image of Nmoc-LW-HBA hydrogel indicating dense nanofibrillar network in gel phase medium. C) Fluorescence microscopy image of gel at 2 mmol* L^{-1} *concentration.*

6.5 Conclusion

In summary, blue light emitting hydrogel upon bicatalytic incorporation of gastrodigenin (*p*-hydroxybenzyl alcohol, HBA) to a Nmoc-protected dipeptide has been discovered. Besides lipase propensity towards the hydrolysis of ester bonds in aqueous medium, its catalytic activity is exploited in the development of fluorescent peptide nanostructures via esterification reaction. The blue light emitting hydrogel could be an ideal biomaterial for bioimaging and bioanalysis of various cell processes.

6.6 References

1. (a) Matson J. B., Stupp S. I. (2012), Self-assembling peptide scaffolds for regenerative medicine, *Chem. Commun*., 48, 26-33 (DOI: 10.1039/C1CC15551B); (b) Olive A. G., Abdullah N. H., Ziemecka I., Mendes E., Eelkema R. van Esch J. H. (2014) Spatial and Directional Control over Self-Assembly Using Catalytic Micropatterned Surfaces, *Angew. Chem., Int. Ed.*, 53, 4132-4136 (DOI: 10.1002/anie.201310776).
2. Mart R. J., Osborne R. D., Stevens M. M., Ulijn R. V. (2006), Peptide-based stimuli-responsive biomaterials, *Soft Matter*, 2, 822-835 (DOI: 10.1039/B607706D).
3. Williams R. J., Smith A. M., Collins R., Hodson N., Das A. K., Ulijn R. V. (2009), Enzyme-assisted self-assembly under thermodynamic contro, *Nat. Nanotechnol*., 4, 19-24 (DOI: 10.1038/nnano.2008.378).
4. Klajn R., Wesson P. J., Bishop K. J. M., Grzybowski B. A., (2009), Writing Self-Erasing images using metastable nanoparticle "Inks", *Angew. Chem., Int. Ed.*, 48, 7035-7039 (DOI: 10.1002/anie.200901119).
5. Boekhoven J., Brizard A. M., Kowlgi K. N. K., Koper G. J. M., Eelkema R., van Esch J. H. (2010), Dissipative self-assembly of a

molecular gelator by using a chemical fuel, *Angew. Chem., Int. Ed.*, 49, 4825-4828 (DOI: 10.1002/anie.201001511).

6. VijayakumarC., Praveen V., Ajayaghosh A. (2009), RGB emission through controlled donor self-Assembly and modulation of excitation energy transfer: A novel strategy to white-light-emitting organogels, *Adv. Mater*., 21, 2059-2063 (DOI: 10.1002/adma.200802932).
7. Tovar J. D. (2013), Supramolecular construction of optoelectronic biomaterials, Acc. Chem. Res.,46, 1527-1537 (DOI: 10.1021/ar3002969)
8. (a) Gao Y., Zhao F., Wang L., Zhang Y., Xu B. (2010), Small peptide nanofibers as the matrices of molecular hydrogels for mimicking enzymes and enhancing the activity of enzymes, *Chem. Soc. Rev.*, 39, 3425; (b) Williams R. J., Smith A. M., Collins R., Hodson N., Das A. K., Ulijn R. V. (2009), Enzyme-assisted self-assembly under thermodynamic control, *Nature Nanotech.*, 4, 19-24 (DOI:10.1038/nnano.2008.378).
9. (a) Schmid R. D., Verger R. (1998), Lipases: Interfacial enzymes with attractive applications, *Angew. Chem., Int. Ed*. 37, 1608-1633 (DOI: 10.1002/(SICI)1521-3773 19980703)37:12<1608:: AIDANIE1608>3.0.CO;2-V); (b) Naik S., Basu A., Saikia R., Madan B., Paul P., Chaterjee R., Brask J., Svendsen A. (2010), Lipases for use in industrial biocatalysis: Specificity of selected structural groups of lipases, *J. Mol. Catal. B: Enzym.***,** 65, 18-23 (DOI:10.1016/j.molcatb.2010.01.002).
10. Chen B., Liu H., Guo Z., Huang J., Wang M., Xu X., Zheng L. (2011), Lipase-catalyzed esterification of ferulic acid with oleyl alcohol in ionic liquid/isooctane binary systems, *J. Agric. Food Chem*., 59, 1256-1263 (DOI: 10.1021/jf104101z).
11. John G., Zhu G., Li J., Dordick J. S. (2006), Enzymatically derived sugar-containing self-assembled organogels with

nanostructured morphologies, *Angew. Chem. Int. Ed.* 45, 4772-4775 (DOI: 10.1002/anie.200600989).

12. (a) Kim S. B., Hattori M., Ozawa T. (2012), Intelligent design of nano-scale molecular imaging agents, *Int. J. Mol. Sci*., 13, 16986-17005 (DOI:10.3390/ijms131216986); (b) Razgulin A., Ma N., Rao J. (2011), Strategies for in vivo imaging of enzyme activity: An overview and recent advances, *Chem. Soc. Rev.*, 40, 4186 (DOI: 10.1039/c1cs15035a).
13. Komatsu T., Kikuchi K., Takakusa H., Hanaoka K., Ueno T., Kamiya M., Urano Y., Nagano T. (2006), Design and synthesis of an snzyme activity-based labeling molecule with fluorescence spectral change, *J. Am. Chem. Soc*., 128, 15946-15947 (DOI: 10.1021/ja0657307).
14. Laschke M. W., van Oijen A. E. V., Körbel C., Scheuer C., Menger M. D. (2013), 4-hydroxybenzyl alcohol: a novel inhibitor of tumor angiogenesis and growth, *Life Sciences*, 93, 44-50 (DOI: 10.1016/j.lfs.2013.05.022).
15. Lehn J.-M. (1995), *Supramolecular chemistry*: concepts and perspectives (VCH, Weinheim, Germany).
16. (a) Ikeda M., Tanida T., Yoshii T., Hamachi I. (2011), Rational molecular design of stimulus-responsive supramolecular hydrogels based on dipeptides, *Adv. Mater.*, 23, 2819-2822 (DOI: 10.1002/ adma.201004658); (b) Raeburn J., Pont G., Chen L., Cesbron Y., Levy R., Adams D. J. (2012), Fmoc-diphenylalanine hydrogels: understanding the variability in reported mechanical properties *Soft Matter*, 8, 1168-1174 (DOI: 10.1039/c1sm06929b/); (c) Mahler A., Reches M., Rechter M., Cohen S., Gazit E. (2006), Rigid, self-assembled hydrogel composed of a modified aromatic dipeptide, *Adv. Mater*., 18, 1365-1370 (DOI: 10.1002/adma.200501765); (d) Yang Z., Gu H., Fu D., Gao P., Lam J. K., Xu B. (2004), Enzymatic formation of supramolecular Hydrogels, *Adv. Mater*.,

16, 1440-1444 (DOI: 10.1002/adma.200400340); (e) Toledano S., Williams R. J., Jayawarna V., Ulijn R. V. (2006), Enzyme-triggered self-assembly of peptide hydrogels via reversed hydrolysis, *J. Am. Chem. Soc.*, 128, 1070-1071 (DOI: 10.1021/ja056549l); (f) Adhikari B., Banerjee A. (2011), Short peptide based hydrogels: incorporation of graphene into the hydrogel, *Soft Matter*, 7, 9259-9266 (DOI: 10.1039/c1sm06330h).

17. Rasale D. B., Maity I., Das A. K. (2012), Emerging π-stacked dynamic nanostructured library, *RSC Adv*., 2, 9791-9794 (DOI: 10.1039/C2RA21334F); (b) Babu S. S., Praveen V. K., Ajayaghosh A. (2014), Functional π-gelators and their applications, *Chem. Rev*.**,** *114*, 1973–2129 (DOI: 10.1021/ cr400195e).

18. Xie P., Zhou Q., Diem M. (1994), IR circular dichroism of turns in small peptides, *Faraday Discuss.*, 99, 233-243 (DOI: 10.1039/ FD9949900233).

19. Rasale D. B., Maity I., Maruthi K., Das A. K. (2013), Peptide self-assembly driven by oxo-ester mediated native chemical ligation *Chem.Commun.*, 49**,** 4815-4817 (DOI: 10.1039/C3CC41475B).

20. (a) Vijayakumar C., Praveen V. K., Ajayaghosh A. (2009), RGB Emission through controlled donor self-assembly and modulation of excitation energy transfer: A novel strategy to white-light-emitting organogels, *Adv. Mater.*, 21, 2059-2063 (DOI: 10.1002/ adma-.200802932); (b) Maity I., Mukherjee T. K., Das A. K. (2014), Photophysical study of a π-stacked β-sheet nanofibril forming peptide bolaamphiphile hydrogel, *New J. Chem.*, 38, 376-385 (DOI: 10.1039/C3NJ00814B).

21. (a) Wall B. D., Diegelmann S. R., Zhang S., Dawidczyk T. J., Wilson W. L., Katz H. E., Mao H.-Q., Tovar J. D. (2011), Aligned macroscopic domains of optoelectronic nanostructures prepared via shear-flow assembly of peptide hydrogels, *Adv. Mater.*, 23,

5009-5014 (DOI: 10.1002/adma.201102963); (b) Giansante C., Raffy G., Schafer C., Rahma H., Kao M.-T., Olive A. G. L., Guerzo A. D. (2011), White-light-emitting self-assembled nanofibers and their evidence by microspectroscopy of individual objects, *J. Am. Chem. Soc*., 133, 316-325 (DOI: 10.1021/ ja106807u).

Chapter 7

Conclusion and Scope for Future Work

7.1 Conclusions

Several methods were used for the development of peptide self-assembly. A number of physical stimuli like variation in pH,[1] temperature,[2] light[3] and sonication[4] were used to exploit peptide self-assembly. The peptide based self-assembled materials have been used in many applications such as drug delivery,[5] tissue engineering,[6] templates for nanofabrication[7] and catalysis.[8] Thus, design and synthesis of such self-assembled materials to further explore in various application is an important task. Fmoc and naphthalene based short peptides have routinely been used by several groups to bring up peptide nanostructures.[9] Here, we have exploited several chemical reactions to direct peptide self-assembly. Several chemical reactions including oxo-ester mediated native chemical ligation, selenoester mediated native chemical ligation, enzyme catalysed peptide hydrolysis and enzyme catalysed esterification of Nmoc-based peptides were used to direct peptide self-assembly.

Chapter 1 described the general introduction to peptide, peptide secondary structures, self-assembly processes, chemical reactions and applications of peptide self-assembly.

Chapter 2 described various spectroscopic and experimental techniques which were used in these studies. This chapter also revealed the materials which were used to carry out these work.

Chapter 3 revealed that naphthalene-*2*-methoxycarbonyl (Nmoc-) based peptide self-assembly via chemical reaction. In this study, we have synthesized Nmoc-protected oxo-esters to further exploit in the self-

assembly process.[10] Nmoc- group offers significant π-π stacking interactions in the self-assembly process. Nmoc-protected oxo-esters were exploited in the peptide self-assembly through chemoselective native chemical ligation. N-terminal cysteines can be efficiently coupled with Nmoc protected peptide oxo-esters through amide bond formation via NCL reaction. Self-assembled dynamic peptide gels are formed via oxidation of the Nmoc-protected peptides synthesized via the NCL reaction. NCL reactions allow the formation of nanofibrillar structures. The entangled nanofibrillar structures are responsible for the formation of self supporting gels.

Chapter 4 reported the results on in situ genereated redox active peptide via selenoester mediated native chemical ligation. Cysteine and Cys-Gly peptide were provided mechanistic insight into the NCL driven self-assembly process. We have also shown the redox active dynamic peptide gels which were formed via oxidation and reduction of the Nmoc-protected peptides synthesized via NCL reactions. The gel-sol transition was highly dependent on the oxidation and reduction of cysteine and cystine based peptides. Peptides were self-assembled via hydrogen bonding and π-π stacking interactions and peptides were redox active in nature. The selenoester mediated NCL reactions were responsible for nanofibrillar structure in gel phase medium.

Chapter 5 demontrated a new kind of dynamic supramolecular hydrogel by introducing an N-terminus protecting aromatic moiety i.e. the naphthalene-2-methoxycarbonyl (Nmoc) group. Enzyme catalyzed hydrogelation leads to the formation of a dynamic library. A simple nanostructured predominating product was generated by the dynamic peptide library that self-assembled through π-π stacking interactions. A real-time morphological change was also described in this chapter.

Chapter 6 described blue light emitting peptide hydrogel upon bicatalytic incorporation of gastrodigenin (*p*-hydroxybenzyl alcohol, HBA) with Nmoc-protected dipeptides. Besides the lipase propensity towards the hydrolysis of ester bonds in aqueous medium, we have exploited catalytic activity of lipase in the development of fluorescent peptide nanostructures via esterification reaction. The entagled blue light emiiting nanofibrillar networks were obsreved in hydrogel state.

7.2 Scopes for Future Work

The native chemical ligation offers free sulfhydryl group in native peptides which aid to control development of peptide self-assembly. The self-assembly and dis-assembly of native peptides were tuned by oxidation-reduction of disulfide bond in the peptides. This approach can be useful in drug delivery and others clinical research applications. We have first reported selenoester mediated native chemical ligation reactions to develop self-assembled nanostructures. We have used Cys-Gly dipeptide which is active metabolite in biology. The higher concentration of Cys-Gly dipeptide is associated with increased risk in women breast cancer.[11] Therefore, such bioorthogonal approaches can be used to trap such metabolites.

The enzyme catalyzed chemical reactions are more promising due to their propensity to work at physiological conditions. Protease is an active enzyme in biology. We have used protease thermolysin to generate the dynamic peptide library. A single predominating component self-assembles to form self-supporting hydrogel. Aβ (1-42) is formed by sequential cleavage of amyloid precursor protein by the proteases *β*-secretase and *γ*-secretase. Aggregation of this Aβ (1-42) peptide fragment leads to Alzheimer disease (AD).[12] Therefore, the identification of proteins or compounds that block secretase remains a major goal of AD

research. Enzyme catalysed peptide self-assembly could be used to study such processes.

Recently, there is wide interest to design molecules with high fluorescence efficiency to monitor the biological events in the cell. Numrerous π-conjugated aromatic molecules are reported with excellent fluorescence efficiency.[13] However, poor water solubility of these molecules hampers their biological applications. We have exploited lipase catalyzed chemical reaction for regioselective inclusion of gastrodigenin to Nmoc-protected peptides. The resulting product was self-assembled in aqueous medium. A strong blue light emitting hydrogel was observed upon illuminating under UV lamp (365 nm). The self-assembly of peptides in water with efficient fluorescence properties makes it an ideal candidate for biomedical applications. These self-assembled materials can be used in bio-imaging and bioassays.

7.3 References

1. Tena-Solsona M., Miravet J. F., Escuder B. (2014), Tetrapeptidic molecular hydrogels: Self-assembly and co-aggregation with amyloid fragment Aβ1-40, *Chem. Eur. J.*, 20, 1023-1031 (DOI:10.1002/chem.201302651).
2. Miravet J. F., Escuder B., Segarra-Maset M. D., Tena-Solsona M., Hamley I. W., Dehsorkhi A., Castelletto V. (2013), Self assembly of a peptide amphiphile: transition from nanotape fibrils to micelles, Soft Matter, 9, 3558-3564 (DOI: 10.1039/ C3SM 27899A).
3. Haines L. A., Rajagopal K., Ozbas B., Salick D. A., Pochan D. J., Schneider J. P. (2005), Light-activated hydrogel formation via the triggered folding and self-assembly of a designed peptide, *J. Am. Chem. Soc.*, 127, 17025-17029 (DOI: 10.1021/ja054719o).

4. Maity I., Mukherjee T. K., Das A. K. (2014), Photophysical study of a π-stacked β-sheet nanofibril forming peptide bolaamphiphile hydrogel, *New J. Chem.*, 38, 376-385 (DOI: 10.1039/ C3NJ00814B).

5. (a) Ma D., Tu K., Zhang L. M. (2010), Bioactive supramolecular hydrogel with controlled dual drug release characteristics, *Biomacromolecules,* 11, 2204-2212 (DOI: 10.1021/bm100676a); (b) Naskar J., Palui G., Banerjee A. (2009), Tetrapeptide-based hydrogels: For encapsulation and slow release of an anticancer drug at physiological pH, *J. Phys. Chem. B.,* 113, 11787-11792 (DOI: 10.1021/jp904251j); (c) Koley P., Gayen A., Drew M. G. B., Mukhopadhyay C., Pramanik A. (2012), Design and self-assembly of a leucine-enkephalin analogue in different nanostructures: application of nanovesicles, *Small,* 8, 984-990 (DOI: 10.1002/smll.201101685).

6. (a) Lee K. Y., Mooney D. J. (2001), Hydrogels for tissue engineering, *Chem. Rev.*, 101, 1869-1880 (DOI: 10.1021/cr000108x); (b) Tsitsilianis C. (2010), Responsive reversible hydrogels from associative "smart" macromolecules, *Soft Matter,* 6, 2372-2388 (DOI: 10.1039/B923947B); (c) Zhao X. B., Pan F., Xu H., Yaseen M., Shan H., Hauser C. A. E., Zhang S., Lu J. R. (2010), Molecular self-assembly and applications of designer peptide amphiphiles, *Chem. Soc. Rev.*, 39, 3480-3498 (DOI: 10.1039/b915923c).

7. Reches M., Gazit E. (2003) Casting metal nanowires within discrete self-assembled peptide nanotubes, *Science,* 300, 625-627 (DOI: 10.1126/science.1082387).

8. Maity I., Manna M. K., Rasale D. B., Das A. K. (2014), Peptide-nanofiber-supported palladium nanoparticles as an efficient catalyst for the removal of N-terminus protecting groups, *ChemPlusChem,* 79, 413-420 (DOI: 10.1002/cplu.201300348).

9. (a) Orbach R., Mironi-Harpaz I., Adler-Abramovich L., Mossou E., Mitchell E. P., Forsyth V. T., Gazit E., Seliktar D. (2012), The rheological and structural properties of Fmoc-peptide-based hydrogels: The effect of aromatic molecular architecture on self-assembly and physical characteristics, *Langmuir*, *28*, 2015-2022 (DOI: 10.1021/la204426q); (b) Debnath S., Shome A., Das D., Das P. K. (2010), Hydrogelation through self-assembly of Fmoc-peptide functionalized cationic amphiphiles: Potent antibacterial agent, *J. Phys. Chem. B*, 114, 4407-4415 (DOI: 10.1021/ jp909520w); (c) Das A. K., Collins R., Ulijn R. V. (2008), Exploiting enzymatic (reversed) hydrolysis in directed self-assembly of peptide nanostructures, *Small*, 4, 279-287 (DOI: 10.1002/smll.200700889).

10. (a) Rasale D. B., Maity I., Das A. K. (2012), Emerging π-stacked dynamic nanostructured library, *RSC Adv.*, 2, 9791-9794 (DOI: 10.1039/C2RA21334F); (b) Rasale D. B., Maity I., Konda M., Das A. K. (2013), Peptide self-assembly driven by oxo-ester mediated native chemical ligation, *Chem. Commun.*, 49, 4815-4817 (DOI: 10.1039/C3CC41475B).

11. (a) Tang C. W., VanSlyke S. A., Chen C. H. (1989), Electroluminescence of doped organic thin films, *J. Appl. Phys.*, 65, 3610-3616; (b) Burn P. L., Lo S. C., Samuel I. D. W.(2007), The Development of light-emitting dendrimers for display, *Adv. Mater.*, 19, 1675-1688 (DOI: 10.1002/adma.200601592); (c) Wu C. C., Lin Y. T., Wong K. T., Chen R. T., Chien Y. Y. (2004), Efficient organic blue-light-emitting devices with double confinement on terfluorenes with ambipolar carrier transport properties *Adv. Mater.*, 16, 61-65 (DOI: 10.1002/ adma.200305619); (d) Baldo M. A.,Thompson M. E., Forrest S. R. (2000), High-efficiency fluorescent organic light-emitting devices

using a phosphorescent sensitizer, *Nature*, 403, 750-753 (DOI:10.1038/35001541).

12. Selkoe D. J., (1999), Translating cell biology into therapeutic advances in Alzheimer's disease, *Nature*, 399, 23-31 (DOI:10. 1038/19866).

13. Lin J., Manson J. E., Selhub J., Buring J. E., Zhang S. M. (2007), Plasma cysteinylglycine levels and breast cancer risk in women, *Cancer Res.*, 67, 11123-11127 (DOI:10.1158/0008-5472).

APPENDIX-A

Characterization Data of Thioesters: Chapter 4

1. High Performance Liquid Chromatograpgy

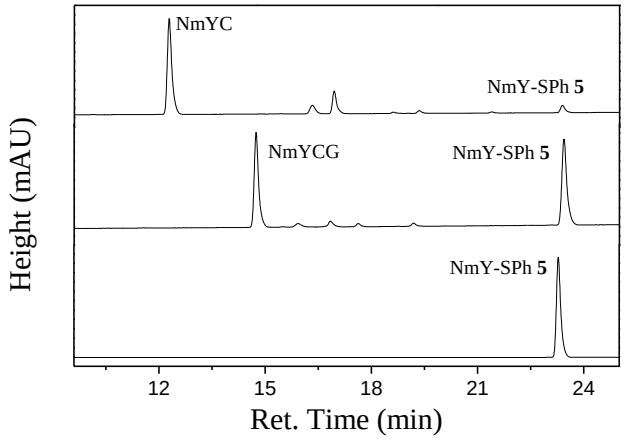

Figure A1. *Overlaid HPLC chromatograms for compound **5** showing peak NmYCG after native chemical ligation with Cys-Gly and peak **NmYC** for ligation reaction of **5** with cysteine.*

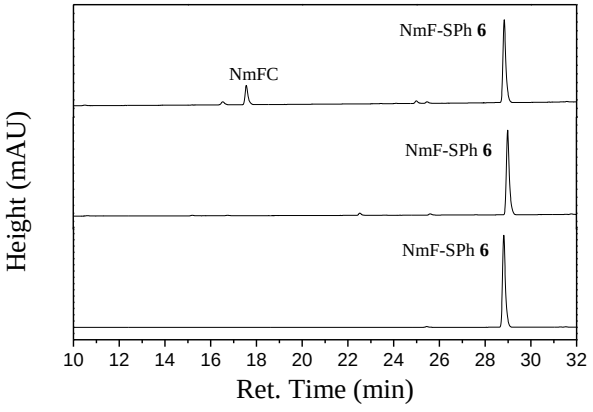

Figure A2. *Overlaid HPLC chromatograms for compound **6** showing **NmFC** ligation product with Cys-Gly. The 16.14 % **NmFC** product was observed upon ligation of **6** with Cysteine.*

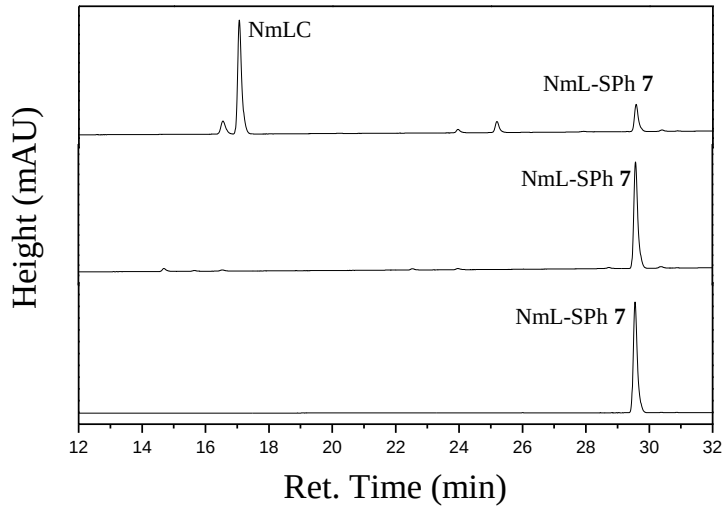

Figure A3. *Overlaid HPLC chromatograms for compound* ***7*** *showing ligation product* ***NmLC*** *with Cys-Gly. The 80.79 %* ***NmLC*** *product was observed upon ligation of* ***7*** *with Cysteine.*

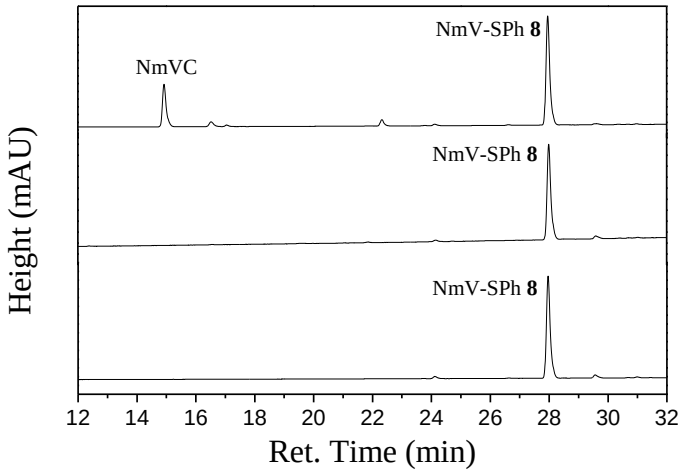

Figure A4. *Overlaid HPLC chromatograms for compound* ***8*** *showing ligation product NmVC with Cys-Gly. The 27.74 %* ***NmVC*** *product was observed upon ligation of* ***8*** *with Cysteine.*

Table A1. *Native chemical ligation reactions with different thioesters*

Entry	Substrate	Cys-Gly[a] and Cys[b]	Product conversion in inert atm. [%]	Product conversion in air [%]	Gel /Sol [c]
1.	NmY-SPh **5**	Cys-Gly	62.33 NmYCG	28.53 $(NmYCG)_2$	S
2.	NmF-SPh **6**	Cys-Gly	0 NmFCG	0 $(NmFCG)_2$	S
3.	NmL-SPh **7**	Cys-Gly	7.47 NmLCG	7.16 $(NmLCG)_2$	S
4.	NmV-SPh **8**	Cys-Gly	0 NmVCG	0 $(NmVCG)_2$	S
5.	NmY-SPh **5**	Cysteine	92.86 NmYC	90.5 $(NmYC)_2$	S
6.	NmF-SPh **6**	Cysteine	16.14 NmFC	8.13 $(NmFC)_2$	S
7.	NmL-SPh **7**	Cysteine	80.79 NmLC	78.03 $(NmLC)_2$	S
8.	NmV-SPh **8**	Cysteine	27.74 NmVC	26.03 $(NmVC)_2$	S

[a]Cys-Gly dipeptide, [b]Cysteine, [c]G = gel, S = solution

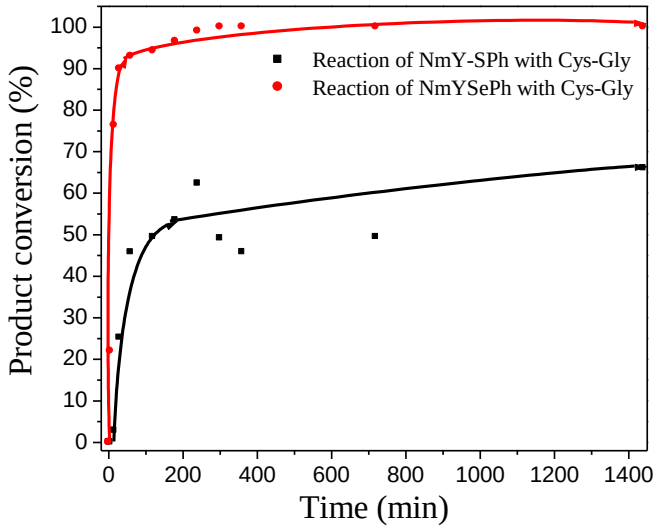

Fiureg A5. *HPLC analysis for* ***NmYCG*** *formation as function of time upon reaction of* ***NmY-SePh*** *and* ***NmY-SPh*** *with* ***Cys-Gly****. Selenoester gives 90%* ***NmYCG*** *conversion at 30 min while only 25%* ***NmYCG*** *conversion was observed from thioester at 30 min.*

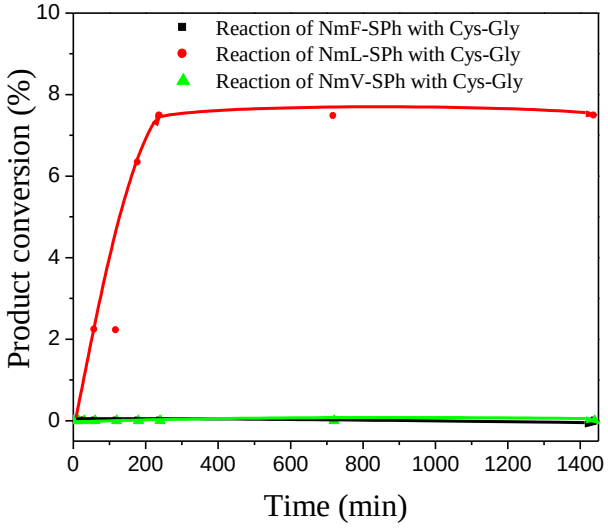

Figure A6. *HPLC analysis for product* ***NmFCG****,* ***NmLCG*** *and* ***NmVCG*** *formation as function of time upon reaction of* ***NmF-SPh****,* ***NmL-SPh*** *and* ***NmV-SPh*** *with cysteine.*

2. ^{1}H , ^{13}C NMR and ESI-MS Characterization of Thioesters

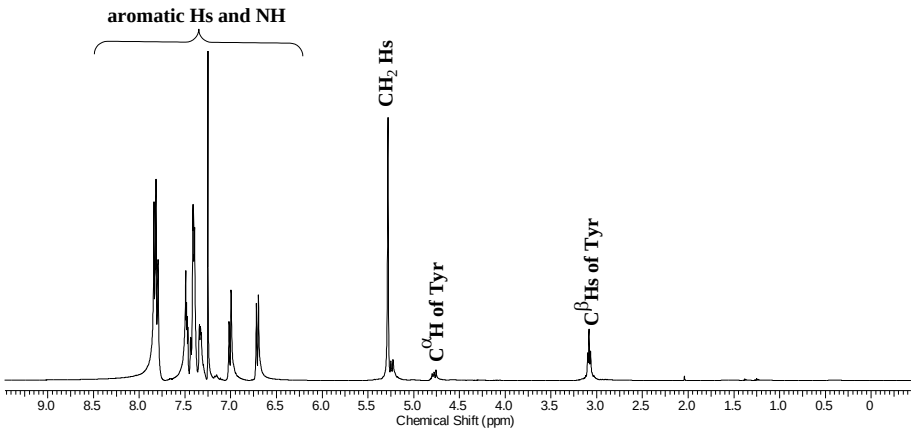

Figure A7. *400 MHz ^{1}H NMR spectrum of* ***5 (NmY-SPh)*** *in $CDCl_3$.*

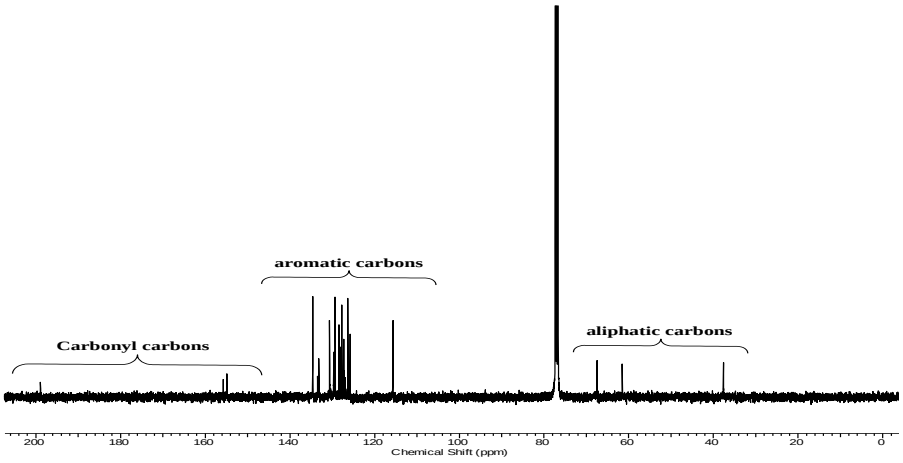

Figure A8. *100 MHz ^{13}C NMR spectrum of* ***5 (NmY-SPh)*** *in $CDCl_3$.*

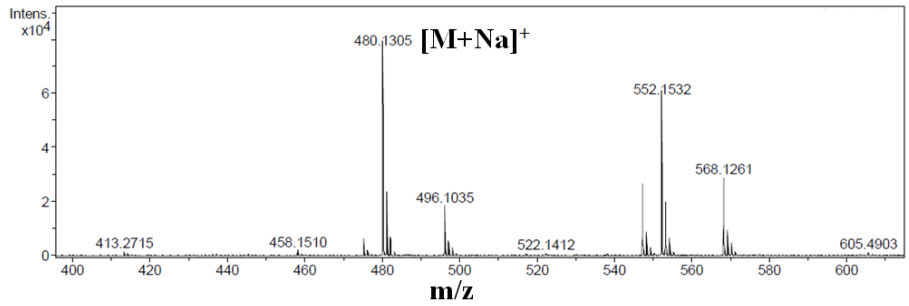

Figure A9. *ESI-MS spectrum of* ***5 (NmY-SPh)****.*

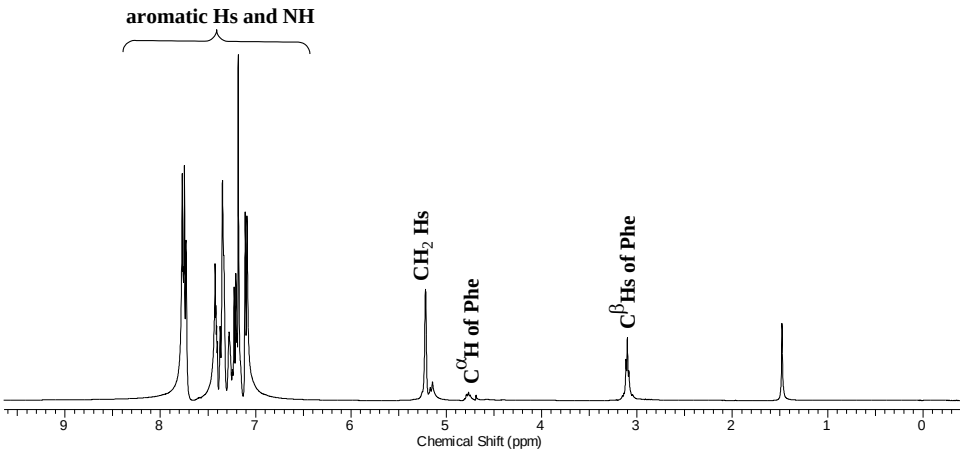

Figure A10. *400 MHz ^{1}H NMR spectrum of* ***6 (NmF-SPh)*** *in $CDCl_3$.*

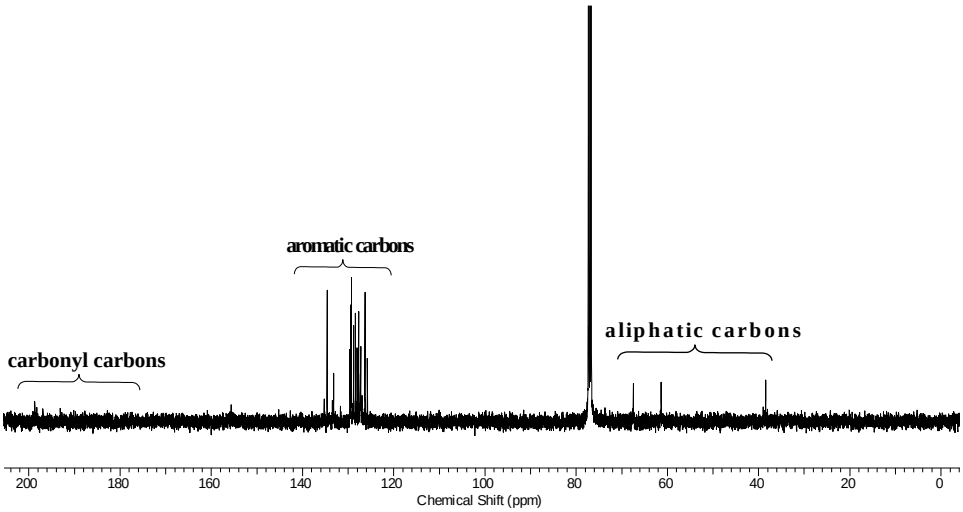

Figure A11. *100 MHz ^{13}C NMR spectrum of* ***6 (NmF-SPh)*** *in $CDCl_3$.*

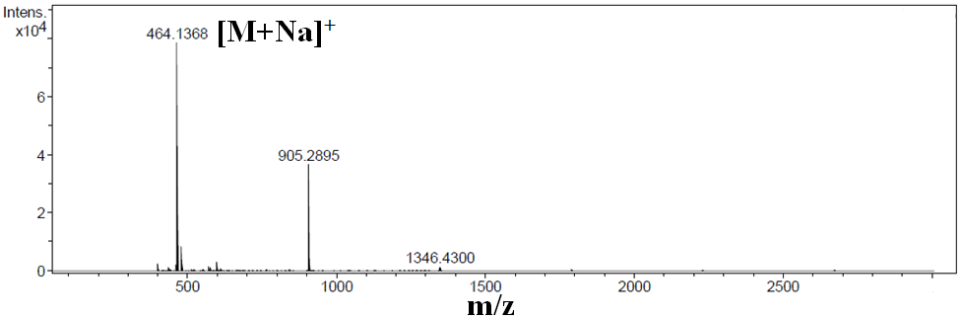

Figure A12. *ESI-MS spectrum of* ***6 (NmF-SPh)***.

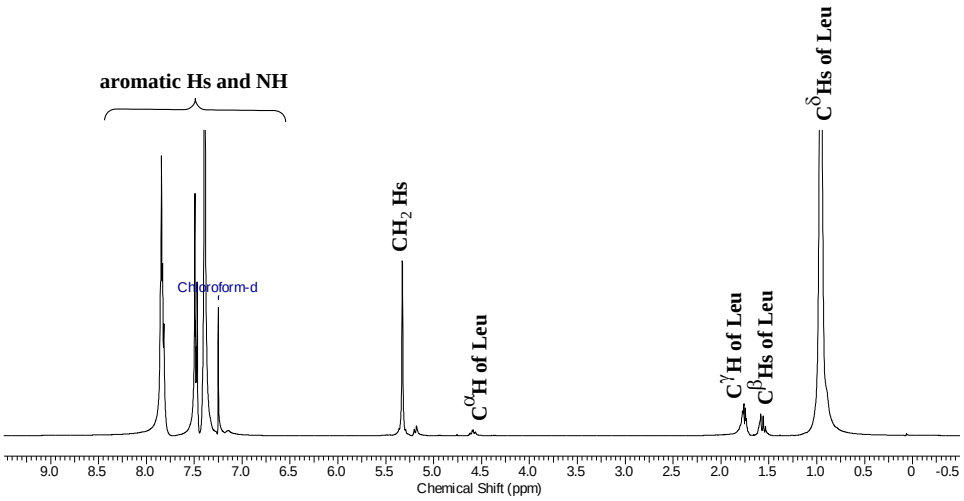

Figure A13. *400 MHz ^{1}H NMR spectrum of* ***7 (NmL-SPh)*** *in $CDCl_3$.*

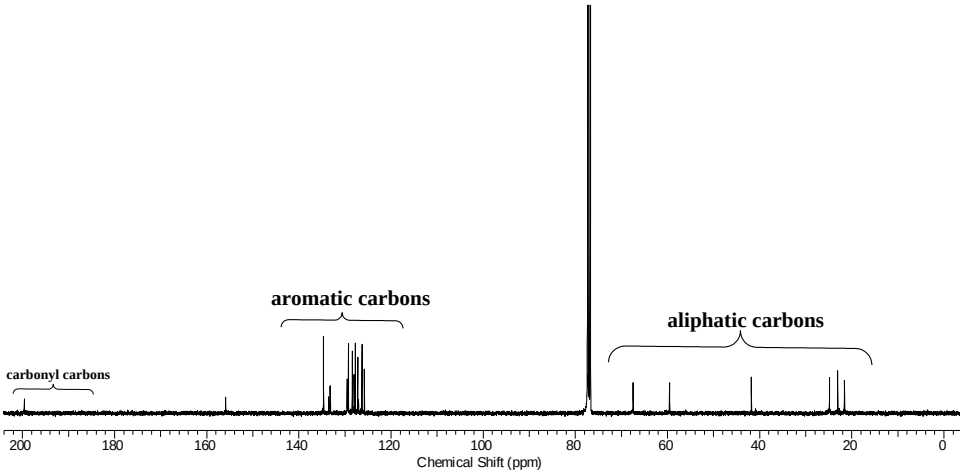

Figure A14. *100 MHz ^{13}C NMR spectrum of* ***7 (NmL-SPh)*** *in $CDCl_3$.*

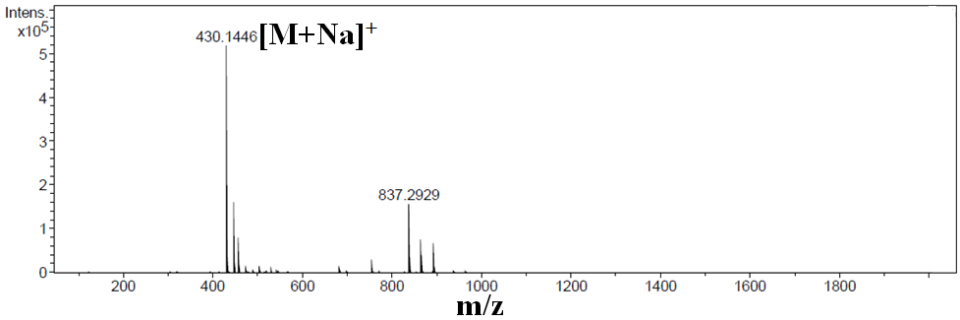

Figure A15. *ESI-MS spectrum of* ***7 (NmL-SPh)****.*

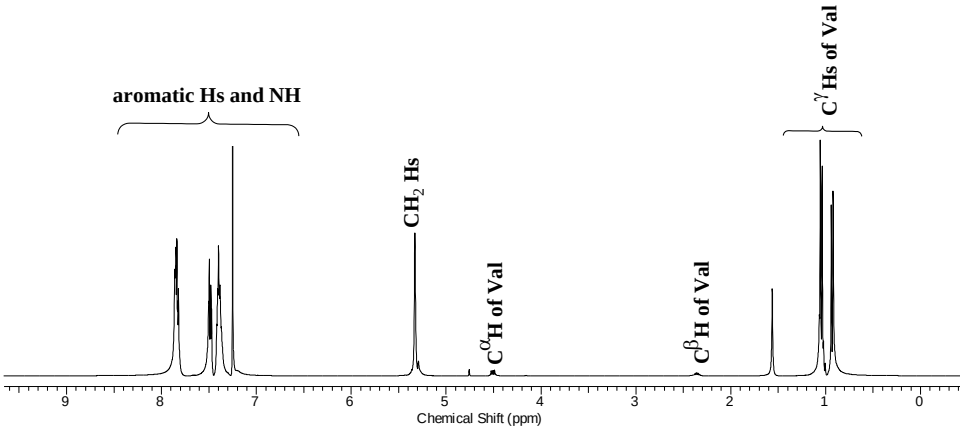

Figure A16. *400 MHz ^{1}H NMR spectrum of* ***8 (NmV-SPh)*** *in $CDCl_3$.*

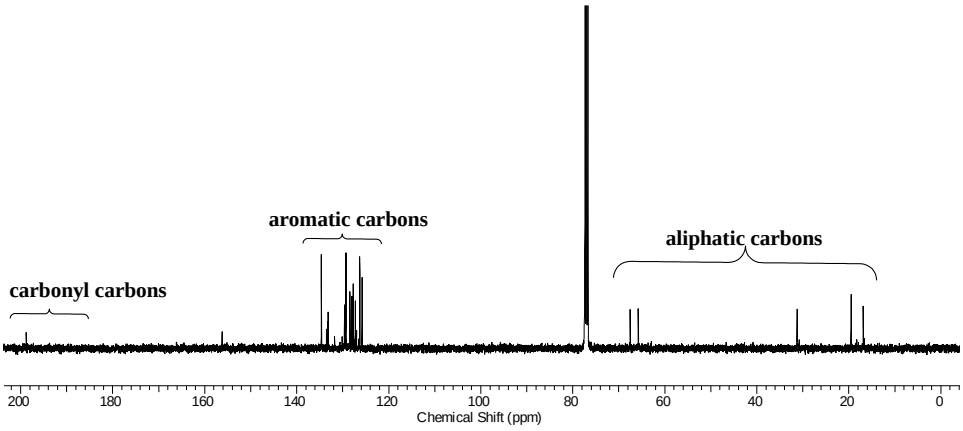

Figure A17. *100 MHz ^{13}C NMR spectrum of* ***8 (NmV-SPh)*** *in $CDCl_3$.*

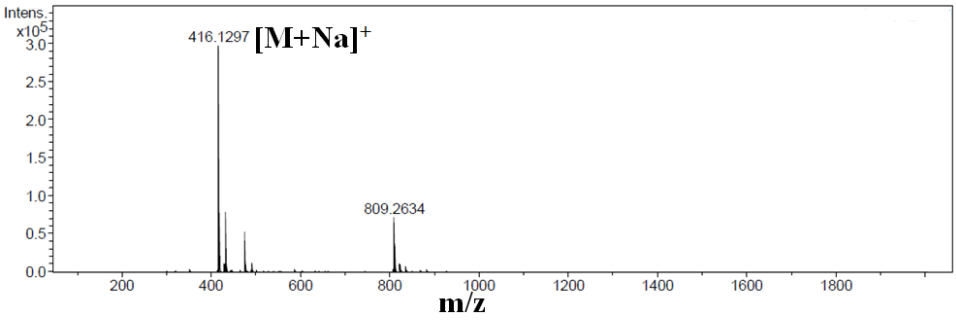

Figure A18. *ESI-MS spectrum of* ***8 (NmV-SPh)****.*